

Copyright is owned by the Author of the thesis. Permission is given for a copy to be downloaded by an individual for the purpose of research and private study only. The thesis may not be reproduced elsewhere without the permission of the Author.

Studies on Abscission Cell Differentiation in  
*Sambucus nigra* and *Phaseolus vulgaris*

*Submitted in partial fulfilment of the degree of  
Doctor of Philosophy  
in Plant Biology*

Institute of Molecular BioSciences  
Massey University  
Palmerston North  
New Zealand

Simone Flight  
BSc (Hons)  
2002

# Abstract

This thesis examines aspects of abscission cell differentiation in *Sambucus nigra* and *Phaseolus vulgaris*. The experimentation is divided into two sections; an *in vivo* study examining the cell wall proteins from the leaf rachis abscission zones of *S. nigra*, to identify proteins that denote the abscission zone as a fully differentiated cell type, and an *in vitro* study examining aspects of secondary or adventitious abscission zone formation in petiole explants of *P. vulgaris*.

As an initial approach to identify abscission cell-specific proteins, a survey of the total cell wall bound proteins in four tissues, leaf mid-rachis (MR), ethylene-treated leaf mid-rachis (MRE), 0 h, or freshly excised leaf rachis abscission zone (OZ) and ethylene-treated abscission zone (ZONE) was undertaken. The study also involved surveying these tissues over the vegetative seasons (spring, summer, autumn). Separation of these protein extracts using SDS-PAGE revealed proteins that were putatively uniquely expressed in each of the tissues. Moreover, the expression of some proteins changed from spring through to autumn. Further fractionation of the extracts using hydrophobic interaction chromatography (HIC), and separation of the fractions using SDS-PAGE, illustrated there were many more proteins that had not been resolved in the initial survey of wall extracts.

In total, four proteins of ca. 10, 28, 38 and 43 kDa were identified in the OZ tissue only and six proteins (ca. 10, 34, 36, 40, 74 and 75 kDa) were detectable in the OZ and ZONE tissues. Three of the putative OZ-specific proteins (designated OZ10, OZ28 and OZ43) were trypsin-digested and some initial amino acid sequence data obtained. The OZ10 tryptic fragment had closest identity to a lipid transfer protein (LTP) from spinach, and the OZ43 fragment had closest identity to an aldose-1-epimerase-like protein expressed in tobacco. Two peptides were sequenced from the OZ28 protein; one had highest identity to a superoxide dismutase and the second had identity to a ribonuclease. Two of these, OZ10 and OZ43 were characterised further. Antibodies raised to LTPs protein from *Daucus carota* and *Arabidopsis thaliana* recognized a protein of 10 kDa that was expressed in both the rachis and abscission zone tissues of *S. nigra* before and after ethylene treatment. Moreover, the LTP antibodies detected a ca. 10 kDa protein in freshly excised and ethylene-treated distal pulvinus, primary

abscission zone and petiole tissues of *P. vulgaris* with highest expression in ethylene-treated petiole tissue. The second protein, to be characterised further was most similar in sequence to a nuclear pore membrane protein identified in tobacco suspension cells and designated gp40. This protein appears to be an aldose-1-epimerase-like enzyme (otherwise known as mutarotase) from its homology to bacterial forms of mutarotase. An antibody to gp40 recognized a ca. 43kDa protein in the non-ethylene treated rachis and zone cell wall extracts of *S. nigra*, the putative OZ43. This same antibody did not recognize any proteins in the protein extract from porcine and lamb kidney, tissues that have mutarotase activity. A coupled enzyme assay was developed to measure the mutarotase activity in the plant samples. Although mutarotase activity was measured in both the soluble and cell wall bound fractions of the rachis cells, purification of the OZ43 protein using column chromatography or through cell fractionation revealed that the ca. 43 kDa protein recognised by the gp40 antibody did not appear to be responsible for this activity.

For the second part of this thesis, the *in vitro* study, the aim was to measure the levels of IAA, ethylene and ACC oxidase enzyme activity in bean petioles explants during IAA-induced secondary abscission zone formation. In the bean explant system, the secondary zone forms at a site along the petiole which is removed from the primary zone and governed by the concentration of IAA added. The petiole tissue that links the primary zone with the secondary zone (the distal segment) remains green and, in this thesis, is designated as G1. The petiole tissue proximal to the zone senesces and yellows, and is divided into Y2 (immediately proximal to the secondary zone), Y3 (mid way) and Y4 (the most proximal petiole tissue).

To measure changes in IAA concentration during secondary zone formation, an immunoassay (ELISA) was developed, initially using polyclonal antibodies to IAA, but the titre of these antibodies was not sufficient and so monoclonal antibodies were used. During secondary zone formation, the concentration of free IAA in the petiole tissue changed dramatically, with measurements ranging between 6 and 2608 pmol/g fresh weight (FW) of tissue. The IAA concentration in the petioles at separation at the primary zone before IAA was added was lower in the G1 and Y2 sections (ca. 30 pmol/g FW) when compared with the Y3 and Y4 sections (166 and 271 pmol/g FW respectively).

At 6 h after the application of IAA, the concentration of IAA had increased to 146 pmol/g FW in the G1 section, remained the same in the Y2 section and increased to 208 and 423 pmol/g FW in the Y3 and Y4 sections, respectively. At 26 h after the application of IAA, and approximately the time of initiation of differentiation of the secondary zone, the IAA concentration was similar to the petioles after 6 h (179 and 21 pmol/g FW for G1 and Y2 respectively) and significantly lower in the Y3 and Y4 sections (35 and 69 pmol/g FW respectively). At the first point at which the green:yellow tissue can be ascertained (at 52 h) the IAA concentration was dramatically higher in the G1 and Y2 tissues (1125 and 1090 pmol/g FW respectively) compared to measurements in the Y3 and Y4 sections at 52 h of 17 and 107 pmol/g FW respectively. At separation at the secondary abscission zone, the IAA measurements in the G1, Y2 and Y4 sections were 405, 315 and 1198 pmol/g FW respectively.

The ethylene produced from freshly excised pulvinus and petiole tissue was ca. 0.20 nmol/h/g FW and increased to 1.7 nmol/h/g FW in the pulvinus, 0.39 nmol/h/g FW in the G1 petiole section and 0.67 nmol/h/g FW in the Y2/Y3/Y4 pooled petiole sections at separation at the primary zone. At separation of the secondary zone, ethylene evolution measurements of 1.73 nmol/h/g FW in G1 and 4.37 nmol/h/g FW in the Y2/Y3/Y4 tissue were observed. However, the activity and expression of ACC oxidase was higher in the fresh tissues and non-senescent petiole region (G1), but was lowest in the senescent (Y2, Y3 and Y4) tissue at the formation of the secondary zone.

# Acknowledgements

Like all of the students of my supervisor Michael McManus that have gone before me, I would like to express my sincere gratitude for his excellent supervision throughout the research and writing of my thesis. I know I would not have reached this point without his encouragement, guidance and patience. I'd also like to acknowledge my co-supervisor David Fountain who has helped make my project as stress free as possible.

I wish to thank all the people in the IMBS and IFS who have freely given their time, advise and trustingly loaned me equipment. In particular, Dick Poll for his help with the ins and outs of column chromatography, Chris Burrows for the coupled enzyme assay, Simon Fielder for helping with the distillation of diazomethane and Dr. Ian Andrew for his help with the enzyme activity assay.

I am very grateful for the three years of financial assistance provided by the Marsden Fund and appreciate the travel grants given to me by the New Zealand Society of Plant Physiologists.

To all of the awesome people in Michael's team, thank you for your practical help and for making the lab an enjoyable place to be. Special thanks to Richard for being so generous and obliging, and to Anya for keeping us organised (good luck with the growing family). There is also Greg, who has taught me a lot, and the very kind and compassionate Ning. To the newer lab additions, Balance, Jan, Rachel and Elizabeth, it was nice to know you guys and all the best for the future.

Others members of Michael's crew I'd like to acknowledge who have come and gone since I started are; Lyn Watson (who was absolutely fantastic), Alicia, Trish, Vikki, Don, Sang Dong, Demming, Celia and Alison.

I'd like to acknowledge Tim White, not only for his assistance with research but also for his fanaticism to help me with anything from work to babysitting and for entertaining me with his great sense of humour. In the same faction is Suzanne D'Ath, who has been absolutely fabulous.

Someone who has been of great support to me over the years is Aly Coulter. Thankyou so much for everything, I don't think I could put into words how much I have appreciated your friendship and unwavering support in every area.

I'd like to thank my family for their support during my time as a PhD student. Brendon and his grandparents have been greatly supportive of my efforts. My parents have always been there for me and, at this very sad and difficult time, I want them to know how much I love them and cherish every moment they are here. Finally, to my children, Danielle and Sonja who have grown into little (and not so little) girls, this is for you.

# Table of Contents

Abstract.....	ii
Acknowledgements.....	v
List of Figures.....	xiii
List of Tables.....	xx
1. Introduction.....	1
1.1 Abscission zone cells: A model for studying plant cell differentiation.....	1
1.2 Overview of the abscission process.....	1
1.2.1 Cell-cell separation during plant growth and development.....	2
1.2.2 Differentiation and cell-cell separation of abscission zone cells.....	3
1.3 The plant cell wall.....	5
1.3.1 The structural proteins of plant cell walls.....	6
1.3.2 Defence-related proteins in plant cell walls.....	8
1.4 Cell wall enzymes associated with cell-cell separation of abscission zone cells.....	9
1.4.1 Hydrolases.....	9
1.4.1.1 Endo $\beta$ -1, 4-glucanhydrolase.....	9
1.4.1.2 Polygalacturonase.....	11
1.4.2 Pectin methylesterase.....	12
1.4.3 Peroxidase.....	12
1.4.4 Pathogen-related proteins inducing during abscission zone cell-cell separation.....	13
1.5 The study of abscission cell differentiation.....	13
1.5.1 Mutant studies and the control of differentiation.....	13
1.5.2 Introduction of the <i>in vivo</i> approach to study abscission and abscission cell differentiation .....	15
1.5.3 Examination of cell wall proteins in <i>S. nigra</i> .....	15
1.5.4 Identifying antigenic protein determinants in the cell wall.....	16

1.6 Control of abscission cell differentiation: Introduction of the <i>in vitro</i> approach to study abscission cell differentiation.....	18
1.6.1 Overview of secondary abscission zones and their formation.....	18
1.6.2 The hormonal control of the abscission process.....	19
1.6.2.1 Ethylene.....	20
1.6.2.2 ACC oxidase.....	21
1.6.2.3 Auxin (IAA).....	22
1.6.3 Secondary abscission formation is a transdifferentiation event.....	24
1.6.4 Control of secondary abscission zone formation in explants of <i>P. vulgaris</i> .....	26
1.7 Thesis Aims.....	29
<b>2. Materials and Methods.....</b>	<b>30</b>
2.1 Growth and explant preparation of <i>Phaseolus vulgaris</i> .....	30
2.1.1 Cultivar and growing media.....	30
2.1.2 Harvest and explant preparation.....	30
2.1.3 Ethylene and IAA treatment of explants.....	32
2.2 Collection and preparation of <i>Sambucus nigra</i> .....	34
2.2.1 Gathering of <i>S. nigra</i> plant material.....	34
2.2.2 Preparation of the tissue samples of <i>S. nigra</i> .....	34
2.3 Biochemical and chemical methods.....	38
2.3.1 Protein extraction and fractionation using column chromatography.....	38
2.3.1.1 Extraction of the soluble protein fraction in plant tissues.....	38
2.3.1.2 Extraction of cell wall-associated proteins.....	38
2.3.1.3 Fractionation of cells using ultracentrifugation.....	39
2.3.1.4 Extraction of proteins from lamb kidney.....	39
2.3.1.5 Concentrating protein, solution exchange and dialysis.....	40
2.3.1.6 Separation of proteins using hydrophobic interaction chromatography and Fast Protein Liquid Chromatograph, (FPLC).....	40
2.3.1.7 Ion exchange column chromatography.....	41
2.3.1.8 Gel filtration chromatography.....	42
2.3.2 The Bradford protein assay.....	44

2.3.3 Sodium Dodecyl Sulfate-polyacrylamide gel electrophoresis (SDS-PAGE).....	45
2.3.3.1 Preparing and running SDS-PAGE mini-gels.....	45
2.3.4 Two-dimensional gel electrophoresis.....	48
2.3.4.1 First dimension isoelectric focusing.....	48
2.3.4.1.1 <i>Rehydration of polyacrylamide gel strips</i> .....	48
2.3.4.1.2 <i>Isoelectric focusing of the polyacrylamide gel strips</i> .....	49
2.3.4.2 Second Dimension SDS-PAGE gel.....	51
2.3.4.3 Staining the acrylamide gels from the second dimension.....	52
2.3.5 Western analysis of SDS-PAGE gels.....	54
2.3.5.1 Immunodevelopment of electroblotted proteins.....	55
2.3.5.1.1 <i>Immunodevelopment of the electroblotted membranes</i> .....	55
2.3.5.2 Amino acid sequencing of internal peptide sequences.....	55
2.3.6 ACC oxidase activity measurements in petiole tissues.....	56
2.3.6.1 Extraction of ACC from petiole tissue.....	56
2.3.6.2 Preparation of samples for ACC oxidase assay using Sephadex G-25 spin columns.....	57
2.3.6.3 ACC oxidase assay.....	57
2.3.7 Measurement of ethylene production by intact petiole sections.....	58
2.3.7.1 Measurement of ethylene using gas chromatography.....	58
2.3.7.2 Calculation of ethylene concentrations.....	59
2.3.8 Measurement of aldose-1-epimerase activity.....	59
2.3.8.1 Preparation of plant extracts for the activity assay.....	59
2.3.9 Preliminary activity assays.....	60
2.3.9.1 Optimisation of the coupled enzyme assay.....	60
2.3.10 Calculation of the standard errors.....	61
2.4 Immunological methods.....	62
2.4.1 Production of polyclonal antibodies to indole-3-acetic acid (IAA).....	62
2.4.1.1 Conjugation of IAA to BSA.....	62
2.4.1.2 Immunisation of rabbits with the BSA-IAA conjugate.....	64

2.4.1.3 Antisera preparation and IgG purification.....	64
2.4.2 The Enzyme Linked Immuno-Sorbant Assay (ELISA) for the determination of IAA content in plant tissues.....	65
2.4.2.1 Extraction and methylation of IAA .....	65
2.4.2.1.1 <i>Preparation of diazomethane</i> .....	65
2.4.2.1.2 <i>Extraction and methylation of IAA in bean tissues</i> .....	67
2.4.2.1.3 <i>Methylation of IAA in a stock solution</i> .....	68
2.4.2.2 Synthesis of the IAA-alkaline phosphatase conjugate (tracer).....	68
2.4.2.3 Optimising the volume of the IAA-alkaline phosphatase tracer for use in the ELISA .....	69
2.4.2.4 Antibody immobilised ELISA.....	70
2.4.3 Affinity purification of antisera raised to a glutathione S-transferase (GST)-fusion protein to remove the GST epitopes.....	71
<b>3. Results: Abscission cell-specific proteins that denote the differentiated state</b>	
3.1 Identification of proteins in the rachis and leaflet abscission zones of <i>Sambucus nigra</i> .....	73
3.1.1 Introduction.....	73
3.1.2 Changes in the cell wall protein profile from MR, MRE, OZ and ZONE samples collected in spring, summer and autumn.....	74
3.1.3 Fractionation of cell wall extracts to discover unique or preferentially- expressed proteins in the ethylene and non-ethylene treated tissues.....	78
3.1.4 Identification of proteins revealed by HIC by amino acid sequencing.....	85
3.2 Characterisation of the OZ43 protein.....	89
3.2.1 Initial identification of OZ43 as an aldose-1-epimerase-like protein.....	89
3.2.2 Biochemical characterisation of OZ43.....	93
3.2.2.1 Preliminary mutarotase activity assays.....	93
3.2.2.1.1 <i>Examination of the <math>\alpha</math>-D-glucose and <math>\beta</math>-D-glucose anomeric equilibrium</i> .....	93
3.2.2.1.2 The coupled aldose-1-epimerase enzyme assay.....	97
3.2.2.1.3 Investigating the sensitivity of the coupled enzyme assay using porcine kidney mutarotase.....	102
3.2.2.2 Immunological identification of OZ43 in cell wall fractions using an antibody raised to the gp40 protein.....	104

3.2.2.3 Mutarotase activity assays of cell wall fractions containing the gp40 antibody-recognised OZ43 .....	107
3.2.2.4 Mutarotase activity assays of soluble and insoluble components of plant tissues, and immunological identification using gp40 antibodies.....	109
3.2.3 Determination of the immunological relationship of OZ43 with gp40 and mammalian mutarotase.....	114
3.2.4 The effect of ethylene on the OZ43 protein and mutarotase activity.....	116
3.3 Examination of OZ10 as a lipid transfer protein .....	120
3.4 Identification of other cell wall proteins using specific antibodies.....	126
4. Results: Changes in indole-3-acetic acid (IAA) and ethylene biosynthesis during the time course of secondary abscission zone formation in bean petiole explants.....	129
4.1 Introduction.....	129
4.1.1 Secondary abscission zone formation in bean petiole explants.....	129
4.2 Development of an ELISA for IAA measurement using polyclonal antibodies.....	132
4.2.1 Polyclonal antibody production.....	132
4.2.1.1 Titres of partially purified polyclonal IAA antisera.....	132
4.3 IAA ELISA using the monoclonal antibody.....	136
4.3.1 Cross-reaction test to support the accuracy of using the monoclonal antibody for measurement of IAA samples.....	139
4.3.2 Measurement of IAA in bean tissues.....	141
4.3.3 Measurement of IAA during the time course to secondary zone formation.....	143
4.4 Ethylene evolution from petiole sections from fresh to secondary abscission.....	146
4.5 ACC oxidase activity and expression in petiole tissue from fresh to secondary abscission .....	149
5. Discussion.....	153
5.1 The <i>in vivo</i> approach to study abscission and abscission cell differentiation.....	153
5.1.1 Introduction.....	153
5.1.2 The survey of cell wall proteins in <i>S.nigra</i> tissue.....	155

5.1.3 Separation of cell wall extracts using SDS-PAGE.....	155
5.1.4 Separation of cell wall HIC fractionated extracts using one and two-dimensional SDS-PAGE.....	156
5.1.5 The major group of cell wall proteins in the crude and fractionated cell wall extracts.....	156
5.1.6 Identification of cell-specific proteins .....	158
5.1.7 Superoxide dismutase in the abscission zone cell walls of <i>S. nigra</i> .....	159
5.1.8 Ribonuclease in the abscission zone cell walls of <i>S. nigra</i> .....	161
5.1.9 Characterisation of a ca. 43 kDa abscission zone cell wall-associated protein from <i>S. nigra</i> .....	161
5.1.10 The identification of a putative lipid transfer protein in abscission zone cell walls of <i>S. nigra</i> .....	167
5.1.11 Cellulase in the zone cell wall of <i>S. nigra</i> .....	169
5.2 The <i>in vitro</i> approach to study abscission zone cell differentiation.....	170
5.2.1 The role of auxin in the determination of abscission zones.....	170
5.2.2 The role of ethylene in the differentiation of abscission zones.....	178
5.3 Summary.....	186
5.3.1 Abscission and abscission cell differentiation: The <i>in vivo</i> approach.....	186
5.3.2 Abscission and abscission cell differentiation: The <i>in vitro</i> approach.....	188
5.4 Future directions.....	191
Appendix A.....	192
Appendix B.....	193
Bibliography.....	194

# List of Figures

<b>Figure 2.1.</b> Primary leaf of <i>Phaseolus vulgaris</i> approximately 14 days after germination. The explants were excised from the plant at this stage of development. ....	33
<b>Figure 2.2.</b> Freshly excised 15 mm petiole explant with the pulvinus attached.....	33
<b>Figure 2.3.</b> A Glass dish used for the ethylene treatment of the petiole explants containing petiole racks set into agar.....	33
<b>Figure 2.4.</b> Excision of petiole segments during the formation, or at separation of the secondary zones. For IAA measurements, the G1, Y2, Y3 and Y4 segments were excised as separate tissues. For ethylene evolution and ACC oxidase activity measurements the Y2, Y3 and Y4 segments were pooled. For all measurements, the shaded areas were discarded.....	35
<b>Figure 2.5.</b> A shrub of <i>Sambucus nigra</i> (elderberry) in flower.....	36
<b>Figure 2.6.</b> A compound leaf of <i>Sambucus nigra</i> .....	36
<b>Figure 2.7.</b> The segmented <i>S. nigra</i> rachis explant (explant shaded green).....	37
<b>Figure 2.8.</b> The leaflet abscission zones from <i>S. nigra</i> after 36 h ethylene treatment of the rachis explant shown in Figure 2.7. The arrows indicate the separated ZONE tissue and the boxed area represents the MRE tissue.....	37
<b>Figure 2.9.</b> Assembly of the Western blotting apparatus.....	54
<b>Figure 2.10a.</b> Elution of BSA from the Phenyl Superose HR 1/1 hydrophobic interaction column (section 2.3.1.6).....	63
<b>Figure 2.10b.</b> Elution of the BSA-IAA conjugate from the Phenyl Superose HR 1/1 hydrophobic interaction column (section 2.3.1.6).....	63
<b>Figure 2.11.</b> The diazomethane ( $\text{CH}_2\text{N}_2$ ) forming reaction.....	66
<b>Figure 3.1a.</b> Separation of cell wall protein extracts of MR, MRE, OZ and ZONE tissues collected in the spring using SDS-PAGE through a 12 % polyacrylamide gel. Proteins are visualised with Coomassie blue R-250 staining.....	76
<b>Figure 3.1b.</b> Separation of cell wall protein extracts of MR, MRE, OZ and ZONE tissues collected in the summer using SDS-PAGE through a 12 % polyacrylamide gel. Proteins are visualised with Coomassie blue R-250 staining.....	76
<b>Figure 3.1c.</b> Separation of cell wall protein extracts of MR, MRE, OZ and ZONE tissues collected in the autumn using SDS-PAGE through a 12 % polyacrylamide gel. Proteins are visualised with Coomassie blue R-250 staining.....	76

<b>Figure 3.2a.</b> Separation of a MR cell wall sample through a hydrophobic interaction column (Phenyl Superose HR 1/1).....	80
<b>Figure 3.2b.</b> Separation, using SDS-PAGE, of HIC fractions D (eluted with 60-65 % buffer B) and E (eluted with 65-70 % buffer B) obtained from the Phenyl Superose column chromatography separation of spring-collected MR, MRE, OZ and ZONE tissue. Proteins are visualised with Coomassie blue R-250 staining. The arrows indicate proteins of interest summarised in Table 3.2.....	81
<b>Figure 3.2c.</b> Separation, using SDS-PAGE, of HIC fractions F (eluted with 70-75 % buffer B) and G (eluted with 75-80 % buffer B) obtained from the Phenyl Superose column chromatography separation of summer-collected MR, MRE, OZ and ZONE tissue. Proteins are visualised with Coomassie blue R-250 staining. The arrows indicate proteins of interest summarised in Table 3.2.....	81
<b>Figure 3.2d.</b> Separation, using SDS-PAGE, of HIC fractions H (eluted with 80-85 % buffer B) and I (eluted with 85-90 % buffer B) obtained from the Phenyl Superose column chromatography separation of autumn-collected MR, MRE, OZ and ZONE tissue. Proteins are visualised with Coomassie blue R-250 staining. The arrows indicate proteins of interest summarised in Table 3.2.....	82
<b>Figure 3.2e.</b> Separation, using SDS-PAGE, of HIC fractions J (eluted with 90-95 % buffer B) and K (eluted with 95-100 %+ buffer B) obtained from the Phenyl Superose column chromatography separation of spring-collected MR, MRE, OZ and ZONE tissue. Proteins are visualised with Coomassie blue R-250 staining. The arrows indicate proteins of interest summarised in Table 3.2.....	82
<b>Figure 3.2f.</b> Two-dimensional separation of OZ HIC fraction I (eluting at 85-90 % buffer B). The proteins were separated using isoelectric focusing in the first dimension and SDS-PAGE in the second dimension. Protein spots are visualised using Coomassie blue G-250.....	84
<b>Figure 3.2g.</b> Two-dimensional separation of MR HIC fraction I (eluting at 85-90 % buffer B). The proteins were separated using isoelectric focusing in the first dimension and SDS-PAGE in the second dimension. Protein spots are visualised using Coomassie blue G-250.....	84
<b>Figure 3.3a.</b> SDS-PAGE separation of fraction E from a Phenyl Superose column chromatography separation of autumn-collected tissue. The proteins arrowed (OZ10, OZ28(a), OZ28(b) and OZ43) were then subjected to tryptic digestion and selected tryptic fragments from each protein were sequenced.....	87
<b>Figure 3.3b.</b> Sequences from a tryptic fragments obtained from the protein bands excised from the SDS-PAGE separation shown in Figure 3.3a.....	87
<b>Figure 3.3c.</b> Amino acid sequence alignment of the internal peptide from OZ28(a) with a ribonuclease from <i>A. thaliana</i> . Gen-bank accession number AAA51406.....	88
<b>Figure 3.3d.</b> Amino acid sequence alignment of the internal peptide from OZ28(b) with a superoxide dismutase from <i>A. thaliana</i> .	

Gen-bank accession number AAF01529.....	88
<b>Figure 3.3e.</b> Amino acid sequence alignment of the internal peptide from OZ43 with gp40 from <i>N. tabacum</i> . Gen-bank accession no. TO1933.....	88
<b>Figure 3.3f.</b> Amino acid sequence alignment of the internal peptide from OZ10 with a lipid transfer protein from spinach. Gen-bank accession no. AAA34032.....	88
<b>Figure 3.4a.</b> Alignment of the amino acid sequence from a tryptic peptide of OZ43 to amino acid sequences of probable and putative and aldose-1-epimerase proteins and aldose-1-epimerase-like proteins from a range of species. The boxed regions contain the amino acids that are the most highly conserved throughout the species examined (present in this alignment in at least 80 % of those plant species compared).....	91
<b>Figure 3.4b.</b> Western analysis, using a monospecific gp40 antibody, of ethylene and non-ethylene treated tissues eluted from the HIC column and separated using SDS-PAGE. Antibody recognition was detected using an alkaline-phosphatase conjugated secondary antibody.....	92
<b>Figure 3.5a.</b> The spontaneous anomeric transformation of $\alpha$ -D-glucose to $\beta$ -D-glucose measured as the change in absorbance at 340 nm over time (minutes).....	96
<b>Figure 3.5b.</b> The spontaneous anomeric transformation of $\beta$ -D-glucose to $\alpha$ -D-glucose measured as the change in absorbance at 340 nm over time (minutes).....	96
<b>Figure 3.6a.</b> Reaction scheme for aldose-1-epimerase assay coupled to the formation of D-glucono $\delta$ -lactone by glucose dehydrogenase at pH 7.6.....	100
<b>Figure 3.6b.</b> Changes in D-glucono $\delta$ -lactone formation (measure at 340 nm) from the glucose dehydrogenase catalysed conversion of $\beta$ -D-glucose to D-glucono $\delta$ -lactone over the range of $\beta$ -D-glucose concentrations indicated.....	101
<b>Figure 3.6c.</b> Changes in D-glucono $\delta$ -lactone formation (measured at 340 nm) from the glucose dehydrogenase catalysed conversion of $\beta$ -D-glucose to D-glucono $\delta$ -lactone over the range of $\alpha$ -D-glucose concentrations indicated.....	101
<b>Figure 3.7a.</b> Increase in formation of D-glucono $\delta$ -lactone (measured at 340 nm) in response to an increase in added porcine kidney mutarotase enzyme unit as shown.....	103
<b>Figure 3.7b.</b> The rate of formation of D-glucono $\delta$ -lactone (measured as change in absorbance at 340 nm with time) over a range of porcine kidney mutarotase enzyme units as shown.....	103
<b>Figure 3.8a.</b> Western analysis using the gp40 antiserum, of specific fractions	

from the chromatographic columns with positive identification of a 43 kDa protein. Antibody recognition was determined using an alkaline-phosphatase conjugated secondary antibody.....	105
<b>Figure 3.8b.</b> Protein staining after SDS-PAGE separation of the OZ43 positive fractions (as identified by Western analysis with the gp40 antiserum) from successive purification columns using FPLC.....	105
<b>Figure 3.8c.</b> The calibration curve of protein standards generated from elution volumes of each protein from the gel filtration column. Each labelled point represents a protein standard where a = 12.5 kDa, b = 29 kDa, c = 66 kDa, d = 150 kDa and e = 22 kDa. The elution volume of the gel filtration fraction containing OZ43 corresponded to a protein between 29 and 66 kDa.....	106
<b>Figure 3.9a.</b> Mutarotase activity rates in fractions from the chromatographic columns indicated that had been determined to contain the OZ43 protein recognised by the gp40 antiserum.....	108
<b>Figure 3.9b.</b> Expression of mutarotase specific activity rates determined by comparing the activity measurements of the partially purified (gp40 antibody-recognised) OZ43 protein (Figure 3.9a) to the activity of the porcine mutarotase (Figure 3.7b).....	108
<b>Figure 3.10a.</b> Diagrammatic representation of the fractionation of rachis cell extracts. The bold borders denote those samples that were analysed for gp40 antibody recognition and aldose-1- epimerase enzyme activity.....	111
<b>Figure 3.10b.</b> (a) Western analysis, using the gp40 antiserum, of the sub-cellular fractions of MR cell wall tissue as indicated in Figure 3.10a, after separation using SDS-PAGE. Antibody recognition was determined using an alkaline-phosphatase conjugated secondary antibody. (b) Protein staining after SDS-PAGE separation of the sub-cellular fractions of MR cell wall tissue subjected to Western analysis in (a).....	112
<b>Figure 3.10c.</b> Mutarotase activity in the sub-cellular fractions of MR cell wall tissue as indicated in Figure 3.10a and examined with SDS-PAGE Figure 3.10b(a) and Western analysis using the gp40 antiserum in Figure 3.10b(b).....	113
<b>Figure 3.11.</b> Mutarotase activity, measured using the coupled enzyme assay, in the HIC fractions from the lamb kidney membrane protein extract.....	115
<b>Figure 3.12a.</b> Western analysis, using the gp40 antiserum, of (a) mid-rachis (MR), (b) ethylene treated mid-rachis (MRE) and (c) ethylene and 1-MCP treated mid-rachis (MRE-MCP) cell wall extract fractions 11 to 17 (as indicated) from the HIC column after separation using SDS-PAGE. Antibody recognition was determined using an alkaline-phosphatase conjugated secondary antibody.....	118
<b>Figure 3.12b.</b> Mutarotase activity in fraction 14 of the HIC separation of MR, MRE and MRE-MCP tissues, as indicated.....	119

<b>Figure 3.13a.</b> Partial internal sequence of OZ10 aligned with the corresponding fragments of lipid transfer sequences from other plant species (from Kader 1997,1996 and Sterk <i>et al</i> 1991).....	122
<b>Figure 3.13b.</b> Western analysis, using the carrot lipid transfer protein antibody, of the cell wall protein extracts of MR, MRE, OZ and ZONE tissues of <i>S. nigra</i> collected in the summer and separated using SDS-PAGE. Antibody recognition was determined using an alkaline-phosphatase conjugated secondary antibody.....	123
<b>Figure 3.13c.</b> A representation of a leaf of <i>P. vulgaris</i> with the pulvinus, abscission zone and petiole indicated.....	124
<b>Figure 3.13d.</b> Western analysis, using the carrot lipid transfer protein antibody, of the cell wall protein extracts from the ethylene and non-ethylene treated bean petiole tissues. The tissues at 0 h are shown as pulvinus0, 1 <sup>o</sup> zone0 and pulvinus0 (as shown in Figure 3.12c), and these three tissues at 36 h of ethylene treatment are indicated as pulvinus36, 1 <sup>o</sup> zone36 and petiole36. Antibody recognition was determined using an alkaline-phosphatase conjugated secondary antibody.....	124
<b>Figure 3.13e.</b> Western analysis, using the <i>A. thaliana</i> lipid transfer protein antibody, of the cell wall protein extracts from the ethylene and non-ethylene treated bean petiole tissues. The tissues at 0 h are shown as pulvinus0, 1 <sup>o</sup> zone0 and pulvinus0 (as shown in Figure 3.12c), and these three tissues at 36 h of ethylene treatment are indicated as pulvinus36, 1 <sup>o</sup> zone36 and petiole36. Antibody recognition was determined using an alkaline-phosphatase conjugated secondary antibody.....	124
<b>Figure 3.13 f.</b> Western analysis, using the carrot lipid transfer antibody, of a cell wall extract from the MR tissue of <i>S. nigra</i> and the petiole tissue of <i>P. vulgaris</i> after separation using SDS-PAGE. Antibody recognition was determined using an alkaline-phosphatase conjugated secondary antibody.....	125
<b>Figure 3.14a.</b> Western analysis, using the BAC antibody, of cell wall extracts of MR, OZ, MRE and ZONE after separation using SDS-PAGE. Antibody recognition was determined using an alkaline-phosphatase conjugated secondary antibody.....	128
<b>Figure 3.14b.</b> Western analysis, using the BAC antibody, of ethylene and non-ethylene treated bean petiole tissues as indicated in Figure 3.13d. after separation using SDS-PAGE. Antibody recognition was determined using an alkaline-phosphatase conjugated secondary antibody.....	128
<b>Figure 4.1a.</b> A freshly excised explant.....	131
<b>Figure 4.1b.</b> Day 0 bean petiole (at abscission at the primary zone with the pulvinus attached).....	131
<b>Figure 4.1c.</b> Day 3 bean petiole (52 h).....	131
<b>Figure 4.1d.</b> Day 5 bean petiole (98 h).....	131

<b>Figure 4.2a.</b> A schematic representation of the reactions involved in the antibody immobilised ELISA using the polyclonal IAA antibody.....	134
<b>Figure 4.2b.</b> The optimised IAA standard curve for the polyclonal IAA antibodies generated. The polyclonal IAA-CH <sub>3</sub> antisera displaying the highest titres (from bleed three) were used to generate the curve. *%B refers to the percentage binding of the alkaline-phosphatase conjugate tracer to the immobilised IAA antibody.....	135
<b>Figure 4.2c.</b> The maximum difference in absorbance measured with antibody immobilised ELISA between IAA concentrations of 0 and 1000 pmole/0.1mL using the polyclonal antisera generated from the two rabbits, as indicated, against IAA-CH <sub>3</sub> .....	135
<b>Figure 4.3a.</b> The absorbance difference between 0% and 100% binding of the IAA-alkaline phosphatase conjugate to IAA antibodies, as indicated, using ELISA. The rabbit antisera used are those in Figure 4.2b for comparison with the monoclonal antibody.....	137
<b>Figure 4.3b.</b> The IAA standard curve using the polyclonal IAA IgG (from Figure 4.2a) compared to the optimised standard curve generated using the monoclonal antibody to IAA. *%B refers to the percentage binding of the alkaline-phosphatase conjugate to the immobilised IAA antibody.....	138
<b>Figure 4.4.</b> Cross-reactivity curves used to validate the measurements of IAA in bean extracts using ELISA.....	140
<b>Figure 4.5.</b> Concentration of IAA in pmol/g fresh weight in extracts of fresh tissues (as indicated) excised from 14-day-old bean plants. The numbers refer to values of IAA as pmol/g fresh weight for each tissue.....	142
<b>Figure 4.6.</b> Changes in endogenous free IAA concentrations in bean petioles from separation at the primary zone to separation at the secondary zone. Values listed in the table at displayed on the adjacent graphs.....	145
<b>Figure 4.7a.</b> Ethylene evolution from wounded fresh petiole and 98 h petiole explants.....	148
<b>Figure 4.7b.</b> Ethylene evolution from petiole segments (G1) and pooled sections (Y2, Y3 and Y4) of explants that are freshly excised (fresh), at abscission of the pulvinus at the primary zone (primary abscission) and at formation of the secondary zone (secondary abscission).....	148
<b>Figure 4.8a.</b> Ethylene evolved in the ACC oxidase activity assay from petiole segments (G1) and pooled sections (Y2, Y3 and Y4) of explants that are freshly excised (fresh), at abscission of the pulvinus at the primary zone (primary abscission) and at formation of the secondary zone (secondary abscission).....	151

- Figure 4.8b.** Western analysis, using the ACC oxidase antibody, from petiole segments (G1) and pooled sections (Y2, Y3 and Y4) of explants freshly excised (fresh), at abscission of the pulvinus at the primary zone (primary abscission) and at formation of the secondary zone (secondary abscission)..... 151
- Figure 4.8c.** A comparison of ethylene evolution and ACC oxidase activity from petiole segments (G1) and pooled sections (Y2, Y3 and Y4) of explants that are freshly excised (fresh), at abscission of the pulvinus at the primary zone (primary abscission) and at formation of the secondary zone (secondary abscission)..... 152
- Figure A.** Optimised standard curve generated using the monoclonal antibody. \*%B refers to the percentage binding of the alkaline-phosphatase conjugate to the IAA antibody..... 192

# List of Tables

<b>Table 2.1.</b> Names and addresses of the manufactures of reagents and specialised equipment.....	30
<b>Table 2.2.</b> Protein standards used for determination of the molecular weight of proteins eluting from the Separose 12 gel filtration column.....	42
<b>Table 2.3.</b> Formulations of buffers and acrylamide gels solutions for SDS-PAGE mini-gels.....	46
<b>Table 2.4.</b> Formulations for solutions used in polyacrylamide gel strip rehydration for isoelectric focusing.....	49
<b>Table 2.5.</b> Running program for isoelectric focusing of polyacrylamide gel strips.....	49
<b>Table 2.6.</b> Components for the second dimension polyacrylamide gels.....	52
<b>Table 3.1.</b> Summary of proteins designated as unique or preferentially-expressed in the cell walls of the tissues indicated, and collected in Spring ((a); from Figure 3.1a) Summer ((b); from Figure 3.1 b) and Autumn ((c); from Figure 3.1c).....	79
<b>Table 3.2.</b> Summary of proteins designated as unique or preferentially-expressed in the tissues indicated after fractionation by HIC and separation using SDS-PAGE (data from Figures 3.2 b, 3.2 c, 3.2 d, 3.2 c).....	85
<b>Table 5.1.</b> The reported IAA concentrations within the tissues of various angiosperms. The IAA units vary between studies so have been converted to pmol/gram FW so they can be compared to the IAA data collected in this thesis.....	177
<b>Table 5.2.</b> Nucleotide homology percentage values between the seven putative ACO clones isolated from fresh petiole tissue by RT-PCR.....	185
<b>Table 5.3.</b> ACC oxidase mRNA sequences in the NCB1 database from plant with the closest similarities to clones 1 to 6 and clone 7 from <i>Phaseolus vulgaris</i> isolated from fresh petiole tissue by RT-PCR.....	185

# Chapter One

## Introduction

### 1.1 Abscission zone cells: A model for studying plant cell differentiation

The positionally differentiated cells of the abscission zone provide a good model for studying the commitment and flexibility of cells within the mature plant body (Roberts *et al* 2000, Osborne and McManus 1986). Osborne and McManus (1986) proposed that in a study of plant cell flexibility and commitment, the cells utilized should have three main features. Firstly, the cells should be of a single cell type that has a specific and easily distinguishable physiological response to a specific signal. Secondly, the cells should possess markers, that is, components (usually proteins) that are specific to the cell and so allow biochemical identification. Finally, it should be possible to examine the physiological and biochemical competence of the cells, and for abscission zone cells, this can be achieved through induction and repression of abscission-associated events (Campillo and Bennett 1996, McManus *et al* 1985).

The research presented in this thesis sets out to examine aspects of the process of abscission zone cell differentiation using two experimental approaches with two distinct aims. The first, an *in vivo* approach, using *Sambucus nigra*, aimed to identify and partially characterise proteins present exclusively in the leaf rachis abscission zone that could be used as markers of abscission zone cell differentiation. The second, an *in vitro* approach using *Phaseolus vulgaris* petiole explants, aimed to examine the hormonal influences of differentiation of cortical cells to secondary abscission zones with the longer term view of using such information to determine the hormone regulation of abscission zone differentiation *in vivo*.

### 1.2 Overview of the abscission process

Abscission is the process of organ shedding, and is a common phenomenon in the life cycle of herbaceous plants. The process of abscission is a very ancient trait, and fossils from the late Silurian period (around 400 million years ago) show evidence of

abscission scars (Addicot 1982). Organs such as leaves, branches, flowers, seeds and fruit may be shed from the parent body at various stages of development and these abscission events are proposed to serve two different functions. Firstly, the shedding of reproductive structures can facilitate species propagation (for example, the dissemination of seeds), and secondly, abscission can remove an organ that is no longer of use to the plant. This later process is usually associated with organ senescence or fruit ripening, both of which can also perform a propagative function (Osborne 1989). The layers of cells that make up the abscission zone can vary in number. In the plants used in this study, the distal pulvinus-petiole abscission zone of *P. vulgaris* is comprised of perhaps three to five layers (Roberts *et al* 2000). In contrast, the leaf rachis abscission zones of *S. nigra* is comprised of between 15 to 30 cell layers that swell and fully separate during the abscission process (Osborne 1989). To date, there does not appear to be a study that has examined the size and the number of cell layers of the abscission zone and compared this to the size of the organ to be shed (Taylor and Whitelaw 2001).

### 1.2.1 Cell-cell separation during plant growth and development

When two plant cells divide, the resulting daughter cells are joined together by a double membrane across the cell filled with pectic material that forms the middle lamella. As the cells grow, cellulose is synthesized and passed out through the newly formed membrane to form a layer of cellulose either side of the membrane (Cosgrove 2000). For much of the plant body, the structural stability and restriction of movement provided by the cell-cell bonding of the middle lamella is maintained throughout the lifespan of the plant. However, for other cells of the plant body it is essential that these cells can separate, and this separation is achieved through environmental and developmental (usually hormonal) cues (Roberts *et al* 2000).

Separating cells involved in abscission and dehiscence (pod shatter) are proposed to be preprogrammed in a distinct way to the surrounding cells, and these cells are often also morphologically different to the adjacent cells (Osborne 1989). Cells of ripening fruit are required to separate but also undergo differentiation as the fruit develops. Cell separation of the outer cells of the root cap serves to assist with the course of the root through the soil because, as the cell layers are sloughed away, mucilage is released and also lessens the resistance of passage of the root (Hawes and Lin 1990). Another

example where cell separation is essential is the development of intracellular spaces in leaves. This cell-cell separation appears to occur in discontinuous locations at the junctions between neighbouring cells and enables gas diffusion to take place (Dale and Milthorpe 1981). However, not all cells of the plant respond and separate to cell-cell separation signals. The majority of epidermal cells do not appear to separate. For example, at the time of abscission, the epidermal cells of the zone do not separate but are typically fractured by the expanding differentiated cortical cells or break with the weight of the subtending organ (McManus *et al* 1998). The epidermal cells of the leaf however must separate to enable the formation of the pore complex flanked by guard cells during the formation of the stomatal complex (Sack 1987).

### 1.2.2 Differentiation and cell-cell separation of abscission zone cells

Cells of the abscission zone often appear as morphologically distinct, small and non-vacuolated. This is proposed to indicate that they have differentiated early in development but their growth is arrested while surrounding cells mature and enlarge. Thus abscission cells maintain a meristematic appearance (Osborne 1989, Addicott 1982, Sexton and Roberts 1982). Another morphological feature of abscission zones, notable in woody species, is their absence of secondary cell wall thickening. This area is not an area of weakness but the absence of this thickening is required to allow for the separation of the primary differentiated pre-determined abscission cells, which results in the shedding of the organ. It is possible that the absence of the secondary cell wall is an important feature in the differentiation of the cell separation zone (Roberts *et al* 2000, Osborne 1989).

Anatomical studies have shown that in some plants, and the leaflet abscission zones of *S. nigra* are an example, the position at which cell separation will take place can be located before abscission begins, usually at the base of the organ to be shed early in development (Gonzalez-Carranza *et al* 1998). The leaflet abscission zone of *S. nigra* differentiates shortly after bud opening, but before the period of rapid leaf expansion, as determined by the ability of ethylene to induce abscission at this time (Osborne and Sargent 1976). In the seeds of *P. vulgaris*, the first pair of leaves is already well differentiated in the embryo at the time of desiccation. However, abscission of the leaf blades cannot be induced until a certain stage of enlargement is reached indicating that differentiation of the abscission zone is a post-germinative event (Osborne 1989).

These observations suggest that the cells of the predetermined abscission zones differentiate early in the development of plant parts and the potential for abscission exists throughout the lifespan of the plant.

The order in which the cells that comprise the abscission zone differentiate from cortical parenchyma cells has been examined in the zone formation of tomato flower pedicels (Bodson and Verhoyen 2000). Abscission zone cell differentiation appears to start with cell division around the epidermal area then, as floral development proceeds, the cells of the abscission zone appear to divide towards the cortex, vascular region and finally to the central parenchyma region. The final differentiated zone is composed of six to eight cell layers with small flat cells across the pedicel.

As a morphologically and anatomically distinct group, the cells of the abscission zone are proposed to have undergone changes around the time of differentiation that give them a unique functional status such that they are able to respond in a different way to ethylene when compared with the surrounding cells (Osborne *et al* 1985). The response of abscission zone cells to ethylene and auxin has been used as a feature to distinguish them from other populations of cells. Abscission cells have been classified as a Type II target cell, where their enlargement is enhanced by ethylene and suppressed by IAA. The cells that make up the majority of the growing body of the plant are largely classified as Type I target cells where IAA promotes their elongation and the growth in this dimension is inhibited by ethylene. However, ethylene does promote lateral expansion (Osborne *et al* 1985). Type III target cells respond to both auxin and ethylene and the cortical cells that mediate leaf epinasty through differential expansion are an example (Osborne 1979).

Thus the abscission process comprises three major facets. The differentiation of the morphologically and anatomically distinct zone cells, the competence to respond in a unique way to ethylene and auxin, and the biochemical dissolution of the wall components to mediate cell-to-cell separation. Each of these aspects is introduced in more detail in the following sections. However, as a starting point, an overview of the structure of the plant cell wall is presented.

### 1.3 The plant cell wall

The plant cell wall is a complex molecular entity made up of polysaccharides, lignin, suberin, waxes, proteins, enzymes, calcium, boron, phenolics, water and possibly lipids. Cell walls are complex structures that confer the shape of cells and ultimately the whole plant. The plant cell is polyhedral in appearance and so is composed of edges, facets and vertices. Each of these three types of walls in any one cell may be structurally and compositionally distinct from the others and hence, may be able to change to new states independent of other elements of the cell (Cassab 1998, Varner and Lin 1989).

The primary cell wall of dicotyledonous plants is composed of cellulose microfibrils that are interconnected by hemicellulose, mainly xyloglucan. This network is the tension-bearing structure of the primary cell wall and is embedded in a matrix of pectins. There are four major types of polysaccharides in the primary cell wall; cellulose and callose, which are synthesized at the plasma membrane, and hemicellulose and pectin, which are synthesized in the Golgi apparatus (Minorsky 2002). Cellulose is the predominant polysaccharide in plant cell walls and consists of  $\beta$ -1, 4-glucan polymers (Smallwood *et al* 1996). Callose consists of  $\beta$ -1, 3-glucan polymers and is synthesized at specific stages of cell wall development in specific cell types (for example, pollen tubes). It is often found where the cell wall has been altered during developmentally-induced changes in the cell shape, and is also used for the repair of the cell wall during the course of pathogenesis (Smallwood *et al* 1996). Cellulose synthase and callose synthase were originally thought to be the same enzyme as partially purified callose synthase can produce  $\beta$ -1, 4-glucan polymers *in vitro*. However, when callose synthase was enriched, the cellulose synthase activity was depleted indicating there are two distinct enzymes for the synthesis of these two polymers (Robertson *et al* 1995). More recently, a putative callose synthase gene has been identified in *Arabidopsis* (*AtGs15*), homologous to yeast  $\beta$ -1, 3-glucan synthase and whose expression partially complements a yeast  $\beta$ -1, 3-glucan synthase mutant (Ostergaard *et al* 2002).

The primary cell wall is laid down while the cell is increasing in volume, and layers produced after the cell has stopped growing comprise the secondary cell wall (Thomas 1988). The cell wall is key to the plant cell being able to achieve a large size and control cell expansion, maintain its shape and confer structural strength. However, the

presence of a rigid or semi rigid wall composed of cross-linked macromolecules stops the movement of proteins and nucleic acids into and out of the cell irrespective of the permeable plasma membrane. The wall also possesses a net negative charge, which means the movement of positively charge molecules through it may be retarded (Brett and Hillman 1985).

In addition to their roles in architecture and protection, plant cell walls also have an active role as ion exchangers, bacterial agglutinins and as sources of cell-to-cell signals (Varner and Lin 1989). Using monoclonal antibodies raised to selected carbohydrate structures of plant cell wall polysaccharides in *Arabidopsis*, differences in the pectic and hemicellulosic polysaccharide structures between the walls of different cell types and even within the same cell type have been discovered in mutant and wild-type *A. thaliana* (Minorsky 2002). These observations illustrate that the insertion of these specific polysaccharide structures in the wall appears to be under tight developmental control, suggesting that the purpose of their placement is to function as part of a highly regulated process.

### 1.3.1 The structural proteins of plant cell walls

A variety of different proteins, glycoproteins and proteoglycans have been identified in the cell walls of land plants and green algae. Up to ten percent of the cell wall of higher plants is composed of proteins, which can be conveniently divided into two main groups. Most of those identified to date have no known enzymatic activity, and become rapidly immobilized in the cell matrix via covalent cross-links (Fry 1995). Accordingly, these proteins are considered to have a structural function although how these proteins contribute to the cell wall architecture is poorly understood (Jose-Estanyol and Puigdomenech 2000).

The most abundant and studied of these proposed structural cell wall proteins are rich in one or two amino acids, contain highly repetitive sequence domains and are highly or poorly glycosylated. These plant cell wall proteins can be divided into four classes, which are the hydroxyproline rich (HPR) proteins or extensins, the arabinogalactan proteins (AGPs), the glycine-rich (GR) proteins, the proline-rich (PR) proteins (Showalter 1993). Within the four main groups are the chimeric proteins that contain extensin-like domains (Cassab 1998). Recent characterisation of newly identified cell

wall proteins show that some of these classifications might be more relevant to sequence domains within the proteins than to the proteins themselves because there are proteins that have a mixture of these domains (Darly *et al* 2001). The variable quantities of HRP, AP, GR and PR proteins in different cells indicate that these proteins influence functions that are specific to cell-type. However, there is little direct evidence as to what these functions might be.

The other main group of cell wall proteins are those that are cell wall-associated, that is, they are not covalently bound to components of the cell wall and can usually be extracted with high salt (1.0 M NaCl). These proteins will be referred to in this thesis as ionically-associated cell wall proteins. Many of these are enzymes and have roles related to assembly, rearrangement or breakdown of the cell wall components. The enzymes in the wall discovered to date catalyse four broad classes of reactions, hydrolysis, transglycosylation, transacylation and the redox reactions (Fry 1995). The majority of the enzymes that have been discovered to be associated with the cell wall are hydrolases (EC 3.\_\_\_\_) and include; galactosidases, glycosidases, glucosidases, polygalacturonases (PGs), pectinesterases, arabinosidases, xyloglucan hydrolases and glycanases (eg. galactanase and xylanase). Other enzymes that have a direct effect on the modification of the cell wall include peroxidases (enzymes that use H<sub>2</sub>O<sub>2</sub> in a range of oxidation reactions), invertase (which catalyses sucrose cleavage), and xyloglucan endo-transglycosylases, a class of enzymes that cleave and rejoin xyloglucan chains (Minorsky 2002, Cassab 1998, Fry 1995). To date, there have been no isomerases (EC 5.\_\_\_\_) identified in the cell wall although there is no obvious reason why they should not be there (Fry 1995). One role for all of these enzymes, because they are involved in maintenance of the cell wall, is in the defence response (Bowles 1990, see section 1.3.2).

As well as a role in the modification of the cell wall structure, there are proteins that are intrinsic components of the cell wall that appear to be involved in mediation of events occurring between the cell and the environment. For example, the acid phosphatases, which regulate the phosphorous level within the plant (Duff *et al* 1994), are markers for autolytic activity (Hall and Sexton 1974), and have been used as tools for the study of protein trafficking mechanisms to the cell surface (Kaneko *et al* 1998). Assuming that the structural components of the cell wall are essentially immobile, the enzymes that are

involved in rearrangements must have some mobility so they are able to find their site of action. The charge and density of pectin in the matrix of the cell wall appears to be an important factor in the regulation of acid phosphatase and pectin methylesterase activity (Micheli 2001). Therefore, it is possible that other enzymes are also regulated by the status of pectin and other cell wall components (Varner and Lin 1989).

### 1.3.2 Defense-related proteins in plant cell walls

The rigid wall provides protection for the plant, providing a barrier against the vast majority of potentially pathogenic organisms. However, the protective function is not just a passive one. A pathogenic organism or some form of stress will induce a defence response leading to the expression of a host of cell wall modifying and pathogen-related (PR) proteins (Hahlbrock and Scheel 1989). Many PR proteins form a heterogeneous group of host-encoded low-molecular-mass proteins that are secreted through the exocytic pathway (Eyal *et al* 1993). They are synthesised by the plant in response to various stimuli, including pathogen attack, exposure to certain chemicals and during the abscission process.

A defense-related protein can be defined as any protein that has a role in the response to stress or pathogen attack. In a review by Bowles (1990), defense-related proteins are divided into three groups. The first are the structural proteins (for example HRGPs) and the enzymes involved in the construction and repair of cell wall components such as callose. The second group are the proteins that act directly on the source of the elicitor, for example, antimicrobial agents such as hydrolases and proteinases. The third group is defined as those proteins, referred to as pathogen related (PR)-proteins, that are induced in response to pathogen invasion yet their function is often not known. For example, the wound-induced cell wall protein (WI12) in the halophyte ice plant with 68% similarity to WUN1, a wound-induced protein in potato (Yen *et al* 2001). Both proteins have unknown functions although they are postulated to act by reinforcing the cell wall after wounding.

A well characterised group of defense-related proteins in the cell wall are the polygalacturonase inhibitor proteins (PGIPs), which have been identified as cell wall-associated in bean (Esquerre-Tugaye *et al* 2000), the roots of white clover (Hay *et al* 1998), in apple fruit (Yao *et al* 1995), and in soybean hypocotyls (Favaron *et al* 1994).

These proteins are leucine-rich thermostable glycoproteins of about 40 kDa and appear to regulate the pectin-endopolygalacturonase signalling system involved in pathogenesis (Shastri *et al* 2002). The endo-polygalacturonase synthesized by the pathogens produces biologically active oligosaccharides from the hydrolysis of the pectin in the middle lamella of the host plant, and these oligosaccharides then stimulate the plant defence response. The PGIP protein acts as another form of defence by inhibiting the pathogen endo-polygalacturonase and thereby preventing hydrolysis of the plants pectic middle lamella. As well as stimulating the formation of PGIP by the host plant and then further defence responses with the release of oligosaccharides, the signals of this system have also been shown to involve the pectic fragments of plant origin (released by pathogen endo-PG), that activate PGIP gene expression in the plant, and endo-PG in the pathogen (Esquerre-Tugaye *et al* 2000).

## 1.4 Cell wall enzymes associated with cell–cell separation of abscission zone cells

### 1.4.1 Hydrolases

#### 1.4.1.1 Endo- $\beta$ -1, 4-glucanhydrolase

Endo- $\beta$ -1, 4-glucanhydrolases (cellulase, EC 3.2.1.4) are enzymes produced in bacteria, fungi and plants that hydrolyse polysaccharides possessing a  $\beta$ -1, 4-glucan backbone, and have been proposed to act primarily on xyloglucan and non-crystalline cellulose in the plant cell wall (Nicol *et al* 1998). Cellulase is encoded by a multigene family in several higher plant species, including poplar (Nakamura *et al* 1995) and avocado (Tonutti *et al* 1995). In *P. vulgaris*, cellulase is encoded by a single gene or several closely related genes (Tucker and Milligan 1991). The mature cellulase proteins characterised to date are generally between 51 and 68kDa (Llop-Tous *et al* 1999, Trainotti *et al* 1999, Bonghi *et al* 1998, Harpster *et al* 1998, Loopstra *et al* 1998, , Lashbrook *et al* 1994).

Ethylene-stimulated bean leaf abscission has been correlated with the induction of a specific isoform of  $\beta$ -1, 4-glucanhydrolase with an isoelectric point of 9.5 (designated as cellulase 9.5) within the cells of the separation layer and adjacent vascular tissue (Durbin *et al* 1981). On exposure of bean explants to ethylene, a 40-fold increase in

cellulase activity has been correlated with a decrease in break-strength at the separation layer (Tucker *et al* 1991). Sexton and collaborators (1980) found if polyclonal antibodies raised to bean abscission cellulase (BAC) were injected into the zones, abscission was delayed. The later study by Thompson and Osborne (Thompson and Osborne 1984), which investigated intertissue signalling, suggested the antibodies injected would not be mobile enough to inactivate the enzyme, but instead that the antibodies may have prevented the release of any biologically active fragments that resulted in the inactivation of the enzyme. A series of studies involving radioimmunoassays (Durbin *et al* 1981), *in situ* and tissue print hybridisation (Tucker *et al* 1991), immunocytochemical localisation (Sexton *et al* 1981), and immunodetection of cellulase on nitrocellulose tissue imprints (del Campillo *et al* 1990), all indicate that the cellulase 9.5 protein is localized in the cortical cells of the separation layer and the vascular bundles of the tissues adjacent to the separation layer. Further, this accumulation occurs at 12 to 18 hours after the start of ethylene treatment. However, the accumulation of BAC mRNA, shown using *in situ* hybridisation with BAC RNA probes, also occurs in vascular cells covering two to four millimetres distal to the separation layer. Tissue-print hybridisation techniques have shown that ethylene-induced cellulase mRNA has the same distribution: two to three cell layers either side of the fracture plane, and extending further from the fracture plane into the vascular tissue consistent with immunolocalisation of cellulase in the same tissue (Tucker *et al* 1991, Tucker 1988). Radioimmunoassays provided no evidence of pre-existing inactive cellulase 9.5 protein (Durbin *et al* 1981), consistent with evidence suggesting ethylene exposure results in the increase synthesis of RNA, with the cellulase protein synthesised *de novo* (Lewis and Varner 1970).

A study by Thompson and Osborne (1994), using the *P. vulgaris* pulvinus-petiole explants, suggests that the activity in the stele of the bean may play an essential role in the coordination of the abscission process. Tucker and collaborators (1981) determined that the abscission-specific bean cellulase 9.5 is induced in both the cortex and the stele of the explant abscission zones during ethylene induced cell-cell separation. Thompson and Osborne (1994) proposed the cells of the cortex around the abscission zone require a signal from the vascular bundles of the stele before they can totally respond to the abscission promoting effects of hormonal treatments such as ethylene. This conclusion was made with results from experiments where the bean explants were treated with

ethylene for periods of time before the stele adjacent to the abscission zone was removed. There appears to be a signal that passes from the abscission zone vascular system (the stele) to the cortex in the first 24 hours of a 5 ppm ethylene treatment of the explants. This unknown signal is required for the synthesis of cellulase 9.5 and for cell-cell separation to occur, and is thought to be a stele-specific polysaccharide breakdown product that either interacts with cell-wall hydrolytic enzymes directly or induces new gene expression (Thompson and Osborne 1994).

#### 1.4.1.2 Polygalacturonase

Anatomical studies of both abscission and dehiscent zones have revealed the primary site of wall breakdown to be at the middle lamella (Peterson *et al* 1996). Since the primary component of the middle lamella is pectin (forming about 35 percent of the dry weight of the cell wall in dicotyledonous plants) a significant direction of research in abscission is the isolation and characterization of pectinases (Micheli 2001). Polygalacturonase (PG; EC 3.2.1.15) is a polyuronide/polygalacturonide/pectin depolymerising and solubilising enzyme (Taylor *et al* 1993). It has been identified as being induced in the middle lamella of tomato fruit cells during ripening (DellaPenna *et al* 1990), during ethylene-stimulated abscission in a similar pattern as cellulase induction (Doorn and Stead 1997, Kalaitzis *et al* 1995, Roberts *et al* 1992) and during a number of other developmental processes thought to involve cell wall breakdown (Hong *et al* 2000).

Kalaitzis and collaborators (1997) examined the expression of three different polygalacturonase enzymes in tomato. A cDNA clone for one of these PGs (pTAPG1) was found to be present in the abscission zones of the tomato leaf and flower and contained 43% identity at the amino acid level with the tomato fruit PG (Kalaitzis *et al* 1997). Hong and collaborators (2000) examined the spatial and temporal expression of *TAPG1* and another abscission zone and pistil-associated polygalacturonase, *TAPG4*, in tomato abscission zones using TAG1 and TAG4 promoter-GUS fusions. The induction of polygalacturonase with ethylene resulted in GUS staining localised more predominantly in the vascular bundles relative to the surrounding cortical cells in the *TAPG4*:GUS transformants. This induction occurred a lot earlier than in the

TAPG1:GUS transformants, where the staining was more evenly distributed across the separation layer.

Analysis of polygalacturonase in the leaflet abscission zones of *S. nigra* has revealed that there are at least two isoforms, which appear to be endo-acting, that are involved in the ethylene-stimulated cell wall separation (Taylor *et al* 1993). In a study by Roberts and collaborators of cellulase and polygalacturonase during leaf abscission of *S. nigra*, the mRNAs encoding these enzymes were degraded when examined by Northern analysis (Roberts *et al* 1992). However, the mRNA of other pathogen-related proteins remained intact. There have been two proposed reasons for this observation. Firstly, it may be the mRNA of the hydrolyzing enzymes is targeted for breakdown. Secondly, it is possible there are two types of cells that make up the abscission zone. The first secretes the wall degrading enzymes and the mRNA in these cells is turned over rapidly. The second cell-type produces proteins that protect the cells immediately exposed to the fracture surface from pathogen attack, and so longer-lived mRNA and protein may occur in these cells.

#### 1.4.2 Pectin methylesterase

Pectin methylesterase (EC 3.1.1.11) is a pectinase that catalyses the demethylesterification of cell wall polygalacturonans in dicotyledonous plants releasing acidic pectin and methanol (Micheli 2001). These enzymes are involved in developmental processes such as cellular adhesion and fruit maturation and have also been reported to increase during the ethylene-stimulated abscission process (Burns and Lewandowski 2000), although a role in abscission for this pectin-degrading enzyme is unclear (Micheli 2001).

#### 1.4.3 Peroxidase

Peroxidases (EC 1.11.1.7) have been postulated to play a role in the mediation of cell-cell separation (McManus 1994, Vizzotto *et al* 1986, Hall and Sexton 1974) and have been shown to be induced during the abscission process of a variety of organs in a range of species, including peach fruit and leaves (Vizzotto *et al* 1986), cotton pedicels (Liu *et al* 1984) and *P. vulgaris* leaves (Kenis and Trippi 1982, Poovaiah and Rasmussen 1973). In the petiole-pulvinus abscission zone of the bean, there is an

increase in the peroxidase activity during ethylene-stimulated abscission, but no apparent increase of an abscission-specific isoenzyme of peroxidase in the abscission zone (McManus 1994).

#### 1.4.4 Pathogen-related proteins induced during abscission zone cell-cell separation

A host of pathogen-related (PR) proteins are induced during the abscission process and many of these have been identified in the separation layer of bean (Campillo and Lewis 1992). It has been suggested that the synchronised accumulation of these PR proteins, early in abscission, could be important as part of the induced resistance to possible fungal attack after the plant part is shed (Campillo and Lewis 1992). Coupe and co-workers (1997) found that the majority of proteins induced in ethylene-treated leaf abscission zones of *S. nigra* encode PR proteins including polyphenol oxidase, a proteinase inhibitor, a metallothionine-type protein and a chitinase. Various forms of the chitin-hydrolysing enzyme chitinase have been noted to appear early at the onset of abscission, consistent with the induction of other PR proteins (Mauch *et al* 1988). Chitinase has no known substrate in plants, but chitin is a major component of fungal cell walls. One form of chitinase accumulates concomitantly with the increase in cellulase 9.5, and could therefore play a more direct role in the abscission process (Campillo and Lewis 1992). Other PR proteins induced in the early stages of bean leaf abscission include the  $\beta$ -1, 3-glucanhydrolases (the substrate of which is callose, present in only small amounts in plant cell walls), and which act synergistically with chitinase in inhibiting fungal growth (Mauch *et al* 1988), and a thaumatin-like protein, often induced in leaves upon infection with necrotising pathogens.

## 1.5 The study of abscission cell differentiation

### 1.5.1 Mutant studies and the control of differentiation

An approach used to investigate the differentiation of abscission zone cells is to create mutants showing impaired abscission zone cell differentiation. To date, there are few examples of phenotypes where the normal developmental events leading to abscission zone differentiation have been impaired (Gonzalez-Carranza *et al* 1998). *Arabidopsis thaliana*, a commonly used model plant, does not possess leaf abscission zones but instead leaves undergo a process of desiccation followed by attrition of the dehydrated

tissues. However, *A. thaliana* does have abscission zones at the base of petals and at the funiculus junction of seeds, but the amount of material that can be extracted from these sites for molecular and biochemical analysis is minute (Roberts *et al* 2000).

A mutant that has been identified and studied is that of the tomato mutant *jointless*, which does not form a normal flower and fruit pedicel abscission zone and carries a recessive mutation at two loci on chromosome 11 designated *j-1* and *j-2* (Wing *et al* 1994). A study by Szymkowiak and Irish (1999) investigated the characteristics of different periclinal and mericlinal chimeras of wild-type and *jointless* tomato plants. In common with other higher plants, there are three layers of meristematic cells in the shoot apical meristem of tomato and it has been established that epidermal tissue is derived from the L1 cells, subepidermal tissue from the L2 cells and the remaining tissues from the L3 cells (Satina *et al* 1940). The findings of the Szymkowiak and Irish study show that it is the outer most cells of the L3 layer that play the most important role in the induction of abscission zone differentiation. When the periclinal chimera consisted of *jointless* L1 and L2 layers and wild-type L3 layer, the L3 layer appeared to coordinate the L1 and L2 cells as if they were wild-type, resulting in a phenotypically wild-type abscission zone. A mericlinal chimera, where half the L3 cells were of the *jointless* genotype and the other half wild-type, resulted in an abscission zone forming across the wild-type half of the pedicel only. This result would indicate there is no lateral communication between the cell layers. These results revealed what cells are affected by the abscission signal but does not indicate the timing of the developmental signals that prompt them to differentiate. It is also unclear what mechanisms are operating in the *jointless* mutant to give the observed affects. Recently, the *JOINTLESS* gene has been identified as a MADS-box gene and is the first gene isolated that is directly involved in the development of a functional abscission zone (Mao *et al* 2000). The MADS-box genes form a large family and many have been found to be important in the development of plant organs such as floral structures (Jang *et al* 1997). Phylogenetic alignment of the deduced amino acid sequence of *JOINTLESS* with sequences in GenBank revealed it has profound homology with other MADS-box genes. Of the 20 MADS-box sequences that were most similar to *JOINTLESS*, none were from those previously found in tomato, indicating this is a new kind of MADS-box gene expressed in tomato. In the phylogenetic analysis by Mao and collaborators,

*JOINTLESS* clusters with genes that are not associated with any known phenotype although several are known to be expressed in vegetative tissues (Mao *et al* 2000).

In other studies, the hormone gibberellic acid has been linked with the differentiation of these cells in tomato. A lateral repressor (Ls) gene has been cloned from tomato with abnormal pedicel formation, and shown to encode a new member of the VHIID family, a putative transcriptional regulatory protein (Schumacher *et al* 1999). Although the role of this protein is unclear it appears to have similarity to transcriptional regulators involved in gibberellic acid and signal transduction (Peng *et al* 1999). This is a conclusion that is drawn from the research of Peng and collaborators (1999) who discovered that the *GAI* gene of gibberellin insensitive mutants (from *Arabidopsis*) encodes proteins that resemble nuclear transcription factors and contain an SH2-like domain indicating that phosphotyrosine may participate in gibberellin signalling. Since gibberellins are proposed to regulate stem elongation, it may be that they serve to arrest specific cells in development during abscission cell differentiation.

### 1.5.2 Introduction of the *in vivo* approach to study abscission and abscission cell differentiation

The use of *S. nigra* as a model plant is designed to identify and partially characterise proteins present exclusively in the leaf rachis abscission zone that could be used as markers of abscission zone cell differentiation *in vivo*. The abscission zone cells examined thus far are those from the zones that transverse the leaf rachis and the leaflet base of compound leaf. The large size of the leaf abscission zone (between 15 and 30 cell layers) enables the collection of highly enriched abscission zone cell samples which makes *S. nigra* a good model plant for the examination of abscission cell proteins. Proteins that are either unique or preferentially expressed in this cell type have been previously identified in these cells (McManus and Osborne 1990, 1990a). Theoretically, the appearance of these proteins can be used to monitor the temporal and spatial differentiation of the leaflet abscission zone cells.

### 1.5.3 Examination of cell wall proteins in *S. nigra*

Proteins occupy every part of the plant cell. In addition to the cell wall proteins, there are those that are attached to, or are integral to, the plasma membrane, cytoplasmic or soluble proteins, and proteins associated and/or within the organelles and their

membranes (Cassab 1998). A convenient way to handle the analysis of the total cell protein is to separate it into two fractions, the soluble protein fraction and the ionically-bound putatively cell wall fraction. The soluble proteins are those that are extracted from the cell with a low ionic strength buffer and include organelles and the plasma membrane washed from the shattered cells. The cell wall proteins utilised in this thesis are those removed from the cell wall tissue (after the soluble proteins are extracted) with high salt (1.0 M NaCl). These are referred to throughout this thesis as the ionically-associated cell wall proteins and are primarily those that are peripheral to the cell wall.

#### 1.5.4 Identifying antigenic protein determinants in the cell wall

The commitment of cells to a particular differentiation pathway can normally be identified by the physiological response that is evoked by special environmental or chemical signals or alternatively, by antigenic components unique to the cell type. Since cells of the abscission zone are structurally and functionally distinct from their non-target neighbours, Osborne and McManus (1986) predicted that they should also express a specific protein complement. McManus and Osborne (1990) published the first study to identify specific or preferentially-expressed peptides in functionally differentiated abscission cells. The approach used in this research utilised antibodies raised to different tissue extracts. McManus and Osborne found three polypeptides (34, 32 and 28 kDa) in the total protein extract of *S. nigra* cells that appear to be abscission-cell specific up to the limits of detection (McManus and Osborne 1990a). Tissue-specific protein differences were initially identified between the leaf tissue, OZ (fresh abscission zone), MR (mid-rachis) and ZONE (separated abscission zone cells after ethylene treatment) tissues by challenging each of these extracts with antibodies raised against OZ extracts using Ouchterlony immuno-diffusion. This is a simple technique that compares the differences between the spectrum of antigenic determinants in each tissue. Identification of specific antigenic determinants in the OZ tissue was achieved using a combination of immuno-competition and immuno-affinity chromatography removing proteins that were common to both the MR and OZ tissues. A polypeptide of 34 kDa eluted from the OZ antibody-immobilised immuno-affinity column that appeared, on SDS-PAGE gels, to be preferentially expressed in the OZ tissue. Western analysis, using antibodies raised to this peptide, detected a protein that was expressed in both the OZ and ZONE tissue and was absent from the MR tissue

(McManus and Osborne 1990a). The presence of this protein in the ZONE tissue indicates that it is cell-specific, as the collection of the ethylene-treated abscission cells comprises a homogeneous population. Moreover, this protein did not appear in the leaf, root or stem tissue indicating its tissue-specific location.

In the search for *S. nigra* abscission cell-specific proteins, an antibody was raised to the pooled soluble and cell wall extracts for both the mid-rachis (non-abscission) tissue and the ethylene-treated abscission zone tissue. The polyclonal antibodies generated to the MR and ZONE extracts were coupled to Sepharose, and were then used as separate immuno-affinity columns. The anti-MR protein column was used to remove peptides and proteins in the MR extract that were also in the ZONE, and the non-binding eluates resolved using SDS-PAGE. This approach identified a protein of ca. 34 kDa that appeared to present exclusively in the abscission zone cells. This pre-absorbed fraction was bound to the anti-ZONE column and then eluted with a combination of high and low pH and resolved using SDS-PAGE. This approach revealed two major proteins of ca. 32 and ca. 34 kDa. An antibody was raised to the ca. 34 kDa protein by direct immunisation of the peptide after excision from the polyacrylamide gel. Using Western blotting, this antibody recognized a ca. 34 kDa protein in the zone cells before and after ethylene treatment that was absent from the mid-rachis extracts (McManus and Osborne 1990a). A protein of ca. 34 kDa was identified again in the leaf rachis abscission zone of *S. nigra*, but this time it appeared to be associated with the cell wall, and almost completely abscission-specific. The protein was identified with Western analysis using a monoclonal antibody raised against extracts from separated abscission zone cells of *S. nigra*, that recognises a specific N-linked oligosaccharide structure (McManus *et al* 1988). Proteins that are recognized by this antibody are glycoproteins and have a xylose/fucose mixed-type N-linked oligosaccharide structure (McManus and Osborne 1991).

In the distal pulvinus:petiole abscission zone of *P. vulgaris*, immune-competition approaches in which abscission zone extracts were passed through an affinity column of antibodies raised to petiole and pulvinus IgG, identified a protein of 68 kDa that was preferentially expressed in the ZONE. McManus and Osborne also identified an antigenic determinant that is specific to the cell wall of bean abscission zone cells (McManus *et al* 1990). This cell-specific protein was found by raising polyclonal

antibodies to bean abscission zone cell wall-specific peptides between 30 and 45 kDa after immune-competition using antibodies to the petiole (non abscission zone) tissue, and using them for immunolocalisation of the antigenic determinants. Electron micrograph of the gold-labelled anti-rat IgG tissue sections showed a different pattern of staining in the zone cell walls of *P. vulgaris* underlining that the abscission target tissue might be comprised of cells with an altered cell wall (McManus *et al* 1989). In *P. vulgaris*, two proteins of 45 kDa and 36 kDa were identified in the putative cell wall fraction (McManus and Osborne 1990).

## 1.6 Control of abscission cell differentiation: Introduction of the *in vitro* approach to study abscission cell differentiation

The second of the two approaches used in this thesis involves examining aspects of the formation of secondary abscission zones in bean (*P. vulgaris*) petiole explants *in vitro*. The formation of secondary abscission zones in explants is based on the observation that plant cells will generally exhibit a higher degree of flexibility in their development and differentiation in culture, where the cells are not restricted by the signals of the intact plant and the environment (Osborne and McManus 1986).

### 1.6.1 Overview of secondary abscission zones and their formation

Secondary or adventitious abscission is the formation of an abscission zone in a position along a stem, branch, pedicel, petiole or phyllomorph tissue, which unlike the naturally-occurring abscission zones, is not predetermined early in development. These abscission zones have been observed primarily in *in vitro* systems involving pear and pear pedicels (Pierik 1980 and 1977) stems of *Impatiens* (Warren Wilson 1988a, 1988 and 1987), mulberry stems (Suzuki 1991), orange stems (Plummer *et al* 1991) and bean petiole explants (McManus *et al* 1998). However, the formation of secondary abscission zones on stems, branches and petioles can also occur *in vivo* in response to tissue injury or infection (Addicot 1982). Where these late forming zones appear *in vitro*, their position appears to be determined by a proposed hormone concentration gradient, with IAA thus far appearing as the most significant compound in determining the site at which these zones will form (McManus *et al* 1998, Warren Wilson *et al* 1988a, Warren Wilson *et al* 1988, Pierik 1980). Other hormones that have been

observed to promote this process are cytokinins in pear pedicels (Pierik 1980 and 1973), abscisic acid in orange stems (Plummer *et al* 1991) and gibberellic acid in cotton stems (Bornmann *et al* 1968). The formation of secondary abscission zones may not occur in all tissues. Pierik (1980) showed that secondary abscission could be induced in pear pedicels but not in apple (Pierik 1977) It is possible that secondary zones can be induced in the pedicel tissue of apple but not under the same experimental conditions used to differentiate this cell type in pear.

The explants of *P. vulgaris* used in this thesis for the study of secondary abscission zone formation *in vitro* were first described by Osborne (1968). Each bean explant contains the distal pulvinus (with the leaf blade excised) and a segment of petiole immediately proximal to the abscission zone. The plant hormone ethylene is used to induce separation of the pulvinus, after which IAA is added to the now exposed primary abscission zone. The added IAA and exogenously supplied ethylene are both required for the differentiation of these zones, although their role in the process is unclear. However, this dual control by auxin and ethylene represents one of the central themes in the regulation of the abscission process.

### 1.6.2 The hormonal control of the abscission process

La Rue (1936) was one of the first to show how IAA has an inhibitory effect on the abscission process, assisting in maintaining the cells of the abscission zone in an arrested state. Since then, the hormonal data gathered supports the following scheme for the control of abscission, and is described by Reid (1985). There is a gradient of auxin from the subtended organ to the plant axis and this maintains the abscission zone in an insensitive state. As long as the attached organ is in a non-senescent condition then abscission will not occur. The auxin gradient is maintained by factors that inhibit senescence of the organ such as auxin, cytokinins, light and a supply of adequate nutrients. Reduction or reversal of the supply of auxin to the plant axis causes the abscission zone to become sensitive to ethylene. Therefore, removing the leaf blade, application of auxin proximal to the abscission zone, shading, poor supply of nutrients or the application of ethylene hastens abscission. Early evidence supporting auxin as the hormone that suppresses abscission activity came with the observation that when a subtending leaf blade was removed, separation would not occur if auxin were applied to the resulting stump (reviewed in Osborne 1989).

Stresses enhancing ethylene production or exogenously applied ethylene may also hasten abscission by reducing auxin synthesis and/or interfering with auxin transport from the leaf (Epstein and Sagee 1992). An extra tier of regulation of the abscission process by ethylene and auxin comes with the observation that IAA induces the production of ethylene. Thus the highly regulated balance between these two hormones appears to be a significant determining factor in the timing of organ shedding.

Other plant growth regulators have also been shown to influence the regulation of the abscission process in these specialised cells. For example, in bean petiole explants, jasmonic acid and its methyl ester have been shown to accelerate abscission (Ueda *et al* 1996) and to a much lesser degree cytokinins and gibberellins have been shown to inhibit the abscission process (Stuttle and Gage 1990). Abscisic acid generally stimulates abscission indirectly by either stimulating the production of ethylene or interfering with the production, transport, or action of auxin (Osborne 1989).

#### 1.6.2.1 Ethylene

The gaseous plant hormone ethylene is widely recognized as a signal that promotes abscission in the majority of abscission systems studied, although there are exceptions (Sexton *et al* 2000). The pathway for ethylene biosynthesis was first elucidated by Yang and collaborators in the early 1970s (Yang and Hoffman 1984) and has provided the basis for all subsequent molecular genetic and biochemical analysis since. The conversion of *S*-adenosylmethionine (AdoMet) by the enzyme 1-aminocyclopropane-1-carboxylate (ACC) synthase (EC 4.4.1.14) to ACC is generally accepted as primarily the rate determining enzymatic step to the formation of ethylene. ACC is then converted to either ethylene, CO<sub>2</sub> and HCN by ACC oxidase [(EC 1.4.3); originally called the ethylene forming enzyme] or conjugated to either N-malonyl-ACC (MACC) by malonyl-ACC transferase (Hoffman *et al* 1982) or 1- $\gamma$ -L-glutamyl-ACC by glutamyl-ACC transferase (Fluhr and Mattoo 1996).

However, of particular relevance to the research in this thesis, is the production of endogenous ethylene during the transdifferentiation of secondary abscission zone cells from cortical cells in bean petiole explants and the regulation of ACC oxidase. Thus in place of reviewing the large amount of literature on ethylene biosynthesis, and the

effects of the hormone on plant tissues, it is most relevant to introduce the enzyme ACC oxidase.

#### 1.6.2.2 ACC oxidase

The first ACC oxidase gene was isolated in tomato by differential screening of a cDNA library (Slater *et al* 1985) and later verified as the ethylene-forming enzyme by a series of antisense experiments involving transgenic plants (Hamilton *et al* 1990). In these experiments, a chimeric *pTOM13* antisense gene was constructed containing a fragment of the *pTOM13* coding sequence inserted in the reverse order driven by the CaMV 35S promoter. The vector containing the antisense gene was then transformed into tomato plants. Ethylene production from wounded leaves of the primary anti-sense *pTOM13* transformants was inhibited by 68% and by 87% in ripening fruit. The results from the experiments by Hamilton and collaborators strongly suggested that the protein encoded by *pTOM13* was involved in ethylene synthesis. The deduced amino acid sequence of the *pTOM13* revealed that it had a 58% similarity to a flavone-3-hydroxylase sequence, which is an iron and ascorbate-dependent dioxygenase (Hamilton *et al* 1990). It was proposed, therefore, that the enzyme required these compounds as cofactors, and so an *in vitro* ACC oxidase assay subsequently developed (Ververidis and John 1991).

Since these findings, ACC oxidase has been identified as encoded by a multigene family in a range of plant species (Wang *et al* 2002) and differential expression of these genes has been shown in a wide number of species (Hunter *et al* 1999). Accordingly, although ACC synthase appears to control the rate of production of ethylene, the differential expression of the ACO genes suggests that ACC oxidase also has a role in the regulation of ethylene production by plant tissues (Johnson and Ecker 1998).

The ACC oxidase protein has been purified and biochemically characterised in a number of species including avocado (McGarvey and Christofferson 1992), apple fruit (Kuai and Dilley 1992), white clover (Gong and McManus 2000, Hunter *et al* 1999), melon (Smith *et al* 1992), carnation flowers (Kosugi *et al* 1997), cherimoya fruit (Escribano *et al* 1996), pear (Vioque and Castellona 1994), citrus peel (Dupille and Zacaris 1996), papaya fruit (Dunkley and Golden 1998) and banana fruit (Moya-Leon and John 1995). The published range for the molecular weight of the ACC oxidase protein is between 35 and 41 kDa although there has been a report of an ACC oxidase

of 27.5 kDa identified in papaya fruit using SDS-PAGE (Dunkely and Golden 1998). There is some evidence to suggest the enzyme is either associated with the plasma membrane (Ramassamy *et al* 1998) or the apoplast (Latche *et al* 1992). However, it does not contain any membrane spanning domains or a N-terminal signal sequence targeting it for translocation to the plasma membrane (*via* the endoplasmic reticulum) and its primary sequence suggests that it is a cytosolic enzyme (Hamilton *et al* 1991). There is no evidence to date that there are plant secretory proteins that do not have a signal peptide targeting them for secretion, although it has been shown that the mammalian cytokinin interleukin 1b protein lacks a signal peptide, but is secreted through endocytic vesicles (Andrei *et al* 1999). More recent immunolocalisation studies of an apple ACO protein have shown it to be located in the cytosol, and lacks any ER plasma membrane signal peptide (MeiChu *et al* 2002).

In common with the differential expression of ACC oxidase multigene families, isoforms of ACC oxidase have also been shown to be kinetically distinct (Gong and McManus 2000). Taken together, the biochemical studies confirm that the conversion of ACC to ethylene by ACC oxidase does represent a further tier of control of ethylene biosynthesis.

#### 1.6.2.3 Auxin (IAA)

It has long been accepted that IAA is an important regulator of the development of plant form (Cooke *et al* 2002). IAA is involved in the mediation of plant cell growth, cell expansion and morphogenesis (differentiation of vascular tissue and lateral root formation). In addition, IAA mediates responses in the environment such as gravitropism and phototropism though little is known about its mode of action (Luschuig 1999).

The dramatic effects IAA has as a plant growth regulator necessitates tight regulation of its concentration in cells. It is believed that the hormone acts primarily as the free acid and the endogenous concentrations of the free IAA are regulated *in vivo* through its synthesis, oxidation, conjugation and transport. The chemical structure of IAA has been known since the early 1930s to be a 3-substituted indole-like tryptophan (reviewed in Park *et al* 2001). Evidence suggests that IAA is synthesized through two main pathways; a tryptophan-dependent and a tryptophan-independent pathway

although the precise routes for its biosynthesis are unknown and to date only the enzymes for the tryptophan-independent pathway have been cloned (Ljung *et al* 2002). Results using IAA biosynthetic mutants of *Arabidopsis* suggest the tryptophan-dependent pathway does not appear to be a significant source of IAA in higher plants (Bartel *et al* 2001), although mutants of *Arabidopsis*, that overproduce IAA, have been shown to have upregulated genes in the tryptophan biosynthetic pathway (Smolen and Bender 2002).

IAA has been shown to form conjugates with sugars, amino acids and small peptides which are believed to be involved in the storage, transport, or degradation of the hormone and thus act as a means to control the homeostatic pool. Conjugate hydrolysis is thought to be one of the most important events controlling auxin homeostasis (Magnus *et al* 1992). When the total IAA content in *Arabidopsis* seeds was analysed it was found that less than one percent was present as free IAA, four percent occurred as ester-linked conjugates, seventeen percent as amino acid conjugates and seventy eight percent as protein conjugates (Park *et al* 2001). In five-day-old seedlings of *Arabidopsis*, free IAA still accounts for less than one percent of the total pool (Ribnicky *et al* 1998). However, the free IAA content of the coleoptile tips of oat, where IAA is synthesised, accounts for about 30 percent of total IAA (Ribnicky *et al* 1998). The *Arabidopsis* IAA mutant, *sur2*, contains high levels of free IAA, that correlate with lower than wild-type levels of conjugated IAA (Delarue *et al* 1998), yet this mutation causes a conditional increase in the free IAA pool size through upregulation of IAA biosynthesis (Barlier *et al* 2000). Conjugation is sometimes a catabolic event, as some conjugates cannot be hydrolyzed back to free IAA (Ljung *et al* 2002, Ostin *et al* 1998, Normanly 1997, Bandurski 1995, Tuominen *et al* 1994, Hangarter and Good 1981, Cohen and Bandurski 1978).

Conjugation and oxidation processes modify the indole ring or auxin side chain and cause loss of biological activity. IAA catabolism appears to be primarily through decarboxylative and non-decarboxylation pathways, two of which have been elucidated (Tuominen *et al*, 1994). Decarboxylative metabolism of IAA usually involves the modification of both the side chain and the indole ring. These complex reactions are catalysed by a variety of peroxidases often referred to as IAA oxidases. Although, there is evidence that IAA oxidases play a significant role in IAA metabolism and

activity *in vivo* (Ljuang *et al* 2002), the products of the reactions are seldom identified as endogenous constituents of plants so this is not considered to be the major pathway of IAA catabolism (Ostin 1998, Lagrimini 1991). Moreover, IAA oxidase does not appear to be present in plants in amounts large enough to have any significant impact on the breakdown of IAA. The major catabolic pathway for IAA in *Arabidopsis* is non-decarboxylative oxidation (Ostin 1998). Similar pathways have been described in other plants although the products often differ significantly between species (Ljuang *et al* 2002).

IAA moves through the plant in two ways; either rapidly through the phloem both acropetally and basipetally, or slowly through from cell to cell from the site of synthesis in the apex to the base in a polar manner. In roots, this unidirectional transport continues throughout the root central cylinder to the root apex but the polar flow moves basipetally (away from the meristem) in the outer cell layers of the root. Polar auxin transport is a unique process that is specific to plants and IAA. Much of the research has focused on polar transport because of the observed effects of differential distribution of the hormone to the plant form and, through use of chemical inhibitors of auxin transport, the physiological importance of auxin transport (Friml and Palme 2002). These experiments led to the chemiosmotic model that explains the transport of auxin through the action of efflux and influx carriers (Rubery and Sheldrake 1974). The AUX and PIN gene families identified in *Arabidopsis* are certainly involved in auxin transport (Palme and Galweiler 2000), but although knowledge about the developmental importance of auxin carriers is rapidly advancing with most of the research focus on efflux carriers (Parry *et al* 2001), there is still no direct evidence that establishes the function of the AUX and PIN genes as carriers.

However, of most relevance to this thesis is the role of IAA and ethylene in the regulation of secondary abscission zone formation *in vivo*.

### 1.6.3 Secondary abscission formation is a transdifferentiation event

Plant cell differentiation, in common with other eukaryotes, can occur *via* cell division with the daughter cells displaying a new competence or through the direct change in cellular competence and function without cell division (transdifferentiation). Fukuda and Komamine (1982) illustrated, using lignin as a marker of cell differentiation,

procambial parenchyma cells differentiate into tracheary elements (TE) without prior cell division. Mechanical wounding often induces transdifferentiation of TEs and inhibitors of ethylene biosynthesis often suppress TE differentiation *in vitro* although there is no direct evidence suggesting ethylene has a role in TE differentiation (Fukuda 1997). These examples demonstrate that, in some cases, a change in the functional capabilities of a cell does not require cell division, i.e. these are transdifferentiation events. The change in function of the cortical cells to secondary abscission zone cells in the bean petiole explant system has also been shown to be a transdifferentiation event (McManus *et al* 1998).

To show this, McManus and collaborators examined the cell layers comprising the secondary abscission zone in both induced and endogenous zone explants. Microscopic examination revealed the parenchyma cells on the green side were turgid and rounded like those at the petiole primary zone, and cells on the yellow side eventually became flaccid and collapsed. There were also similarities in the induction of the cellulase 9.5 that occurs in both primary and secondary zones. The cytoplasmic activity, including dilation of dictyosomes and increased vesicle formation, are also similar in both primary and secondary zones. Analysis of petioles at all stages from primary to secondary zone formation using light microscopy of sectioned petiole explants revealed at no stage was there any evidence of cell division. Microdensitometry readings indicated that the DNA content did not double in quantity during this differentiation event so confirming that there was no cell division. However, endoreduplication of portions of DNA may have occurred but these events resulted in microdensitometry readings that were in the range of variation. Although there was no cell division observed (supported by the lack of formation of cell plates), there were changes in the nuclei of the different tissues. Just before abscission, the zone cells on the green side displayed dispersed chromatin typical of highly active cells and appeared under light microscopy to have higher genomic activity.

There are examples where cell division does occur in the differentiation of secondary zones. For example, in stem explants of *P. vulgaris* (Webster and Leopold 1972) and the stem of excised GA-treated cotyledonary nodes of cotton (Bormann *et al* 1968), differentiation of cells into adventitious abscission zone cells is clearly preceded by cell division.

#### 1.6.4 Control of secondary abscission zone formation in explants of *P. vulgaris*

In the bean petiole system, differentiation of secondary abscission zones and the cell-cell separation at the differentiated site appears to proceed without pause, whereas in normal abscission the position is defined early in development but the abscission event does not occur until later when the organ senesces. At the time of cell-cell separation of secondary zone cells the morphology and biochemistry within these cells is indistinguishable from those of the predetermined abscission zones (McManus *et al* 1998).

The concentration of applied IAA, at the distal face of the explant, determines the position along the petiole at which the secondary zone will form. A mathematical model has been described that explains how applied concentrations of IAA can effect the position of abscission zone formation (Warren Wilson *et al* 1988). It was postulated that the positioning of the induced abscission site within a stem explant of *I. sultani* depends on the accumulation of basipetally transported auxin. From this research the general hypothesis is that abscission occurs where the auxin concentration decreases in the morphologically upward direction, i.e. accumulates at the base and sets up a 'reverse' concentration gradient from the base to the apex. This is supported by the observation that when IAA is added at the base or middle of the explant, abscission occurs at a position more apical to the point of application. This was confirmed by Warren Wilson and collaborators (1999) in nodal explants of *I. sultani*. In the bean explant system however, the addition of IAA to the base of the explant (the original proximal end) does not result in the formation of any adventitious abscission zone.

Warren Wilson and collaborators (1987) proposed the theory of a morphogenic field, which determines the position of formation of the secondary zone by IAA concentration. Warren Wilson and collaborators also found that certain forms of wounding of internodal explants could induce abscission near the wound site. Two auxin mechanisms were postulated to explain this; the first suggests that the induction of the zone may be due to the oxidative catabolism of auxin at the wound surface and the second that there may be an increase in the auxin concentration where the wound severs the vascular strands through which the auxin normally moves basipetally (Warren Wilson 1988). In the bean petiole explants, if IAA is not applied, an

adventitious abscission zone will form in a small percentage of explants with the same orientation of green:yellow tissues as at the primary zone, that is: yellow (senescent) tissue distal to the zone and green tissue proximal to the zone. The mechanisms operating that signal the petiole cells to differentiate in these explants may be similar to the wound induced abscission zones in stems of *Impatiens*, with the zone forming near the site of wounding.

In the bean explant system used in this thesis, the higher the concentration of applied IAA, the further removed from the distal primary zone the secondary zone differentiates (McManus *et al* 1998). Although the chemical signals that are transmitted by adjacent senescing and non-senescing tissues are unknown, it has been observed in all explants that the cells that differentiate to secondary zone cells form on the green tissue side of the abscission zone, in the same fashion as in predetermined abscission zones. There does not appear to be a predetermined polarity of perception of the transdifferentiation signal, which may occur if the zones formed only when the distal tissue became senescent. It may be that the applied IAA maintains the distal side of the explant in a non-senescing state, with its concentration determining the portion of petiole that remains green. If this were the case a particular threshold concentration, or concentration difference between adjacent cells, combined with signals provided by ethylene, may trigger a row of cortical cells to differentiate to zone cells. It is possible, therefore, there are other morphogenic compounds acting to influence the position of the zone (Warren Wilson 1987).

An increase in cellulase 9.5 protein has also been measured in secondary abscission zones in bean petiole explants (McManus *et al* 1998). The timing of the induction of cellulase 9.5 during the transdifferentiation of these adventitious abscission zones has not been measured. It is possible that the transcript is transported from the primary petiole-pulvinus abscission zone and translated at the site of secondary zone formation. Alternatively, the cellulase 9.5 mRNA may be present in the petiole cortical cells and the signals provided by auxin and ethylene determine which cells will translate the message to the active cellulase 9.5 enzyme. The possibility of a role for cellulase in the differentiation of cortical cells to secondary abscission zones has not been examined, and the time at which these cells first differentiate is also unknown. Determining the temporal induction of cellulase 9.5 during the formation of secondary zones and

combining this information with ultrastructural changes and the endogenous concentrations of ethylene and auxin, it may be possible to postulate a function for cellulase 9.5 during this specialised cell differentiation event.

## 1.7 Thesis Aims

This thesis sets out to examine aspects of the regulation of abscission cell differentiation using both an *in vivo* approach with *S. nigra* as the model species, and an *in vitro* approach with *P. vulgaris* as the model species.

The thesis aims, and hence the research plan, is therefore divided into two sections.

The *in vivo* approach:

A protein that is expressed only in abscission zone cells (and not the surrounding non-zone cells) could theoretically be used as a marker of the specialised cell type and the onset of the expression of this protein a spatial and temporal indicator of abscission cell differentiation. The aims of the *in vivo* section of research were to identify and characterise one or more of these proteins by screening for either unique or preferentially-expressed proteins in the leaf rachis abscission zone of *S. nigra*, and use amino acid sequencing to identify any proteins of interest. Furthermore, using the identity of any unique or preferentially-expressed proteins, determine a role (if any) for these proteins in the abscission process.

The *in vitro* approach:

Elucidating the role of the abscission-associated plant hormones ethylene and auxin in the regulation of abscission cell differentiation will add to the knowledge required to develop techniques to control the spatial and temporal differentiation of adventitious (and perhaps predetermined) abscission zones. The aims of the *in vitro* section of research were to

- Measure the IAA concentration along in the petiole explants which form secondary zones to determine if there is a correlation between the concentration of IAA and the position where these zones differentiate.
- Investigate the regulation of the ethylene biosynthesis (ACC oxidase activity and accumulation) in the petiole explants as they form secondary abscission zones.

## Chapter 2

# Materials and Methods

Unless otherwise stated, all of the chemicals used were from BDH Laboratory Supplies or Sigma Chemical Company. All solutions were made using water purified using reverse osmosis (RO), followed by filtration by microfiltration (Milli-Q, Millipore Corporation). The details of these and the manufacturers of the other reagents and specialised equipment are listed in Table 2.1.

### 2.1 Growth and explant preparation of *Phaseolus vulgaris*

#### 2.1.1 Cultivar and growing media

The cultivar of *Phaseolus vulgaris* used for all experimentation was cv. Tender Green (Watkins NZ Ltd, New Plymouth, New Zealand). Trays of growing media were prepared by adding dolomite (3 g/L) and iron sulfate (0.5 g/L) together with agricultural lime (2 g/L) to a horticultural bark base (formulation by the Plant Growth Unit, Massey University). Approximately 25 seeds were sown per tray. The seedlings were watered twice daily and grown in a temperature-regulated glass house (maintained between 15 and 25 °C) under natural daylight.

#### 2.1.2 Harvest and explant preparation

The bean seedlings were harvested at a similar developmental time point in which the petioles of the 2 primary leaves had extended to 2 cm (approximately 14 days after germination) (Figure 2.1). To prepare the explants, each leaf was first cut away from the lamina:pulvinus junction and the petiole excised to include a length of 15 mm proximal to the pulvinus:petiole abscission zone and so incorporate the primary abscission zone and the distal pulvinus (Figure 2.2). Glass dishes (1 L) were prepared several h earlier containing plastic petiole holders set into 2% (w/v) agar (Figure 2.3). The petiole explants were carefully laid into the plastic holders with a pair of tweezers. The rim of each dish had been ground to a flat surface and petroleum jelly was spread on the ground glass to assist in making an airtight seal between the dish and lid.

Company	Full Company Name	Company Address
ACROS Organics	ACROS Organics	NJ, USA
Ajax	Ajax Chemicals	Auburn, NSW, Australia
Alltech	Alltech Associates Inc.	Deerfield, IL, USA
American National	American National Can.	Chicago, IL, USA
Amersham	Amersham Biosciences	Buckinghamshire, UK
Anthos	Anthos Labtech Instruments	Salzberg, Austria
Applied Biosystems	Applied Biosystems	Foster City, CA, USA
Benton Dickenson	Benson Dickenson Medical Pte Ltd	Singapore
BDH	British Drug Houses	Poole, Dorset, UK
Bio-Rad	Bio-Rad Laboratories	Hercules, CA, USA
BOC Gases	BOC Gases (NZ) Ltd	Palmerston N, New Zealand
Calbiochem	Calbiochem Corporation	La Jolla, CA, USA
Difco	Difco Laboratories	Detroit, MI, USA
Gibco-BRL	Life Technologies Gibo-BRL	Gathersbury, MD, USA
Idetek	Idetec Inc.	Sunnyvale, CA, USA
Immobilin	Millipore Corporation	Bedford, MA, USA
Medicell	Medicell International Ltd	London, UK
Micron Separations	Micro Separations Inc.	MI, USA
Nunc	Nalge Nunc International	Roskilde, Germany
Pall Filtron	Pall Filtron	Ann Arbor, MI, USA
Reidel-de haen ag seelze	Reidel-de haen ag seelze	Hannover, Germany
Roche	Roche diagnostics GmbH	Mannheim, Germany
Savant	Savant Instruments Inc.	Farmingdale, NY, USA
Serva Feinbiochemica	Serva Feinbiochemica	Heidelberg, Germany
Shimadzu	Shimadzu Corporation	Kyoto, Japan
Sigma	Sigma Chemical Company	St Louis, MO, USA
Tropix	Tropix	Bedford, MA, USA
Univar	Univar	Auburn, NSW, Australia
Vertis	The Vertis Company	Gardiner, NY, USA
Whatman	Whatman International Ltd	Maidstone, UK
Wheaton	Wheaton Glass	Milville, NJ, USA
Zentech	Zentech	Dunedin, New Zealand

Table 2.1. Names and addresses of the manufactures of reagents and specialised equipment.

### 2.1.3 Ethylene and IAA treatment of explants

To induce the formation of secondary abscission zones, ethylene and then IAA were applied to the explants. Ethylene (1 mL of a 10 000 ppm ethylene standard) was injected through the rubber bung into the glass dishes containing the freshly excised explants to give a final ethylene concentration of 10 ppm. The dishes were then placed in an illuminated growth cabinet and incubated at 25 °C for 36 h, by which time the pulvini had visibly senesced and separated from the petioles. The ascinded pulvini were removed with tweezers and IAA (1 µL aliquots from a 1 mM stock) was applied with a pipette to the exposed abscission zone cells on the petiole. The dishes were re-sealed and ethylene (1 mL of 10 000 ppm) was injected through the rubber bungs. The second and final application of IAA was placed on the primary abscission face 8 h after the first and ethylene (1 mL of 10 000 ppm) added as before. Each day, over the remaining 5 days of the time course, the dishes were aerated, resealed and injected with ethylene.

At the appropriate time intervals tissues were collected. During the formation of, or at secondary zone separation, the green petiole tissue was harvested as the green segment (designated as G1) and the yellow petiole tissue as three segments (Y2, Y3, Y4)(Figure 2.4). These were collected separately for the IAA experiments and pooled for the ethylene evolution and ACC oxidase experiments. In all experiments the damaged distal end of the petiole, the fracture plane (for both primary and secondary zones) and the callus on the proximal end were cut away and discarded (ca. 1 to 2 mm of tissue in each case).

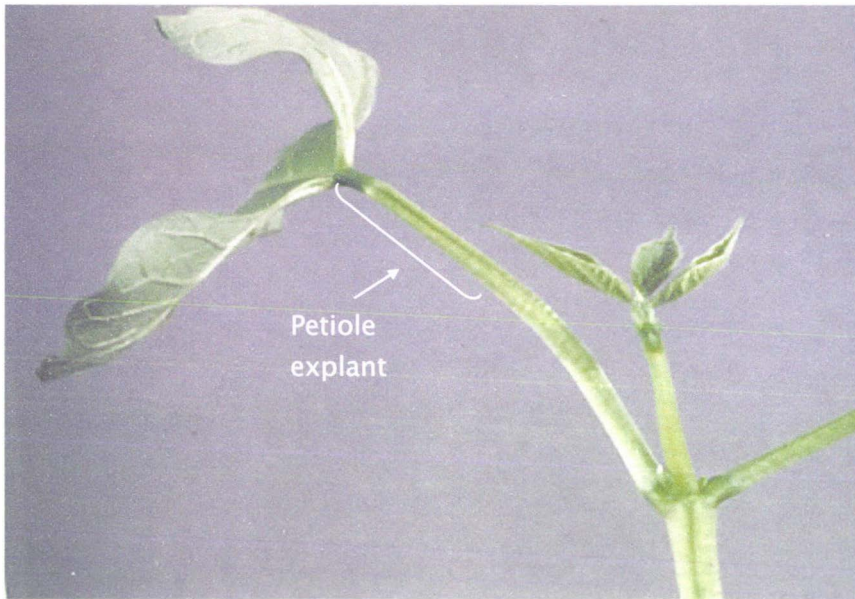


Figure 2.1. Primary leaf of *Phaseolus vulgaris* approximately 14 days after germination. The explants were excised from the plant at this stage of development.

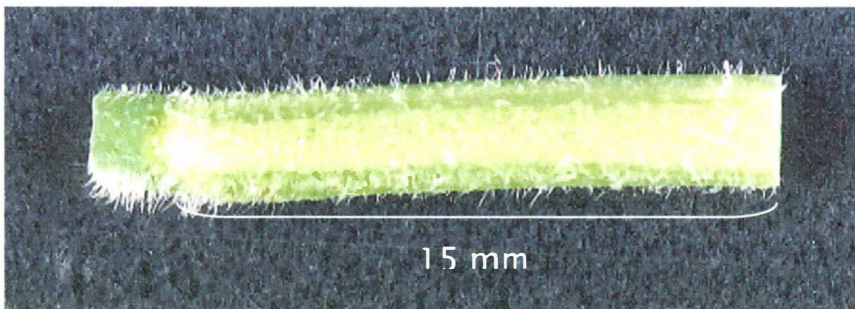


Figure 2.2. Freshly excised 15 mm petiole explant with the pulvinus attached.

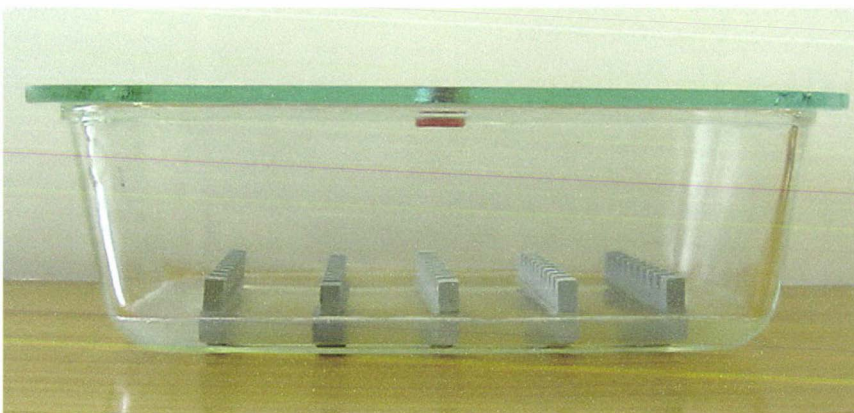


Figure 2.3. A glass dish used for the ethylene treatment of the petiole explants containing petiole racks set into agar.

## 2.2 Collection and preparation of *Sambucus nigra*

### 2.2.1 Gathering of *S. nigra* plant material

Plant material was collected from elderberry shrubs (Figure 2.5) growing locally in areas surrounding the Massey University campus in Palmerston North. Collected material (compound leaves), was taken to the laboratory and processed immediately. A record of the date and the amount collected from each shrub was kept to ensure an even contribution of each shrub (or group of shrubs) towards each tissue type.

### 2.2.2 Preparation of the tissue samples of *S. nigra*

Four samples were excised from the collected leaves. Mid-rachis (MR) tissue was collected as the middle third of the rachis between the point of insertion of each set of compound leaflets. Cells of the leaflet abscission zone prior to ethylene treatment, labeled OZONE (OZ), were collected by slicing out the leaf rachis abscission zone between the compound leaflets with a scalpel blade. The areas of MR and OZ tissue collection from the rachis (Figure 2.6) are illustrated in Figure 2.7.

To collect ethylene-treated tissues, molten agar [2% (w/v)] was poured to a depth of about 1 cm into the glass dishes illustrated in Figures 2.3 and left to set. Explants containing the leaflet abscission zone cells were excised from the rachi (Figure 2.7), forced gently into the agar (approximately 1 per 2 cm<sup>2</sup>) and the dishes sealed as in section 2.1.2. Ethylene (1 mL of 10 000 ppm) was injected through the rubber bungs in the lids of the dishes containing the explants, which were then placed into a fluorescent illuminated growth cabinet at 25 °C for 36 h. At 36 h, the separated cells of the abscission zone (ZONE) were collected with a blunt scalpel by gently scraping the area (Figure 2.8). The ethylene treated mid-rachis tissue (MRE) was collected from these explants [as the lower section of rachis tissue from the explant (Figure 2.8)] after the removal of the zone cells. The 1-methylcyclopropene (1-MCP)-treated MRE tissue (MRE-MCP) was prepared in the same way as the MRE tissue, but with the addition of 1 ppm 1-MCP in the glass dishes containing the explants. All tissues were collected directly into liquid nitrogen and stored at -80 °C.

Distal end of  
the explant

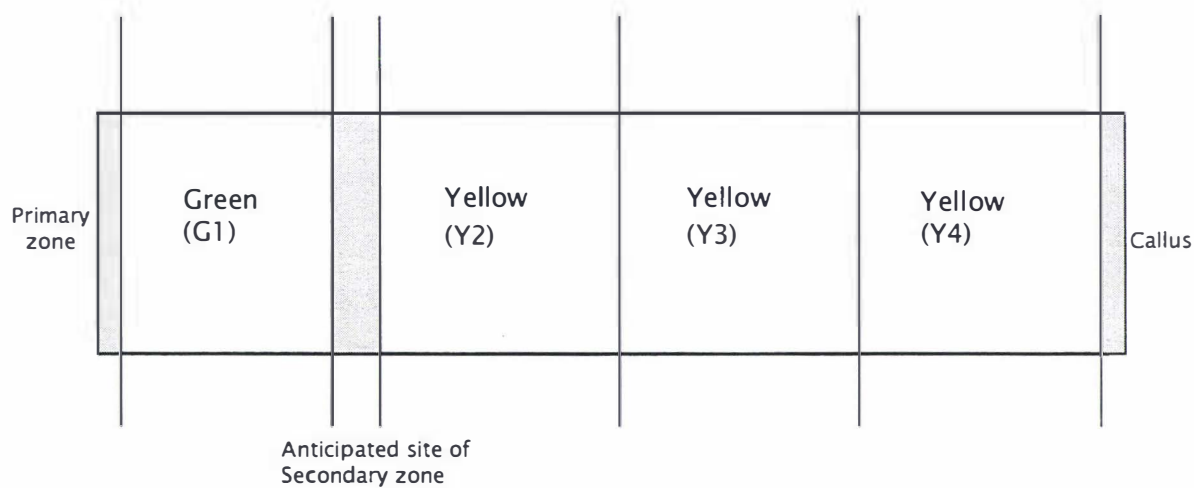


Figure 2.4. Excision of petiole segments during the formation, or at separation of the secondary zones. For IAA measurements, the G1, Y2, Y3 and Y4 segments were excised as separate tissues. For ethylene evolution and ACC oxidase activity measurements the Y2, Y3 and Y4 segments were pooled. For all measurements, the shaded areas were discarded.



Figure 2.5. A shrub of *Sambucus nigra* (elderberry) in flower.



Figure 2.6. A compound leaf of *Sambucus nigra*.

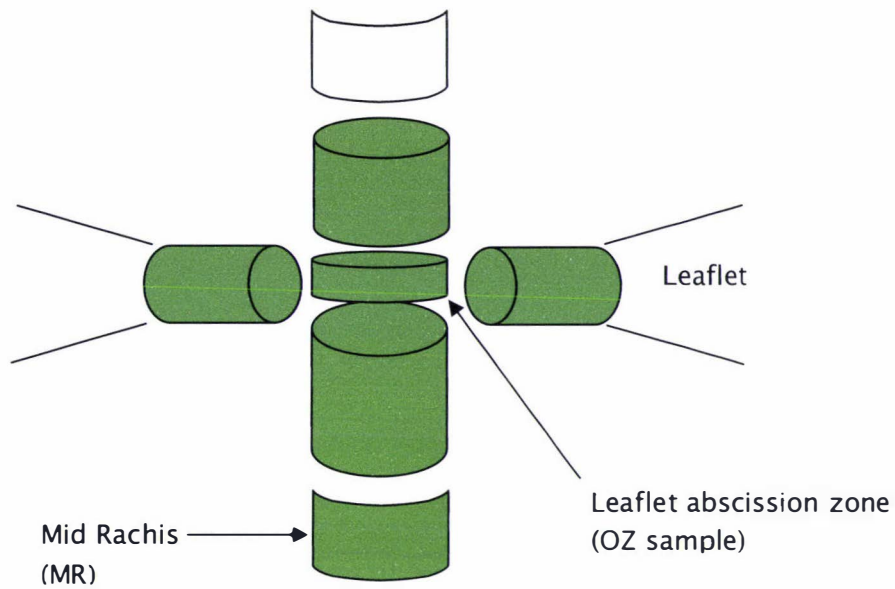


Figure 2.7. The segmented *S. nigra* rachis explant (explant shaded green).

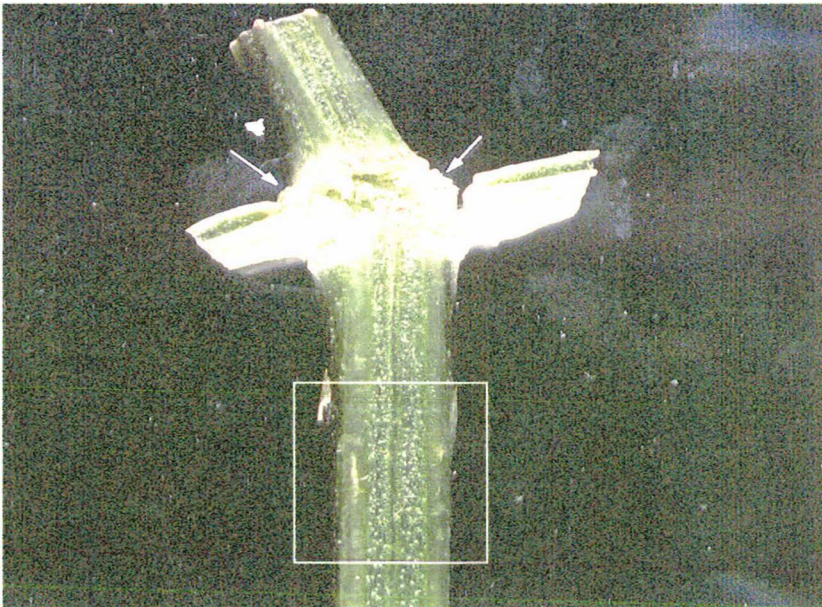


Figure 2.8. The leaflet abscission zones from *S. nigra* after 36 h ethylene treatment of the rachis explant shown in Figure 2.7. The arrows indicate the separated ZONE tissue and the boxed area represents the MRE tissue.

## 2.3 Biochemical and chemical methods

### 2.3.1 Protein extraction and fractionation using column chromatography

#### 2.3.1.1 Extraction of the soluble protein fraction in plant tissues

##### Reagent

2-mercaptoethanol

To extract the ZONE tissue, the collected cells were powdered with a mortar and pestle in liquid nitrogen and then transferred to a centrifuge tube containing 50 mM 2-mercaptoethanol to give a ratio of 3 mL: 1 g fresh weight (FW) of tissue. The other samples (MR, MRE, MRE-MCP and OZ) were extracted by placing the frozen tissue (frozen in liquid nitrogen and stored at  $-80^{\circ}\text{C}$ ) into a Waring blender and then adding 50 mM 2-mercaptoethanol to give a ratio of 3 mL: 1 g FW of tissue. The tissues were blended at high speed for about 5 min or until a fine suspension was obtained. At this point, all samples were incubated for 30 min at room temperature with agitation, and then centrifuged (12 000g for 15 min at  $4^{\circ}\text{C}$ ). The supernatants were decanted and either used for Western analysis (section 2.3.5) or for cell fractionation studies (section 2.3.1.3). The remaining pellet was resuspended in 50 mM 2-mercaptoethanol at a 3 mL: 1 g FW ratio, and then centrifuged as before. The supernatant was then removed and the pellet washed with 50 mM mercaptoethanol, as described. After the three 2-mercaptoethanol washes, the same volume of Milli-Q water was added to all the samples, and the pellet resuspension washing step performed a further 12 times. A small sample of the supernatant from each wash was kept for protein estimation (section 2.3.2). After 11 water washes, the soluble protein content had been removed from the tissues (data not shown).

#### 2.3.1.2 Extraction of cell wall-associated proteins

##### Reagent

Sodium chloride

The insoluble pellets remaining after removal of the final supernatant from the water washes (section 2.3.1.1) were extracted twice with 1 M NaCl at a 1 mL:1 g FW ratio. After the first addition of NaCl, the samples were incubated for 1 h at  $37^{\circ}\text{C}$  with

agitation. The NaCl extracted tissues were centrifuged (12 000g for 20 min at 4 °C) and the supernatants pipetted into 50 mL-capacity plastic tubes. The second NaCl incubation was for 24 h at 4 °C. The tissues were centrifuged as before and the supernatant containing the wall-associated proteins collected. The protein content of each of the extracts was measured (section 2.3.2), the extracts then pooled and stored at -20 °C.

### 2.3.1.3 Fractionation of cells using ultracentrifugation

The initial supernatant obtained after centrifugation of the 50mM 2-mercaptoethanol extract (section 2.3.1.1) was centrifuged at 10 000g to separate the components that pellet at low centrifugal force, e.g. the nuclear membranes and most of the organelles. The resulting supernatant was centrifuged at 100 000g for 30 min to separate the remaining complexes and organelles in the pellet from the truly soluble proteins in the supernatant. Ultracentrifugation of the 1 M NaCl mid-rachis cell wall extract (section 2.3.1.2) at 100 000g for 30 min separated the cell wall and plasma membrane components from the cell wall associated proteins. A diagrammatic representation of the fractionation scheme is shown as Figure 3.10a.

### 2.3.1.4 Extraction of proteins from lamb kidney

#### Reagents

Ammonium sulfate

Sodium chloride

Lamb kidney (2.8 g) was powdered with liquid nitrogen with a mortar and pestle. Eight mL of 0.5 M NaCl was then added to the powdered kidney and the mixture incubated for 1 h at 4 °C. The extract was transferred to microfuge tubes and centrifuged (15000g for 10 min at 4 °C). The supernatant was transferred to dialysis tubing and dialysed against 2 M ammonium sulfate (3 changes of 0.5 L over 72 h at 4 °C). Proteins in the kidney extract that precipitate at 2 M ammonium sulfate [i.e. after the dialysis step] were removed by centrifugation (12 000g for 10 min at 4 °C). The resulting supernatant was filtered (section 2.3.1.6) before injection onto the Hydrophobic Resource<sup>R</sup> column (Amersham). The conditions used for the elution of the proteins

from the hydrophobic column in the lamb kidney extract are the same as those described in section 2.3.1.6.

### 2.3.1.5 Concentrating protein, solution exchange and dialysis

#### Reagent

Tris[hydroxymethyl]amino methane (Tris; Gibco-BRL)

Extract volumes from previous sections that were up to 1 L in volume were concentrated to volumes of less than 10 mL using Macrosep<sup>TM</sup> centrifugal concentrators [molecular weight cut off (MWCO) 10K; Pall Filtron] and centrifugation in a 45° fixed angle rotor (SS-34, Sorvall) at 3000g at 4 °C. Smaller volumes were concentrated using Nanosep<sup>TM</sup> microconcentrators (MWCO 10 K; Pall Filtron) to enable resolution on a SDS-PAGE mini-gel, and to reduce the sample volume prior to loading onto the Phenyl Superose HR 1/1 column (Amersham).

Concentrated samples (each containing ca. 3 mg/mL of protein) required removal of the NaCl for resolution using SDS mini-gels. The microconcentrators (Pall Filtron) were used for the desalting of small samples (about 15 µg), taken from the concentrated extracts. To do this, a 25 mM Tris solution (pH 7.4) was added to the concentrators containing the samples to make each up to a volume of 400 µL. The concentrators were centrifuged (3 000g at 4 °C) until the sample volumes had reduced to 50 µL then more Tris solution was added (to return the total volume to 400 µL) and the concentrators centrifuged until the final volume reached 20 µL. The protein content of each sample was measured (section 2.3.2) to ensure equal loading on the SDS-PAGE mini-gels. The desalted samples were then resolved on an SDS-PAGE mini-gel using the method described in section 2.3.3.

### 2.3.1.6 Separation of proteins using hydrophobic interaction chromatography and Fast Protein Liquid Chromatograph, (FPLC)

#### Reagents

Ammonium sulfate

Potassium phosphate

To prepare samples for hydrophobic column chromatography, concentrated extracts (from section 2.3.1.5) were dialysed against 3 changes of 50 volumes of 2 M ammonium sulfate over 72 h at 4 °C. The dialysis step exchanged the samples into the same salt (ammonium sulfate) and at the same salt concentration (2 M) as the equilibrated Phenyl Superose<sup>R</sup> column (section 2.4.1.1) ensuring maximum binding of the extract to the column when loaded. The dialysed extracts were stored at -20 °C until separation on the column.

Prior to separation, the dialysed samples were filtered by forcing the protein solutions, using a syringe, through a Cameo 25GAS filter (0.22 µM; Micron Separations). The protein content (section 2.3.2) of the filtered extracts was determined to ensure equal loading of sample protein onto the column.

The Phenyl Sepharose HR 1/1 (Amersham) column or the higher capacity HR 5/5 (Amersham) column was used depending on the protein concentration of the extract. Each column was equilibrated for 30 min with buffer A [2M ammonium sulfate, pH 5.6] using a flow rate of 0.5 mL/min for the HR1/1 column and 2 mL/min for the HR 5/5 column. After sample loading, a linear elution gradient, at 2 mL/min, was used for all samples; the percentage of buffer B (20 mM potassium phosphate, pH 7.0) increased from 0 to 100 in 45 min (beginning at time zero). Buffer B was kept at 100 % for 30 min to ensure late eluting proteins had disassociated from the column. Prior to use, all FPLC buffers were filtered through GH-Polypro hydrophilic polypropylene membrane filters (47 mm, 0.2 µM; Pall Filtron) using a glass filtering apparatus (Zentech, Dunedin, New Zealand).

Fractions were collected from the column, using a fraction collector (Frac-100, Amersham), at 5% increments of buffer B, and so corresponding to one fraction every 2.25 min. An absorbance profile (280 nm) was obtained using a chart recorder (Recorder 102).

### 2.3.1.7 Ion exchange column chromatography

#### Reagents

Sodium chloride

Tris

Fraction(s) containing the proteins of interest from the hydrophobic Phenyl Sepharose HR1/1 or HR 5/5 columns were located using Western analysis (section 2.3.5). All positive fractions were pooled and dialysed against Mono-Q column buffer A [3 x 100 volumes of 50 mM Tris-HCl (pH 7.5) over 48 h]. The Mono-Q column (H/R 1/1, Amersham) was equilibrated with at least 5 volumes of buffer A at a flow rate of 0.5 mL/min. Samples were then loaded onto the column at 1 mL/min (HR 1/1) or 5 mL/min (HR 5/5), and proteins were eluted within a gradient of 100% buffer A: 0% buffer B [50 mM Tris-HCL, (pH 7.5) containing 1 M NaCl] to 0% buffer A: 100% buffer B over 45 min.

### 2.3.1.8 Gel filtration column chromatography

#### Reagents

Sodium chloride

Fraction(s) from the Mono-Q ion-exchange column (section 2.3.1.7) which contained the proteins of interest were identified by Western analysis (section 2.3.5). Positive fractions were pooled and concentrated to a volume of 200  $\mu$ L using NanoSep<sup>TM</sup> concentrators (section 2.3.1.5) in preparation for loading on to the Superose 12 gel filtration column (Amersham). Optimal separation was obtained by adjusting the sample to 0.5 M NaCl and this was achieved by reducing the volume of the Mono-Q eluate to 50  $\mu$ L in a 400  $\mu$ L concentrator, making up the volume to 400  $\mu$ L with 0.5 M NaCl and then reducing the volume again to 50  $\mu$ L. This was repeated a total of 3 times, before the final volume was made up to 200  $\mu$ L for injection on to the Separose 12 column.

The molecular masses ( $M_r$ ) of the proteins eluting from the column was measured by comparing the elution volume ( $V_e$ ) of proteins of known molecular weight (Molecular Weight Marker Kit for Gel Filtration Chromatography (molecular weight range 12 000

to 200 000 kDa, Sigma) with the elution volumes of the sample proteins (Table 2.2). A plot of the elution volume divided by the void volume versus the log ( $M_r$ ) was used to determine the molecular weight of the sample fractions with known elution volumes.

Protein Standard	Molecular Weight	Log $M_r$	Elution Volume (Ve)	$V_e/V_0$
Cytochrome C	12.5 kDa	1.10	15	2
Carbonic anhydrase	29 kDa	1.46	13.95	1.86
Bovine serum albumin	66 kDa	1.82	12.80	1.7
Alcohol dehydrogenase	150 kDa	2.18	12.0	1.6
$\beta$ -Amylase	200 kDa	2.30	10.95	1.46
Blue Dextran 2000	Void Volume ( $V_0$ )		7.5	

Table 2.2. Protein standards used to determine the molecular weight of proteins eluting from the Superose 12 gel filtration column.

### 2.3.2 The Bradford protein assay

Protein concentrations in tissue extracts or column eluates were estimated with a microassay version of Bradford's method (Bradford 1976) using a commercially available dye (Coomassie Brilliant Blue R-250 concentrate dye preparation, from Bio-Rad).

Samples containing the protein to be measured were pipetted into 96-well microtiter plates and made up to 160  $\mu\text{L}$  with Milli-Q water. The Bio-Rad reagent (40  $\mu\text{L}$ ) was then added to each sample and mixed by drawing up and down the pipette. The mixtures were incubated for 10 min at room temperature, and then the absorbance values of the samples read at 595 nm using a microtiter plate reader (Anthos htII plate reader).

A protein standard curve was constructed to determine the protein concentration of sample solutions using a 1  $\mu\text{g}/\text{mL}$  BSA solution (Bovine serum albumin, Serva Feinbiochemica). The samples used for protein estimation had absorbance readings in the linear region of the BSA curve (containing between 0.5 and 7  $\mu\text{g}$  protein per 200  $\mu\text{L}$  reaction). An equation to determine the protein concentration from absorbance readings (shown below) was derived from the linear portion of the BSA curve.

$$\mu\text{g (protein in sample)} = (\text{Absorbance reading } 595 \text{ nm} \times 8.55) - 2.41$$

The equation to determine the protein concentration may not be the same for every batch of the Bio-Rad protein dye as the dye concentrations may change slightly. Therefore, a new standard curve should be constructed for each batch of the dye.

### 2.3.3 Sodium Dodecyl Sulfate–polyacrylamide gel electrophoresis (SDS–PAGE)

SDS-PAGE separates proteins electrophoretically through a polyacrylamide gel on the basis of molecular mass, and was originally described by Laemmli (1970).

#### Reagents

Acetic acid

Acrylamide stock solution [40% (w/v); Bio-Rad]

Ammonium persulfate (APS; Univar)

Bromophenol blue

Coomassie Brilliant Blue R-250 (Bio-Rad)

Glycerol

Glycine

Methanol

2-Mercaptoethanol (Reidel-de haen ag seelze)

SDS

*N,N,N',N'*-tetramethylethylenediamine (TEMED; Reidel-de haen ag seelze).

Tris

#### 2.3.3.1 Preparing and running SDS–PAGE mini-gels

Mini-gels used for SDS-PAGE contained 12 to 15% (w/v) acrylamide and were run using the Bio-Rad mini-gel apparatus. The formulations for the buffers, gels and Coomassie protein stain are listed in Table 2.3, and the volumes and amounts stated are sufficient for 2 mini-gels. The separating gel was pipetted between the glass plates leaving a 3 cm gap below the top of the gel to the shortest plate to allow for the loading wells (10 wells; 1.5 x 0.5 cm) in the stacking gel. An overlay of Milli-Q water was pipetted onto the separating gel to prevent atmospheric oxidation. When the separating gel had polymerised (approximately 30 min), the overlay was tipped off and the separating-stacking gel interface washed with Milli-Q water and dried with filter paper. The prepared stacking gel was then pipetted onto the separating gel and the combs inserted. After about 30 min, the stacking gel had polymerised and the prepared gels were placed into the electrophoretic apparatus. Running buffer was poured into the electrophoretic tank (about 800 mL), submersing the gels, and the combs removed from

the stacking gel. Samples were prepared by adding the sample in solution to an equal volume of 2 x SDS gel loading buffer [60 mM Tris-HCL, pH 6.8 containing 20% (v/v) glycerol, 5.0% (w/v) SDS, 10% (w/v) 2-mercaptoethanol and 0.01% (w/v) bromophenol blue]. Four  $\mu\text{L}$  of prestained molecular markers [low range (ca. 15 to 110 kDa) or kaleidoscope markers (3.8 to 37 kDa), Bio-Rad] were loaded in at least 1 well per gel. The samples were placed into boiling water for 3 min, cooled, centrifuged (12 000g for 1 min at room temperature) and the supernatants pipetted into the wells of the prepared gels. The loading wells have a capacity of 40  $\mu\text{l}$  with the best resolution in samples that contained between 2 and 10  $\mu\text{g}$  of protein. The gels were run until the dye front had eluted from the bottom of the gel. When examining molecular weight proteins above 20 kDa, the gel was run until the lowest molecular weight marker (approximately 20 kDa) had reached the bottom of the gel resulting in greater separation of the larger proteins. All mini-gels were run at a constant 200 V. At the conclusion of electrophoresis, the gels were either subjected to Western analysis (section 2.3.5) or stained with Coomassie brilliant blue (Table 2.3) and destained with 30% (v/v) ethanol.

Separating buffer		Stacking buffer		Running buffer	
Tris	45 g	Tris	6.0 g	Tris	3.0 g
SDS	1.0 g	SDS	0.4 g	SDS	1.0 g
		Glycine	14.4 g		
Milli-Q water to 400 mL		Milli-Q water to 150 mL			
Make up to 500 mL after adjusting pH to pH 8.8 with 1 M HCL		Make up to 200 mL after adjusting pH to 6.8 with 1 M HCL		Made up to 1 L with Milli-Q water	
Separating gel (12%)		Stacking gel		Coomassie Brilliant Blue stain	
Acrylamide	3 mL	Acrylamide	1 mL	Coomassie Blue	0.1 g
Separating buffer	5 mL	Stacking buffer	5 mL	Methanol	100 mL
Milli-Q water	2 mL	Milli-Q water	4 mL	Milli-Q water	325 mL
APS (10%)	100 $\mu$ L	APS (10%)	100 $\mu$ L	Mixed on a magnetic stirrer until dissolved then 50 mL of acetic acid added	
TEMED	10 $\mu$ L	TEMED	10 $\mu$ L		

Table 2.3. Formulations of buffers and acrylamide gel solutions for SDS-PAGE mini-gels.

## 2.3.4 Two-dimensional gel electrophoresis

Two-dimensional electrophoresis is used to separate proteins and peptides on the basis of their isoelectric point and molecular mass. The first dimension involves isoelectric focusing of the proteins in the sample along a polyacrylamide gel strip containing an immobilised pH gradient. The second dimension involves eluting the proteins from the first dimension gel strip using SDS-PAGE. The resulting slab gel was stained using a colloidal stain.

### 2.3.4.1 First dimension isoelectric focusing

All components used for isoelectric focusing, aside from those described in other methods, were obtained from Amersham unless otherwise stated.

#### 2.3.4.1.1 Rehydration of polyacrylamide gel strips

##### Reagents

Ampholine<sup>R</sup>

3-[(3-cholamidopropyl)dimethylammonio]-1-propanesulfonic acid (CHAPS)

Dithiothreitol (DTT)

Tris

Urea

In all experiments in this study, polyacrylamide gel strips (Immobiline Drystrips) were rehydrated in a solution containing the sample. The total polyacrylamide strip rehydration solution consisted of rehydration solution (400  $\mu$ L), sample denaturing solution (50  $\mu$ L) and sample [50  $\mu$ L in 10 mM Tris (pH 7.4) after buffer exchange (section 2.3.1.5)]. The solutions are listed in Table 2.4. Ampholine<sup>R</sup> is a buffering solution that consists of numerous polyamino and polycarboxylic acids of low molecular weight which act as ampholytes. The buffering capacity is in the pH range of 3.5 to 10.

To rehydrate the Immobiline Drystrips, the protective plastic coating is first pulled off the polyacrylamide strip. The delivery ends of plastic 2 mL disposable pipettes (1 for each strip) were covered with parafilm and the strips placed into the pipettes. The

sample and the strip solutions were pipetted down the non-delivery end of the pipettes onto the gel side of the strip. The open ends were covered with parafilm and the strips placed on a rocking table (or vertical rotary mixer) for 18 h at 20 °C. After this rehydration time, the strips had absorbed the entire sample solution.

#### 2.3.4.1.2 Isoelectric focusing of the polyacrylamide gel strips

##### Reagents

##### Silicone oil

The isoelectric focusing (I.F) gel strip apparatus was assembled as described in the Immobiline Drystrip manual (Amersham). The first step in assembly is to pipette silicone oil (3 to 4 mL) onto the cooling plate and then place the Immobiline Drystrip tray into position. Silicone oil (9 mL) was then placed on the tray and the Dry Strip holder placed on top.

The rehydrated gel strips from section 2.3.4.1.1 were placed on the Dry Strip holder with the acid ends of all the strips aligned with each other and at the cathode end of the I.F apparatus. Two electrode strips (Whatman) were cut to 11 cm, dampened with Milli-Q water, blotted to remove excess moisture and placed across the acid and basic ends of the Drystrips to ensure the electrode strips were in contact with the gel. The 2 electrodes were then pushed firmly onto the tray covering the electrode strips, silicone oil (90 mL) poured over the gel strips in the tray, and the lid of the I.F apparatus placed on the assembly.

The running program used was that suggested in the Immobiline Drystrip manual for 180 mm Drystrips with a pH range of 3 to 10 (Table 2.5). After isoelectric focusing, the strips were either used for the second dimension (section 2.3.4.2) immediately or stored at -80 °C for periods of up to 30 days.

	Urea	CHAPS	DTT	Ampholine <sup>R</sup>
Rehydration solution	8 M	2% (w/v)	40 mM	2% (v/v)
Sample denaturing solution	8 M	4% (w/v)	0.15 mM	-

Table 2.4. Formulations of solutions used in polyacrylamide gel strip rehydration for isoelectric focusing.

Phase	Voltage (V)	Current (mA)	Watts (W)	Time (h)	Volt h (Vh)
1	500	1	5	4.5	1500
2	500	1	5	5	10000
3	3500	1	6.5	6.5	43750
			Totals	20.5	55250

Table 2.5. Running program for isoelectric focusing of polyacrylamide gel strips.

### 2.3.4.2 Second Dimension SDS-PAGE gel

#### Reagents

Acrylamide [40% (w/v)]

Agarose

Ammonium persulfate (APS)

Bromophenol blue

Sodium Dodecyl Sulfate (SDS)

N,N,N',N'-tetramethylethylenediamine (TEMED)

Tris

One polyacrylamide slab gel (14 cm x 25 cm) was prepared for each first dimension I.F gel strip. The PAGE glass plates were washed with ethanol, wiped and dried. The plastic spacers were cleaned and wiped with petroleum jelly to assist in making a seal. The separating gel solution was made from the components listed in Table 2.6 (column A). Each formulated gel was mixed by swirling, then degassed using the Buchner funnel vacuum system. The components in column B were then added and the gel mixed by swirling. The separating gel was poured up to about 4.5 cm from the smallest plate and water overlaid. After the separating gel had polymerised (30 to 40 min) the water was poured off and the gel surface blotted dry with filter paper. The stacking gel formulation listed in Table 2.6 was mixed, degassed in the same way as the separating gel and the solution pipetted over the separating gel with a single well made using a piece of thin plastic (0.5 cm x 5 cm x 0.1 cm) at one side of the stacking gel. Water was overlaid on the stacking gel using the same procedure described for the separating gel.

The first dimension gel strips from section 2.3.4.1.2 were cut down so they would fit along the top of the gel. Initially 18 cm, each strip was reduced to 13 cm by removing 2 cm from the acidic end and 3 cm from the basic end using a sharp scalpel blade. The gel strips were pressed down onto the stacking gel where complete contact was made between the strip and the gel with no air bubbles. Molten agarose [0.5% (w/v)], containing 0.001% (w/v) of bromophenol blue, was swiftly pipetted across the gel strip. Once set, the gel was clipped into the electrophoresis apparatus (after removal of the bottom spacer) and the tanks filled with running buffer (section 2.3.3). Ten  $\mu\text{L}$  of pre-stained low range molecular weight markers (Bio-Rad) was pipetted into the single

well. The gel was set to run at a constant 20 mA for 6 h or until the bottom marker was about 2 cm from the bottom of the gel. On completion of electrophoresis, the gel apparatus was disassembled and the gel stained with a Coomassie G-250 stain (section 2.3.4.3).

#### 2.3.4.3 Staining the acrylamide gels from the second dimension

##### Reagents

Ammonium sulfate

Coomassie G-250 (Bio-Rad)

Methanol

Phosphoric acid

Each second dimension gel was washed 3 times in Milli-Q water (300 mL per gel), and after the final wash, with water, was replaced with the staining solution [0.4% Coomassie G-250 in 17% (w/v) ammonium sulfate, 2% (v/v) phosphoric acid and 34% (v/v) methanol]. The gels were stained for 4 days (destaining is not required when using this protein stain).

Volumes required for a single gel	Separating gel		Stacking gel	
	A	B	A	B
Acrylamide [40% (v/v)]	10 mL		1.3 mL	
Separating gel buffer (1.5 M Tris, pH 8.8)	7.5 mL		2.5 mL	
Milli-Q water	12 mL		6.1 mL	
SDS [10% (w/v)]		300 $\mu$ L		10 $\mu$ L
APS [10% (w/v)]		150 $\mu$ L		50 $\mu$ L
TEMED		15 $\mu$ L		100 $\mu$ L

Table 2.6. Components for the second dimension polyacrylamide gels.

### 2.3.5 Western analysis of SDS-PAGE gels

#### Reagents

Glycine

Methanol

Tris

Proteins separated on SDS-PAGE mini-gels were blotted onto polyvinyl difluoride membranes (PVDF membrane; Immobiline) using a Trans-Blot Electrophoretic Transfer Cell (Bio-Rad). Prior to the assembly of the apparatus, the PVDF membrane was soaked in methanol for 5 min and then in the transfer buffer [25 mM Tris, 190 mM glycine, 10% (v/v) methanol]. The transfer cassette with gel and membrane was assembled as shown in Figure 2.9, placed in the transfer cell and immersed in transfer buffer. Mini-blots were run at 30 V for 1 h for complete transfer.

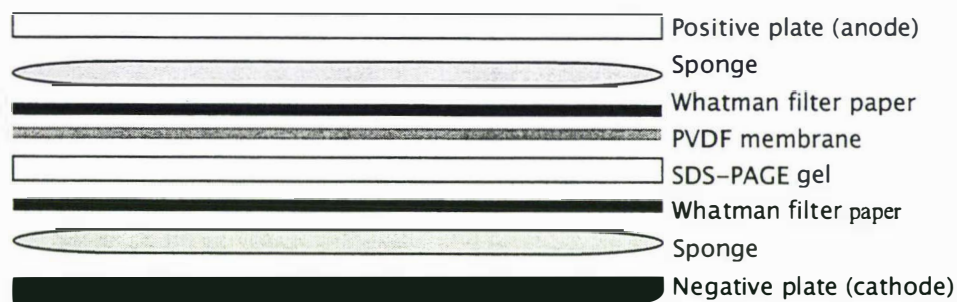


Figure 2.9. Assembly of the Western blotting apparatus

### 2.3.5.1 Immunodevelopment of electroblotted proteins

#### 2.3.5.1.1 Immunodevelopment of the electroblotted membranes

##### Reagents

Developing solution [150 mM Tris-HCL (pH 9.7), containing 0.01% (w/v) 5-bromo-4-chloro-3-indoyl phosphate [(BCIP), 0.02% (w/v) p-nitroblue tetrazolium (NBT), 1% (v/v) dimethyl sulphoxide (DMSO), 8 mM MgCl<sub>2</sub>]

##### I-Block (Tropix)

Phosphate Buffered Saline [PBS; 50 mM sodium phosphate (pH 7.4) containing 250 mM NaCl]

Phosphate Buffered Saline - Tween [PBS-T; PBS containing 0.5% (v/v) Tween 20]

On completion of electrophoretic transfer, the apparatus was disassembled and the membrane placed into a 0.2% blocking solution [PBS-T containing 0.2% (w/v) I-Block] for 1 h. After this time, the membrane was placed directly in the primary antibody solution (typically a 1 in 2000 dilution of antibody in PBS) and incubated for 1 h. The antibody solution was then tipped off, and the membrane washed 3 times (about 5 min for each wash) with PBS-T (ca. 50 mL per wash). The membrane was then incubated for 1 h with the secondary antibody (1 in 10 000 dilution of goat anti-rabbit IgG alkaline phosphatase conjugate). The membrane was then washed twice with PBS and twice more with 150 mM Tris-HCL, pH 9.7, to remove the phosphate that could interfere with the activity of the alkaline phosphatase conjugate. The membrane was then submersed in the developing solution. When the membrane developed the desired colorimetric result (typically between 2 to 15 min), the reaction was stopped by tipping off the developing solution and covering the membrane with water purified using reverse osmosis (RO water). Each incubation step and substrate development was performed at room temperature on a rocking or shaking platform.

#### 2.3.5.2 Amino acid sequencing of internal peptide sequences

Protein bands of interest were excised from SDS-PAGE mini-gels stained with Coomassie R-250 (section 2.3.3.1). The gel pieces were sealed in microfuge tubes filled with Milli-Q water and sent to Ms C. Knight at the School of Biological Sciences, University of Auckland to obtain internal amino acid sequence. The short internal sequences were obtained from the protein(s) from each excised acrylamide gel section

by eluting the protein(s) from the gel, treating with trypsin (which cleaves the peptide bond R-X and K-X, where X is any amino acid). The trypsin-cleaved peptides, that had been separated by micro-bore HPLC, were sequenced with a model 470A gas-phase sequencer, complete with an on-line phenylthiohydantoin amino acid analyzer. The chemicals and programs used for sequence analysis were supplied by the manufacturer (Applied Biosystems).

## 2.3.6 ACC oxidase activity measurements in petiole tissues

### 2.3.6.1 Extraction of ACC from petiole tissue

#### Reagents

Ammonium sulfate

DTT

Glycerol

Sodium ascorbate

Tris

The ACC oxidase assay described by McGarvey and Christoffersen (1992) and Fernandez-Maculet and Yang (1992) was used.

Petiole explant tissue was harvested at the appropriate time intervals, the tissues powdered by freezing in liquid nitrogen and grinding with a mortar and pestle. Six mL/gram (FW) of extraction buffer [0.1 M Tris (pH 7.5) containing 10% (v/v) glycerol, 30 mM sodium-ascorbate, 2 mM DTT] was then added to the frozen powder, and the mixture shaken vigorously on a shaking platform for 1 h at 4 °C.

The extracts were then filtered through 2 layers of Miracloth<sup>R</sup> (Calbiochem, La Jolla, California, USA), and the filtrate partially purified by ammonium sulfate precipitation. Firstly, ammonium sulfate was added to each extract to make a final concentration of 30% (w/v) and the mixture shaken vigorously on ice for 1 h. The extracts were then centrifuged (12 000g, 15 min, 4 °C), the pellet was discarded and the supernatant made to 90% ammonium sulfate saturation and the precipitation carried out as before. After centrifugation, the supernatant was discarded and the pellet dissolved in 1 mL of

Sephadex G-25 column equilibration buffer [50 mM Tris (pH 7.5) containing 10% (v/v) glycerol, 30 mM sodium ascorbate, 2 mM DTT].

#### 2.3.6.2 Preparation of samples for ACC oxidase assay using Sephadex G-25 spin columns

##### Reagents

DTT

Glycerol

Tris

To remove excess ammonium sulfate, the resuspended extracts from section 2.3.6.1 were eluted by centrifugation from Sephadex G-25<sup>R</sup> (Amersham) columns in a method similar to that described by Neal and Florini (1973).

Ten mL disposable syringes (Benton Dickenson) were first packed with 2 layers of GF-A glass microfibre filter paper (Whatman) at the delivery end and the tips sealed with parafilm. Sephadex G-25 column resin was pipetted into the syringe barrels to a volume of 5 mL (5 times the sample volume), the parafilm was then removed and the syringes placed in 50 mL tubes. The resin was then packed down by centrifuging the 50 mL tubes (containing the syringes) at 1000g for 1 min. Each column was then equilibrated with 5 volumes of the equilibration buffer (section 2.3.6.1) by centrifugation 1 mL samples were pipetted onto the columns. The syringes containing the samples were then placed into 50 mL plastic tubes and centrifuged at 1000g for 1 min. The eluates were then transferred to microfuge tubes and stored for short periods (less than 24 h) at  $-20^{\circ}\text{C}$ .

#### 2.3.6.3 ACC oxidase assay

##### Reagents

ACC

DTT

Glycerol

Iron Sulfate ( $\text{FeSO}_4 \cdot 7\text{H}_2\text{O}$ )

Sodium ascorbate

Sodium bicarbonate

Tris

Seven hundred microliters of each ACC oxidase enzyme preparation (section 2.3.6.2) was incubated at 30 °C for 3 min. After this pre-equilibration time, 200 µl (measured in triplicate) was pipetted into 5.5 mL-capacity vacutainer tubes containing 800 µl of a reaction mixture (pre-equilibrated at 30 °C), to give a final concentration of 50 mM Tris-HCL, pH 7.5, 1 mM ACC, 10% (v/v) glycerol, 2 mM DTT, 30 mM sodium ascorbate, 20 mM iron sulfate and 30mM sodium bicarbonate. The tubes were then sealed and the reactions incubated with shaking (175 rpm) at 30 °C for exactly 20 min after which time 1 mL gas samples were removed and the ethylene content determined using gas chromatography (section 2.3.7.1).

### 2.3.7 Measurement of ethylene production by intact petiole sections

Petioles, sampled at the appropriate time points, were cut into 2 sections as described in section 2.1.3. All samples were measured in triplicate. At least 0.2 g of each tissue sample was placed into 5.5 mL-capacity glass tubes, the tubes were then sealed for 1 hour with rubber bungs after which time gas samples of 1 mL were removed. After each sampling, the evolved ethylene samples were contained in the syringes by forcing the syringe needles into hard rubber block until measurement by gas chromatography.

#### 2.3.7.1 Measurement of ethylene using gas chromatography

The concentration of ethylene produced by and evolved from petiole sections was measured using a Gas Chromatograph (Shimadzu; model 3400) containing a 80% Porapak N/20% Porapak Q column (Alltech) and a flame ionization detector. The carrier gas was nitrogen with a flow rate of 40 mL/min. The flame was maintained by hydrogen and air both at 50 kPa. Several hours before use, the carrier gas, O<sub>2</sub> and air were turned on and at least 1 hour before use, the flame was generated. The column and injector temperatures were set at 250 °C.

A 1 mL standard of ethylene (0.99 ± 0.01 ppm; BOC Gases) was injected several times to calibrate the instrument. The ethylene peaks of the 1 mL sample gases were

identified by comparison with the retention time of the ethylene standard peak (typically 90 s).

### 2.3.7.2 Calculation of ethylene concentrations

The concentration of ethylene gas produced by the intact petiole tissues and from the ACC oxidase assay (sections 2.3.7 and 2.3.7.1) is expressed in nmol/h/g tissue FW. The amount of ethylene in ppm was calculated by measuring the height of each sample ethylene peak generated by the chart recorder (the peak with the same retention time of the 0.99 ppm standard ethylene peak) and comparing this measurement to the height of the ethylene peak generated with the 0.99 ppm standard gas. The number of moles the sample peaks represented could then be determined by calculating the number of moles of gas in the vacutainer tube (using the ideal gas equation) and multiplying this by the concentration of ethylene in ppm.

$$n = (PV/RT) \times \text{ppm} \times 10^{-6}$$

The ideal gas equation

n = total number of moles of gas in the vessel

P = pressure (kPa)

V = volume (L)

R = universal gas constant, 8.314 J K<sup>-1</sup> mol<sup>-1</sup>

T = temperature (298.15 K)

## 2.3.8 Measurement of aldose-1-epimerase activity

### 2.3.8.1 Preparation of plant extracts for the activity assay

Reagents

Tris

Soluble and bound proteins were extracted from the plant tissues as described in sections 2.3.1.1 to 2.3.1.3. These plant extracts, or those eluting from the hydrophobic, ion-exchange or gel filtration columns were adjusted to the assay buffer (100 mM Tris-HCl, pH 7.6) using NanoSep<sup>TM</sup> concentrators (section 2.3.1.5). The amount of protein

from the plant samples used in the enzyme assay was 100  $\mu\text{g}$  for crude and ultracentrifuged cell extracts, (section 2.3.1.3) and 8  $\mu\text{g}$  for all other partially purified extracts (except when measuring specific activity, where 20  $\mu\text{g}$  of protein was used for all samples)

## 2.3.9 Preliminary activity assays

### 2.3.9.1 Optimisation of the coupled enzyme assay

#### Reagents

$\alpha$ -D-glucose

Tris

Optimisation of the coupled enzyme assay involved firstly, determining the amount of substrate ( $\alpha$ -D-glucose) required in the coupled enzyme assay to give an appreciable rate but one which was below the  $V_{\text{max}}$  for glucose dehydrogenase (GDh). Secondly, establishing a concentration of glucose dehydrogenase that would result in the reactions reaching a linear rate between 5 to 15 min after the addition of the substrate. The buffer conditions used were for the optimal activity of glucose dehydrogenase [100 mM Tris-HCl (pH 7.6) containing a molar excess of  $\text{NAD}^+$  (0.5 mM) to GDh]. All reactions were performed at 20  $^{\circ}\text{C}$ . Mutarotase is active over a broad pH range (4.0 to 8.5) with the optimal activity of enzymes from mammalian sources at pH 7.4.

Freshly prepared reaction buffer (100 mM Tris-HCl, pH 7.6) was added to a disposable cuvette to give a final reaction volume of 1 mL. Between 0.01 and 15 units of mutarotase (porcine kidney; Roche) was added, and then 1 unit of glucose dehydrogenase (Sigma). In a microfuge tube,  $\alpha$ -D-glucose (10 mg) was added to 1 mL of reaction buffer and mixed by vortex for 10 seconds. The glucose solution (between 5 and 100  $\mu\text{L}$ ) was then rapidly added to the reaction mix in the cuvette and mixed by inversion (3 times over 10 seconds). The cuvette was then quickly placed in the spectrophotometer, which was adjusted to zero (time zero), and absorbance readings (340 nm) recorded every min.

The optimal concentration of  $\alpha$ -D-glucose in each 1 mL reaction was determined to be  $5.5 \times 10^{-4}$  M (equivalent to 0.1 mg per 1 mL reaction) in the coupled assay, containing 0.1 units of GDh. The conditions and the definition for determination of these optimal amounts is described in more detail in section 3.2.2.1.2. All subsequent assays were carried out with this concentration of  $\alpha$ -D-glucose. To assay the enzyme in the plant extract, aliquots of crude or partially purified enzyme (sections 2.3.1.1 to 2.3.1.4 and 2.3.1.6 to 2.3.1.8) were added in place of the porcine kidney enzyme.

#### 2.3.10 Calculation of the standard errors

The variances between data replicates in this thesis are expressed as standard errors. All of the graphs and data were generated, and the standard errors calculated, using the software program Microsoft Excel. The standard error is calculated by first calculating the standard deviation (SD), using the Microsoft Excel SD function, then dividing the SD by the square root of the number of samples.

## 2.4 Immunological methods

### 2.4.1 Production of polyclonal antibodies to indole-3-acetic acid (IAA)

The procedure used for generating polyclonal antibodies is essentially that described in Hock *et al* (1992).

#### 2.4.1.1 Conjugation of IAA to BSA

##### Reagents

Bovine serum albumin (BSA)

1-ethyl-3[3-dimethylaminopropyl]carbodiimide-HCL (EDC)

Indole-3-acetic acid (IAA)

Methanol

PBSalt [20 mM sodium phosphate (pH 7.1) containing 250 mM NaCl]

Sodium hydroxide

The immunoconjugate was synthesised using a carbodiimide reaction. Firstly, 10 mg of IAA was dissolved in 0.1 ml of absolute methanol and then made up to 8 mL with Milli-Q water, and the pH was adjusted to 6.5 with 1 M NaOH. The coupling reagent, EDC (20 mg) was dissolved in 0.5 mL of Milli-Q water and the pH adjusted to 6.5 with 0.01 M NaOH. The IAA and EDC solutions were mixed, then slowly stirred in the dark for 1 h at 25 °C. Over a time period of 15 min, 20 µL aliquots of a 50 mg/mL BSA solution, pH 6.5, were then pipetted into the IAA-EDC solution. To remove the O<sub>2</sub> from the reaction vessel, N<sub>2</sub> gas was blown into the reaction mix for 2 to 3 min and the reaction vessel then sealed. The mixture was then stirred slowly in the dark for 18 h at 25 °C. The BSA-IAA conjugate was then dialysed for 3 days against PBSalt at 4 °C.

The effectiveness of the conjugation was estimated by comparing the elution of conjugated and non-conjugated BSA using hydrophobic Phenyl Superose column chromatography (section 2.3.1.6). Two mg of each protein conjugate was loaded onto the column and it was expected that the conjugated BSA would be more hydrophobic, because of the attached hydrophobic IAA compounds. Therefore, it would elute from the column later than unconjugated BSA. The BSA-IAA conjugate did elute later (at 90% B, Figure 2.10b), when compared with the unconjugated BSA (at 65% B, Figure 2.10a).

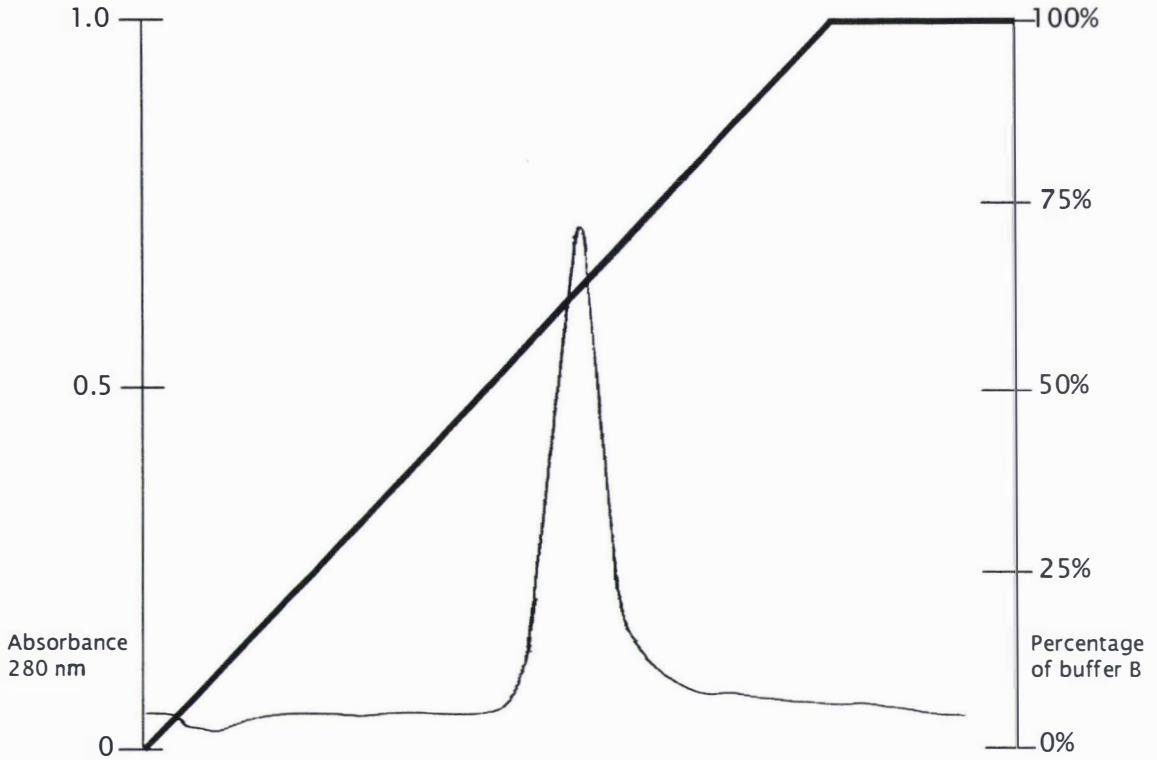


Figure 2.10a. Elution of BSA from the Phenyl Superose HR 1/1 hydrophobic interaction column (section 2.3.1.6).

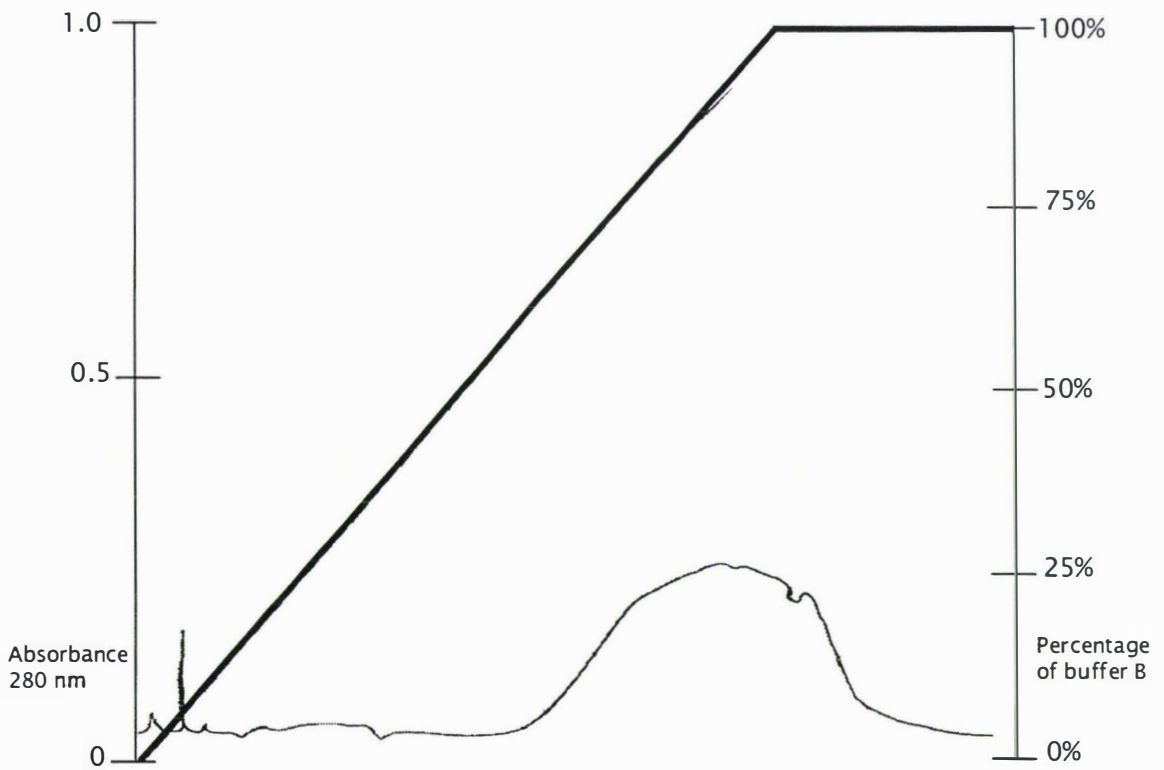


Figure 2.10b. Elution of the BSA-IAA conjugate from the Phenyl Superose HR 1/1 hydrophobic interaction column (section 2.3.1.6).

( — ) = A<sub>280nm</sub>

( — ) = % buffer B

#### 2.4.1.2 Immunisation of rabbits with the BSA-IAA conjugate

Two six-month-old rabbits (NZ White) were initially bled from the ear vein to obtain a control serum (*c.* 5 mL). Each rabbit was then immunised with 0.5 mL of BSA-IAA (*c.* 0.6 mg) emulsified in 0.5 mL of Freund's complete adjuvant (Difco). To emulsify the immunoconjugate and adjuvant, the mixture was vortexed rapidly in 10 mL glass bottles for at least 1 min, until no bilayer formed on standing.

The rabbits were boosted a further 3 times at 4 weekly intervals by subcutaneous injections of the antigen at different positions down the back of the animal. Each boost contained 0.5 mL of IAA-BSA conjugate (*c.* 0.3 mg) with 0.5 mL of Freund's incomplete adjuvant (Difco).

#### 2.4.1.3 Antisera preparation and immunoglobulin G (IgG) purification

##### Reagents

Ammonium sulfate

Sodium hydroxide

Sodium phosphate

The rabbit blood was collected into plastic tubes (15 mL Falcons) and kept for 1 h at room temperature. The clot was then removed from the sides of the tube with a syringe needle and the tube left for a further 18 h at 4 °C for further clotting. The serum was separated from the clot by tipping the entire contents into a small glass funnel, the clot remaining in the top of the funnel, and the serum collecting into microfuge tubes. The microfuge tubes were then centrifuged (5 000g for 10 min at 20 °C), and the supernatant collected.

The portion of the serum containing the IgG fraction was partially purified by ammonium sulfate precipitation. Five mL of saturated ammonium sulfate was added to 10 mL of serum and the pH adjusted to 6.3 with 1 M NaOH. The serum was agitated for 30 min at 20 °C on a shaking platform then centrifuged (10 000g for 10 min at 20 °C). The supernatant was discarded and the pellet re-suspended in 10 ml (the original serum volume) of 0.07 M sodium phosphate, pH 7.4. The serum fraction was then

placed into dialysis tubing (3/4 diameter, GibcoBRL) and dialysed against 3 500 mL changes of 0.07 M sodium phosphate, pH 6.3.

To further purify the IgG fraction, the dialysed serum was eluted from a anion exchange DEAE Sephacel column (Diethylaminoethyl resin; Amersham). The columns were made as described in section 2.6.2 for Sephadex G-25 columns except an equal volume of resin to serum was used. Columns were equilibrated with 5 volumes of 0.07 M sodium phosphate, pH 6.3, before the addition of the dialysed serum. The serum was eluted with the same buffer used to equilibrate the columns, with a flow rate of approximately 0.5 mL/min. Fractions of 1 mL were collected and the protein content of each fraction monitored by measuring the absorbances at 280 nm. The large early eluting protein peak observed contains the IgG fractions. The fractions containing the most protein in this peak were combined and used for the immunoassay. The purified IgG was stored at  $-20^{\circ}\text{C}$  until use.

## 2.4.2 The Enzyme Linked Immuno-Sorbant Assay (ELISA) for the determination of IAA content in plant tissues

### 2.4.2.1 Extraction and methylation of IAA

#### 2.4.2.1.1 Preparation of diazomethane

##### Reagents

Absolute ethanol

Acetic acid

Diazogen<sup>R</sup> (ACROS)

Diethyl ether

IAA

Potassium hydroxide

There are two approaches commonly used to methylate small amounts of compound using diazomethane (DZM). Firstly, DZM can be synthesized, then added to the solution containing the compound with the  $-\text{COOH}$  group to be methylated. Alternatively, in a method that does not require the use of specialised distillation equipment, the methylation of IAA can be done *in situ*, as DZM is being generated

(Hock *et al* 1992). Both the *in situ* and the diazomethane distillation methods were used for the methylation of sample and standard IAA solutions. By comparing ELISA measurements (data not shown), the most effective method of  $-\text{COOH}$  group methylation of IAA appeared to be through adding diazomethane previously prepared, as shown by more sensitive IAA standard curves. Consequently prepared DZM was used for the methylation of sample and standard IAA solutions.

There are three methods for synthesis of DZM described by Schwartz and Bright (1974) and one of these methods, used in this thesis, is described below.

Diazomethane is usually synthesised from the precursor N-methyl-N-nitrosotoluene p-sulphonamide, purchased as Diazogen<sup>R</sup>. Reacting this methyl nitrosamide with potassium hydroxide will form diazomethane (Figure 2.11).



Figure 2.11. The diazomethane ( $\text{CH}_2\text{N}_2$ ) forming reaction.

The specialised distillation equipment, with no ground glass connections (Wheaton) was assembled in the fume hood. Extreme care was taken when handling the distilled diazomethane as it is toxic and forms explosive crystals on ground glass edges.

Absolute ethanol (25 mL) and 7.5 mL of  $\text{H}_2\text{O}$  containing 4.9 g of potassium hydroxide was mixed and placed in a conical flask, partially submerged in a  $65^\circ\text{C}$  water bath, with a dropping funnel. Diazogen (10.5 g) was dissolved in 25 mL of diethyl ether and placed in the dropping funnel. The Diazogen solution was added slowly to the potassium hydroxide mixture containing boiling chips. The gaseous DZM was condensed and collected in a conical flask covered in ice. When all the Diazogen mixture had reacted (approximately 90 min), 10 mL of diethyl ether was placed in the dropping funnel and added slowly to the potassium hydroxide mixture. After the ether had evaporated, the equipment was disassembled and the DZM placed into a Schott bottle and stored at  $-20^\circ\text{C}$ . The methylating efficiency of DZM appears to deteriorate within 21 days (D. Officer, *pers comm*). To check if it is still effective, a small sample

was placed into a conical flask and 1 drop of 0.2 M acetic acid added. If the solution clears then DZM is still present.

#### 2.4.2.1.2 Extraction and methylation of IAA in bean tissues

##### Reagents

Extraction solution [80% (v/v) methanol containing 4.5 mM butylated hydroxytoluene]

Diazomethane (DZM)

Diethyl ether

Tris Buffered Salt [TBSalt; 20 mM Tris-HCL, (pH 7.4) containing 250 mM NaCl]

IAA was extracted from petiole tissues using a method derived from Hock *et al* (1992) and Weir (1978).

Plant tissues, collected as described in section 2.1.3, were ground in microfuge tubes using a Vertis 45 grinder (Vertis) in 10 volumes of extraction solution. The material was then ground further using a mortar and pestle and then shaken vigorously for 1 h at 4 °C. Extracts were then centrifuged (12000g for 10 min at 4 °C) and the supernatant pipetted into microfuge tubes. The remaining ground tissues (pellets) were re-extracted twice with fresh extraction solution by shaking for 1 h at 4 °C, centrifuging, and collecting the supernatants as described.

The volume of each extract was reduced to less than 20% of its original volume, using a Speedvac Dryer (Savant SC200), to ensure the majority of the methanol had been removed. The extracts were then combined and the pH adjusted to 2.5 with 1 M HCL. Diethyl ether (1.5 mL per 1 mL of reduced extract) was added to each of the reduced aqueous samples, the samples then shaken vigorously, the bilayer left to reform and the organic phase containing the IAA removed. The diethyl ether extraction of the aqueous phase was repeated twice to assist with the transfer of the IAA from the aqueous to the organic phase. The three diethyl ether extracts for each sample were combined in microfuge tubes.

Each sample extraction in diethyl ether was methylated by the addition of diazomethane (section 2.3.8.1.1). Ether extracts were cooled to -20 °C prior to methylation to increase the effectiveness of the IAA methylating reaction. Diazomethane was added to

each of the extracts in molar excess (about 0.2 mL of prepared diazomethane solution was added to 1 mL of extract), and the extracts agitated vigorously on a rocking table for 30 min at 4 °C. The excess DZM was then quenched with the addition of 10 µL of 0.2 M acetic acid and the extracts completely dried in the Speedvac Dryer. The methylated sample IAA was dissolved in 0.5 mL of TBS by vertical rotary mixing for 18 h at 4 °C. The samples were assayed immediately using ELISA.

#### 2.4.2.1.3 Methylation of IAA in a stock solution

##### Reagents

Absolute methanol

Acetic acid

Diazomethane (DZM)

IAA

IAA was methylated using the same technique as used to methylate the sample solutions. To make a 10 mM stock solution, IAA (17.92 mg) was dissolved in 9 mL of absolute methanol to which 950 µL of the prepared DZM solution (section 2.4.2.1.1) was added. The mixture was agitated for 30 min at 4 °C. After this time, 50 µL of 0.2 M acetic acid was added and the stock solution transferred to an amber bottle and stored at -20 °C.

#### 2.4.2.2 Synthesis of the IAA-alkaline phosphatase conjugate (ELISA tracer)

##### Reagents

Dimethylformamide

1-ethyl-3[3-dimethylaminopropyl]carbodiimide-HCL (EDC)

Glycerol

Methanol

PBSalt [20 mM sodium phosphate (pH 7.1) containing 250 mM NaCl]

Sodium hydroxide

The IAA-alkaline phosphatase conjugate (tracer) was synthesised as described in Hock *et al* (1992).

Firstly, IAA was attached to the coupling reagent (EDC) by dissolving 10  $\mu\text{mol}$  IAA in 0.2 mL of 50% (v/v) dimethylformamide and adding it to the EDC solution (20  $\mu\text{mol}$  in 0.1 mL of  $\text{H}_2\text{O}$ ). The pH was adjusted to 6.5 with 0.01 M NaOH and incubated with slow stirring for 1 h at 25  $^{\circ}\text{C}$ . Alkaline phosphatase (1 mg, 3000 U/mg, Boehringer) was diluted in 200  $\mu\text{L}$  of 50% (v/v) dimethylformamide and added over at least 90 min, in 20  $\mu\text{L}$  portions, to the IAA-EDC solution. The reaction vessel was then flushed with  $\text{N}_2$  and tightly closed. The mixture was stirred slowly for 18 h at 25  $^{\circ}\text{C}$  in the dark on a magnetic stirrer, then dialysed against 5% (v/v) dimethylformamide for 8 h and subsequently for 3 days against PBSalt. The dialysed tracer was mixed with glycerol in a ratio of 1 to 1.2 (v/v) respectively and stored at  $-20^{\circ}\text{C}$ .

#### 2.4.2.3 Optimising the volume of the IAA-alkaline phosphatase tracer for use in the ELISA

##### Reagents

*p*-nitrophenol phosphate (pNPP)

Diethanolamine (DEA)

Magnesium chloride

To determine the optimal volume of the alkaline phosphatase-IAA conjugate (tracer) that would be required for ELISA, a series of assays was performed that did not require the use of an IAA antibody.

The substrate solution for alkaline phosphatase was prepared by dissolving a pNPP tablet (20 mg) in 0.9 M DEA, pH 9.8, containing 0.3 mM  $\text{MgCl}_2$  (20 ml). A range of volumes of a 1 in 100 dilution of the tracer (0, 1, 5, 10, 20 and 50  $\mu\text{L}$ ) were pipetted into the wells of the microtiter plates (Nunc) with 50  $\mu\text{L}$  of the substrate solution and each made up to a reaction volume of 100  $\mu\text{L}$  with DEA buffer. The reactions were incubated at 37  $^{\circ}\text{C}$  and read every 10 to 15 min at 405 nm with the plate reader (Anthos). An optimal tracer concentration was estimated as the amount required to give an absorbance change of about 1.5 absorbance units (Au) in 15 min at 37  $^{\circ}\text{C}$ . Using this method, the optimal volume of prepared tracer was estimated as 20  $\mu\text{L}$  of a 1 in 100 dilution per assay. Once determined, the tracer concentration was kept constant in polyclonal and monoclonal IAA ELISAs.

#### 2.4.2.4 Antibody immobilised ELISA

##### Reagents

##### I-Block

Methylated IAA (section 2.4.2.1.3)

PBSalt - Tween (PBSalt-T; 20 mM sodium phosphate (pH 7.1) containing NaCl (250 mM) and 0.5% (v/v) Tween 20)

Sodium carbonate

Substrate solution (section 2.4.2.3)

TBSalt (section 2.4.2.1.2)

Tracer (section 2.4.2.2)

The antibody immobilised ELISA, where the primary IAA antibody was coated on to the immuno-microtiter plate first, is described in Weir 1978. Mouse immunoglobulins (IgGs) adsorb poorly to the polystyrene microtiter well surface and so when using the monoclonal IAA antibodies (derived from hybridomas constructed from the spleen cells of mice), a goat anti-mouse immunoglobulin was coated to the plate first, and then the mouse monoclonal attached to the immobilised anti-mouse antibody.

For the monoclonal based assay, goat anti-mouse IgG (whole molecule, Sigma) was dissolved in 50 mM sodium carbonate, pH 9.5, to give an antibody coating concentration of 0.1  $\mu\text{g}/\mu\text{L}$  (10  $\mu\text{g}$  per reaction). Anti-mouse antibody (100  $\mu\text{L}$ ) was added to each well of an immunosorbant microtiter plate (Nunc) and the plate covered and incubated for about 18 h at 4  $^{\circ}\text{C}$ . After incubation, the anti-mouse IgG was tipped off, the plate patted dry with paper towels and the wells washed 3 times with PBSalt-T. After each addition of PBSalt-T, the wells were left for 10 min, the PBSalt-T then tipped off and the plate patted dry. The IAA monoclonal mouse IgG (Idetek) was prepared by dissolving the commercially available lyophilised IgG (1 mg) in coating buffer to give a final concentration of 0.06  $\mu\text{g}/\mu\text{L}$  (6  $\mu\text{g}$  per reaction). The prepared anti-IAA antibody (100  $\mu\text{L}$ ) was added to each well and the plate covered and incubated for 18 h at 4  $^{\circ}\text{C}$ . After this time, the IgG solution was tipped off and the plate washed with PBSalt-T as before. Standard curves for IAA using the monoclonal antibody were constructed as described in the methods accompanying the commercially available monoclonal IAA antibody (Idetek). Standard solutions of IAA were prepared by

diluting a 10 mM stock solution of methylated IAA to 20 pmol/ $\mu$ L and then serial dilutions of 10, 5, 2.5, 1, 0.5, 0.2, and 0.01 pmol/ $\mu$ L were made with TBSalt from this dilution. All standard solutions were made just prior to measurements. Sample solutions for measurements of IAA were prepared as described in section 2.4.2.1.2. After the anti-IAA IgG incubation described above, the sample and standard IAA solutions were added to their respective wells (100  $\mu$ L of each per well) and the plate covered with plastic film. The plate was then incubated for 3 h at 37  $^{\circ}$ C with gentle agitation. After this time, the tracer (20  $\mu$ L) was added to the reactions and the plate incubated at 37  $^{\circ}$ C for 30 min. The reactions were then tipped off and the wells washed and dried as before. Substrate solution (100  $\mu$ l) was then added to each well and the plate incubated for 10 min at 37  $^{\circ}$ C. After this time, the absorbance values were read at 405 nm using the microtiter plate reader. The reactions were incubated at 37  $^{\circ}$ C for longer periods if the absorbance values for the zero standard (no IAA, maximum binding of the tracer) were less than 1.5 Au.

ELISAs using the polyclonal antibodies, generated in rabbits, did not require the pre-coating of a supporting antibody on the immunosorbent plates to assist in adsorption of the IgGs. Aside from this, the assay procedure was the same as that used for the monoclonal antibody. Initially, to assess the IAA IgG titres of the polyclonal antisera, 100  $\mu$ l of a dilution range (undiluted, 10, 100, 1000, 5000 and 10 000-fold) of partial purified antisera (section 2.4.1.3) were coated to the immunosorbent wells. One  $\mu$ g of either BSA or IAA-CH<sub>3</sub> in TBSalt were added to each well in the place of the standard IAA solutions for the monoclonal ELISAs.

The percentage binding (%B) of the IAA tracer to both the polyclonal and monoclonal antibodies for each standard or sample was determined using the calculations in Appendix A. The %B values obtained for the IAA standard solutions were plotted against the IAA standard concentrations using a log-linear scale to generate a standard curve for the measurement of IAA in the plant extracts.

### 2.4.3 Affinity purification of antisera raised to a glutathione S-transferase (GST)-fusion protein to remove the GST epitopes

#### Reagents

Ammonium sulfate

PBS

The IgG component of the antisera was precipitated with a 50% (v/v) saturated ammonium sulfate solution as described in section 2.4.1.3. After dialysis of the IgG against 100 volumes of PBS (3 changes over 48 h), the protein content was measured using the Bradford assay (section 2.3.2) and 500  $\mu\text{g}$  of IgG added to 100  $\mu\text{L}$  of Glutathione Sepharose Resin (Amersham), where 1 mL of resin will bind 5 mg of GST protein. The mixture was then incubated for 1 h at 37  $^{\circ}\text{C}$ . After this time, the resin was centrifuged (5000g for 5 min) and the supernatant containing the affinity purified IgG collected. Another 100  $\mu\text{L}$  of resin was then added to the supernatant and incubated and collected as before.

There were two gp40 antibody preparations used for Western analysis and these are described in section 3.2.2.2. Both the antisera and monospecific antibodies to gp40 were obtained from the laboratory of Heese-Peck and Raikhel (described in Heese-Peck and Raikhel 1998). The affinity purification of gp40 from the antisera, using the method described in this section, did not improve the titer of the gp40 antibodies and so was not used for detection of gp40-like proteins in the cell wall-bound protein extracts.

## Chapter Three

# Abscission cell-specific proteins that denote the differentiated state

### 3.1 Identification of proteins in the rachis and leaflet abscission zones of *Sambucus nigra*

#### 3.1.1 Introduction

An analysis of the ionically-associated cell wall proteins in the rachis and leaflet abscission zone tissue of the elder was conducted to determine whether there were proteins that appeared in these cells that were not present, or present in lower abundance, in the surrounding rachis tissue. Comparisons were also made between the proteins of the abscission zone cells and those of the surrounding tissue after ethylene treatment. This survey of the cell wall fractions from ethylene and non-ethylene treated abscission zone and rachis tissues was conducted over the spring (September to November), summer (December to February) and autumn (March to May) seasons. In terms of terminology for different tissues, the following scheme was used: mid-rachis without ethylene = MR; ethylene treated mid-rachis = MRE; abscission zone tissue prior to ethylene treatment = OZ; ethylene-treated abscission zone at separation = ZONE. For the purposes of this thesis, proteins are identified by an approximate molecular mass (e.g. ca. 40 kDa), calculated from the immediate protein standard markers. This is because the mass of any protein of interest was determined from a plot of the molecular mass of the protein standards against their mobility. However, in this thesis, single percentage (12.5%) mini-acrylamide gels were used, and so the log relationship was often distorted. The author is aware that for accurate determination of molecular weight using SDS-PAGE, acrylamide gradient gels should be used (Hames and Rickwood 1981).

### 3.1.2 Changes in the cell wall protein profile from MR, MRE, OZ and ZONE samples collected in spring, summer and autumn

The initial comparison of the ionically-associated proteins in the cell wall collected over the three seasons (spring, summer and autumn) using SDS-PAGE is given as Figures 3.1 a to 3.1 c and protein bands of interest are summarised in Table 3.1. This comparison investigates major changes in the cell wall protein components that can be seen using one-dimensional SDS-PAGE, and as expected, there are several major proteins that occur in all of the tissues. However, because of the abundance of proteins in the cell wall it is not possible to conclude that bands of the same size in different tissues are the same protein. Nevertheless, in the following comparisons, a protein band that appears in one tissue type and is absent from another will be designated as preferentially-expressed in that tissue. As well as a comparison of proteins between tissues, extraction and separation of cell wall proteins over spring, summer and autumn affords comparison of the influence of seasons on protein expression, and these differences are also shown in Figure 3.1a to 3.1c and summarised in Table 3.1.

The comparison of protein bands revealed five major groups of preferentially-expressed proteins. A description of each of the groups of proteins is as follows: Group I proteins are preferentially-expressed in the non-ethylene treated mid-rachis (MR) tissue; Group II proteins are preferentially-expressed in both the MR and non-ethylene treated abscission zone (OZ) tissues; Group III proteins are preferentially-expressed in the ethylene treated MR tissue (MRE); Group IV proteins are preferentially-expressed in both the ethylene-treated abscission zone cells and rachis tissue (i.e. ZONE and MRE) and Group V proteins are expressed in the OZ tissue only. The arrows on each gel (Figures 3.1 a to 3.1 c) indicate the location of these proteins, and Table 3.1 summaries these proteins into their groups.

Group I comprises proteins of sizes ca. 18, 24 and 72 kDa, with the ca. 24 kDa polypeptide present as a preferentially-expressed protein in all seasons. The ca. 18 kDa polypeptide appeared to preferentially accumulate in the MR tissue, but only in the tissues collected in the summer months. The ca. 72 kDa protein is only preferentially-expressed in the MR tissue collected in spring. There are proteins of this size in the MR tissue collected in the summer and autumn months but they do not appear clearly to be

preferentially-expressed. Group II comprises proteins of sizes ca. 28, 30, 34 and 37 kDa. None of these proteins appear in tissues collected in more than one season although it is possible that the ca. 37 kDa protein is present in tissues collected in the summer gel but is masked by other bands. These proteins are not apparent when these tissues are exposed to ethylene over (48 h; i.e. not present in the MRE and ZONE tissues) possibly due to either a down-regulatory effect of ethylene or deterioration of the proteins over the time taken for ethylene treatment (48 h) i.e. they disappear with tissue ageing. There are six group III proteins, induced specifically in the mid-rachis tissue by ethylene, ranging from ca. 21 to 80 kDa. In common with the group II proteins, the MRE-specific group III proteins do not appear in more than one season. There are four visible group IV proteins of ca. 17, 18, 30 and 36 kDa. The two smaller (17 and 18 kDa polypeptides) are visible in both the spring and summer-collected tissue but are not clear in the autumn- collected tissue. The ca. 36 kDa protein is clearly more abundant in the MRE and ZONE tissues collected in the spring, but this apparently ethylene-induced protein, along with the ca. 30 kDa polypeptide observed in the gel of the spring-collected tissue, is not resolvable in the summer-collected tissue, and does not appear to be present in the autumn-collected tissue. Group V comprises of two proteins of ca. 15 and 38 kDa. The ca. 15 kDa protein may be present in other tissues but appears preferentially-expressed in the summer when compared with the spring and autumn collections. The ca. 38 kDa protein is resolvable only in the autumn tissue, but perhaps is masked in the gel of the summer tissue by other abundant proteins of similar size.

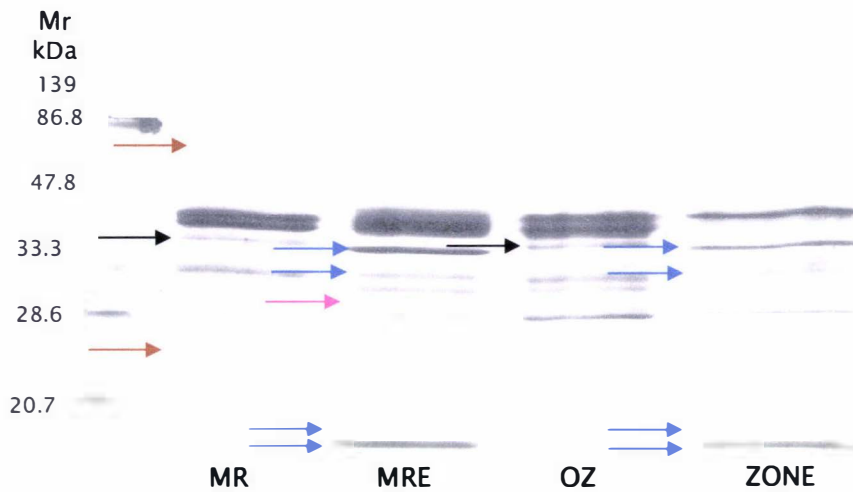


**Figure 3.1a.** Separation of cell wall protein extracts of MR, MRE, OZ and ZONE tissues collected in the spring using SDS-PAGE through a 12 % polyacrylamide gel. Proteins are visualised with Coomassie blue R-250 staining.

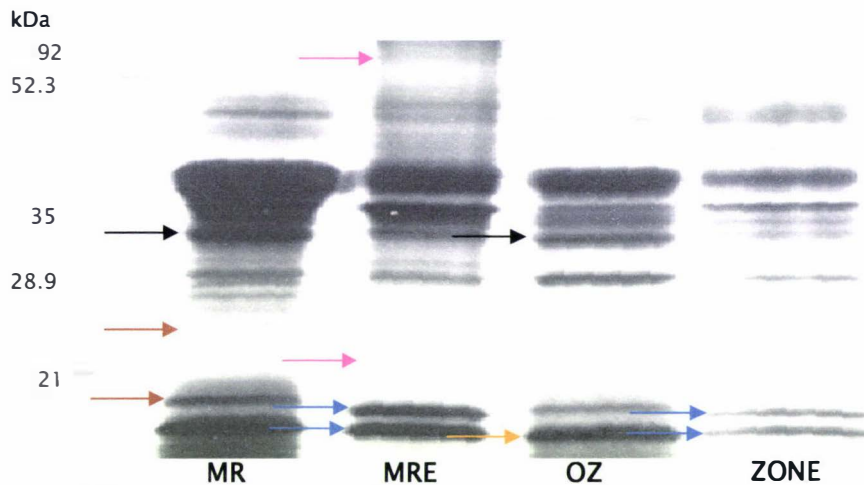


**Figure 3.1b.** Separation of cell wall protein extracts of MR, MRE, OZ and ZONE tissues collected in the summer using SDS-PAGE through a 12 % polyacrylamide gel. Proteins are visualised with Coomassie blue R-250 staining.

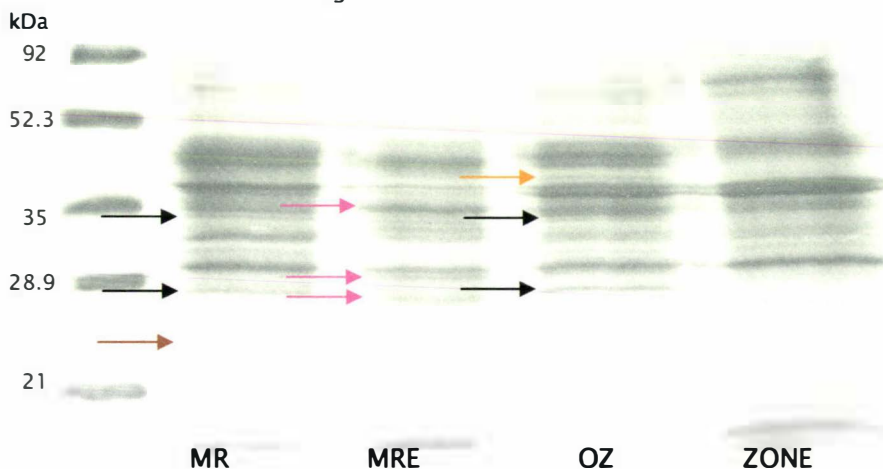


**Figure 3.1c.** Separation of cell wall protein extracts of MR, MRE, OZ and ZONE tissues collected in the autumn using SDS-PAGE through a 12 % polyacrylamide gel. Proteins are visualised with Coomassie blue R-250 staining.

G R O U P	Tissue location of protein bands	Spring (a)	Summer (b)	Autumn (c)
		(from Figure 3.1a)	(from Figure 3.1b)	(from Figure 3.1c)
ca. mass of proteins (kDa)				
I	MR (brown arrows)	24 72	18 24	24
II	MR & OZ (black arrows)	37	30	28 34
III	MRE (pink arrows)	30	21 80	32 27.5 29
IV	MRE & ZONE (blue arrows)	17 18 36 30	17 18	
V	OZ (orange arrows)		15	38

Table 3.1. Summary of proteins designated as unique or preferentially-expressed in the cell walls of the tissues indicated, and collected in Spring ((a); from Figure 3.1a) Summer ((b); from Figure 3.1b) and Autumn ((c); from Figure 3.1c).

### 3.1.3 Fractionation of cell wall extracts to discover unique or preferentially-expressed proteins in the ethylene and non-ethylene treated tissues

The initial investigation using SDS-PAGE identified a wide array of proteins as preferentially-expressed in some tissues, or altered in response to seasonal changes (section 3.1.2). Of most relevance to this investigation are the proteins that appear only in the abscission zone cells either before (OZ) or after ethylene treatment (OZ and ZONE). From the crude cell wall extracts, there appeared to be two proteins (ca. 15 and 38 kDa) which were unique or preferentially-expressed in the cell walls of the leaflet abscission zone cells before ethylene treatment (OZ) and which were not in the surrounding rachis tissue (Group V, Table 3.1). However, analysis of the cell wall extracts using one-dimensional SDS-PAGE is limiting as many less abundant proteins are masked by those more abundant. Therefore, to identify additional proteins, the crude cell wall extracts needed to be separated further. In this study, cell wall extracts from each of the four tissues collected in the spring were separated using hydrophobic interaction chromatography (HIC). Proteins were bound onto the column and eluted using a gradient from 2 M  $(\text{NH}_4)_2\text{SO}_4$  (0 % B) to 20 mM potassium phosphate, pH 7 (100 % B) and fractions collected over 5 % intervals of buffer B during the elution. An example of an FPLC trace from the Phenyl Superose HIC column separation of a MR extract is illustrated in Figure 3.2a. Collected fractions were further allocated a letter (A to K) indicating the percentage B range they eluted from. Fractions A, B and C contain pooled fractions 0 to 20 %, 20 to 40 % and 40 to 60 % respectively. These fractions contained a low concentration of protein and few resolvable polypeptides and so were not examined further. The other extract fractions (D to K) were compared using SDS-PAGE. The separations are shown as Figures 3.2b to 3.2e, and a summary of the results is displayed as Table 3.2.

As with the analysis of the gels of tissue collected in different seasons (section 3.1.2), the proteins that were of initial interest in the HIC fractions were those preferentially-expressed in the OZ tissue only, or in OZ and ZONE tissues. At least six peptides (ca. 10, 34, 36, 40, 74 and 75 kDa) were present in the abscission zone cells before (OZ) and after abscission (ZONE, Table 3.2). In all of the groupings (except MRE and ZONE) there were proteins that appeared in more than one fraction, most notably the ZONE-specific proteins that constituted most of the tissue-specific or preferentially-expressed

peptides (with 13 members). Seven proteins in this ZONE-only grouping (ca. 10, 30, 33, 35, 36, 46 and 76 kDa) appeared to be present in two or more fractions with the remaining 6 proteins (ca. 11, 23, 25, 27, 32 and 29 kDa) appearing in one fraction only (Table 3.2).

The process of fractionating the crude cell wall extracts using HIC highlights proteins of lower abundance. Therefore, the SDS-PAGE gels of these fractions revealed many more proteins that were not discernable in the crude extracts. Resolution of single protein bands on the gels produced from the fractionated extracts was still hindered by the large number of proteins of similar size in each fraction. Therefore, Fraction I (Figure 3.2d) from the OZ and MR samples was examined further because of the relatively high proportion of proteins bands between 36 and 45 kDa that were indistinguishable from one another in the one-dimensional gel. Moreover, fraction I was the fraction with the highest concentration of protein (ca. 100  $\mu$ g), and this ensured that there would be sufficient for two-dimensional (2-D) electrophoretic analysis.

Separation of the proteins in fraction I further using 2-D electrophoresis revealed at least two proteins that are preferentially-expressed in the OZ tissue (Figure 3.2f and g). From the 2-D gel, protein a is estimated to be between 40 and 45 kDa and has a pI of 8.3. A less abundant protein of the same size and a pI of 9.6 can also be seen in the OZ fraction (Figure 3.2f, protein b). Neither of these two spots was discernible in the MR fraction (Figure 3.2g). An attempt was made to determine some internal amino acid sequence from a tryptic digest of protein a (Figure 3.2f) but no sequence was obtained. The failure to obtain any amino acid sequence from the tryptic fragments generated from protein a is thought to be due to the sensitivity limits of the separation and sequencing instruments used. The use of 2-D gel electrophoresis, however, does demonstrate that it is a powerful technique for the resolution and identification of putative cell-specific proteins. However, due to the limited opportunities to repeat the 2-D gels, the emphasis of this thesis moved to the identification of some of the cell wall proteins revealed after HIC separation.

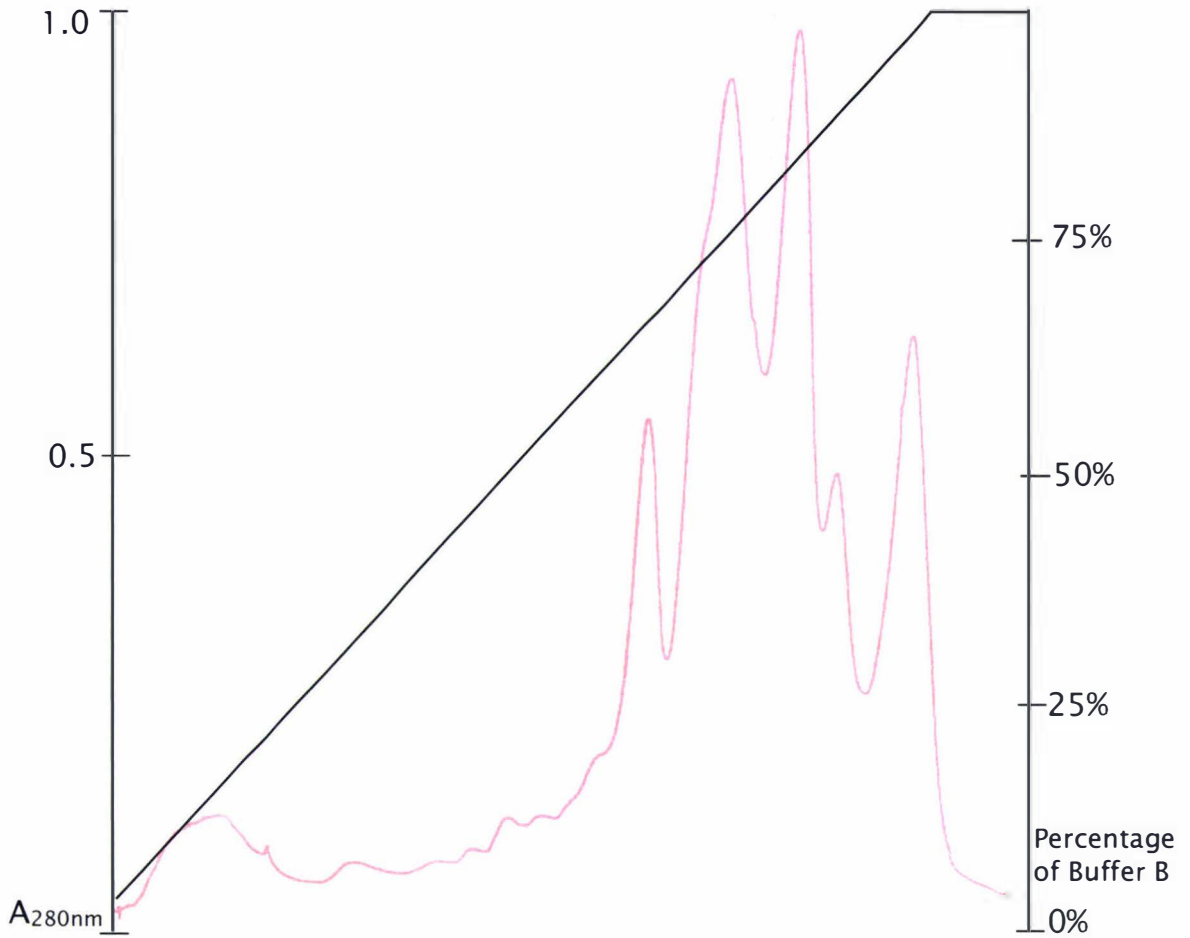


**Figure 3.2 a.** Separation of a MR cell wall sample through a hydrophobic interaction column (Phenyl Superose HR 1/1).

( — ) =  $A_{280\text{nm}}$     ( — ) = % buffer B

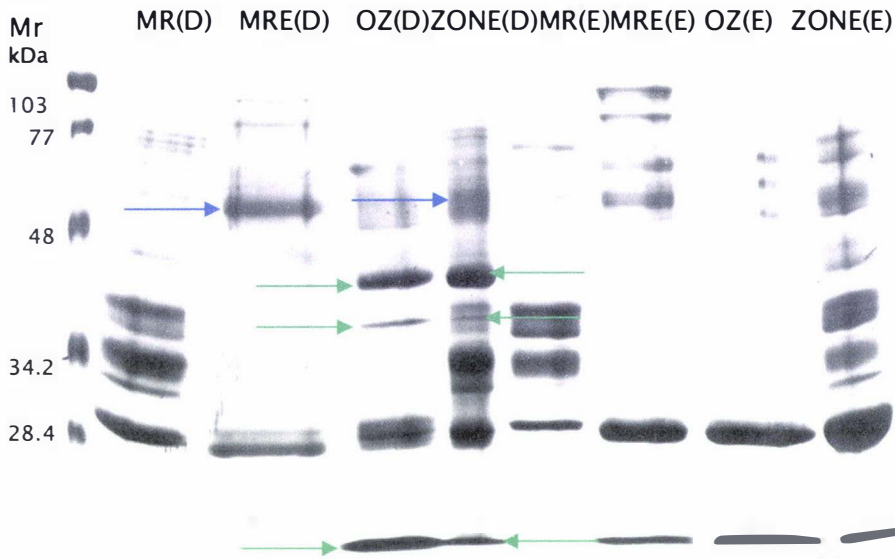


Figure 3.2b. Separation, using SDS-PAGE, of HIC fractions D (eluted with 60–65 % buffer B) and E (eluted with 65–70 % buffer B) obtained from the Phenyl Superose column chromatography separation of spring-collected MR, MRE, OZ and ZONE tissue. Proteins are visualised with Coomassie blue R-250 staining. The arrows indicate proteins of interest summarised in Table 3.2.

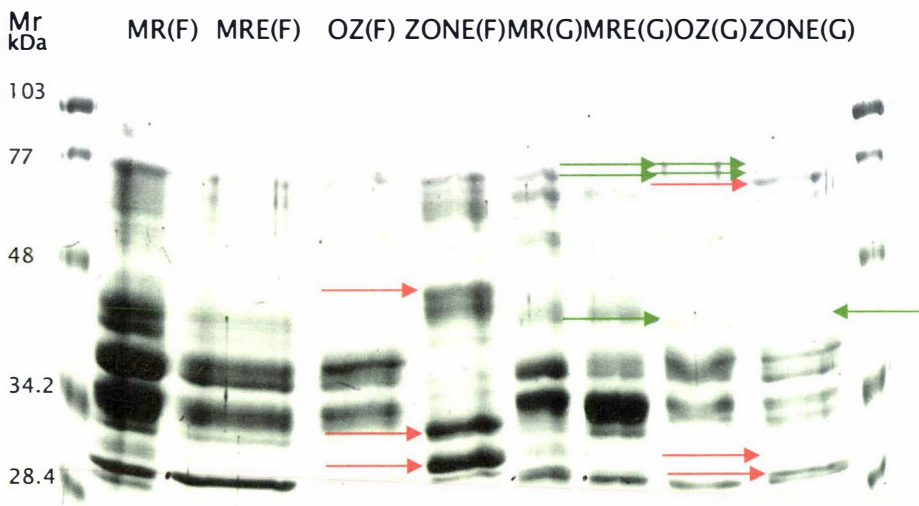


Figure 3.2c. Separation, using SDS-PAGE, of HIC fractions F (eluted with 70–75 % buffer B) and G (eluted with 75–80 % buffer B) obtained from the Phenyl Superose column chromatography separation of spring-collected MR, MRE, OZ and ZONE tissue. Proteins are visualised with Coomassie blue R-250 staining. The arrows indicate proteins of interest summarised in Table 3.2.



Figure 3.2d. Separation, using SDS-PAGE, of HIC fractions H (eluted with 80–85 % buffer B) and I (eluted with 85–90 % buffer B) obtained from the Phenyl Superose column chromatography separation of spring-collected MR, MRE, OZ and ZONE tissue. Proteins are visualised with Coomassie blue R-250 staining. The arrows indicate proteins of interest summarised in Table 3.2.

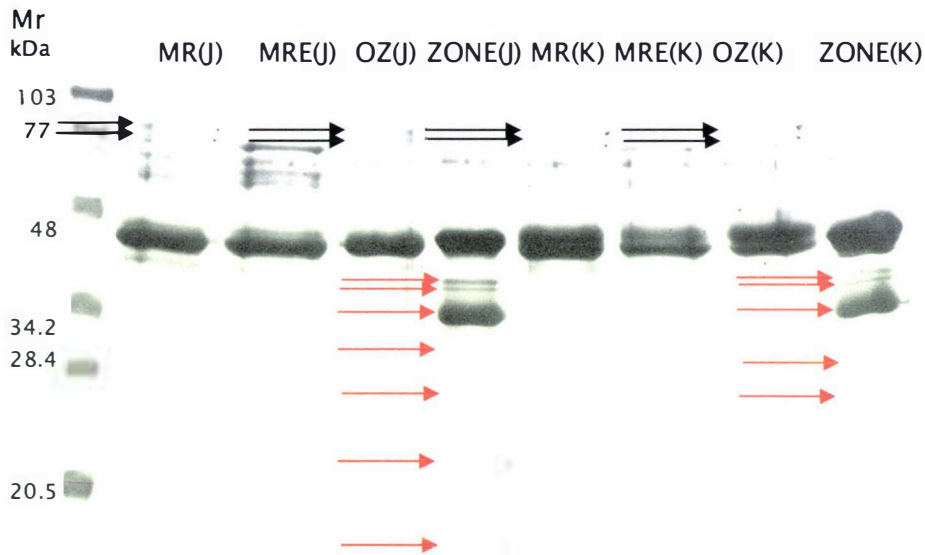


Figure 3.2e. Separation, using SDS-PAGE, of HIC fractions J (eluted with 90–95 % buffer B) and K (eluted with 95–100 %+ buffer B) obtained from the Phenyl Superose column chromatography separation of spring-collected MR, MRE, OZ and ZONE tissue. Proteins are visualised with Coomassie blue R-250 staining. The arrows indicate proteins of interest summarised in Table 3.2.

Fractions from HIC column <sup>a</sup>	Tissue samples where preferentially-expressed proteins were identified			
	OZ & ZONE (green arrows) Group 1	ZONE (red arrows) Group 2	MRE & ZONE (blue arrows) Group 3	MR and OZ (Black arrows) Group 4
Fraction D (60 to 65 % B)	10 36 40 <sup>b</sup>		49	
Fraction E (65 to 70 % B)				
Fraction F (70 to 75 % B)		30 33 46		
Fraction G (75 to 80 % B)	75 74 40	30 32 76		
Fraction H (80 to 85 % B)	34	76 46 33 10		
Fraction I (85 to 90 % B)		76 35 33 29 25 11		
Fraction J (90 to 95 % B)		36 35 33 30 23 10		76.5 77.5
Fraction K (95 to 100 %+ B)		36 35 33 30 27		76.5 77.5

Table 3.2. Summary of proteins designated as unique or preferentially-expressed in the tissues indicated after fractionation by HIC and separation using SDS-PAGE (data from Figures 3.2 b, 3.2 c, 3.2 d, 3.2 c).

<sup>a</sup> The values denote percentage buffer B used in the elution from the Phenyl Superose column

<sup>b</sup> Protein mass as estimated from the marker ladder (kDa)

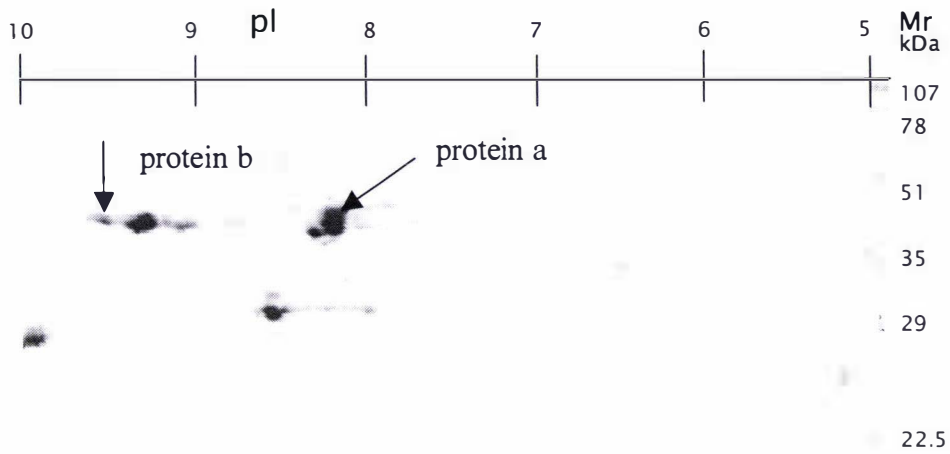


Figure 3.2f. Two-dimensional separation of OZ HIC fraction I (eluting at 85–90 % buffer B). The proteins were separated using isoelectric focusing in the first dimension and SDS-PAGE in the second dimension. Protein spots are visualised using Coomassie blue G-250.

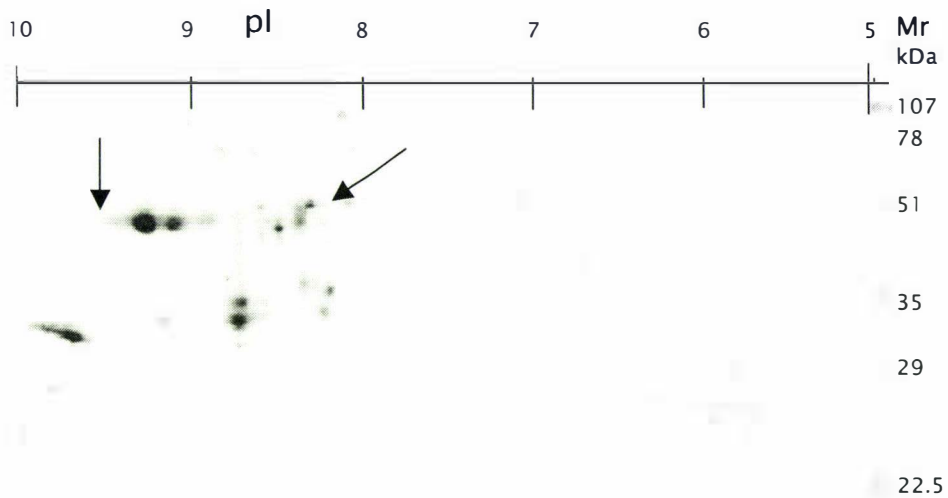


Figure 3.2g. Two-dimensional separation of MR HIC fraction I (eluting at 85–90 % buffer B). The proteins were separated using isoelectric focusing in the first dimension and SDS-PAGE in the second dimension. Protein spots are visualised using Coomassie blue G-250.

### 3.1.4 Identification of proteins revealed by HIC by amino acid sequencing

The HIC comparison undertaken for rachis tissue collected in the spring (section 3.1.3) was also undertaken with tissue collected in summer and autumn-collected tissues (data not shown). One of the HIC fractions, (E), from the OZ autumn tissue, contains three protein bands of sizes ca. 10, 28 and 43 kDa that appeared, on a SDS-PAGE gel, to represent proteins that are expressed preferentially in the OZ tissue (Figure 3.3a). Each of these bands, therefore, is labeled with the prefix OZ followed by its molecular mass, for example OZ10. The fraction (E) separation (Figure 3.3a) is significantly different to the fraction E protein profile observed in the extraction and separation of the spring-collected tissue (Figure 3.2b). However, fraction E for the OZ sample from the autumn-collected tissue does bear some resemblance to fraction D for the OZ sample in the spring-collected tissue with proteins of ca. 10 kDa and 40 kDa prominent as being expressed preferentially in the OZ and ZONE tissue.

The three protein bands highlighted in Figure 3.3a (OZ10, OZ28 and OZ43) were excised from the gel, trypsin-digested and at least one peptide from each digest sequenced. The internal sequences obtained are shown in Figure 3.3b. To identify these peptides, amino acid sequence alignments were undertaken using sequences from previously characterised proteins available on the NCBI database ([www.ncbi.nlm.nih.gov](http://www.ncbi.nlm.nih.gov)). Two forms of comparison are used. The first is the percentage of identity, where the amino acid residues of the comparison sequence match exactly to the amino acid residues of the protein fragment. The second type of expression of homology is the percentage of similarity, where the amino acid residues of the comparison sequence either match exactly or have a different but similar residue in the same position (for example, isoleucine is similar to leucine). The percentage similarity is the same or has a larger value than the percentage identity. The mass of the protein the sequence had significant identity with was also compared to see whether they were within the size range of the OZ proteins. A similarity in size acts as a degree of confirmation of the identification of a protein by amino acid sequence identity although the one-dimensional mini-gel system does not permit a fully accurate sizing of proteins (Figure 3.3c to 3.3f).

The internal peptide sequence for the OZ10 protein had significant identity (11 out of 20 residues) to a LTP from spinach (Figure 3.3f). The OZ10 peptide also had significant identity to many other non-specific lipid transfer proteins previously characterised in plants and this comparison is discussed further in section 3.3.

Two distinct sequences were obtained from the two tryptic fragments sequenced in OZ28, and for sequence comparison these were designated OZ28 (a) and OZ28 (b). OZ28 (a) appeared to share identity (10 out of 13 amino acids) with an internal sequence of a ribonuclease previously characterised in plants (Figure 3.3c). There are many groups and subgroups of ribonucleases with molecular weights ranging from 10 kDa to 40 kDa. A few of approximately 30 kDa have been characterised which may be similar to OZ28a.

The OZ28b tryptic fragment shared sequence identity (8 out of 8 residues) with a superoxide dismutase from *Arabidopsis* (Figure 3.3d). There are three groups of superoxide dismutases (SOD) in plants categorized by the metal ion present at their active site. SOD has been found throughout the plant cell presumably because  $O_2^-$ , a highly reactive and damaging molecule in the cell, cannot cross membranes. SOD in plants is either a dimer or a tetramer of identical subunits of around 15 kDa. The tryptic fragment from OZ28b with sequence identity to an internal portion of a SOD in this study may be a dimeric form of the iron or manganese isoenzyme.

The tryptic fragment from OZ43 protein has significant sequence identity (69%; 11 out of 16 residues) and 88% similarity (14 out of 16 residues) to an internal fragment of aldose-1-epimerase-like enzyme, gp40 (Figure 3.3e). The gp40 protein has been partially characterised in the nuclear pore membrane of tobacco suspension cells (Heese-Peck and Reikhel 1998). Aldose-1-epimerase was originally named mutarotase because of its optically rotating affect on aldose sugars in solution. It is often still referred to by this name, and will be used interchangeably with aldose-1-epimerase in this thesis. Aside from proteins identified with sequence similarities, nothing is known about the amino acid sequence and structure of this enzyme in higher plants although mutarotase activity has been measured in a variety of fruits. Thus the OZ43 protein was characterised further in this study (section 3.2) to further elucidate whether the 43 kDa OZ protein from *S. nigra* functions as a aldose-1-epimerase-like enzyme.

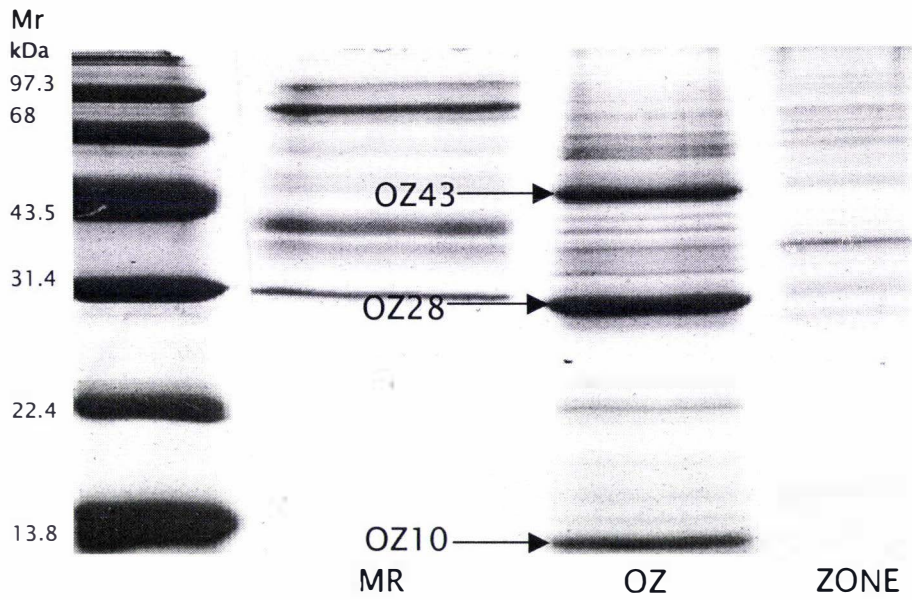


Figure 3.3a. SDS-PAGE separation of fraction E from a Phenyl Superose column chromatography separation of autumn-collected tissue. The proteins arrowed (OZ10, OZ28(a), OZ28(b) and OZ43) were then subjected to tryptic digestion and selected tryptic fragments from each protein were sequenced.

GDFYLHWLGPADS	OZ28(a)
GDASTVVK	OZ28(b)
KATPVNLAQHTYWNLG	OZ43
IAGSIQGINYSYASSLPGKC	OZ10

Figure 3.3b. Sequences from tryptic fragments obtained from the protein bands excised from the SDS-PAGE separation shown in Figure 3.3a.

	G-D-F-Y-L-H-W-L-G- P-A-D-S	OZ28(a) ( <i>S. nigra</i> )
70	G-D-N-Y-D-P-W-L-G--P-A-D-S 82	RNase ( <i>A. thaliana</i> )

Figure 3.3c. Amino acid sequence alignment of the internal peptide from OZ28(a) with a ribonuclease from *A. thaliana*. Gen-bank accession number AAA51406.

	G-D-A-S-T-V-V-K	OZ28(b) ( <i>S. nigra</i> )
81	G-D-A-S-T-V-V-K 88	superoxide dismutase ( <i>A. thaliana</i> )

Figure 3.3d. Amino acid sequence alignment of the internal peptide from OZ28(b) with a superoxide dismutase from *A. thaliana*. Gen-bank accession number AAF01529.

	K-A-T-P-V-N-L-A-Q-H-T-Y-W-N-L-G	OZ43 ( <i>S.nigra</i> )
183	K-A-T-P-I-N-L-S-H-H-P-Y-W-N-I-G 198	gp40 ( <i>N. tobaccum</i> )

Figure 3.3e. Amino acid sequence alignment of the internal peptide from OZ43 with gp40 from *N. tobaccum*. Gen-bank accession no. TO1933.

	I-A-G-S-I-Q--G-I-N-Y-S-Y-A-S-S-L-P-G-K-C	OZ10 ( <i>S.nigra</i> )
56	A-A-N-A-I-K- G-I-N-Y-G-K-A-A-G-L-P-G-M-C 175	lipid transfer protein (Spinach)

Figure 3.3f. Amino acid sequence alignment of the internal peptide from OZ10 with a lipid transfer protein from spinach. Gen-bank accession no. AAA34032.

## 3.2 Characterisation of the OZ43 protein

### 3.2.1 Initial identification of OZ43 as an aldose-1-epimerase-like protein

The identification of the plant aldose-1-epimerase-like protein gp40 has been made through comparison of this sequence with other known aldose-1-epimerase sequences from bacteria, virus and mammals (Heese-Peck and Raikhel 1998). The identification of the *A. thaliana* proteins as possible aldose-1-epimerases has been made through the comparison of the other deduced sequences from *Arabidopsis* to the gp40 protein (Town *et al* 2002, unpublished). The proteins referred to as mutarotase-like or probable mutarotases in *A. thaliana* comprise 358 residues, while the putative mutarotases are between 323 and 490 amino acids in length. The sequence alignments of the plant mutarotases from other species in Figure 3.4a show ten highly conserved residues, all of which are present in OZ43. The residues that are not identical between sequences consist of substitutions of one of three residues. The mutarotase-like proteins and probable mutarotase proteins align at residue 183 with the first residue on the OZ43 fragment, while the putative mutarotases from *A. thaliana* align at different residues.

The cell wall fraction from the hydrophobic interaction chromatography (HIC) column, visualised using SDS-PAGE (Figure 3.3a) was the first step in identifying the OZ43 protein. OZ43 has significant amino acid identity to internal sequence from the putative mutarotase, gp40, isolated from the nuclear pore of tobacco suspension cells (Figure 3.4a). Further, both the OZ43 and gp40 proteins have a similar molecular mass, determined by SDS-PAGE for OZ43 and deduced amino acid sequence for gp40. It was later found in this study, with the information provided by the sequencing of the genome of *Arabidopsis thaliana* (The Arabidopsis Genome Initiative 2001) that there were high percentages of identity between the OZ43 fragment, gp40 and all of the 14 deduced sequences of possible aldose-1-epimerase proteins from *A. thaliana* (Figure 3.4a).

Nevertheless, the 16 amino acid residue OZ43 sequence fragment with a 69 % identity and 88 % similarity to gp40 and hence to the other possible mutarotases in *Arabidopsis*, combined with the similarity in molecular mass, is insufficient evidence to fully confirm that OZ43 and these proteins share significant overall sequence and structural

similarities. To probe such structural similarities further, the overall structure of the OZ43 protein was compared to gp40 using Western analysis on cell wall extracts of OZ and MR, MRE and ZONE tissues (Figure 3.4b) with an antibody raised to gp40 (see section 3.2.2.2). This comparison provided two pieces of information. Firstly, there was clear recognition of a protein of approximately ca. 43 kDa in extracts of *S. nigra* by the gp40 monospecific antibody confirming the similarity of gp40 and OZ43 protein. Secondly, the antibody recognised the ca. 43kDa protein in the separated OZ and MR extracts but not in the ethylene treated MRE and ZONE (data not shown) extracts (Figure 3.4b). This apparent down-regulation of the OZ43 protein by ethylene is investigated further in section 3.2.4.

	K	A	T	P	V	N	L	A	Q	H	T	Y	W	N	L	G	OZ43 <i>S. nigra</i> cell walls
183	K	A	T	P	I	N	L	S	H	H	P	Y	W	N	I	G	Mutarotase-like <i>N. tabacum</i> (T01933)*
183	K	P	T	P	I	N	L	A	L	H	T	Y	W	N	L	H	Mutarotase-like <i>A. thaliana</i> (T0 7719)
183	K	P	T	P	I	N	L	A	L	H	T	Y	W	N	L	H	Mutarotase-like <i>A. thaliana</i> (AAM61410)
183	K	P	T	P	I	N	L	A	L	H	T	Y	W	N	L	H	Mutarotase-like <i>A. thaliana</i> (NP190364)
183	K	A	T	P	I	N	L	A	L	H	T	Y	W	N	L	H	Probable mutarotase <i>A. thaliana</i> (T49949)
183	K	A	T	P	I	N	L	A	L	H	T	Y	W	N	L	H	Probable mutarotase <i>A. thaliana</i> (AAL36040)
183	K	P	T	P	I	N	L	A	L	H	T	Y	W	N	L	H	Mutarotase-like <i>A. thaliana</i> (CAB41863)
183	K	D	T	P	I	N	L	A	Q	H	T	Y	W	N	L	A	Mutarotase-like <i>A. thaliana</i> (BAB02717)
315	K	A	T	P	V	N	L	A	H	H	S	Y	W	N	L	G	Putative mutarotase <i>A. thaliana</i> (CAB89324)
196	K	T	T	P	L	N	L	V	H	R	S	Y	W	N	L	G	Putative mutarotase <i>A. thaliana</i> (AAF03500)
204	K	T	T	P	L	N	L	V	H	R	S	Y	W	N	L	G	Putative mutarotase <i>A. thaliana</i> (AAF26148)
147	K	D	T	P	I	N	L	A	Q	H	T	Y	W	N	L	A	Putative mutarotase <i>A. thaliana</i> (AAK64036)
147	K	D	T	P	I	N	L	A	Q	H	T	Y	W	N	L	A	Putative mutarotase <i>A. thaliana</i> (NP 566594)
315	K	A	T	P	V	N	L	A	H	H	S	Y	W	N	L	G	Putative mutarotase <i>A. thaliana</i> (NP 197018)
213	K	T	T	P	L	N	L	V	H	R	S	Y	W	N	L	G	Putative mutarotase <i>A. thaliana</i> (NP 186775)
167	K	P	C	P	V	N	M	T	N	H	V	Y	F	N	L	D	<i>E. coli</i> (Ui3636)
162	K	D	T	A	L	N	L	T	N	H	T	N	H	T	Y	F	<i>Haemophilus influenzae</i> (C64096)
148	K	D	T	A	L	N	L	N	T	H	T	Y	F	N	L	E	<i>Haemophilus influenzae</i> (U32764)
172	E	S	T	V	F	N	P	T	N	H	V	Y	F	N	L	S	<i>Streptococcus thermophilus</i> (M38175)
167	Q	D	T	L	V	N	P	T	N	H	S	Y	F	N	L	S	<i>Streptococcus pneumoniae</i> (NP 35765)
167	Q	T	T	P	V	N	L	T	N	H	S	Y	F	N	G	F	Porcine mutarotase (BAB18973)
167	Q	A	T	P	V	N	L	T	N	H	S	Y	F	N	L	A	Mutarotase-like <i>Homo sapiens</i> (AAL62476)

Figure 3.4a. Alignment of the amino acid sequence from a tryptic peptide of OZ43 to amino acid sequences of probable and putative and aldose-1-epimerase proteins and aldose-1-epimerase-like proteins from a range of species. The boxed regions contain the amino acids that are the most highly conserved throughout the species examined (present in this alignment in at least 80 % of those plant species compared).

\*Gen-bank accession numbers are listed beside each sequence

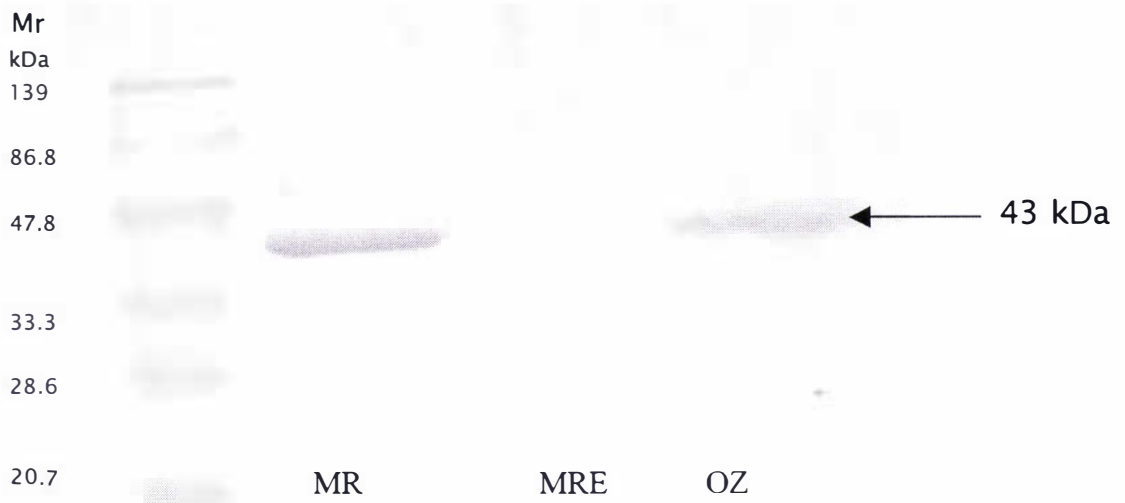


Figure 3.4b. Western analysis, using a gp40 monospecific gp40 antibody, of ethylene and non-ethylene treated tissues eluted from the HIC column and separated using SDS-PAGE. Antibody recognition was detected using an alkaline-phosphatase conjugated secondary antibody.

### 3.2.2 Biochemical characterisation of OZ43

The sequence and antibody data suggested that OZ43 (or a protein in the OZ43 protein band) was related to or identical to gp40, thought to be an aldose-1-epimerase-like protein. However, without obtaining more amino acid sequence from OZ43, or cloning the corresponding gene, any further comparison with gp40 was limited. Therefore, the focus of the study turned to the determination of whether the gp40 antibody-recognised OZ43 protein was active as an aldose-1-epimerase enzyme. This had not been determined for gp40. To date, although there is significant mutarotase activity in extracts from most plant species examined thus far, there has not been a protein isolated from higher plants that has been shown to possess epimerase activity. By purifying and examining the activity of OZ43 with assays designed to measure mutarotase activity, it can be established whether this protein is in fact a mutarotase or has some other function in higher plants. For instance, Heese-Peck and Raikhel proposed that gp40 may be an active sugar transporter based on its cellular distribution and domains with structural likeness to those seen in mammalian sugar transporters (see discussion section 5.1.9).

#### 3.2.2.1 Preliminary mutarotase activity assays

##### 3.2.2.1.1 Examination of the $\alpha$ -D-glucose and $\beta$ -D-glucose anomeric equilibrium

In bacteria, aldose-1-epimerase catalyses the anomeric conversion of aldose sugars and is involved in carbohydrate metabolism. In mammals, the function of this optical rotation by aldose-1-epimerase is not clear and even less is known about this enzyme in plants. In this thesis, the plant extracts containing the OZ43 protein were tested for mutarotase activity. Mutarotase activity can be measured by adding a sample (containing the mutarotase enzyme) to a solution of  $\alpha$ -D-glucose or  $\beta$ -D-glucose (optically active aldose sugars) and measuring the change in absorbance over time as the solution sugar reaches an equilibrium between the  $\alpha$ - and  $\beta$ - forms. However, this anomeric conversion occurs spontaneously, and so this needs to be taken into account when measuring the effect of any added enzyme. As this reaction proceeds in either direction (depending on which form of glucose initially predominates in the solution) the spontaneous, or mutarotase catalysed conversion rate of  $\alpha$ -D-glucose to  $\beta$ -D-glucose is affected by the reforming  $\alpha$ -D-glucose (or vice versa) until equilibrium is reached.

A polarimetric method can be used to detect the optical rotation of  $\alpha$ - and  $\beta$ - anomers and involves using a polarimeter. Some preliminary measurements were performed using a standard polarimeter but these did not produce reproducible rates of change and so this method was not pursued further (data not shown). However, where a polarimeter has been used to measure anomeric interconversion, semiautomatic electronic polarimeter is frequently used (Jain and Singh 1995). This device, which was not available for use in the experiments in this thesis, enables the rapid mixing and measurement of the reaction components without removing and replacing the cell in the polarimeter.

Instead, a spectrophotometric method was used for measuring the change in absorbance at 340 nm as the optical rotation of D-glucose occurred. The first set of experiments examined the spontaneous rate of conversion of  $\alpha$ -D-glucose to  $\beta$ -D-glucose and  $\beta$ - to  $\alpha$ -D-glucose, and was measured using  $\alpha$ - and  $\beta$ -D-glucose concentrations of 11 and 55 mM (Figure 3.5a and 3.5b). These two concentrations, corresponding to 0.1 and 1 mg of glucose in a 1ml assay, were chosen simply to show the effect of a five-fold concentration difference on the equilibrium. The  $\alpha$ -glucose anomer of D-glucose has a higher absorbance at this wavelength when compared with the  $\beta$ - anomer, and so the absorbance decreased over time using  $\alpha$ -D-glucose as the equilibrium was formed with  $\beta$ -D-glucose. The rate of decrease was 0.0058 and 0.0073 absorbance units (Au) per minute for 11 mM and 55 mM glucose concentrations respectively (Figure 3.5a). The rate of increase in the absorbance using  $\beta$ -D-glucose as the substrate was 0.0049 and 0.0107 Au per minute for the 11 mM and 55 mM concentrations respectively (Figure 3.5b). The reaction rate when using 11mM compared to 55 mM doubles in the  $\beta$ -D-glucose assay but increases by only 25% when using  $\alpha$ -D-glucose as the substrate. This is because the D-glucose used for the  $\alpha$ -D-glucose assay was not all in the  $\alpha$ - form whereas the  $\beta$ -D-glucose used was almost 100% in the  $\beta$ -form.

Ten units of a commercial preparation of mutarotase were added to 1 mM of  $\alpha$ -D-glucose and the 11 mM and 55 mM  $\alpha$ -D-glucose reactions (described above) to assess the catalytic effect of the enzyme on the equilibrium. The mutarotase used was from porcine kidney, and a unit is defined as the amount that catalysed the conversion of 1  $\mu$ mol of  $\alpha$ -D-glucose over a period of 1 minute. This concentration of mutarotase did

not have a significant effect on change in absorbance over time for any of the glucose concentrations (data not shown).

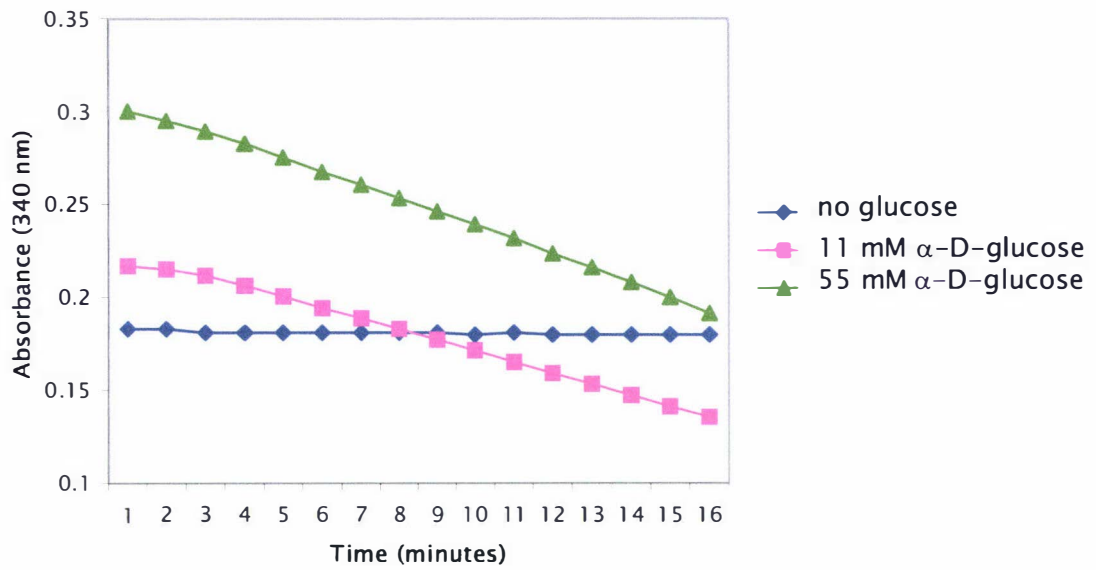


Figure 3.5a. The spontaneous anomeric transformation of  $\alpha$ -D-glucose to  $\beta$ -D-glucose measured as the change in absorbance at 340 nm over time (minutes).

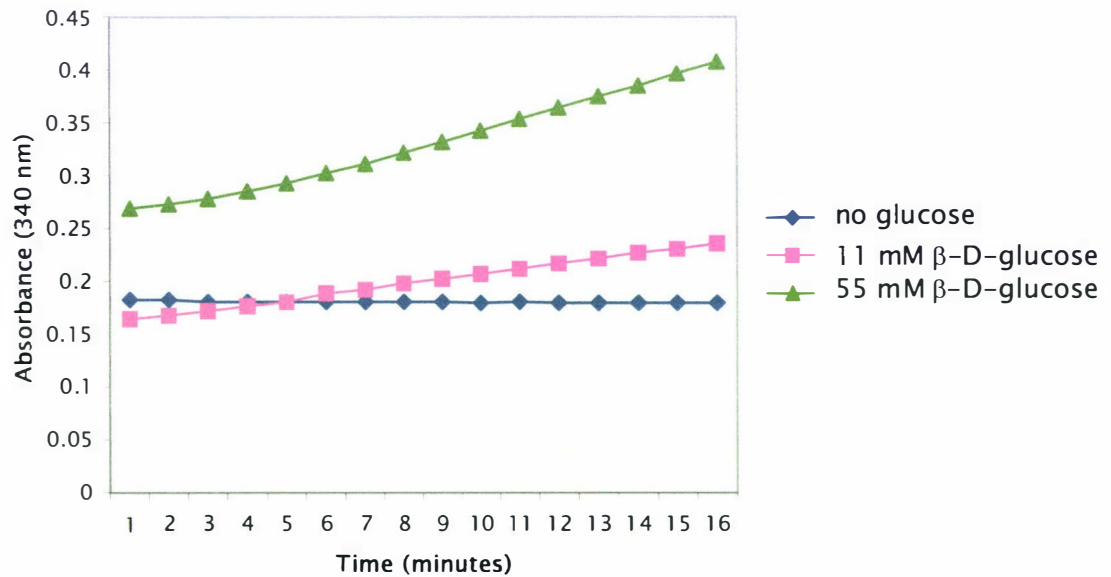


Figure 3.5b. The spontaneous anomeric transformation of  $\beta$ -D-glucose to  $\alpha$ -D-glucose measured as the change in absorbance at 340 nm over time (minutes).

### 3.2.2.1.2 The coupled aldose-1-epimerase enzyme assay

The low rates of the anomeric  $\alpha$ - to  $\beta$ - conversion of D-glucose measured using a spectrophotometer at 340 nm due to the formation of the equilibrium, and the apparent insensitivity to a comparatively high concentration of added mutarotase enzyme were overcome by adding glucose dehydrogenase (GDh, chromatographically purified from *Bacillus megatorium*) to the assay to produce a coupled enzyme assay (Figure 3.6a). The principle of the assay is that by coupling the  $\alpha$ - to  $\beta$ -D-glucose equilibrium to the  $\beta$ -D-glucose-specific GDh enzyme,  $\beta$ -D-glucose is removed as it formed thus driving the reaction forward. The rate of formation of the product of the assay, D-glucono  $\delta$ -lactone is measured (via the formation of NADH) and, providing that the GDh is not limiting, is related to the rate of formation of  $\beta$ -D-glucose (and hence the intrinsic epimerase activity in the extract).

The spectrophotometric method used for the measurement of mutarotase activity in the following assays is similar to the polarimetric method described in Mulhern (1973). In this thesis, aliquots of enzyme-containing extracts were added to freshly prepared  $\alpha$ -D-glucose containing glucose dehydrogenase and the NAD<sup>+</sup> (0.5 mM) cofactor required for this enzyme. NAD<sup>+</sup> is converted to NADH by GDh with the catalysis of  $\beta$ -D-glucose to D-glucono  $\delta$ -lactone. The formation of NADH can be measured, coincidentally, at 340 nm with a spectrophotometer. The cuvettes containing the reaction mixture were placed in the spectrophotometer and the absorbance zeroed. The absorbance readings using  $\alpha$ -D-glucose as the substrate increased over time for the coupled assay, while the change in Au for the equilibrium reaction (section 3.2.2.1.1), with no added GDh gave a negative rate when  $\alpha$ -D-glucose was the substrate. While both reactions are measured at 340 nm, the negative absorbance rate caused by the reduction in  $\alpha$ -glucose concentration (Figure 3.5b) does not impact on the positive absorbance rate comparisons between different  $\alpha$ -D-glucose concentrations caused by the formation of NADH.

In initial determinations using added porcine kidney enzyme, the absorbance readings were recorded every minute and these reached a stable linear rate of increase for  $\alpha$ -D-glucose (between 0.0275 to 11 mM) after 7 min which continued for over 40 min (data not shown). However, recordings for each reaction were stopped after 15 min, allowing

enough points for calculation of the linear rate (3.6b and 3.6c, 3.7a). The rates measured with  $\alpha$ -D-glucose as the substrate in over concentrations between 0.275 and 11 mM, appeared to be slower from 1 to 6 min than from 7 to 15 min (Figure 3.6c). The slow initial rates may have been due to a warming of the solution in the spectrophotometer over time as it was observed that higher reaction mixture temperatures resulted in higher rates in absorbance change (data not shown). It should be noted that a water-jacketed cuvette holder was not used in these assays. However, the same effect is not apparent in the reaction containing  $\beta$ -D-glucose with GDh (Figure 3.6b), which suggests the slow initial increase in the coupled assay with  $\alpha$ -D-glucose is a feature of the reaction. Nevertheless, it was the calculations made from the observed relationship between the linear rates that were used for quantification of mutarotase in the plant samples. Further characterisation of the kinetics of this reaction was not necessary (see section 3.2.2.1.3).

Although the pH may affect the rate of the mutarotase enzyme, in these experiments the pH is kept constant at 7.6, as it is optimal for the glucose dehydrogenase enzyme. In species of higher plants in which it has been examined, aldose-1-epimerase activity is reported to have a broad pH optima (between 4 to 8.5 pH units) with maximum activity at pH 7.4 (Bailey *et al* 1967). The two mammalian forms of this enzyme used in this thesis [porcine kidney and lamb (section 3.2.3)] are also reported to have the same pH optima of 7.4 (Keston 1954).

The changes in absorbance with time for variable concentrations of  $\beta$ -D-glucose illustrate the characteristic activity curves of a first order reaction (Figure 3.6b). The conversion of  $\alpha$ -D-glucose to D-glucono  $\delta$ -lactone through  $\beta$ -D-glucose in the coupled assay, aside from the slow increase in the rates, have different characteristic rate curves (Figure 3.6c). The  $V_{\max}$  for glucose dehydrogenase can be calculated with the data used to construct Figure 3.6b (and is also stated in the product information). However, the  $V_{\max}$  for glucose dehydrogenase with  $\beta$ -D-glucose as the substrate is not the same as the concentration of  $\alpha$ -D-glucose that results in the  $V_{\max}$  of GDh in the coupled reaction. Thus it is imperative that the coupled enzyme reaction operates under the  $V_{\max}$  of GDh when  $\alpha$ -D-glucose is the substrate so any increase in the rate of conversion of  $\alpha$ -D-glucose to  $\beta$ -D-glucose (due to the presence of the mutarotase enzyme) will increase the reaction rate (see discussion section 3.5). A plot was selected from Figure 3.6c using an

$\alpha$ -D-glucose concentration of 0.55 mM that gave a considerable reaction rate, but was significantly below the lowest  $\alpha$ -D-glucose concentration where the highest rate was reached (5.5 to 11 mM), i.e. at a concentration of  $\alpha$ -D-glucose between 5.5 and 11 mM, GDh is operating at its maximum velocity ( $V_{\max}$ ) and at concentrations of  $\alpha$ -D-glucose that are higher than this,  $\beta$ -D-glucose is being produced faster than GDh can convert it to D-glucono  $\delta$ -lactone. At concentrations of  $\alpha$ -D-glucose where GDh is operating above its  $V_{\max}$ , the reforming of  $\alpha$ -D-glucose from the pooling  $\beta$ -D-glucose affects the characteristic linear curves of the lower concentrations of  $\alpha$ -D-glucose (Figure 3.6c).

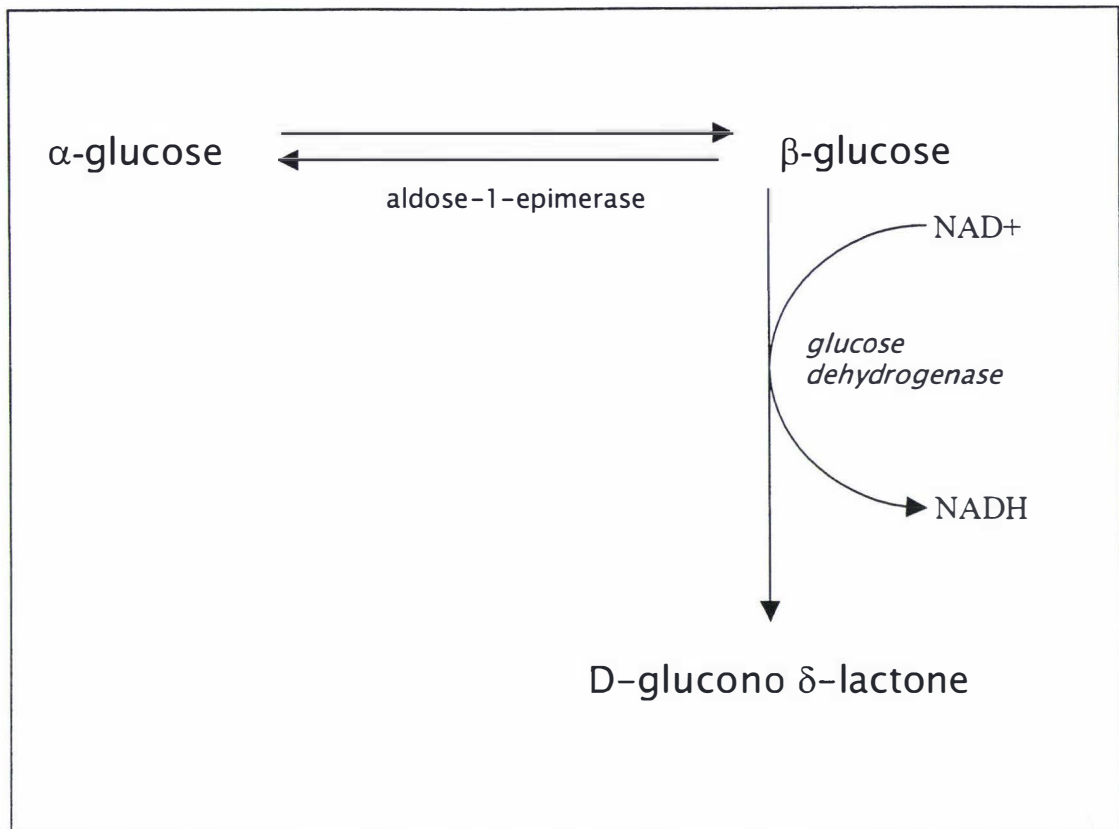


Figure 3.6 a. Reaction scheme for aldose-1-epimerase assay coupled to the formation of D-glucono  $\delta$ -lactone by glucose dehydrogenase at pH 7.6.

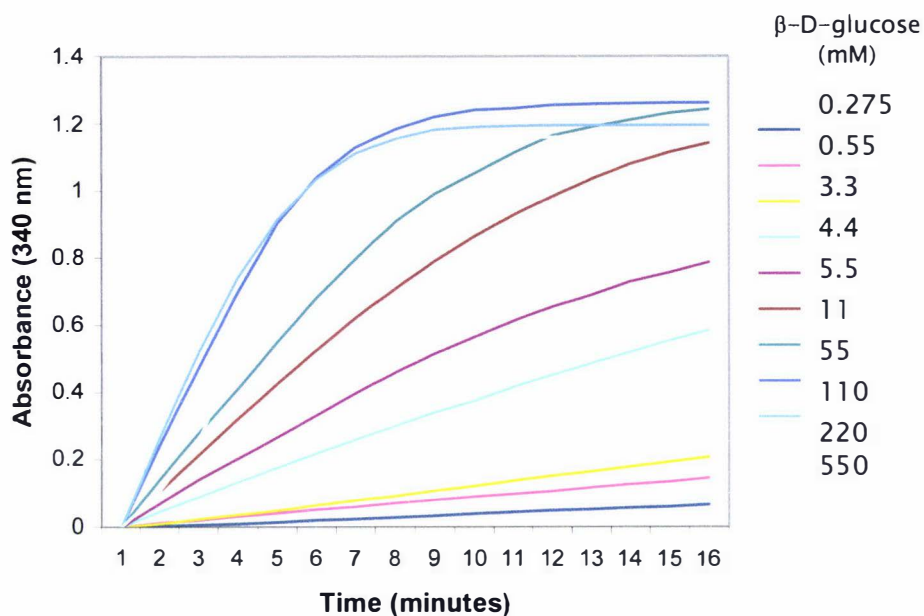


Figure 3.6b. Changes in D-glucono  $\delta$ -lactone formation (measured at 340 nm) from the glucose dehydrogenase catalysed conversion of  $\beta$ -D-glucose to D-glucono  $\delta$ -lactone over the range of  $\beta$ -D-glucose concentrations indicated.

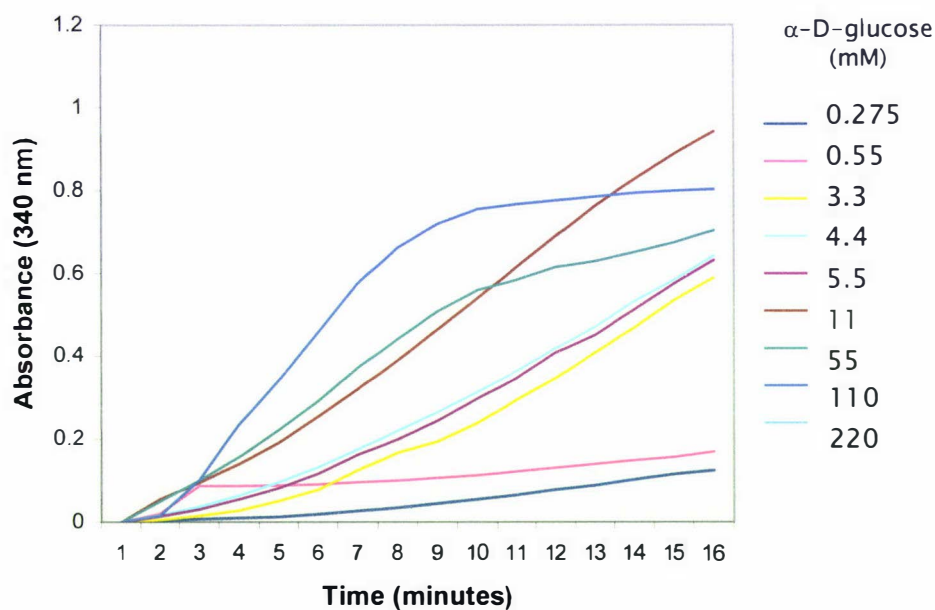


Figure 3.6c. Changes in D-glucono  $\delta$ -lactone formation (measured at 340 nm) from the glucose dehydrogenase catalysed conversion of  $\alpha$ -D-glucose to D-glucono  $\delta$ -lactone over the range of  $\alpha$ -D-glucose concentrations indicated.

### 3.2.2.1.3 Investigating the sensitivity of the coupled enzyme assay using porcine kidney mutarotase

The range of mutarotase concentrations over which the optimised coupled enzyme assay was sensitive was measured by the determination of reaction rates with different amounts of porcine kidney mutarotase added (Figure 3.7a). The concentration of the enzyme is measured in units, where one unit is the amount of enzyme that will convert one  $\mu\text{mole}$  of  $\alpha\text{-D-glucose}$  to one  $\mu\text{mole}$  of  $\beta\text{-D-glucose}$  in 1 min at  $25\text{ }^{\circ}\text{C}$ . Each of the reactions shown in Figure 3.7a is representative of a different amount of added porcine kidney mutarotase in a 1 mL assay, and the rate of each reaction *versus* the units of enzyme used in the assay is shown as Figure 3.7b. For reasons discussed in section 3.2.2.1.2, the slow initial rates of the reactions were not included in the calculations. Instead, the linear sections of the curves (between 9 and 15 min) were used for calculation of the rates. There is an increase in the reaction rate as more kidney enzyme is added up until there are 0.1 units of enzyme in the 1 ml reaction (Figure 3.7b). After this point there is no significant increase in the reaction rate, which demonstrates that, with 0.55 mM glucose, and 0.1 units of glucose dehydrogenase added, the reaction is sensitive to concentrations of between 0.005 and 0.1 units of mutarotase. The spontaneous mutarotation of  $\alpha\text{-D-glucose}$  to  $\beta\text{-D-glucose}$  caused a consistent background rate of 0.004 Au/min (Figure 3.7b).

The units of mutarotase activity in the plant samples were estimated by measuring the reaction rates (the change in absorbance with time) and then comparing these with the rates obtained from the porcine kidney mutarotase assays containing known units of enzyme. Measuring activity in units allows for a comparison of the activity of different forms. However, the author is aware that there will be differences in the kinetic properties of the mammalian and plant enzymes (Bailey *et al* 1967) and so one unit of plant enzyme will probably have a different concentration of active enzyme compared with 1 unit of the porcine enzyme.

Once established, the mutarotase activity assay was used to determine whether there was activity in the cells of *S. nigra*, and if it was catalysed by cell-wall-associated OZ43 protein recognised by the gp40 antibody.

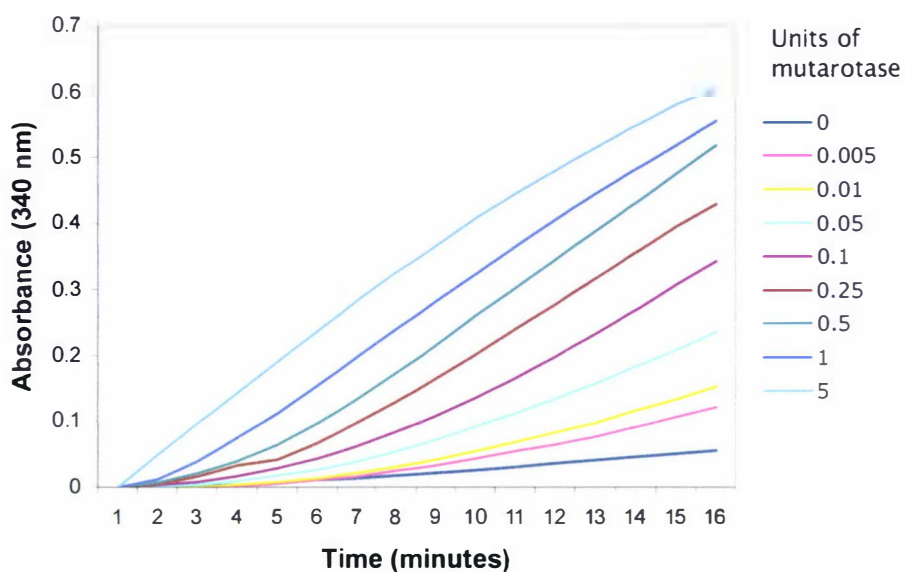


Figure 3.7a. Increase in formation of D-glucono  $\delta$ -lactone (measured at 340 nm) in response to an increase in added porcine kidney mutarotase enzyme units as shown.

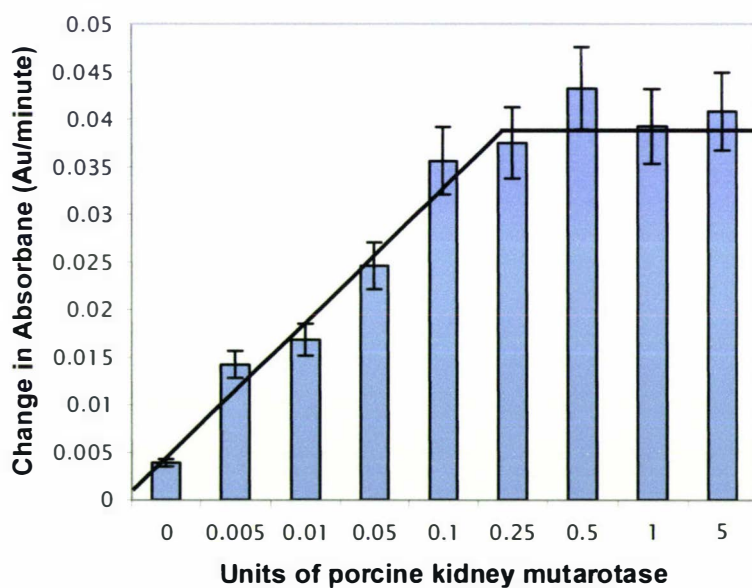


Figure 3.7b. The rate of formation of D-glucono  $\delta$ -lactone (measured as change in absorbance at 340 nm with time) over a range of porcine kidney mutarotase enzyme units as shown.

### 3.2.2.2 Immunological identification of OZ43 in cell wall fractions using antibodies raised to the gp40 protein

To investigate whether aldose-1-epimerase activity was associated with the gp40 antibody-recognised OZ43 protein extracted from the autumn tissue, the protein was partially purified using FPLC. The column fractions from the hydrophobic interaction (Resource), the ion-exchange (Mono-Q), and the gel filtration FPLC columns (Sephacrose 12) containing the OZ43 protein were identified with the gp40 antibody using Western analysis after separation by SDS-PAGE (data not shown). The gp40 antibody detected a protein of ca. 43 kDa in certain fractions from each column and a summary Western is shown as Figure 3.8a. Protein bands of ca. 43 kDa are apparent on the SDS-PAGE gel in the samples purified using HIC and ion exchange but cannot be identified with any certainty in the crude extract (Figure 3.8b). This was expected as the crude extracts contain many proteins, and only the more abundant can be seen by using SDS-PAGE without previous purification (section 3.1.2).

To determine the native molecular weight of this OZ43 eluting from the gel filtration column, the column was calibrated (see section 2.3.1.8) and the standard curve generated from these calculations is shown as Figure 3.8c. This curve was used to establish the elution volume of the OZ43 and thus its molecular mass. The OZ43 protein correlated with proteins of ca. 29 to 66 kDa (with an elution volume from the column of between 12.8 and 13.95 ml), and the gp40 antibody through Western analysis determined that the OZ43 was ca. 43 kDa. Therefore, the evidence suggests the protein recognised by the gp40 antibody exists as a monomer.

The gp40 antibody obtained for the initial identification of OZ43 was a monospecific polyclonal antibody (Heese-Peck and Raikhel 1998) and this is used in Figure 3.4b. This antibody had been generated to a recombinant gp40-GST fusion protein that had been expressed in *Escherichia coli*, the insoluble expressed protein isolated from an SDS-PAGE gel for immunisation of rabbits. The gp40 antisera obtained initially for the experiments in this thesis had been made monospecific by depleting the GST epitopes from the antisera. The depleted antibodies were then enriched further by affinity purifying against gp40-GST immobilised on PVDF membranes. When this supply of antibody became exhausted, all further identification of the gp40-recognised OZ43 protein was done using the gp40-GST antisera without enrichment.

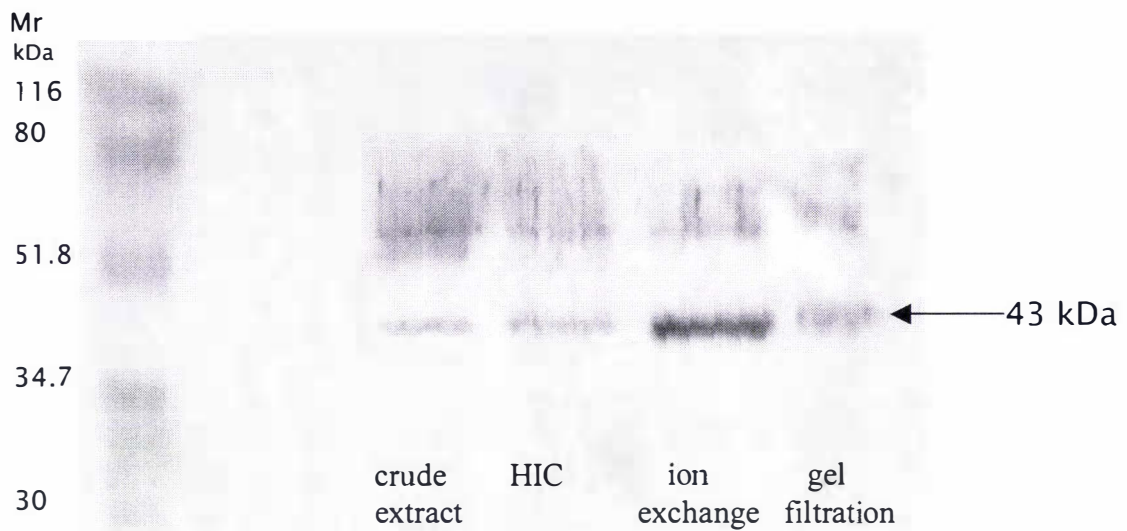


Figure 3.8a. Western analysis using the gp40 antisera, of specific fractions from the chromatographic columns with positive identification of a 43 kDa protein. Antibody recognition was determined using an alkaline-phosphatase conjugated secondary antibody.

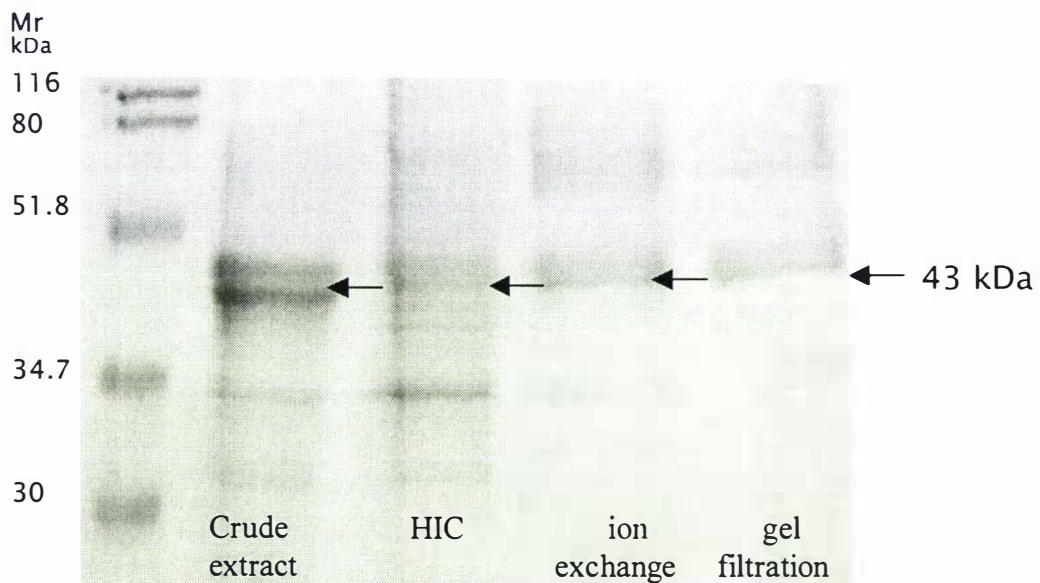


Figure 3.8b. Protein staining after SDS-PAGE separation of the OZ43 positive fractions (as identified by Western analysis with the gp40 antisera) from successive purification columns using FPLC.

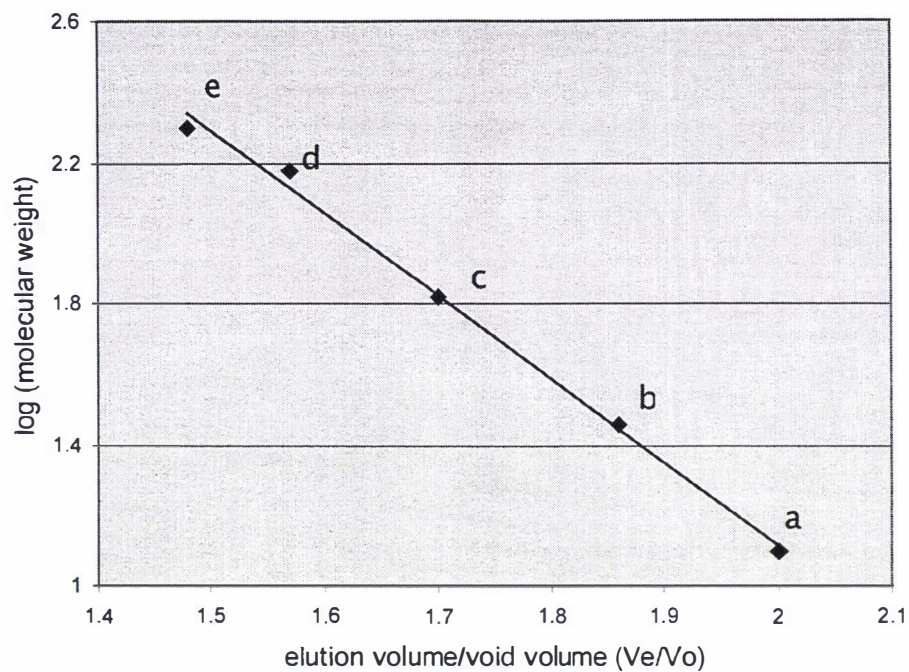


Figure 3.8c. The calibration curve of protein standards generated from elution volumes of each protein from the gel filtration column. Each labelled point represents a protein standard where a = 12.5 kDa, b = 29 kDa, c = 66 kDa, d = 150 kDa and e = 200 kDa. The elution volume of the gel filtration fraction containing OZ43 corresponded to a protein between 29 and 66 kDa.

### 3.2.2.3 Mutarotase activity assays of cell wall fractions containing the gp40 antibody-recognised OZ43

The partial purification of the cell wall extract fraction after HIC column chromatography (where OZ43 was initially identified) using ion exchange and gel filtration column chromatography is described in section 3.2.2.2. There was an expectation that if OZ43 (as recognised by gp40) possessed mutarotase activity, the specific activity of the fractions containing the OZ43 protein would increase with successive purification. Therefore, mutarotase activity was measured in each of the gp40 positive fractions (Figure 3.9a). The initial cell wall extract contained a mutarotase activity of 0.026 Au/minute/20  $\mu$ g of protein (20  $\mu$ g of protein was used in all of the assays when measuring specific activity) and this activity increased in the positive OZ43 from the HIC column to 0.028 Au/minute/20 $\mu$ g of protein (Figure 3.9a). Using the porcine kidney mutarotase data, these values translated into 2.5 and 3.75 enzyme units/mg of protein respectively (Figure 3.9b). However, there was much less activity detectable in the gp40 antibody positive fraction from the ion exchange column and none detectable in the gp40 antibody positive fractions following the gel filtration column. Although mutarotase is robust and will remain active for many months at 4  $^{\circ}$ C, the data suggest that either the mutarotase has lost activity through the purification process or the mutarotase activity is associated with another protein which co-purified with OZ43 protein recognised by the gp40 antibody after HIC chromatography but is separated after ion exchange chromatography. Therefore, mutarotase activity was assayed for in the other fractions that elute from the ion-exchange column. There was no activity measured in any of the other Mono-Q column fractions, indicating the activity of the enzyme, which may be OZ43, has been lost through the purification process either through degradation or because of the removal of an unknown cofactor during the purification process.

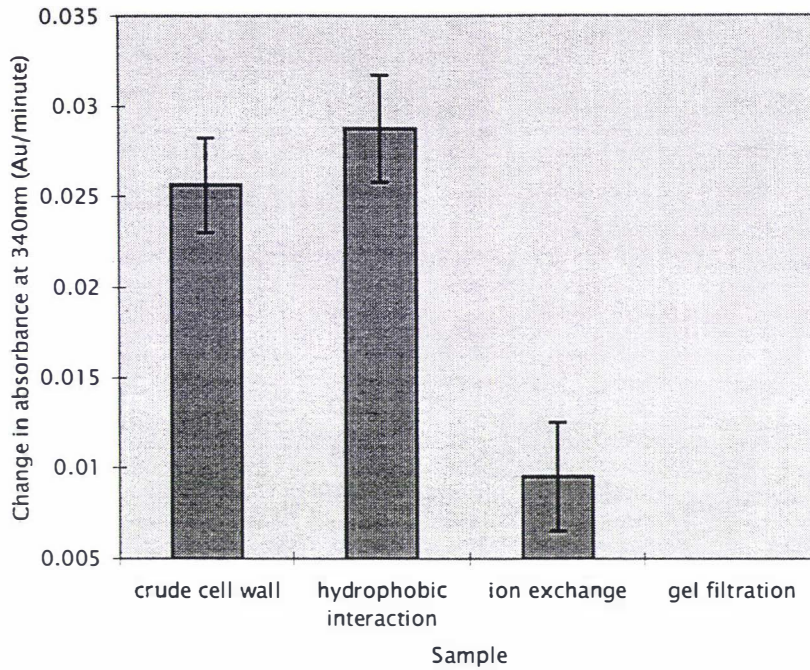


Figure 3.9a. Mutarotase activity rates in fractions from the chromatographic columns indicated that had been determined to contain the OZ43 protein recognised by the gp40 antibody.

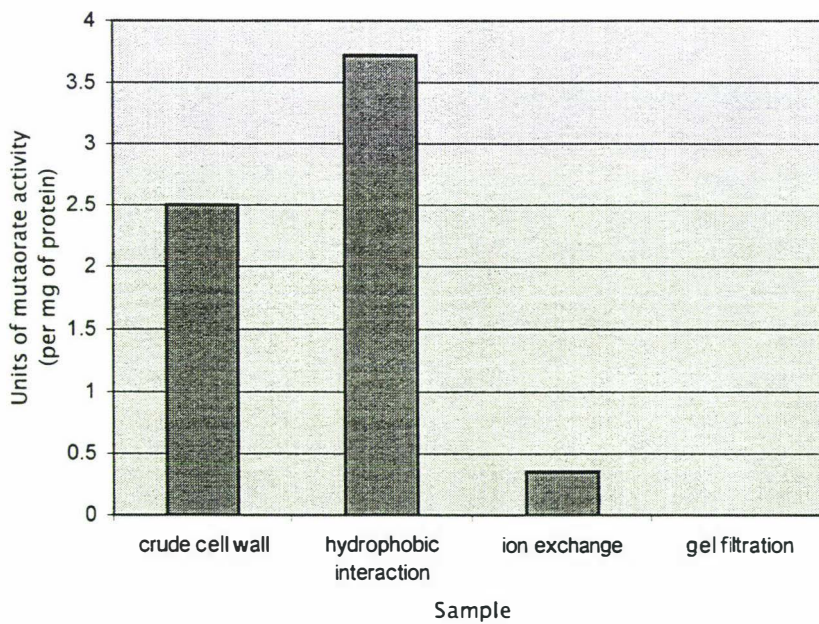


Figure 3.9b. Expression of mutarotase specific activity rates determined by comparing the activity measurements of the partially purified (gp40 antibody-recognised) OZ43 protein (Figure 3.9a) to the activity of the porcine mutarotase (Figure 3.7b).

### 3.2.2.4 Mutarotase activity assays of soluble and insoluble components of plant tissues, and immunological identification using gp40 antibodies

To examine the putative aldose-1-epimerase activity further, sub-cellular localisation of the gp40 antibody-recognised OZ43 protein was undertaken and the enzyme activity determined in these fractions. The cells of the rachis (MR) were fractionated, using ultracentrifugation, into separate components as outlined in Figure 3.10a. The activity of the enzyme in the five preparations (denoted as Preps I to V in the bold borders) and the presence of OZ43 by immunological recognition was then established. The detection of OZ43 using Western analysis with the gp40 antibody is shown as Figure 3.10 b and the corresponding activity measurements in each of the extracts are shown as Figure 3.10 c. The OZ43 protein is detected on the gp40 Western blot in the cell wall supernatant fraction (the crude cell wall 1.0 M NaCl extract that was centrifuged at 100 000g for 30 min). This fraction (Prep V) contains putatively cellular proteins which are not attached or integrated into the cell wall or attached to membranes, but rather those which have dissociated from the cell wall with the high (1M) salt treatment. Analysis of the corresponding protein stained gel [Figure 3.10b(b)] revealed a band of ca. 43 kDa in the 100 000g supernatant from the cell wall preparation (Prep V), but which is absent from Preps I and II. A band of ca. 43 kDa can also be detected in Prep III (but was not recognised by the gp40 antibody).

In terms of the location of the enzyme activity, there is significant activity detected in the cell wall supernatant fraction (Prep V) where the OZ43 was detected with gp40 antibody [Figure 3.10b(a)]. However, the highest mutarotase activity was observed in the soluble supernatant (100 000g fraction; Prep III). This fraction contains the truly soluble proteins as the cell membranes have been pelleted by ultracentrifugation (Prep II). There was no OZ43 detected in Prep II by Western analysis, but there was small but significant enzyme activity. This may be due to the presence of mutarotase in the small soluble components that pellet under the centrifugation conditions, or possibly because of the inclusion of the mutarotase present in the supernatant crossing into the pellet sample as the 100 000g soluble pellet had a upper portion of dense slurry that was included in the pellet sample. It appears from this data that there are mutarotase enzymes associated with the cell wall, that are solubilised by the 1 M salt elution, as well as soluble enzymes in the cytosol of the cell and possibly enzyme associated with

cellular membranes. OZ43, as detected by Western analysis with the gp40 antibody, appears to be present only in the cell wall supernatant fraction, suggesting this protein plays little or no role in contributing to the mutarotase activity detectable in the other fractions.

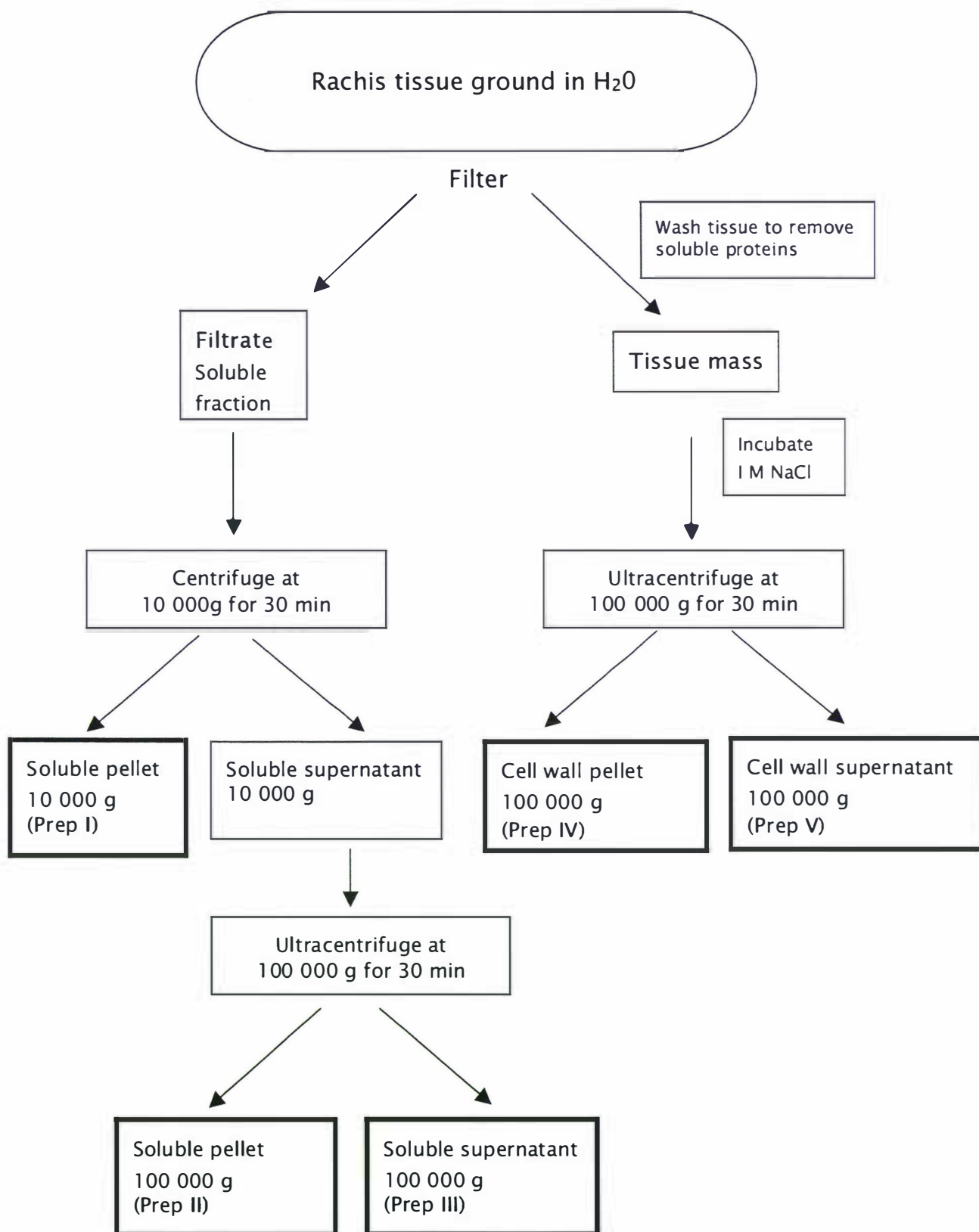


Figure 3.10 a. Diagrammatic representation of the fractionation of rachis cell extracts. The bold borders denote those samples that were analysed for gp40 antibody recognition and aldose-1-epimerase enzyme activity.

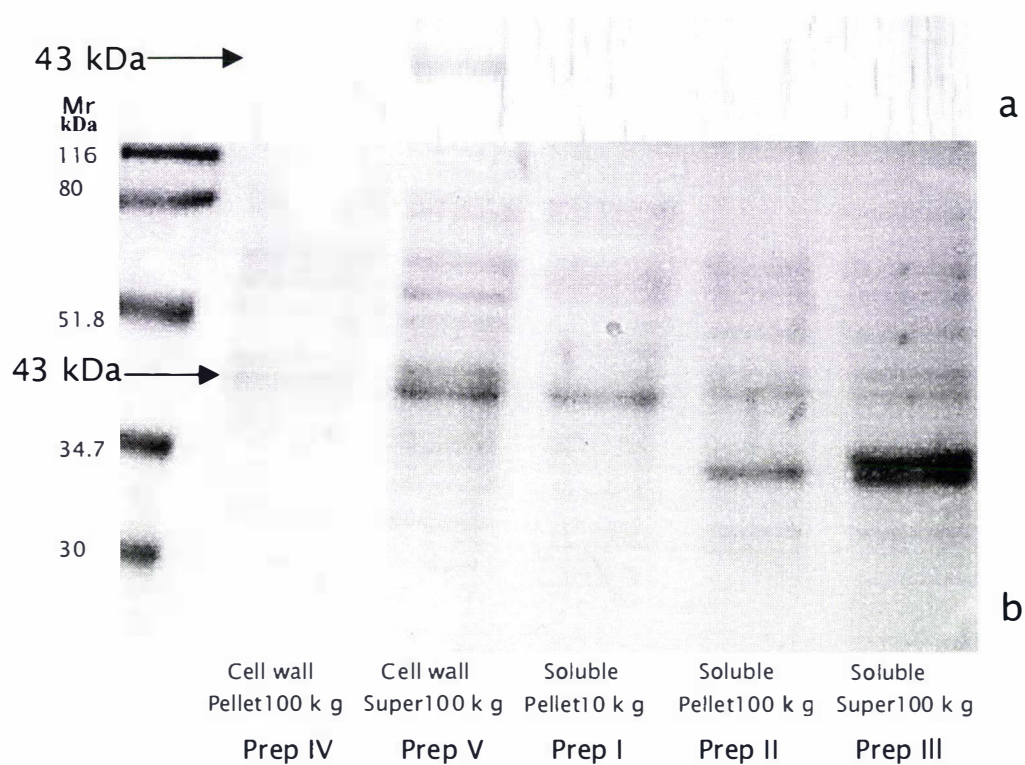


Figure 3.10b. (a) Western analysis, using the gp40 antibody, of the sub-cellular fractions of MR cell wall tissue as indicated in Figure 3.10a, after separation using SDS-PAGE. Antibody recognition was determined using an alkaline-phosphatase conjugated secondary antibody. (b) Protein staining after SDS-PAGE separation of the sub-cellular fractions of MR cell wall tissue subjected to Western analysis in (a).

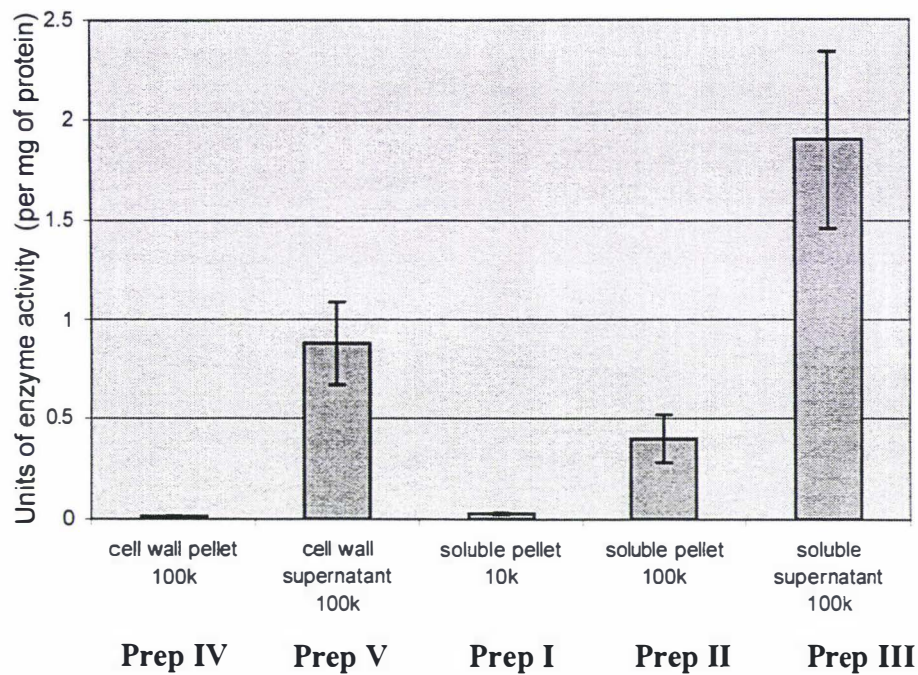


Figure 3.10c. Mutarotase activity in the sub-cellular fractions of MR cell wall tissue as indicated in Figure 3.10a and examined with SDS-PAGE Figure 3.10 b(a) and Western analysis using the gp40 antibody in Figure 3.10b(b).

### 3.2.3 Determination of the immunological relationship of OZ43 with gp40 and mammalian mutarotase

The partial purification (section 3.2.2.3) and the subcellular fractionation (section 3.2.2.4) of the OZ43 protein recognised by the gp40 antibody revealed that there was a disparity between protein recognition by the gp40 antibody and enzyme activity. As a complementary approach to determining whether protein(s) recognised by the gp40 antibody do have associated aldose-1-epimerase activity, the antibody was challenged against a mammalian extract known to contain the enzyme. To do this, the proteins associated with the plasma membrane of lamb kidney cells were extracted using 0.5 M NaCl, and fractionated using the HIC (Resource column) in the same way as the plant extracts (Figure 3.11). The resulting fractions were subjected to Western analysis using the gp40 antibody and assayed for mutarotase activity using the same conditions as for the plant samples. The highest mutarotase activity was found in fraction 13 from the Resource column (1.3 units of activity/mg protein). However, the gp40 antisera did not recognise either the mammalian mutarotase or any protein of around 40 kDa from fractions 10 to 17 of the lamb kidney extract. Interestingly, the elution of aldose-1-epimerase activity from lamb kidney suggests that there maybe at least two isoforms. The activity in fractions 0 and 1 may represent enzyme that has not bound to the column, but then two peaks of activity as observed in fraction 5 and fraction 13.

Purified porcine kidney mutarotase, used for calibrating the activity assays, was also used in a Western blot with gp40 as the primary antibody, but no detection of any protein was observed (data not shown). This data suggests that the OZ43 protein from *S. nigra* rachis cell wall tissue is more closely related immunologically to the putative plant mutarotase protein, gp40 than the active mammalian enzymes. Examination of the aligned amino acid sequences from a fragment of the porcine enzyme and one from human (a sequence has not been published for lamb mutarotase) to the OZ43 tryptic peptide and putative plant mutarotases (Figure 3.4a) suggests the OZ43 protein has a higher sequence identity to the plant proteins than the mammalian mutarotases. This conclusion has been made on the basis that two of the highly conserved amino acids in the plant enzymes (K<sub>183</sub>, W<sub>195</sub>) are not present in the porcine and human mutarotase fragments respectively.

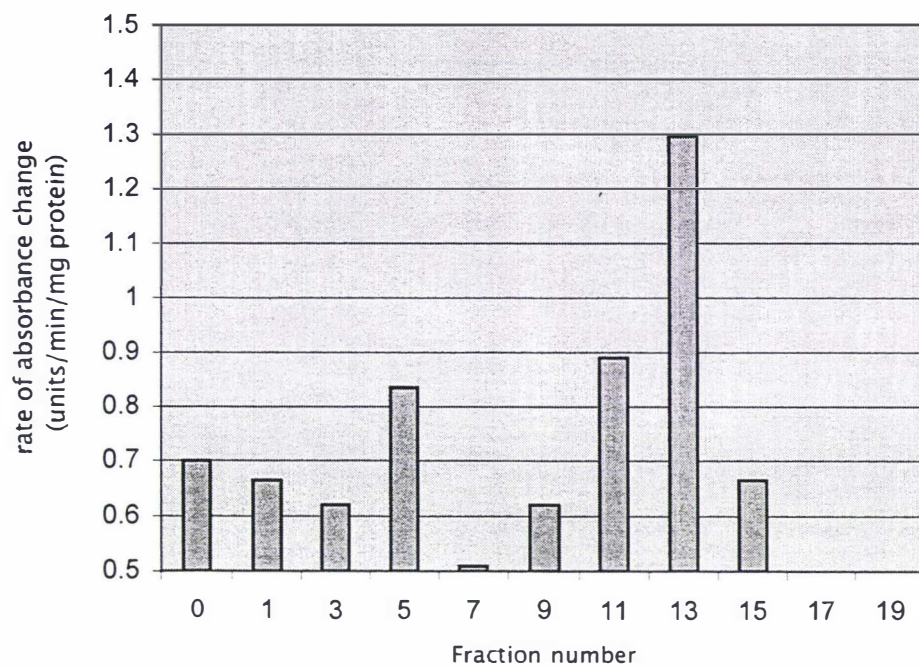


Figure 3.11. Mutarotase activity, measured using the coupled enzyme assay, in the HIC fractions from the lamb kidney membrane protein extract.

### 3.2.4 The effect of ethylene on the OZ43 protein and mutarotase activity

The gp40 antibody was used as part of the initial identification of the OZ43 protein to see whether it was immunologically related to the gp40 aldose-1-epimerase-like glycoprotein identified in the nuclear pore membrane of tobacco suspension cells. The gp40 antibody detected a protein of ca. 43 kDa in the non-ethylene treated tissues (MR and OZ) but the protein was not present in the ethylene-treated MR (MRE) and OZ (ZONE) (Figure 3.4b).

This reduction or elimination of the gp40 antibody-recognised OZ43 in ethylene treated tissues could be caused by either the down-regulation of the protein by ethylene, or the deterioration of the protein in these tissues over time as the MRE and ZONE extracts were prepared from explants treated with ethylene for 36 h. To establish whether this was an ageing affect or a direct hormonal affect, MR tissue was exposed to ethylene in the presence or absence of 1-methylcyclopropene (1-MCP) that is reported to block the effects of ethylene (Sisler *et al* 1999). Tissue extracts of MR, MRE and MRE treated with 1-MCP were fractionated using FPLC and the fractions that were known to contain the OZ43 protein (or the fractions where OZ43 was expected to elute) were subjected to Western analysis using the gp40 antibody. The gp40 antibody recognised a protein band of ca. 43 kDa in fraction 14 of the MR separation [Figure 3.12a(a)] and in fraction 14 of the MRE-MCP preparation [Figure 3.12a(c)]. No recognition of a ca. 43 kDa protein in fraction 14 of the MRE separation was observed [Figure 3.12a(b)], or in any of the other HIC fractions (data not shown).

One fraction each from the tissues where a ca. 43 kDa protein was detected with gp40 (i.e. MR and MRE-MCP) was used for the mutarotase activity assays. There was no detection of a ca. 43 kDa protein in the MRE HIC fractions so fraction 14 was assayed (corresponding to the fractions in MR and MRE-MCP which contained gp40 antibody recognition of the OZ43 protein). These activity profiles (Figure 3.12b) were compared to the Western blots for each of the three samples. The activity of mutarotase in the ethylene treated MR (MRE) drops sharply compared to the OZ43 positive MR fraction. This correlates with the expression of the OZ43 protein seen on the Western blot [Figures 3.12 a (a) and 3.12 a (b)] where the gp40 antibody does not visually detect OZ43 in MRE. The OZ43 protein is present in the MRE-MCP tissue fraction

[Figure 3.12a(c)] but there appears to be no significant increase in mutarotase activity when compared with the MRE fraction. This data suggests that the OZ43 protein that is recognised by the gp40 antibody is down-regulated with ethylene treatment, but the mutarotase enzyme may deteriorate as a result of ageing of the tissue.

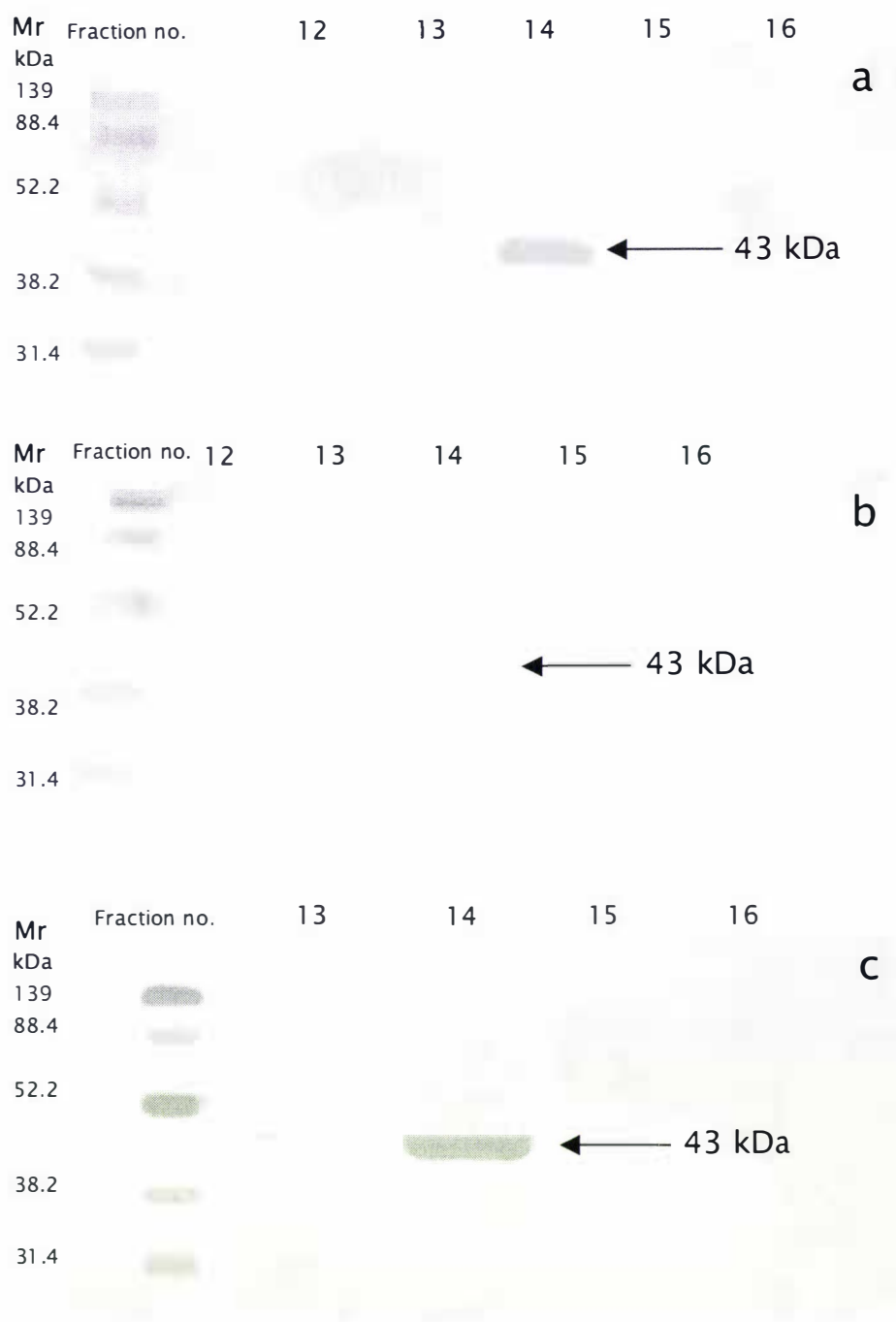


Figure 3.12a. Western analysis, using the gp40 antibody, of (a) mid-rachis (MR), (b) ethylene treated mid-rachis (MRE) and (c) ethylene and 1-MCP treated mid-rachis (MRE-MCP) cell wall extract fractions 11 to 17 (as indicated) from the HIC column after separation using SDS-PAGE. Antibody recognition was determined using an alkaline-phosphatase conjugated secondary antibody.

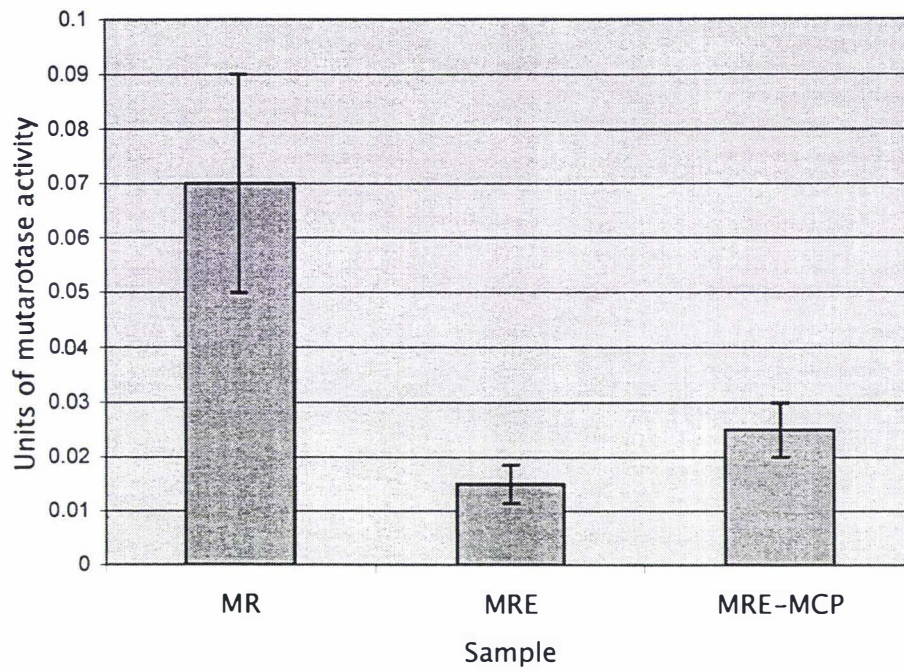


Figure 3.12b. Mutarotase activity in fraction 14 of the HIC separation of MR, MRE and MRE-MCP tissues, as indicated.

### 3.3 Examination of OZ10 as a putative lipid transfer protein

The amino acid sequence of a tryptic peptide from OZ10 (section 3.1.4) appears to have significant identity (between 35 % and 55 %) with lipid transfer proteins (LTPs) from plants, and an alignment with 12 LTPs that have been previously sequenced from plants is shown (Figure 3.13a). The LTPs with which the OZ10 sequence shares identity with all belong to a family of non-specific LTPs. To date, all of the LTPs identified in plants appear to have no exclusive function, i.e. all LTPs that have been identified in plants are non-specific. All nsLTPs have six to eight strictly conserved cysteine residues (C<sub>74</sub>) which form disulfide bridges as well as two to three charged amino acids at positions 45 to 47 from the presumed signal sequence cleavage site. One of the cysteine residues in the OZ10 sequence aligns with a highly conserved cysteine residue in the other compared sequences. There are four other residues in the OZ10 fragment (A<sub>57</sub>, N<sub>64</sub>, A<sub>68</sub> and P<sub>72</sub>) that are conserved across most of the LTPs sequences compared in Figure 3.13a.

Two antibodies were obtained that had been raised to LTP proteins. One had been raised to a recombinant protein generated from a cDNA cloned from embryonic cell cultures of carrot (*Daucus carota*). The other was generated from a purified LTP from *Arabidopsis*. Both of these antibodies recognised proteins of ca. 10 kDa in fractionated cell wall extracts of *S. nigra* (Figure 3.13b, with the carrot anti-LTP shown). There was no apparent OZ10 expression difference in the tissues tested suggesting that the protein(s) recognised by these LTP antibodies in *S. nigra* is/are not associated with ageing of the tissues or ethylene treatment. There was no recognition of the protein in the soluble extracts of each of the tissues of *S. nigra* examined (data not shown).

The two LTP antibodies also displayed the same recognition pattern in the cell wall extracts from the different tissues of the bean (*P. vulgaris*) that were examined (Figures 3.13 d and 3.13e) although some differences in the intensity of recognition were observed. In the non-ethylene treated tissues of the bean leaf pulvinus, distal abscission zone and petiole tissues immediately proximal to the abscission zone (Figure 3.13d and 3.13 e), both antibodies demonstrated highest recognition in the abscission zone (Figures 3.13 d and 3.13 e). After ethylene treatment for 36 h (at which time the pulvinus had abscinded), the recognition of the LTP protein in the zone remains the same, or is slightly diminished, but recognition of the target protein in the petiole tissue

has increased. In common with *S. nigra*, there was no protein detected by either LTP antibody in the soluble fractions from bean (data not shown).

The low range protein marker standards used to estimate protein band sizes throughout this thesis do not have a low enough range to accurately size any peptides smaller than 13 or 14 kDa (as this is typically the size of the smallest protein standard). Therefore, a kaleidoscope protein standard marker with a range of 3.8 to 37 kDa was used to more accurately assess the size of OZ10 in *S. nigra* and *P. vulgaris* tissue (Figure 3.13f). Using the kaleidoscope marker (the standard protein bands have been darkened for resolution purposes), it was observed that the carrot LTP antibody detected a peptide of ca. 10 kDa in both the cell wall extracts.

	I	A	G	S	I	Q	-	G	I	N	Y	S	Y	A	S	S	L	P	G	K	C	<i>S. nigra</i> (OZ10)
56	A	A	A	G	V	S	-	G	I	N	A	G	N	A	A	S	I	P	S	K	C	75 Maize
	A	A	N	A	I	K	-	G	I	N	Y	G	K	A	A	G	L	P	G	M	C	Spinach
	A	A	A	R	F	P	-	T	I	K	Q	D	A	A	S	S	L	P	K	K	C	Castor bean
	I	A	R	G	I	H	-	N	L	N	E	D	N	A	R	S	I	P	P	K	C	Wheat
	A	A	R	G	I	K	-	G	L	N	A	G	N	A	A	S	I	P	S	K	C	Rice
	I	A	R	G	I	H	-	N	L	N	L	N	N	A	A	S	I	P	S	K	C	Barley
	A	G	K	E	I	K	-	G	L	N	I	D	L	V	A	A	L	P	T	T	C	Rape
	T	A	N	A	V	T	-	G	L	N	L	N	A	A	A	G	L	P	A	R	C	Carrot
	I	L	A	A	N	T	-	R	I	N	L	N	N	A	N	S	L	P	G	K	C	Gerbera
	A	A	G	A	I	S	-	G	I	N	L	G	K	A	A	G	L	P	S	T	C	Tobacco
	A	A	N	A	L	P	-	T	I	N	V	A	R	A	A	G	L	P	K	A	C	Broccoli
	A	A	K	A	V	G	P	G	L	N	T	A	R	A	A	G	L	P	S	A	C	76 <i>Arabidopsis</i>

Figure 3.13a. Partial internal sequence of OZ10 aligned with the corresponding fragments of lipid transfer protein sequences from other plant species (from Kader 1997,1996 and Sterk *et al*/1991).

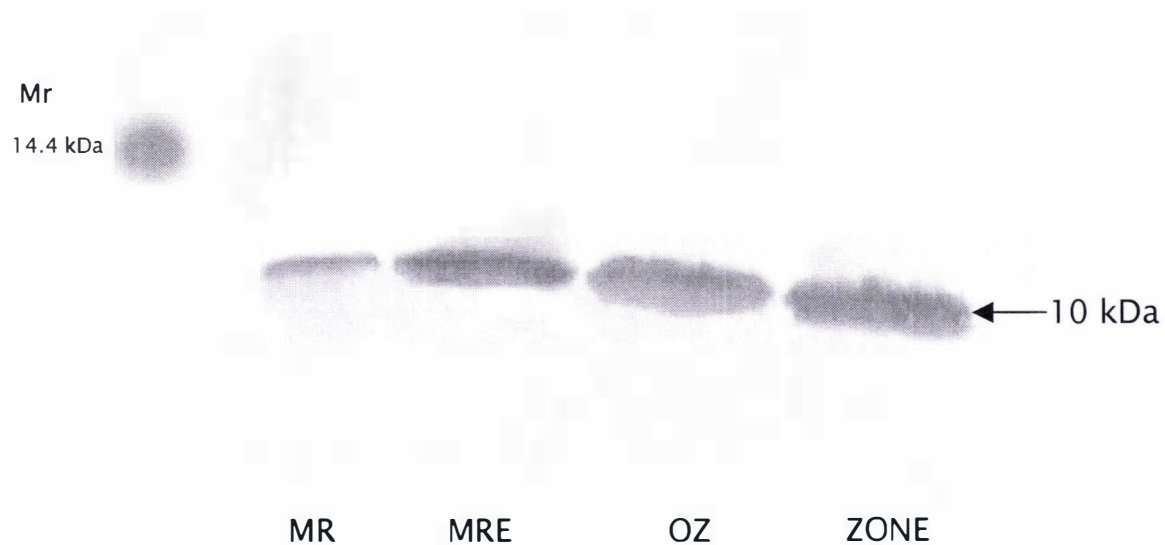


Figure 3.13b. Western analysis, using the carrot lipid transfer protein antibody, of the cell wall protein extracts of MR, MRE, OZ and ZONE tissues of *S. nigra* collected in the summer and separate using SDS-PAGE. Antibody recognition was determined using an alkaline-phosphatase conjugated secondary antibody.

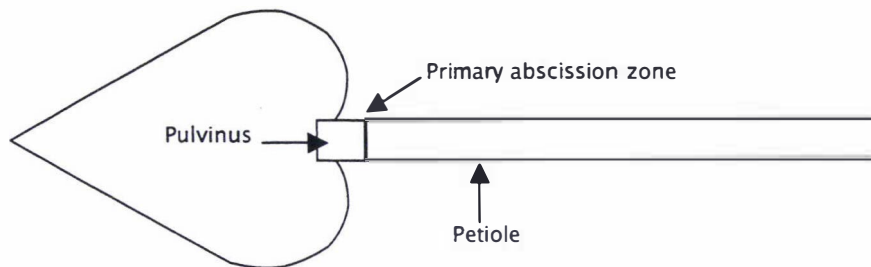


Figure 3.13c. A representation of a leaf of *P. vulgaris* with the pulvinus, abscission zone and petiole indicated.

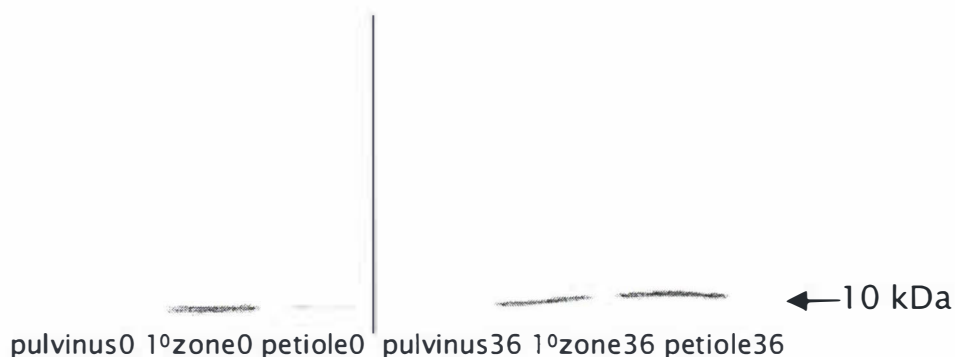


Figure 3.13d. Western analysis, using the carrot lipid transfer protein antibody, of the cell wall protein extracts from the ethylene and non-ethylene treated bean petiole tissues. The tissues at 0 h are shown as pulvinus0, zone0 and petiole0 (as shown in Figure 3.12 c), and these three tissues at 36 h of ethylene treatment are indicated as pulvinus36, zone36 and petiole36. Antibody recognition was determined using an alkaline-phosphatase conjugated secondary antibody.

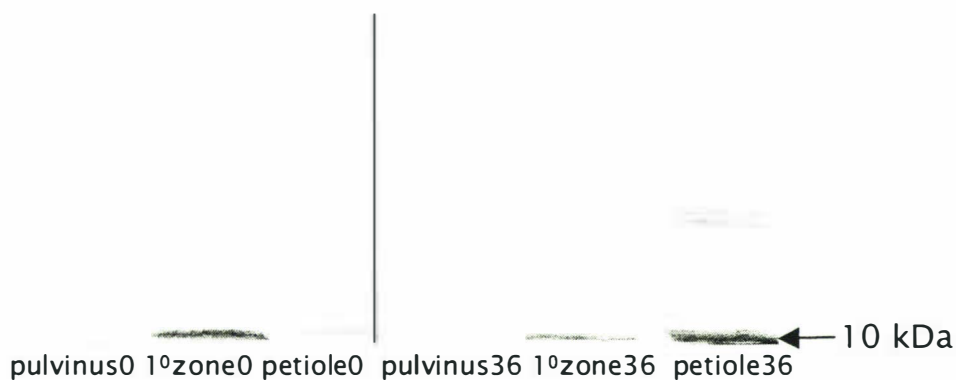


Figure 3.13e. Western analysis, using the *A. thaliana* lipid transfer protein antibody, of the cell wall protein extracts from the ethylene and non-ethylene treated bean petiole tissues. The tissues at 0 h are shown as pulvinus0, zone0 and pulvinus0 (as shown in Figure 3.12c), and these three tissues at 36 h of ethylene treatment are indicated as pulvinus36, zone36 and petiole36. Antibody recognition was determined using an alkaline-phosphatase conjugated secondary antibody.

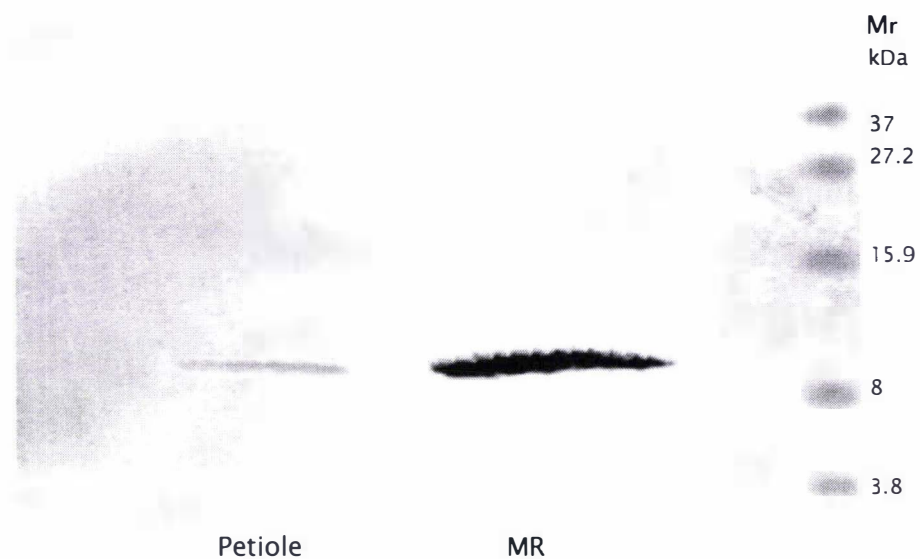


Figure 3.13f. Western analysis, using the carrot lipid transfer antibody, of a cell wall extract from the MR tissue of *S. nigra* and the petiole tissue of *P. vulgaris* after separation using SDS-PAGE. Antibody recognition was determined using an alkaline-phosphatase conjugated secondary antibody.

### 3.4 Identification of other cell wall proteins using specific antibodies

The original screening for abscission cell-specific proteins (sections 3.1.2 and 3.1.3) also identified a series of proteins that were specifically induced by ethylene in the abscission zone (the ZONE extracts). There appears to be at least thirteen proteins detected in the fractionated cell wall extracts that are specific to the ZONE cells (Table 3.2).

The plant growth regulator ethylene is closely associated with promoting abscission, and in doing so induces the expression of a specific isoform (pI 9.5) the cell wall degrading enzyme endo- $\beta$ -1,4- glucanhydrolase (cellulase). The induction of this enzyme is reported in the abscission zone cells of *S. nigra* and *P. vulgaris*, the model plants used in this thesis. Therefore, to identify if any of the proteins identified in *S. nigra* as ZONE-specific were identical to the pI 9.5 isoform of endo- $\beta$ -1,4- glucohydrolase an antibody raised to an abscission induced cellulase in *P. vulgaris*, known as bean abscission cellulase (BAC)(Tucker and Milligan 1991), was used against the *S. nigra* tissues. This antibody was prepared from proteins expressed from pBAC10 in *E. coli* by M.T.McManus (IMBS, Massey University).

The BAC antibody detected a 36 kDa protein in both the MRE and ZONE cell wall extracts from the tissue collected in the summer (Figure 3.14a). This is not consistent with an abscission-associated endo- $\beta$ -1,4-glucohydrolase in *S. nigra* reported as being 54 kDa and only induced in the cells of the leaflet abscission zone (Taylor *et al* 1994). The original survey of the total cell wall extracts (section 3.1.2) revealed at least six proteins that appeared to be induced in both the MRE and ZONE cell wall tissues (Table 3.1). Most notably, a protein in the spring gel (Figure 3.1a), of ca. 36 kDa, appears to be expressed preferentially in the ethylene-exposed tissues. It is possible that the protein observed in the initial spring cell wall extracts is the same as that detected by the BAC antibody in the same tissues. In the HIC fractionated extracts, there were at least eight ethylene-induced proteins between 10 and 49 kDa and five of these are between 29 and 36 kDa (Table 3.2). However, most of these ethylene-induced proteins appear to be confined to the ZONE cells. There is only one protein resolvable in the HIC fractionated extracts of 49 kDa that appears in both the MRE and ZONE cell wall extract (Table 3.2).

In contrast with *S. nigra*, the BAC antibody recognised a 51 kDa protein in the cell wall extracts of the petiole-pulvinus primary abscission zone cells that is consistent with the size of bean abscission  $\beta$ -1,4-endo glucohydrolase (Figure 3.14b). The protein is present only in the ethylene treated pulvinus and primary abscission zone (sampled at 36 h) and not in other tissues.

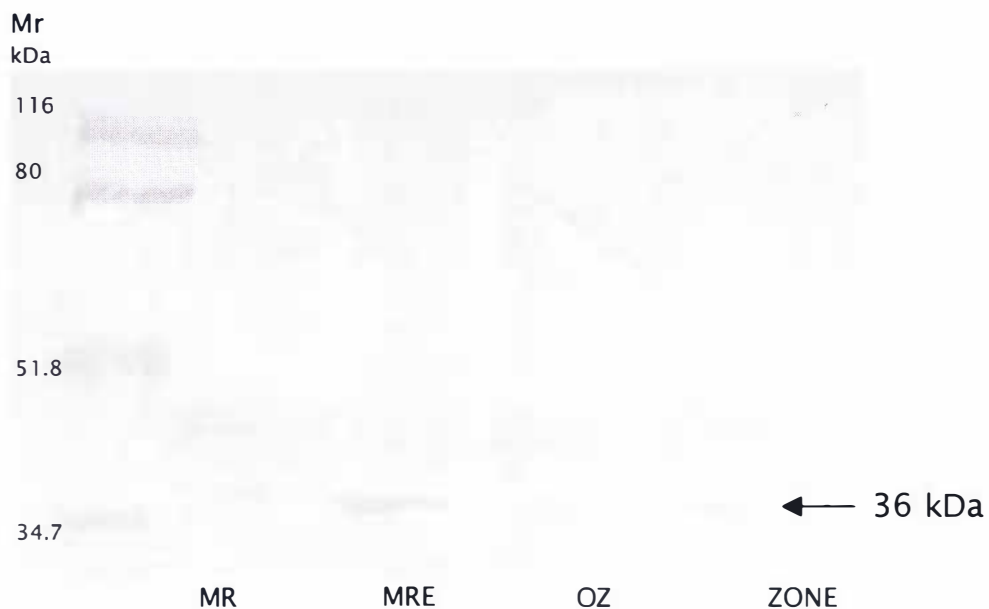


Figure 3.14a. Western analysis, using the BAC antibody, of cell wall extracts of MR, OZ, MRE and ZONE after separation using SDS-PAGE. Antibody recognition was determined using an alkaline-phosphatase conjugated secondary antibody.

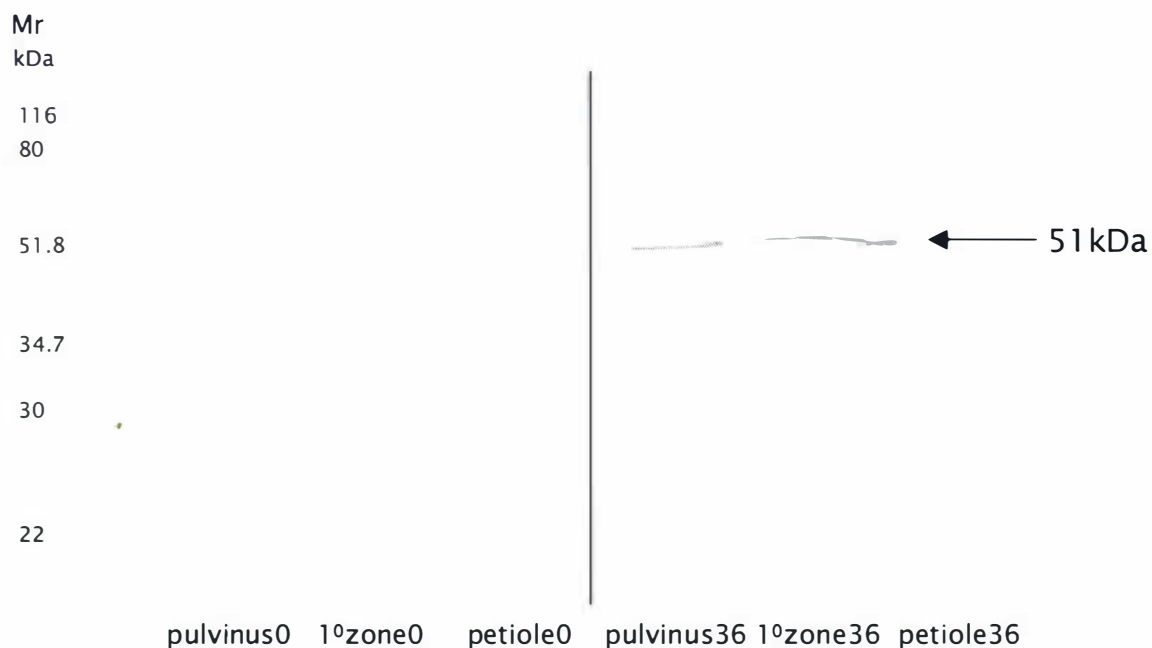


Figure 3.14b. Western analysis, using the BAC antibody, of ethylene and non-ethylene treated bean petiole tissues as indicated in Figure 3.13d, after separation using SDS-PAGE. Antibody recognition was determined using an alkaline-phosphatase conjugated secondary antibody.

## Chapter Four

### Changes in indole-3-acetic acid (IAA) and ethylene biosynthesis during the time course of secondary abscission zone formation in bean petiole explants

#### 4.1 Introduction

Adventitious, or secondary abscission zones form in stems, branches, pedicels and petioles in places not predetermined at the time of cell differentiation (Osborne 1989). In the plant species examined thus far, the two plant hormones ethylene and IAA (the principal naturally-occurring auxin) are documented to control the timing and position of the formation of these zones. In this study, adventitious abscission zones were induced in petiole explants of bean, and the endogenous levels of IAA and ethylene measured in the different regions of the petiole explant. Measuring the concentration of IAA involved the development of an IAA immunoassay with, initially, an attempt at polyclonal antibody production for use in an ELISA. The use of polyclonal antibodies (PcAb) was then extended to the use of a commercially available monoclonal antibody (McAb). ACC oxidase enzyme activity was also measured and compared to the ethylene evolved directly from the various segments of tissue examined.

##### 4.1.1 Secondary abscission zone formation in bean petiole explants

The procedure to obtain secondary abscission zones is described in section 2.1.3. A pictorial depiction of the progress from freshly-excised explant to cell-to-cell separation at the secondary abscission zone is shown as Figures 4.1 a to 4.1 d. It has been found previously that the amount of IAA added to the primary abscission zone after the distal pulvinus has abscinded, determines the position along the petiole where the secondary abscission zone will form (McManus *et al* 1998). The higher the concentration of applied IAA, the further away along the petiole (from the primary zone) the secondary zone forms, and the larger the portion of green petiole maintained.

In this study, the concentration of applied IAA was kept constant (1.0 mM) and the abscission zone formed 3 mm from the primary petiole-pulvinus abscission zone

(Figures 4.1 c and 4.1 d). It was important when excising tissues during the early stages of the differentiation process, that the position along the petiole where the secondary zone would form could be predicted as there was no morphological indication until about day 3 (Figure 4.1c). The four regions of each petiole that were sampled during the differentiation process are also indicated (Figure 4.1a to 4.1d). The ca. 2 mm section containing the secondary zone was excised and not included in the IAA, ethylene and ACC oxidase measurements. A 1 mm slice of callus tissue from the proximal end of the explant, and a ca. 2 to 3 mm slice encompassing the primary zone at the distal end of the explant were discarded.

The secondary zones formed with a success rate of between 65 to 80% of IAA-treated petioles (data not shown) and two principle factors emerged as important in controlling the percentage of success. The first was the initial condition of the bean plants, with the plants having thicker petioles tending to form zones with more success. Secondly, the damage caused by the cutting of the explant appeared to be important. A sharper cleaner cut resulted in less damage to the tissues and a higher chance of a secondary zone forming.

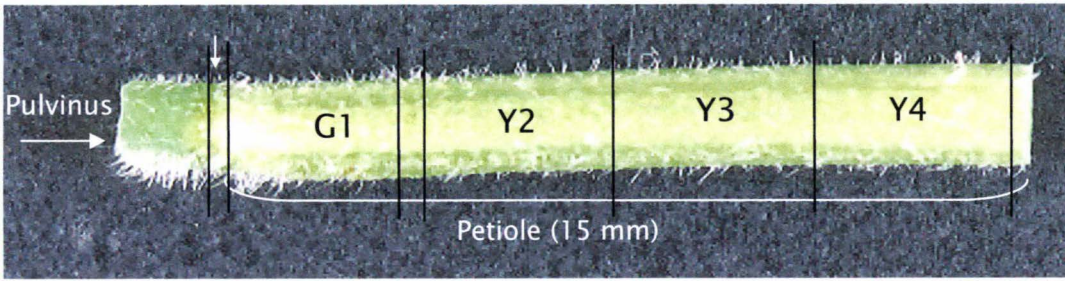


**Figure 4.1a.** A freshly excised explant. The unlabelled arrow denotes the primary abscission zone.

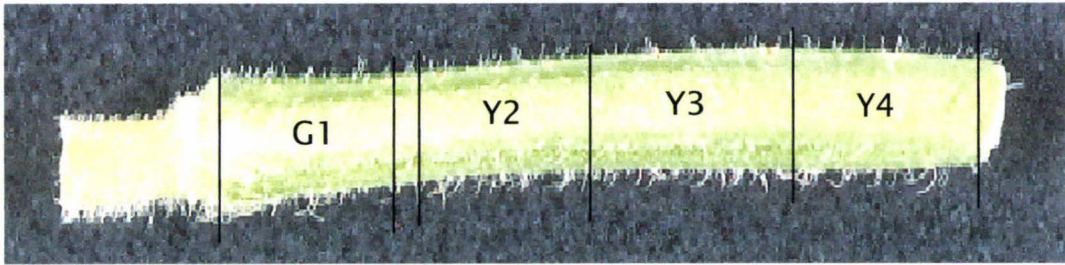


**Figure 4.1b.** Day 0 bean petiole (at abscission at the primary zone with the pulvinus attached).

After 36 h, the pulvinus senesces and separates (or can be easily removed with tweezers). At this time, IAA is first applied to the exposed primary abscission zone followed by a second application, 8 h later.

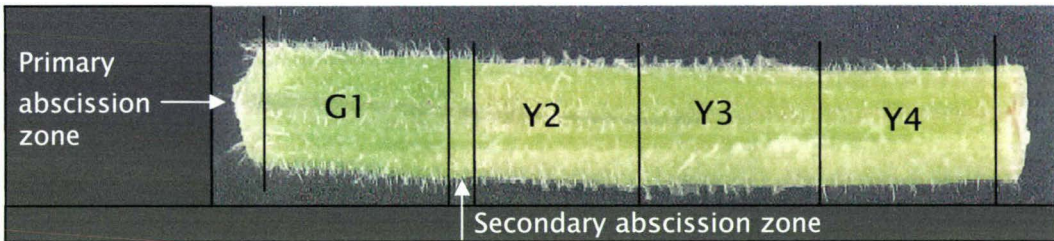


**Figure 4.1c.** Day 3 bean petiole (52 h).

Three days after the second application of the IAA, a junction appears 3 mm from the primary abscission zone in the petiole. Yellowing of the major proximal portion of the petiole is also observed.

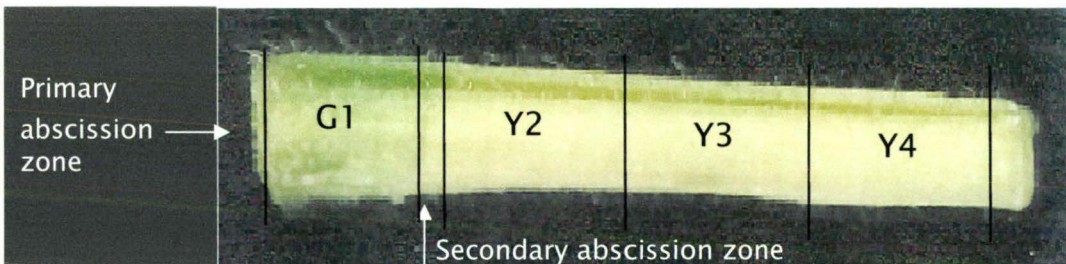


**Figure 4.1 d.** Day 5 bean petiole (98 h).

Four to five days after the application of IAA, the proximal portion had senesced further and an epidermal fracture appears transversing the petiole at right angles. This is deemed the site of secondary zone formation.

## 4.2 Development of an ELISA for IAA measurement using polyclonal antibodies

The concentration of IAA was measured in sectioned segments of petiole explants induced to form secondary zones (Figure 4.1) using an ELISA with both polyclonal and monoclonal antibodies. The following section describes the data gathered in the raising of the polyclonal antibodies.

### 4.2.1 Polyclonal antibody production

An enzyme-linked immunoassay was developed based on that outlined in Weir (1978) and Hock *et al* (1992). For this, an attempt was made to produce polyclonal antibodies to IAA by immunising rabbits with a BSA-IAA conjugate (as IAA alone is a weak immunogen).

#### 4.2.1.1 Titres of partially purified polyclonal IAA antisera

Bleeds were obtained before rabbits were immunised (pre-immune bleed) and at three week intervals after each immunisation with the BSA-IAA conjugate. A total of four boosts, as well as the initial immunisation, of the BSA-IAA antigen were given to the two rabbits over a period of about six months (approximately four weeks between each injection). The immunoglobulin (IgG) proteins were isolated from the collected samples by ammonium sulfate precipitation and DEAE-sephacel resin (section 2.4.1.3).

It was anticipated that the antisera raised to the BSA-IAA conjugate would contain a higher titre of IgG against BSA compared to the less immunogenic IAA. Therefore, comparisons were made between the recognition of the partially purified antisera to IAA and BSA using the ELISA.

The concentration of the partially purified antisera, which resulted in the saturation of the ELISA, i.e. where there was no change in the absorbance with increased dilution of the antisera, was used to estimate the antibody titres of BSA when compared to IAA-CH<sub>3</sub>. Each reaction contained 1 µg of either BSA or IAA-CH<sub>3</sub>. For the BSA reactions, the dilution of antisera where the assay saturated (i.e. decreasing the dilution of PcAb

gave no further change in the absorbance) was at 1/5000 and 1/1000 for rabbits 1 and 2 respectively. The IAA-CH<sub>3</sub> assays saturated at no dilution of antisera for both rabbits. Therefore, the calculated theoretical maximum titres of the IgGs were  $1.05 \times 10^{-4}$  mol/L of IAA-CH<sub>3</sub> for both rabbits and  $3.65 \times 10^{-4}$  mol/L and  $7.3 \times 10^{-5}$  mol/L of BSA for rabbits 1 and 2 respectively (see Appendix B for sample calculations).

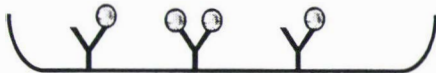
It can be ascertained if the assay is sensitive enough to measure IAA concentrations in plant tissue extracts by constructing the log-linear curve of percentage binding of the IAA-alkaline phosphatase tracer (to the IAA antibody) against the IAA concentration. There is not an exact expected rate of reaction or change in Au between the maximum IAA concentration (where IAA is saturating the antibody sites) in the assay (0% binding) and no IAA (non-specific binding). The calculations are comparative between these two IAA samples. If there is a low titre of IAA antibodies, there will be 0% binding of the tracer at low concentrations of IAA. Figure 4.2a illustrates the scheme for the binding of IAA and the tracer to the PcAb antibody in the antibody immobilised ELISA. The standard curve constructed using the antisera from rabbit two after the third bleed is shown in Figure 4.2b. The binding sites on the polyclonal antisera appeared to become saturated at an IAA concentration of 50 pmol/0.1mL. The absorbance readings in the assays for concentrations of IAA above 50 pmol/0.1mL did not change and hence the percentage binding (%B) was close to zero after this point.

In addition to the requirement of a high titre of IAA antibodies in the polyclonal antisera, the total absorbance change over the IAA concentration range required to generate an IAA standard curve sufficiently sensitive for measuring the sample concentrations of IAA (0 to 1000 pmol/0.1mL) was estimated to be at least 0.6 Au units. This is a value estimated from the results obtained using the suggested monoclonal antibody dilution stated in the literature accompanying the IAA commercially-available monoclonal antibody-based IAA immunoassay kit. The maximum difference in the absorbance, for the concentration range of IAA measured, was 0.17 and 0.19 for the undiluted antisera from bleed 2 from rabbits 2 and 1 respectively (Figure 4.2c).

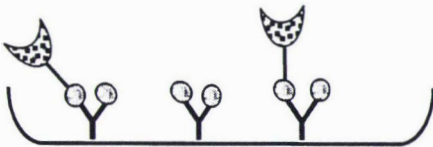
Figure 4.2a. A schematic representation of the reactions involved in the antibody immobilised ELISA using the polyclonal IAA antibody.



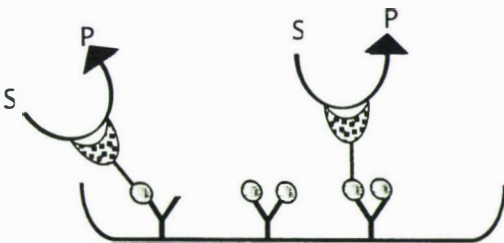
The polyclonal IAA antibody is coated to the wells




The polyclonal IAA antibody with free IAA added from the standard solution or in the plant extracts



The polyclonal IAA antibody with free IAA and the IAA - alkaline phosphatase tracer



The polyclonal IAA antibody with free IAA, the tracer and the substrate (pNPP). The amount of product formed depends on the amount of binding of the free IAA in the sample (%B). When the %B is zero there is no free IAA bound and the tracer occupies all of the IAA binding sites

Y	IAA IgG
⊙	Free IAA
	IAA - alkaline phosphatase conjugate (tracer)

Key. The symbols used in Figure 4.2 a. to represent the components of the antibody immobilised polyclonal ELISA.

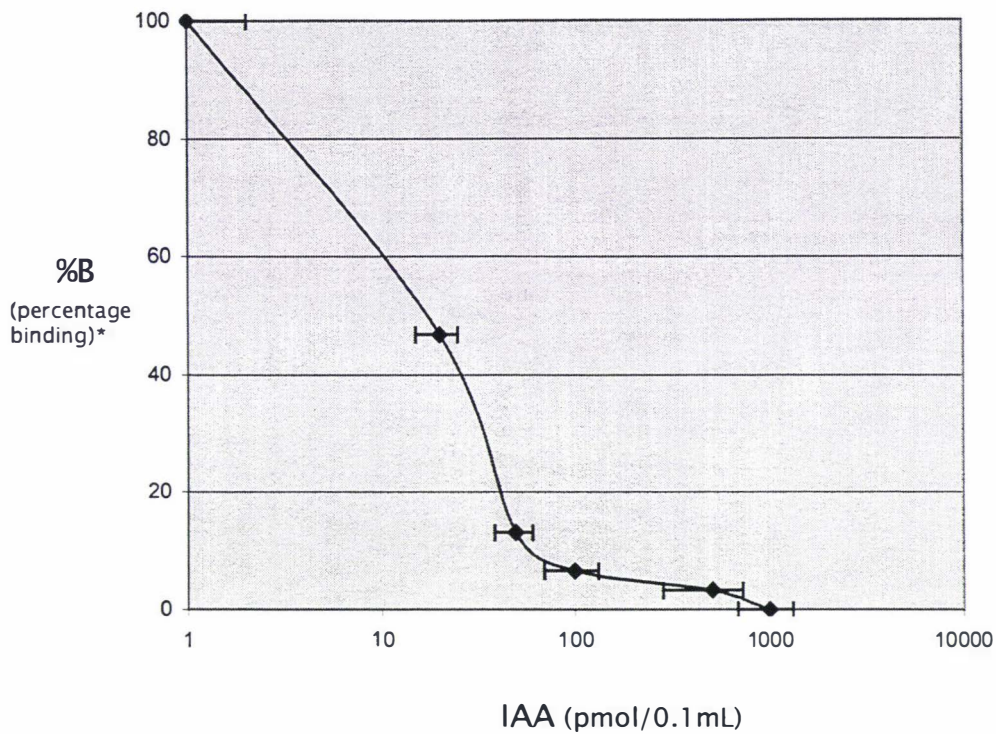


Figure 4.2b. The optimised IAA standard curve for the polyclonal IAA antibodies generated. The polyclonal IAA-CH<sub>3</sub> antisera displaying the highest titres (from bleed three) were used to generate the curve. \*%B refers to the percentage binding of the alkaline-phosphatase conjugate tracer to the immobilised IAA antibody.

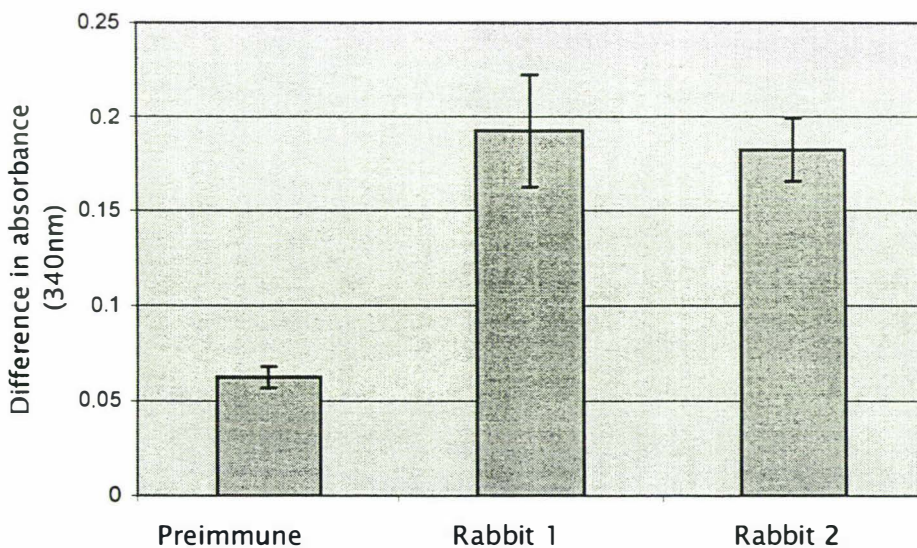


Figure 4.2c. The maximum difference in absorbance measured with antibody immobilised ELISA between IAA concentrations of 0 and 1000 pmole/0.1 mL using the polyclonal antisera generated from the two rabbits, as indicated, against IAA-CH<sub>3</sub>.

### 4.3 IAA ELISA using the monoclonal antibody

The low titres of the polyclonal antibodies raised to the BSA-IAA conjugates, for reasons that will be assessed later in the discussion section, resulted in an immunoassay that was insensitive to detect relatively large changes in IAA concentration. To overcome this, a commercially available monoclonal-based IAA detection kit was obtained and then assessed for use to measure the IAA concentrations in plant tissue extracts using ELISA. The commercially available monoclonal antibody was then used to determine the amounts of IAA in the bean tissue and petioles during the time course of secondary abscission. The antibody was diluted 30 times the recommended dilution because at the stated dilution, the reaction proceeded too rapidly, with full development of the assay within five minutes of substrate addition. Initially, the monoclonal assay activity and curve generated from IAA standards was compared with the polyclonal antiserum raised against the IAA-BSA conjugate (Figures 4.3 a and 4.3 b).

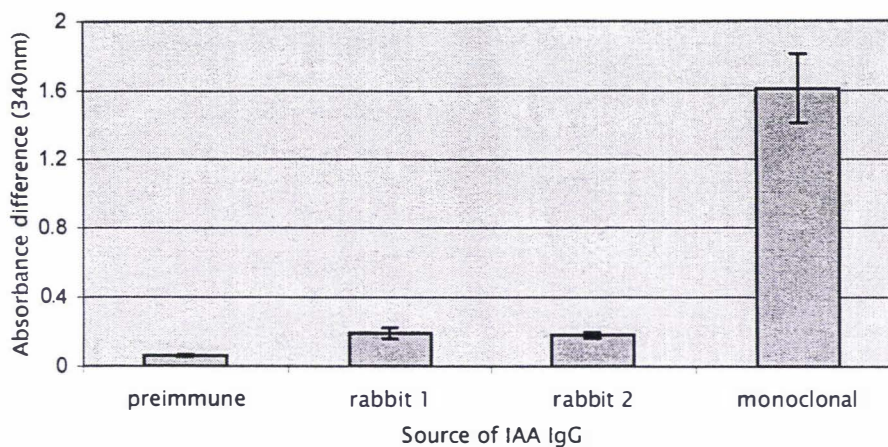


Figure 4.3a. The absorbance difference between 0% and 100% binding of the IAA-alkaline phosphatase conjugate to IAA antibodies, as indicated, using ELISA. The rabbit antisera used are those in Figure 4.2b for comparison with the monoclonal antibody.

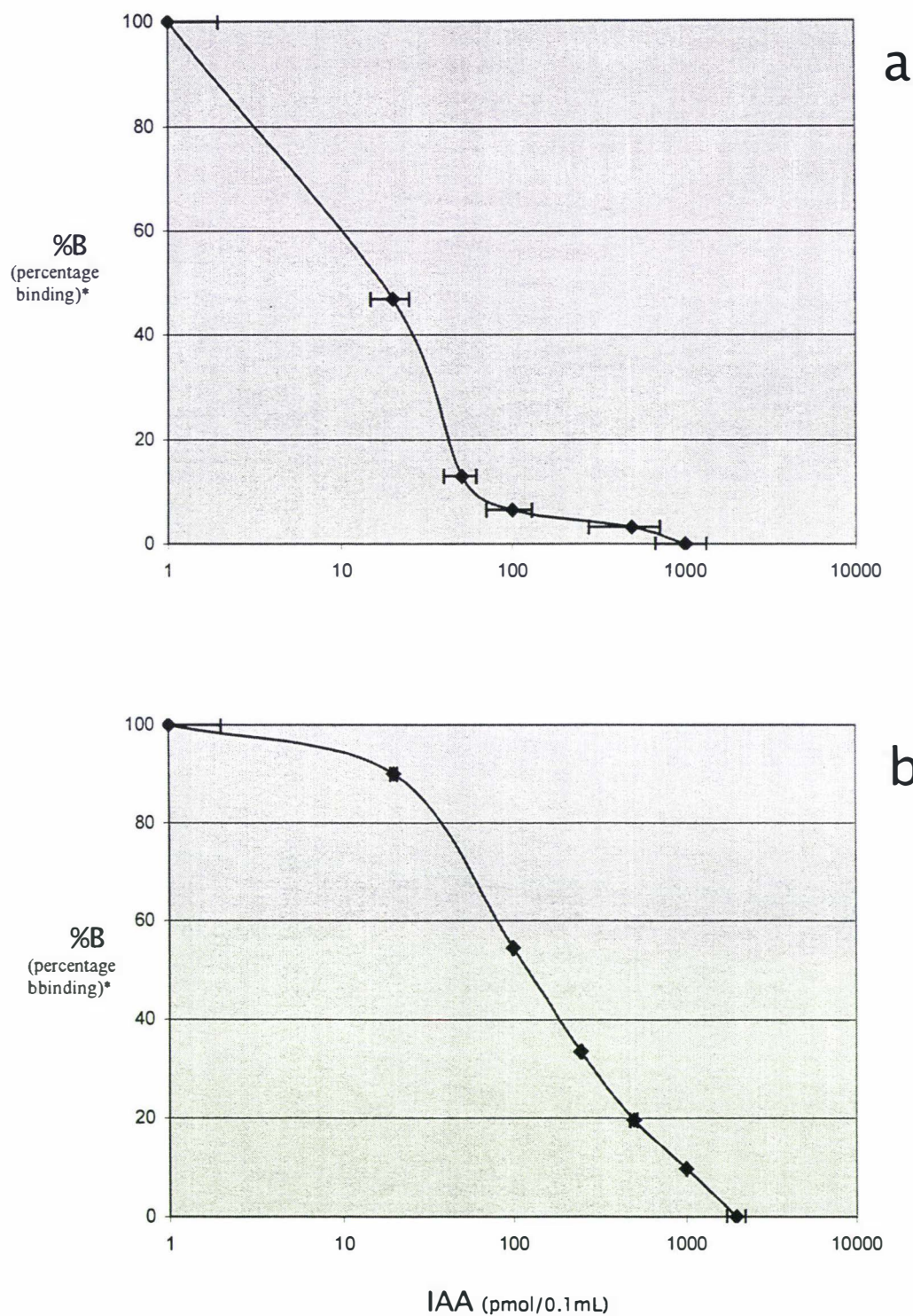


Figure 4.3b. The IAA standard curve using the polyclonal IAA IgG (from Figure 4.2a) compared to the optimised standard curve generated using the monoclonal antibody to IAA. \*%B refers to the percentage binding of the alkaline-phosphatase conjugate to the immobilised IAA antibody.

#### 4.3.1 Cross-reaction test to support accuracy of using the monoclonal antibody for measurement of IAA in samples

Before using the monoclonal antibody to measure the concentration of IAA in bean tissue extracts, curves were constructed to establish whether there were any compounds in the sample extracts that may interfere with the ELISA. The method used to construct these curves is similar to that described by Quarrie and colleagues (1988).

The curve represented by the blue points (Figure 4.4) was generated from the standard IAA concentrations, and is used as an indicator of any change in the IAA concentration values calculated when the plant extracts are present i.e. the relationship is linear as the x and y values, the standard IAA concentrations (1, 50, 100, and 250), are the same. The second curve, represented by the pink points, was generated with 50  $\mu$ L of fresh petiole extract present in each of the standard IAA reactions. The parallel nature of these curves indicates there are no compounds in the plant extract interfering with the assay. Curves of this nature that are not parallel indicate the presence of interfering compounds that must be removed before further analysis (Caruso *et al* 1995). Interference of the antibody generally gives a lower value of binding when all of the antibody sites are occupied by free IAA ( $B_0$ ), and consequently an overestimation of the endogenous hormone. That is, if there are other compounds in the extract binding to the IAA sites of the antibody this will prevent the binding of the tracer and so give a calculated value for free extract IAA that is higher than the actual amount.

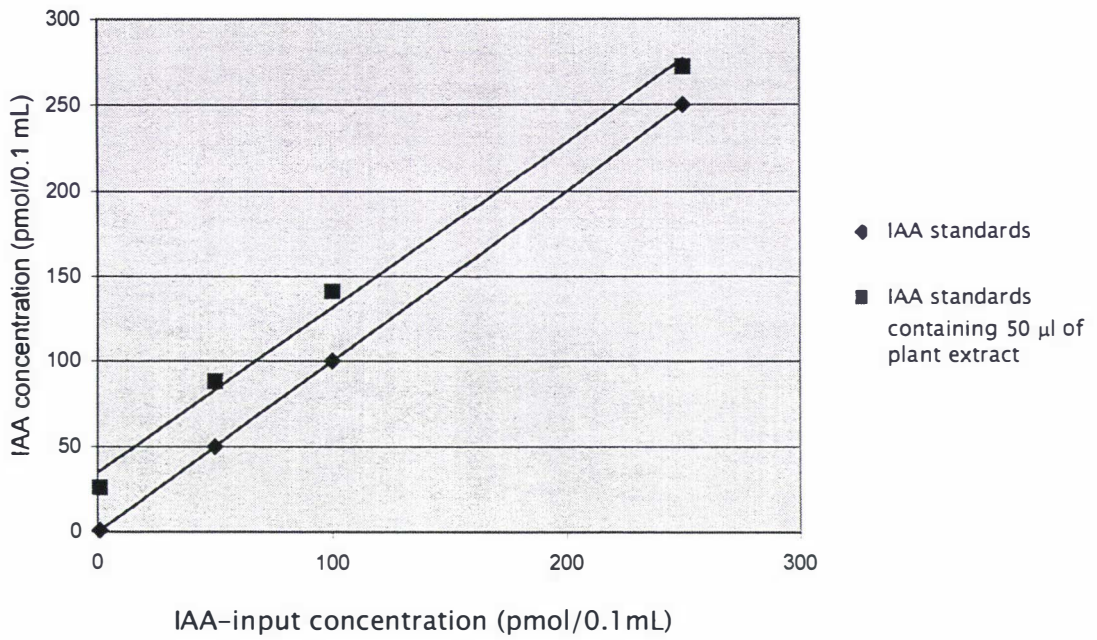


Figure 4.4. Cross-reactivity curves used to validate the measurements of IAA in bean extracts using ELISA.

### 4.3.2 Measurement of IAA in bean tissues

Prior to use in the measurement of IAA concentrations during secondary zone formation, the antibody was further tested in terms of the determination of IAA in different plant tissues. The hypocotyl, epicotyl, petiole, shoot, and leaf from 14-day-old bean plants were collected and the IAA extracted as described in section 2.4.2.1.2.

The amounts of IAA in these tissues, as measured by IAA ELISA using the monoclonal antibody, are shown in Figure 4.5. The concentration of IAA is higher in the shoot tissue (750 pmol/g FW) when compared with the other tissues assayed. The leaf tissues, which are also known to be a source of IAA production, had a concentration of IAA that was considerably higher than the petiole, hypocotyl and epicotyl tissues (190 in the leaf compared to 20 to 40 pmol/g FW in the other tissues).

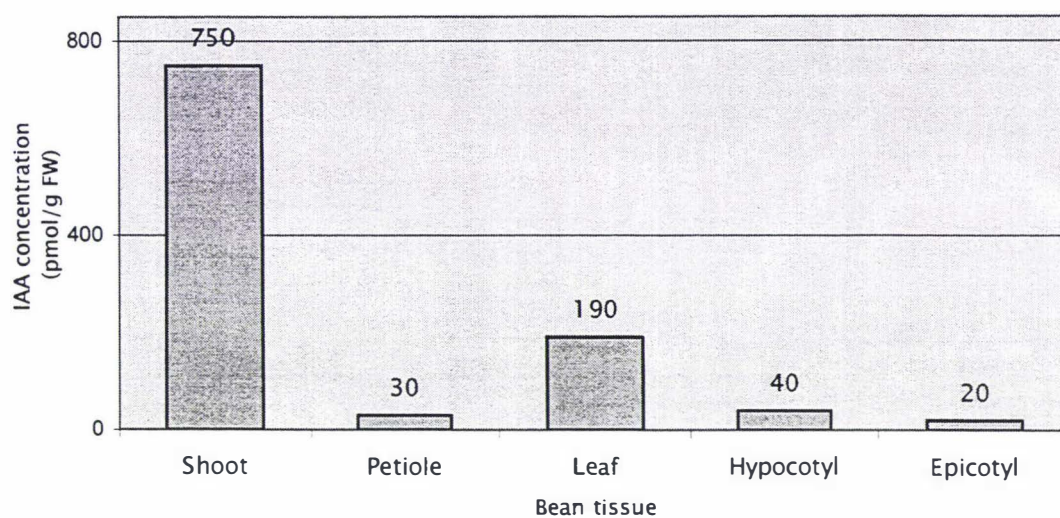


Figure 4.5. Concentration of IAA in pmol/g fresh weight in extracts of fresh tissues (as indicated) excised from 14-day-old bean plants. The numbers refer to values of IAA as pmol/g FW for each tissue.

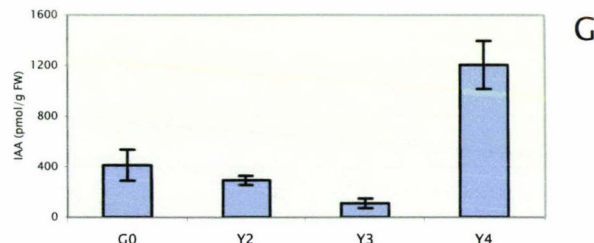
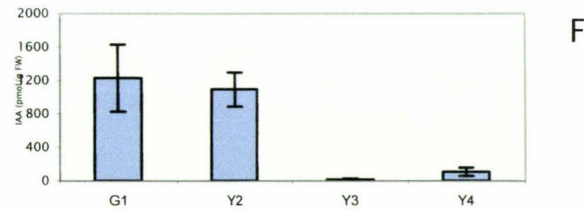
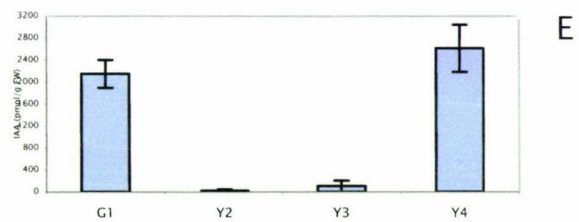
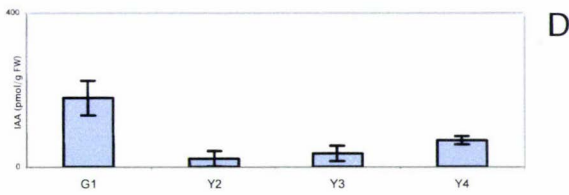
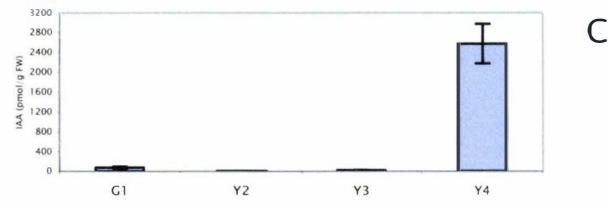
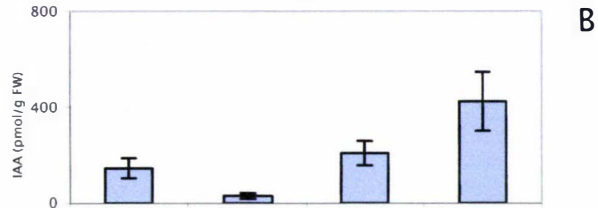
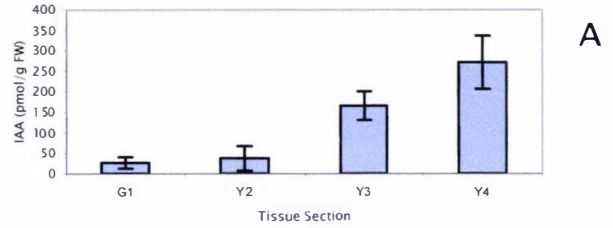
### 4.3.3 Measurement of IAA during the time course of secondary zone formation

Secondary zones were generated as described in section 2.1.3. Seven time points were assayed; 0 h, where the senescing pulvinus was removed before any application of IAA; 6 h after the second and final addition of IAA to the primary abscission layer (there was one IAA application at the time of primary abscission and one 8 hours later), and then 16 h, 26 h, 40 h and 52 h after the final IAA addition (refer to Figure 4.1d). Each petiole piece was divided into four 3 mm sections to establish differences in IAA concentrations along the petiole. Sections are labelled one to four, where one is the section at the distal end of the petiole (proximal to the primary zone) and four is the proximal end. An additional label G or Y has been added to indicate either the green, distal portion (G1) or the (later) senescing yellow (Y) portions (sections 2, 3 and 4). These sections, with labels as described above, are illustrated on petioles in Figures 4.1 a to 4.1 d. The concentrations of IAA were calculated and expressed in pmol/g fresh weight (FW). The results in this section have been calculated from two biological duplicates. That is, two separate experiments in forming secondary zones were performed and the IAA determinations are a triplicate assay from each experiment. The standard errors were calculated for the two biological duplicates separately and the greater error presented graphically. The results are presented in Figure 4.6 (a to g).

At the time of primary abscission, there was a definite increase in the concentration of IAA from the distal abscission end to the proximal end of the explant (Figure 4.6a). The first two sections (G1 and Y2) have about the same concentration of IAA (between  $26 \pm 14$  and  $37 \pm 30$  pmol/g respectively) with the end section (Y4) containing the most IAA ( $271 \pm 65$  pmol/g). The difference in the concentration of these hormones is dramatic with approximately 6-fold more IAA in the Y3 section and 10-fold more IAA in the Y4 section when compared with the G1 section. Six h after the final IAA addition there is a similar distribution pattern of IAA along the petiole, although the concentration has increased in the green section (G1) and the concentration in the Y2 section has remained the same. Although the overall IAA concentration of approximately 800 pmol/g in the petiole explant six h after abscission is higher (almost twice that of the petioles at primary abscission), it is considerably less than the amount of IAA applied to the primary abscission face. By 16 h, the amount of IAA in the Y4 section compared to the Y4 section at 6 h has increased six-fold (from  $423 \pm 123$  to

2570 ± 408 pmol/g). This is a dramatic increase in the total amount of free IAA and may influence the spatial and temporal differentiation of the secondary zone. The release or breakdown of IAA conjugates and a pooling of free IAA could explain the very high concentration of IAA at 16 h in the Y4 section. There is a striking distribution change at 26 h where the overall IAA concentration drops dramatically (from 2677 to 304 pmol/g) and the G1 section (179 ± 45 pmol/g) contains the highest amount of IAA. By observing the petiole explants, this appears to be around the time the secondary zones differentiate. By 40 h, the pattern of IAA distribution is similar to 26 h with a dramatic rise in overall concentration of IAA within the petiole explant (from 304 pmol/g to 4882 pmol/g). The IAA increase is principally in the G1 (12-fold) and Y4 (37-fold) sections. There is a proportionally larger rise in the IAA concentration in the Y4 tissue when compared with the G1 section, i.e., where at 26 h the IAA in the Y4 section accounted for 22% of the explant IAA but at 40 h the Y4 section made up 53% of the total free IAA. At 52 h, where the colour differences become apparent and there is visible mechanical weakness at the adventitious abscission zone, the amount of IAA in the Y4 section is low (a 24-fold drop from the 40-h petiole sample) and for the first time point there is a massive increase in the concentration of IAA in the Y2 section (1090 ± 209 pmol/g). Finally, at full separation (98 h) when the proximal end of the petiole explant is senescent and the zone has separated, the concentration of IAA in the Y4 section (1198 ± 47 pmol/g) is still relatively high compared to the other three sections (between 3 and 12-fold higher) with the green G1 section (405 ± 268 pmol/g) the next highest.

Tissue Sample	Time Point (h)	IAA Concentration (pmol/gram)
G1	0 Primary zone separation	26 ± 14
Y2		37 ± 30
Y3		166 ± 35
Y4		271 ± 65
G1	6	146 ± 42
Y2		30 ± 12
Y3		208 ± 50
Y4		423 ± 123
G1	16	80 ± 20
Y2		6 ± 3
Y3		21 ± 5
Y4		2570 ± 408
G1	26	179 ± 45
Y2		21 ± 23
Y3		35 ± 20
Y4		69 ± 11
G1	40	2147 ± 251
Y2		24 ± 23
Y3		103 ± 101
Y4		2608 ± 430
G1	52 Visible colour difference	1225 ± 405
Y2		1090 ± 207
Y3		17 ± 9
Y4		107 ± 10
G1	98 Secondary zone separation	405 ± 268
Y2		315 ± 10
Y3		107 ± 13
Y4		1198 ± 47



## 4.4 Ethylene evolution from petiole tissues

The ethylene evolved from the petiole sections was measured using gas chromatography. The scheme used to label the explant sections is shown in Figures 4.1 a to 4.1 d and described in section 4.1.1. For experiments measuring ethylene evolution from the petioles, explants were cut into two sections. The first section was the G1 tissue used in the IAA experiments, while the second section comprised the Y2, Y3 and Y4 segments as a pooled tissue. Three time points were assayed; the first was from freshly excised explants, the second was at abscission of the primary zone (0 h) and the third at the time of secondary zone separation (98 h).

Cutting of the explants resulted in ethylene production, and this was considered to be the putative wound-induced ethylene peak (Figure 4.7a). Two samples of petiole (freshly-excised petiole and 98 h explants) were analysed further to establish when this wound response stabilised. Firstly, a fresh bean plant was wounded by the excision of a petiole explant, the excised petiole was sealed in a glass tube of known volume and the ethylene evolved was measured hourly. The tube containing the petiole was aired and resealed after each hourly sample was removed. The aged explant (98 h) was wounded by cutting into three approximately even sections, and the ethylene evolved was measured in the same way as described for the freshly-excised explants.

The ethylene evolution data obtained from these wounding experiments is shown as Figure 4.7a. There was a significant increase in the ethylene produced two h after wounding in the fresh tissue (0.63 nmol/g/h in the first hour to 0.94 nmol/g/h in the second hour). The evolved ethylene then decreases dramatically in the fresh tissue between 2 and 3 h from wounding by approximately 0.6 nmol/g/h, and between 3 and 4 h there is a moderate increase of 0.13 nmol/g/h. The 98 h secondary abscission zone explant, which is in fact 144 h post excision, broadly followed the same pattern of wound ethylene evolution as the fresh tissue but with less significant differences in changes of ethylene evolution over the time course, and a lower overall amount of ethylene produced. However, both samples stabilised 6 h after wounding, and produced about the same amount of ethylene (0.07 to 0.08 nmol/g/h) between 6 and 7 h. With this information, petiole sections for the three time points [freshly excised, at primary abscission (0 h) and at secondary abscission (98 h)] were cut and left to air for 6 h in a

humidified container, sealed for an hour and then a 1 mL sample removed for analysis using gas chromatography.

When compared with the fresh explants, the production of ethylene was 2 to 3-fold greater in the explants at abscission of the pulvinus at the primary zone and then increased dramatically by 8 to 20-fold in the secondary zone explants (Figure 4.7b). In freshly excised explants, the level of ethylene evolution was similar in the G1 tissue ( $0.19 \pm 0.12$  nmol/h/g) and the pooled Y2, Y3 and Y4 tissues ( $0.10 \pm 0.06$  nmol/h/g). At the time of abscission of the pulvinus, the level of ethylene had increased 2-fold in the G1 tissue ( $0.39 \pm 0.13$  nmol/h/g) and approximately 7-fold in the Y2, Y3 and Y4 ( $0.67 \pm 0.25$  nmol/h/g). At 98 h, the time of formation of secondary zones, the ethylene evolution had increased to  $1.73 \pm 0.29$  nmol/h/g in the G1 tissue and to  $4.37 \pm 0.25$  nmol/h/g in the Y2, Y3 and Y4 tissue. The ethylene evolved in the Y2, Y3 and Y4 tissue was significantly higher than in the G1 tissue. In this study, the senescent pulvinus, at the time of primary abscission produced 2 to 3 times more ethylene ( $1.7 \pm 0.34$  nmol/h/g) compared to the Y2, Y3 and Y4 sections of the petiole from which it had separated.

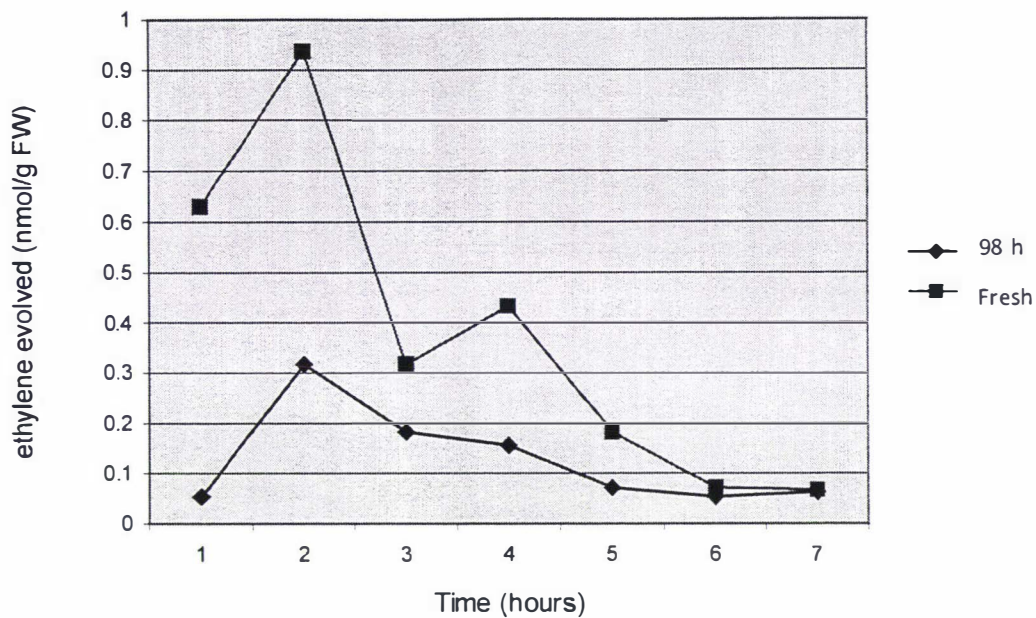


Figure 4.7a. Ethylene evolution from wounded fresh petiole and 98-h petiole explants.

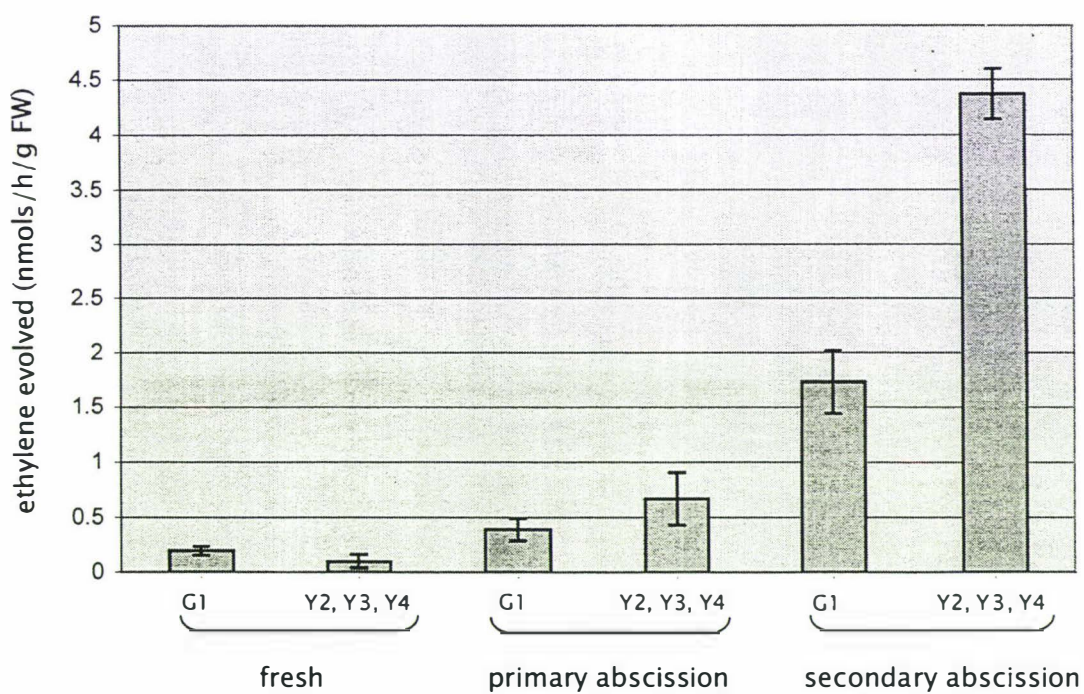


Figure 4.7b. Ethylene evolution from petiole segments (G1) and pooled sections (Y2, Y3 and Y4) of explants that are freshly excised (fresh), at abscission of the pulvinus at the primary zone (primary abscission) and at formation of the secondary zone (secondary abscission).

## 4.5 ACC oxidase activity and expression in petiole tissues

ACC oxidase activity was also determined for the same tissues, and at the same time points, as for the ethylene evolution measurements (Figure 4.8a). The freshly excised tissue had the highest ACC oxidase activity when compared with the tissues at separation of the pulvinus at primary abscission, and at secondary zone formation. In freshly excised tissue, the activity in the Y2, Y3 and Y4 pooled fresh petiole sections ( $0.29 \pm 0.07$  nmol/h/mg protein) was approximately the same as the G1 segment ( $0.22 \pm 0.05$  nmol/h/mg protein). At the time of separation of the primary zone, the ACC oxidase activity was approximately six times lower in the G1 section ( $0.053 \pm 0.006$  nmol/h/mg protein) when compared with the fresh G1 section and about 20-times lower in the Y2, Y3 and Y4 tissue of the primary zone ( $0.021 \pm 0.001$  nmol/h/mg protein) when compared with the fresh tissue. At the time of separation of the secondary zone, the ACC oxidase activity increased in the G1 petiole section to  $0.097 \pm 0.008$  nmol/h/mg protein but remained the same (in the Y2, Y3 and Y4 tissue).

Using SDS-PAGE and Western analysis, the extracts from which the ACC oxidase activity was measured were also challenged with an antibody raised to the gene product of an ACC oxidase gene in expressed leaf tissues of *Trifolium repens* (white clover)(designated TR-ACO2). A protein band of ca. 42 kDa, that is within the size range of previously characterised ACC oxidase enzymes, was the most strongly recognised of the proteins detected (Figure 4.8b). The expression of the ca. 42 kDa band corresponds closely to the ACC oxidase activity measured in the same samples (Figure 4.8a), with the highest expression in the fresh tissues, followed by the G1 tissue of the petioles at separation of the primary and secondary zone, and the least abundance in the yellow-pooled sections at separation of both zones. The detection observed of the other bands could be due to the recognition, by the ACC oxidase antibody, of similar epitopes to the ACC oxidase enzyme presented on these other proteins. Alternatively, the antisera used for this blot may contain other antibodies directed to other proteins of lower abundance. The bands other than the ca. 42 kDa do not appear to change in abundance in each of the tissues. However, there is recognition of a protein band of ca. 29 kDa that follows the expression pattern of the ca. 42 kDa protein, the presumed ACC oxidase, which may be a product of the cleavage of a larger ACC oxidase enzyme.

Both the ACC oxidase activity and ACC oxidase protein accumulation did not correlate with the ethylene evolution data. Figure 4.8c compares the ACC oxidase activity data with the ethylene evolution data. The units for the ACC oxidase activity data presented on Figure 4.8b were adjusted from nmol/h/mg of protein to nmol/h/g (FW), the same as the units of the ethylene evolution data. Because the amount of ethylene evolved from the tissue sections is 10 to 100-fold greater than the ethylene evolved from the ACC oxidase assay, the units for the ACC oxidase data have been multiplied by 100 so each sample can be clearly compared on the same graph. By expressing the ACC oxidase measurements in fresh weight, the difference between the amount of ethylene evolved from the fresh tissue and the tissues at separation becomes more dramatic. The ACC oxidase activity is now greater in the fresh tissues compared to those at separation, probably because the petioles at separation have more protein per milligram of tissue as they weigh less and appear less hydrated than the fresh tissue. However, overall the ethylene evolution data follows a pattern almost opposite to that of the ACC oxidase activity. For example, in the Y2, Y3 and Y4 tissue sections at secondary separation, the ethylene evolved is the highest of the six samples (4.37 nmol/h/g) with the ACC oxidase activity the lowest, equal to the yellow-pooled sections at primary separation (approximately 0.002 nmol/h/g).

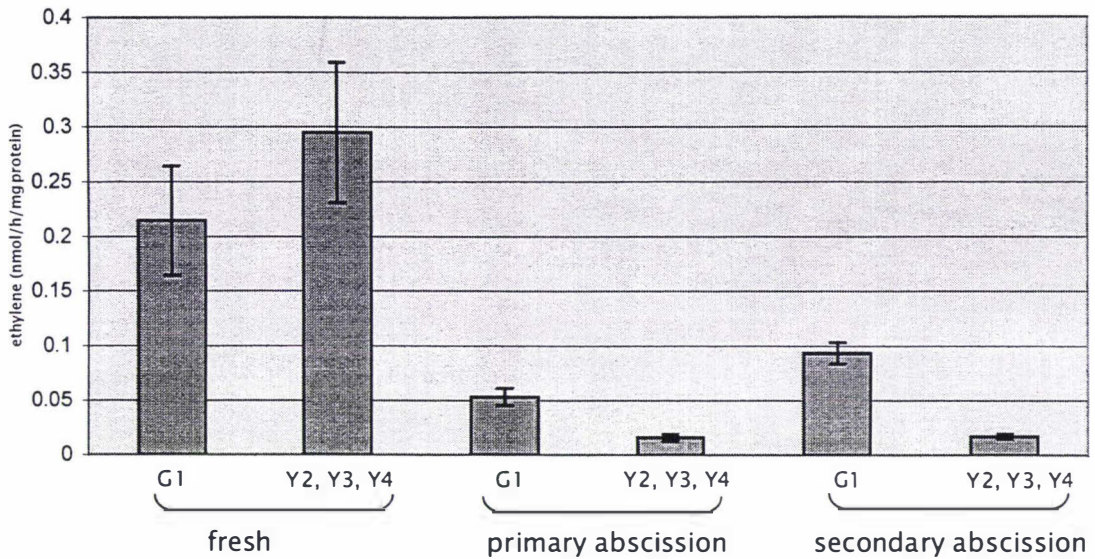


Figure 4.8a. Ethylene evolved in the ACC oxidase activity assay from petiole segments (G1) and pooled sections (Y2, Y3 and Y4) of explants that are freshly excised (fresh), at abscission of the pulvinus at the primary zone (primary abscission) and at formation of the secondary zone (secondary abscission).

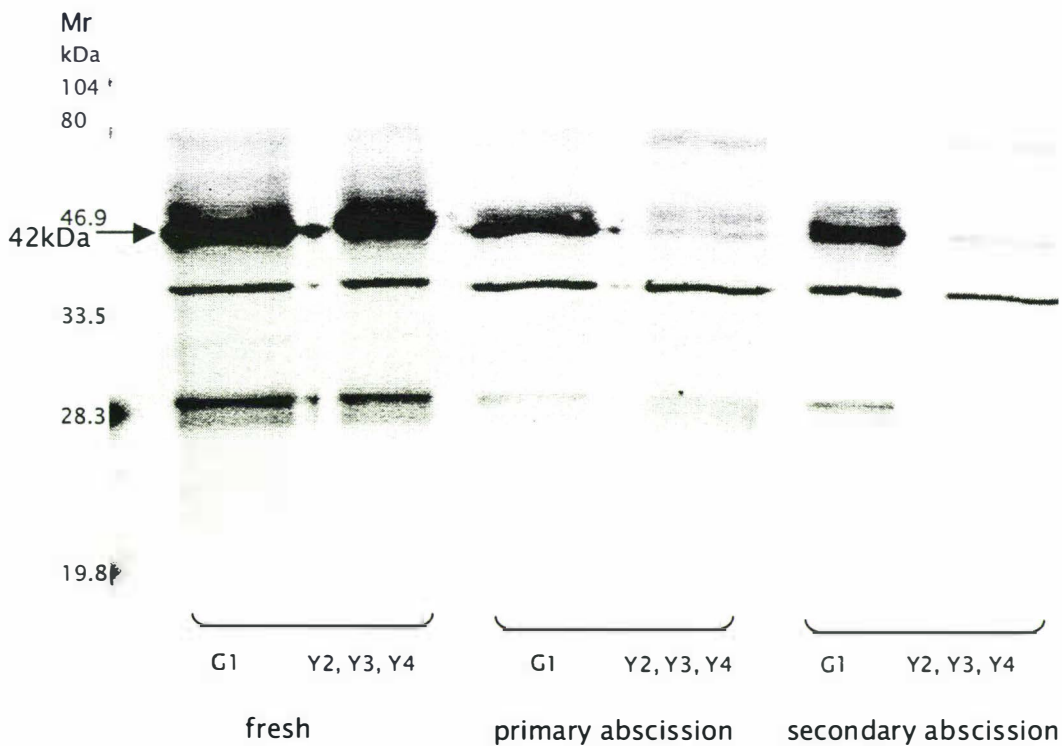
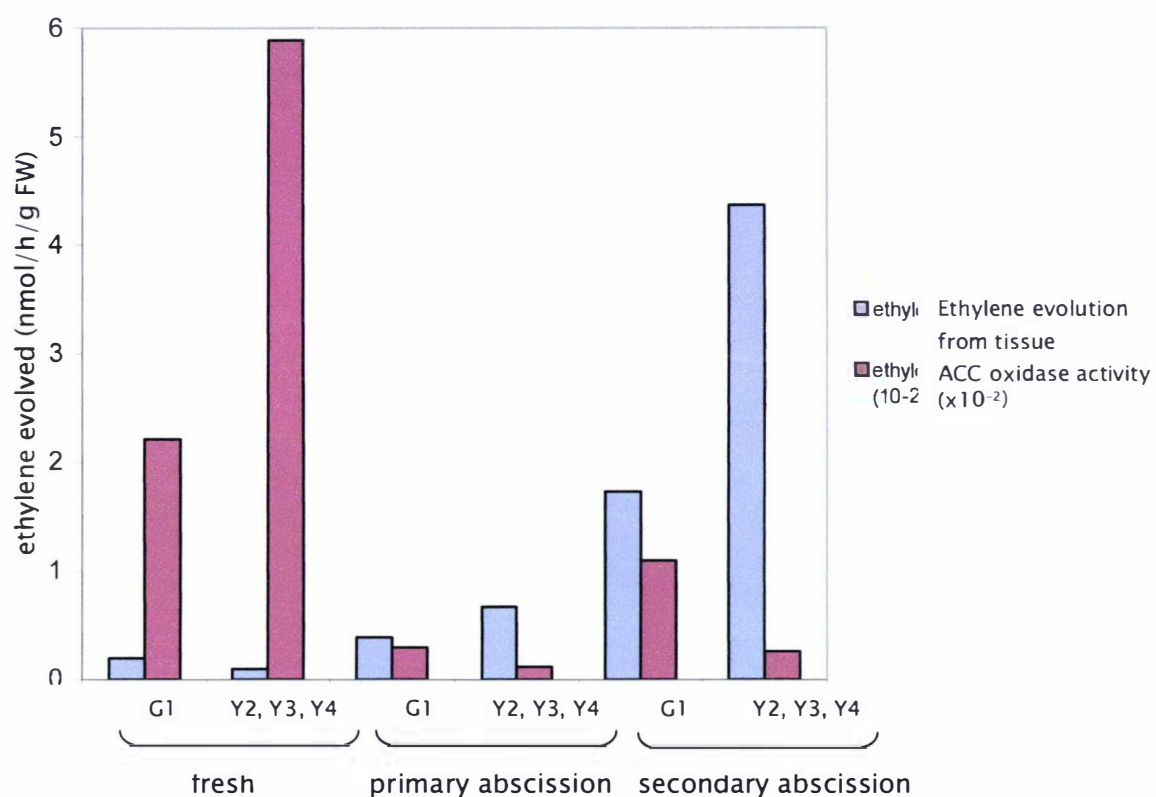


Figure 4.8b. Western analysis, using the ACC oxidase antibody, from petiole segments (G1) and pooled sections (Y2, Y3 and Y4) of explants freshly excised (fresh), at abscission of the pulvinus at the primary zone (primary abscission) and at formation of the secondary zone (secondary abscission).



**Figure 4.8c.** A comparison of ethylene evolution and ACC oxidase activity from petiole segments (G1) and pooled sections (Y2, Y3 and Y4) of explants that are freshly excised (fresh), at abscission of the pulvinus at the primary zone (primary abscission) and at formation of the secondary zone (secondary abscission).

## Chapter Five

# Discussion

### 5.1 The *in vivo* approach to study abscission and abscission cell differentiation

#### 5.1.1 Introduction

The initial aim of the research presented in this section was to identify proteins that were either preferentially expressed or unique to the leaf rachis abscission zone cells in *S. nigra*. *S. nigra* is used to study aspects of abscission because it has between 15 and 30 layers of terminally-committed cells in its leaflet abscission zone that swell and separate when exposed to ethylene (Osborne 1989). It is thus possible to collect these separated cells as a homogeneous cell class. It has been proposed that cell-specific proteins expressed in abscission zone cells and not in the surrounding rachis tissue can be used as markers of cell differentiation (Osborne and McManus 1986). Antibodies generated to cell-specific proteins could then be used as probes revealing the location of the protein and at what point during plant cell differentiation it accumulates. These exclusive proteins may have a role relating to the structural differences observed between zone and rachis cells or may be involved in the unique response of zone cells, to ethylene and auxin.

#### 5.1.2 The survey of cell wall proteins in *S. nigra* tissue

Initially, the research of this thesis aimed to purify and characterise the 34 kDa protein expressed in the cell walls of zone cells (OZ and ZONE) of *S. nigra* zone previously identified by McManus and Osborne (1991). In addition to the 34 kDa peptide, other potential cell-specific proteins were also screened for. For the purposes of this thesis, proteins were extracted from the cell wall with 1 M NaCl and referred to as ionically-associated cell wall proteins. It is possible that during the extraction process proteins that are normally within the soluble fraction became associated with the cell wall and are not removed from the tissue with the water washes. However, the technique for cell wall bound protein extraction used in this thesis is the same as that used by McManus

and Osborne (1991) and there is no evidence in these studies that suggests that there is soluble protein contamination in the cell wall extracts. However, to show definitively that a protein is cell wall associated, immunolocalisation of the protein in the cell wall is required. The localisation of a protein can be confirmed through immunolocalisation, as illustrated by McManus and Osborne (1989), with the immunolocalisation of an unidentified protein in the abscission zone cell walls of *P. vulgaris*.

### 5.1.3 Separation of cell wall extracts using SDS-PAGE

One-dimensional SDS-PAGE of cell wall extracts revealed one protein of 38 kDa that appeared to be expressed only in the OZ cell walls in the extract from the tissue collected in the autumn months (Table 3.1, group V). At this level of resolution, there were no apparent abscission zone cell-specific proteins (i.e. expressed in the ZONE and/or the OZ tissues) of 34 kDa in any of the total cell wall extracts.

Previous analysis of the elongating hypocotyl of mung bean, using two-dimensional electrophoresis, revealed there were at least 250 peptides that could be extracted from the cell wall with 1 M NaCl (Corke and Roberts 1997). Assuming that there are a similar number of proteins in the cell walls of *S. nigra*, then the one-dimensional minigels, used to separate the total cell wall extracts, will have limitations in resolving individual peptides as it is probable there are many peptides that will have similar molecular weights. Consequently, a band that appears to be a single peptide may contain several different proteins or isoforms of the same protein.

### 5.1.4 Separation of cell wall HIC fractionated extracts using one and two-dimensional SDS-PAGE

To resolve single peptides, the proteins in the cell wall extracts were separated further using hydrophobic interaction chromatography (HIC). Each of the wall extracts was fractionated into over 20 fractions that were then separated with SDS-PAGE using the minigel system. In three of the fractions (from the extracts of spring collected tissues) there appeared to be a total of six peptides that were present only in the OZ and ZONE tissues (Table 3.2). One of these, resolvable in fraction H (Figure 3.2d), was a ca. 34 kDa protein, the same size as one of the previously identified abscission zone cell-specific proteins (McManus and Osborne 1991).

Fractionation of the extracts with column chromatography reduced the number of peptides separated using SDS-PAGE (Figures 3.2b to 3.2e). However, with most of the protein eluting after 60 percent buffer B [i.e. in only 40 percent of the fractions (Figure 3.2a)], there were still densely staining areas in many of the fractions where single peptides were not resolvable. To separate the peptides further, one of the fractions (fraction I) was selected for two-dimensional electrophoresis. This technique separates proteins on the basis of their isoelectric point and molecular mass. This method resolved what appeared to be single proteins and revealed the presence of at least two proteins of ca. 42 kDa with different isoelectric points of 8.3 and 9.6. An attempt was made to obtain amino acid sequence from these spots by excising them from the gel, but although the spots appeared to contain enough protein for amino acid sequencing of fragments generated using trypsin, there was no sequence returned. Apparently, the concentration of protein was not high enough for the sequencing technique used.

#### 5.1.5 The major groups of cell wall protein in the crude and fractionated cell wall extracts

In terms of the survey of cell wall proteins, five major groups were identified (Table 3.1 and 3.2). Proteins that appear either exclusively or preferentially expressed in the non-ethylene treated MR and OZ tissues (Table 3.1, group 2) are examples of proteins that are down-regulated or have reduced expression with ageing or ethylene treatment. One of these, a putative isomerase (OZ43), was identified and partially characterised (see section 5.1.9).

There appears to be several proteins of 18, 24 and 72 kDa that are rachis-specific (MR) or preferentially expressed in the tissue with reduced abundance (or are absent) in the abscission zone cells and the ethylene treated tissues (Table 3.1, group I). The absence of these proteins associated with the OZ cell walls could be a result of functional differences within rachis cells when compared with the abscission zone cells and/or a consequence of the anatomical cell wall differences. Proteins that are unique to the rachis cells could be used as biochemical markers of cell differentiation of MR to OZ cells as the loss of the protein in the OZ may signal the onset of abscission cell-differentiation.

The cells of the rachis (MR) constitute type I target cells and the abscission zone (OZ) are classified as type II cells based on their response to ethylene and auxin (Osborne 1989). As the biological response of these two cell types to ethylene and auxin is quite different, it appears likely there are some different proteins induced in the cell walls of MR when compared with the OZ tissue. The peptides expressed only in the MRE tissue (Table 3.1, group III) may function in a MR ethylene response that differs to that observed in the abscission zones cells.

Thirteen peptides that are ZONE cell-specific were identified from fractionation of the cell wall extracts using HIC (Table 3.2, group 2), compared to six MRE-specific peptides in the total bound wall extracts (Table 3.1, group III). Previous reports show that most of the ZONE-specific proteins have roles in protecting the exposed fracture surface from the invasion of bacteria and fungi (Coupe *et al* 1995). Coupe and co-workers found that, of the nine ethylene up-regulated proteins in the leaflet abscission zone of *S. nigra* they isolated, seven had significant sequence similarity to previously characterised pathogen related (PR) proteins. One of the nine proteins they characterised further was a ca. 7.5 kDa metallothionine-like protein with unknown function that was identified previously through cDNA characterisation (Coupe *et al* 1995). A protein previously isolated from ZONE cell tissue of 20 kDa (not specifically associated with cells walls), with its significant sequence identity with the carboxy terminus of an extensin protein, is a possible regulator of cell wall integrity (Ruperti *et al* 1999).

The peptides in MRE and ZONE cell walls are listed in group IV of Table 3.1, and their accumulation represents an ethylene-response common to both cell types. These may include proteins that are commonly induced by ethylene, including the peroxidases (McManus 1994) and the chitinases (Boller *et al* 1983).

In the initial one-dimensional gel survey (Table 3.1), it was observed that some of the proteins extracted from the cell wall changed in abundance over the vegetative season. For example, a peptide of ca. 15 kDa appeared to be highly expressed in the OZ tissue in the summer months but was only a minor component in the spring and autumn OZ gels. A change in the abundance of some proteins throughout the seasons seems probable as the physiological processes and morphology of the rachi change from

spring to autumn. In spring, the cells of the rachis are rapidly dividing and elongating, as the tissues are actively growing. In summer, the tissues have stopped elongating as rapidly and have a higher level of primary cell wall thickening, and the shrub flowers and fruits during the summer collection period. During the autumn collection period, some of the leaves are beginning to show signs of senescence (loss of chlorophyll) and the rachis tissue appears thicker and more weathered.

The same procedure of total cell wall protein extraction and fractionation using HIC with tissues from the spring months (Table 3.2) was repeated for tissues collected in the summer and autumn months. As well as differences in expression of proteins between tissue types and changes in the abundance of individual proteins through the seasons, there were again differences in the expression of proteins resolvable in the fractions between seasons. However, it was observed that many proteins were not resolvable in the same HIC fractions in the spring, summer and autumn collections. This made it difficult to find and isolate a particular protein over the course of several extractions covering the three seasons.

#### 5.1.6 Identification of cell-specific proteins

From the survey of the cell wall proteins in the four tissue samples there was one 34 kDa protein that appeared in fraction H after HIC fractionation (Table 3.2, group 1) that appeared to be abscission zone cell specific (i.e. in both the OZ and ZONE tissues). As this was the same size as one of the cell wall proteins previously identified by McManus and Osborne (1990) as being abscission-zone specific, more tissue was collected (in the summer and autumn months) but fractionation of these tissues did not reveal the putatively zone-specific 34 kDa protein. However, a protein fraction separated using HIC from the tissue collected in the autumn months appeared to have several other candidates for cell-specific proteins present in the OZ tissue. Therefore, internal amino acid sequence data from tryptic fragments of ca. 43, 28 and 10 kDa proteins were obtained, and putative identities obtained using the BLAST-P function. Four fragments were sequenced (two from the ca. 28 kDa protein) and database matches identified the ca. 43 kDa protein putatively as gp40 (an aldose-1-epimerase-like protein), one of the ca. 28 kDa proteins putatively as a superoxide dismutase and the second ca. 28 kDa protein putatively as a ribonuclease I. The ca. 10 kDa protein was identified putatively as a lipid transfer protein.

From these four putative identities, three antibodies were obtained. Two for the ca. 10 kDa protein, that appeared to be a lipid transfer protein (LTP), and one for the ca. 43 kDa protein, that had identity with the gp40 protein. The LTP antibodies recognised a peptide of the same molecular mass as the OZ10 protein. Likewise, the antibody to the gp40 protein recognised a protein of ca. 43 kDa. The combination of sequence identity, molecular weight and recognition by an antibody raised against the proposed protein is compelling evidence for the identification of a gp40-like protein and the lipid transfer protein. However, it is possible that even though the antibodies recognised proteins that were the same size as the protein bands from which the sequence fragment was initially obtained, the antibodies could be detecting different proteins than those of the sequences they had similarity too. For example, two internal fragment sequences were obtained from the protein band of ca. 28 kDa and were identified as superoxide dismutase and a ribonuclease indicating there is more than one protein in this band. Each one is discussed in more detail in the following sections.

#### 5.1.7 Superoxide dismutase in the abscission zone cell walls of *S. nigra*

The identification of a putative superoxide dismutase in the OZ tissue was not pursued further as a candidate for an abscission-zone cell-specific protein as it is well known that these enzymes are associated with abiotic stress. Therefore, it would be expected to be expressed in both the ZONE cells and the ethylene-treated MR tissue (MRE). Moreover, the fragment size (eight residues) is perhaps not sufficient to deduce its function by comparison to a whole protein previously characterised. However, this short sequence may be from an isoform of SOD that is specific to the OZ cells and not induced by ethylene.

The localisation of SOD in the cell walls of abscission-zone cells has been observed (Henry and Ananich 1986), although its presence was not measured and compared to other cell types. Both the reduced oxygen species  $O_2^{\cdot-}$  (a superoxide radical) and  $H_2O_2$  (hydrogen peroxide) do not appear to cause the plant any harm at physiological concentrations. However, the toxicity *in vivo* occurs when they are converted into hydroxyl radicals in a metal-ion dependent reaction. These radicals and their derivatives are amongst the most reactive species known to chemistry (Cadenas 1989). Because the hydroxyl radicals are very reactive, defence mechanisms are designed to

control the level of superoxide and hydrogen peroxide within the cell. Plants possess higher levels of intracellular oxygen than in other organisms because they are oxygen-evolvers and therefore have several tiers of defence against oxygen derived free radicals. The defence mechanisms against free radical damage in plants are both enzymatic and non-enzymatic. The enzymatic defences include peroxidases and catalases that remove  $H_2O_2$ , and superoxide dismutases that catalyse the transformation of superoxide radicals to hydrogen peroxide and dihydrogen. Non-enzymatic defences include glutathione and ascorbate along with a range of less predominant compounds (Larson 1988).

Superoxide dismutase is a relatively abundant protein present in three different forms in plants as determined by the metal ion present in the active site. The three groups that have been identified are an iron SOD and a manganese SOD that are both very similar in structure, and a copper/zinc SOD which appears structurally unrelated to the iron and manganese forms (Steffens *et al* 1986). The SOD identified in this study appears to be either an iron or manganese form but most likely a manganese form as, to date, iron forms have been found only in chloroplasts (Bowler *et al* 1994). Examination of the subcellular locations and functions in the plant cell reveal that some form of SOD appears present in most parts of the cell. However, in response to stress only the copper/zinc form is induced with metal treatment of the plant (Obereggar *et al* 2000).

#### 5.1.8 Ribonuclease in the abscission zone cell walls of *S. nigra*

Ribonucleases catalyse the cleavage of ribonucleic acid with varying specificities depending on the type of enzyme. The study of the functions of plant ribonucleases is complicated by a complex profile of RNase activities detected in tissues (ZhengHua and Droste 1996). For example, a highly polymorphic family of at least 20 genes encodes the intracellular pathogen-related RNase proteins from *P. vulgaris*. There are many reports of the induction of RNases in response to different stress inducing factors. Most of the reported research examines the changes in RNase activities in response to a water deficit (for example Biswas and Choudhuri 1984, Tatt 1980, Yi and Todd 1979). In consideration of the protein size (ca. 28 kDa) and the cell wall location, it is most likely that if the OZ28 protein is a RNase, it is a member of the group I enzymes, although it is not clear what their function in abscission is.

### 5.1.9 Characterisation of a ca. 43 kDa abscission zone cell wall-associated protein from *S. nigra*

A major part of the research in this part of the thesis involved the characterisation of the protein from which the OZ43 tryptic fragment was obtained. The peptide sequence obtained for OZ43 has significant similarity to an aldose-1-epimerase-like protein (gp40) in tobacco suspension cells (Heese-Peck and Raikhel 1998). This identification for the OZ43 protein makes it one of the more likely candidates for an abscission cell-specific protein as it has not been associated with stress responses. However, very little is known about gp40 and whether this protein functions as a mutarotase enzyme with which it shares significant sequence identity.

The initial identification of OZ43 (or a protein within the SDS-PAGE band) as a putative gp40-like (a possible mutarotase) protein was from the sequence identity of a small internal tryptic peptide of 16 amino acid residues. The short OZ43 sequence contained two of the five residues that are highly conserved between all of the bacterial forms of mutarotase examined to date, gp40, pig, human and 11 of the 14 possible forms of mutarotase in *Arabidopsis*. The five conserved residues modelled in the gp40 active site (Fishman *et al* 1973) are two histidine (H-115, H-192), two tyrosine (Y-163, Y-194) and one tryptophan (W-121). The histidine at position 192 and the tyrosine at 194 are present in the OZ43 sequence fragment (the OZ43 fragment did not contain amino acids in the range of the other conserved residues). Alignment of the gp40 sequence with the OZ43 fragment and the possible mutarotase sequences from *Arabidopsis* reveals there are 10 highly conserved residues within the plant enzyme. Three of the seven putative mutarotases from *Arabidopsis* do not have a H-192 residue. This is replaced with an arginine at this position, but this is adjacent to histidine at position 191.

In a structural examination of mutarotase by Thoden and Holden (2002), a survey of the SWISS-PROT data bank revealed that there are about 45 amino acid sequences that code for probable mutarotases. Amino acid sequence alignments of these proteins demonstrate that they have sequence similarities ranging from 45 to 58 percent and identities ranging from 26 to 38 percent. Interestingly, the probable mutarotases show no sequence identity to other proteins in the data bank.

The sequence of the tobacco suspension cell nuclear pore membrane gp40 mutarotase-like protein was found to share significant identities (35 to 41 percent) to mutarotase proteins from bacteria and yeast (Heese-Peck and Raikhel 1998). With the sequencing of the *Arabidopsis* genome, there have been five mutarotase-like (about 60 percent identity), two probable (about 55 percent identity) and seven putative (about 43 percent identity) mutarotases identified by comparison of amino acid sequences deduced from DNA sequences with that of the tobacco gp40 sequence.

The immunological identification of the OZ43 protein at ca. 43 kDa with the gp40 monospecific antibody, in the same HIC fraction as the band from which the OZ43 sequence was obtained, was good evidence that the amino acid sequence fragment from OZ43 and the ca. 43 kDa protein recognised by the gp40 antibody were the same protein. The gp40 antibody did not detect the porcine kidney mutarotase or any proteins in the lamb kidney extract suggesting the plant OZ43 and the tobacco membrane located gp40 protein are more closely related in overall structure to each other than to the mammalian mutarotases with which gp40 shares significant sequence identity.

Mutarotase activity has been measured in bacteria, yeast, mould, fungi, birds, fish, mammals and higher plants. In higher plants, the mutarotase activity was measured in a variety of different species although no activity was also recorded in some species (Bailey *et al* 1967). The pepper family revealed the highest activity of those species examined with only enzyme activity in the fruit measured. Although activity has been measured in higher plants, no active enzyme has been isolated, and despite its widespread distribution no definite function has yet been ascribed to the enzyme in higher plant species. Therefore, once OZ43 (as recognised by the gp40 antibody) was identified as a mutarotase-like protein, it was of interest to determine if any enzyme activity was associated with the protein.

To establish whether the gp40-like OZ43 protein possessed mutarotase activity, a method to measure this activity was developed using a coupled enzyme assay. The development of the coupled enzyme assay began with testing different concentrations of  $\alpha$ -D-glucose and measuring how the spontaneous mutarotation increased with increasing amounts of substrate. Because of the equilibrium between  $\alpha$ -D- and  $\beta$ -D-

glucose, the change in absorbance at 340 nm (reducing in value as  $\alpha$ -D-glucose equilibrates to  $\beta$ -D-glucose) was not changed significantly by a relatively high concentration of added  $\alpha$ -D-glucose in comparison to the coupled assay. The same pattern was observed for high concentrations of added  $\beta$ -D-glucose. However, by coupling the D-glucose anomeric equilibrium to the glucose dehydrogenase specific conversion of  $\beta$ -D-glucose to D-glucono  $\delta$ -lactone, the  $\beta$ -D-glucose is removed as it forms thereby preventing it converting back to  $\alpha$ -D-glucose. The formation of NADH from the NAD<sup>+</sup> cofactor was measured optically at 340nm as an increase in absorbance. The coupling resulted in a considerably more sensitive assay providing the substrate ( $\alpha$ -D-glucose) concentration was significantly below the  $V_{\max}$  of glucose dehydrogenase (i.e. the conversion of  $\beta$ -D-glucose by glucose dehydrogenase was not the rate-limiting step, but rather the concentration of the mutarotase enzyme determined the reaction rate).

All the measurements of mutarotase activity were performed on samples that had been desalted using concentrators with a 10 kDa molecular mass cut-off range. Compounds that have been shown to inhibit the mutarotase enzyme in mammals, for example 1-deoxyglucose and 1-methylglucoside (Bailey *et al* 1967), are of low molecular weight (<10 kDa) and so should be removed in the concentration and desalting process. To eliminate any effects of different pH, the samples were exchanged into a 100 mM Tris-HCL, pH 7.6, buffer.

During the purification process, the specific activity of mutarotase in the HIC fraction, containing the gp40-identified OZ43 protein appeared to increase slightly when compared with the crude cell wall extract. Considering the HIC fraction with OZ43 contained about 10 percent of the total protein loaded onto the column, the specific activity may have been expected to increase significantly (about 10-fold) if this was the protein that was displaying the enzyme activity. Several of the other HIC fractions assayed appeared to have activity, but none as high as the fraction containing the OZ43 protein. The activity then decreased dramatically in the fraction from the ion exchange (Mono-Q) column that contained the OZ43 protein (as identified through Western analysis using the gp40 antibody). However, the other fractions from the Mono-Q column did not possess any activity either indicating that the enzyme had lost activity during purification either through deterioration or through the removal of some essential cofactor. There is no other evidence that indicates there is a cofactor requirement for

mutarotase in bacteria and mammals, but this does not rule out the possibility of a plant enzyme cofactor requirement, including the role for a chaperone protein.

The fractionation of the cell into cell wall and soluble components was another way to assess whether the gp40 antibody was detecting an active mutarotase. If the activity did not correspond to gp40 antibody detection, then it is likely the activity is not caused by the OZ43 protein. In the fractionation experiment, most activity was found in the soluble supernatant containing the truly soluble proteins, but there was no detection of OZ43 (or any other protein) with the gp40 antibody. However, there was also significant activity in the cell wall supernatant fraction (the ionically-bound wall proteins) where there was detection of a 43 kDa protein. This may be coincidental as there could be another protein that is associated with the cell wall that has mutarotase activity. Certainly, this data does demonstrate there is another active mutarotase in the soluble protein fraction that is not recognised by gp40.

The experiments with the plant hormone ethylene indicate that accumulation of OZ43 (as detected with the gp40 antibody) decreases with exposure to ethylene over a period of 48 h. The decrease in OZ43 expression in the MRE tissues (compared to the MR) is not induced by tissue ageing, because when 1-MCP (a blocker of ethylene action) was used, the OZ43 protein was expressed to similar levels as in the fresh tissue (MR).

The mutarotase activity also fell in the ethylene treated tissues, but the small increase in activity in the 1-MCP treated tissue did not parallel the larger increase in protein expression apparent on the Western blots. This may suggest that the protein with which the mutarotase activity is associated appears to degrade over time, an effect that is exacerbated by the tissue damage caused by the stress responses to ethylene. This would explain why the 1-MCP treated MRE tissues have slightly higher activity than the MRE tissue. However, the OZ43 protein appears to be down-regulated by ethylene as OZ43 in the 1-MCP tissue is expressed in similar levels as in the MR tissue.

Ethylene, intimately linked with senescence, has been shown to regulate the activity of many enzymes in senescing tissues as the plant mobilises storage materials and breaks down structural components (Kende and Zeevaert 1997). The OZ43 protein associated with the cell wall may have some role in the assembly of the cell wall components,

transporting sugars or in signalling processes, and maybe down-regulated during senescence. The observations within this thesis do not elucidate the function of this mutarotase-like OZ43 protein in higher plants except that its role in the cell probably does not require the epimerisation of ketoses and hexoses, with glucose the most metabolically significant. The extraction of the OZ43 protein from the cell wall suggests it may have a function in cell wall maintenance. However, there is no evidence to show there are any processes in construction, maintenance or breakdown of cell walls that require aldose sugars to be of a particular optical status (Henrissat *et al* 2001, Fry 1995). In all living organisms, the synthesis of the glycoside components of the cell wall are performed by glycosyltransferases, which utilise activated sugar donors such as UDP or GDP-mono, di or polysaccharides (Reiter and Vanzin 2001). Therefore, if OZ43 were a mutarotase enzyme it would probably not have a role in cell wall maintenance. However, the data in this thesis suggests that OZ43 may not possess mutarotase activity but is similar in structure to a mutarotase-like protein. The sequence similarities of the plant proteins to the sugar binding mammalian, bacterial and yeast mutarotases combined with the lack of any homology to previously characterised proteins, suggests a role for OZ43 in the binding of sugars.

In primitive bacteria, glucose is directly oxidised through glucose oxidase, a catalysis that can only occur via the  $\beta$ - anomer of glucose. Therefore, there was a requirement for mutarotase to provide glucose oxidase with the specific glucose substrate. During glucose utilisation in less primitive organisms, oxidation occurs via the  $\beta$ - anomer of glucose 6-phosphate. The spontaneous mutarotation of this compound is extremely rapid and not accelerated by mutarotase (Bailey *et al* 1967). The function of mutarotase in glucose metabolism in bacteria and primitive organisms should have become redundant with the evolution of phospholytic pathways of glucose utilisation. However, the prolonged evolutionary history and the apparent stable physical and catalytic properties of the enzyme, when taken in conjunction with the lack of its requirement in glucose metabolism, indicates a significant alternative function must have evolved. It has been observed that the distribution of mutarotase in less primitive organisms is not consistent with the location of glycolytic enzymes (Bailey *et al* 1967). Clear evidence to support its role as a sugar transporter is supported by the observation that the increase in the influx of glucose into the kidney parallels the expression of the mutarotase protein as this tissue develops (Bailey *et al* 1970). Further, inhibitors of mutarotase have

also been shown to inhibit the active transport of glucose across the cell membrane of calf kidney cells and intestinal mucosa (Mulhern *et al* 1973).

The mutarotase-like gp40 from tobacco (localised to the nuclear rim) is postulated to have a role that involves the transport and/or binding of sugars, a feature of the aldose-1-epimerase enzymes. Heese-Peck and Raihkel (1998) postulate that gp40 may have a role in the sugar-specific nuclear import of glycoproteins, a process that has been illustrated with the sugar-dependent (nuclear leader sequence (NLS)-independent) nuclear import of glycosylated BSA (Duverger *et al* 1995). Heese-Peck and Raihkel did not attempt to measure the mutarotase activity for the gp40 glycoprotein as during the gp40 purification process they modified the O-linked terminal *N*-acetylglucosamine (O-tGlcNAc) residues with galactose using galactosyltransferase (GalTF) producing Gal- $\beta$ -1, 4-GlcNAc. Galactosylated tGlcNAc interacts specially with *Erythrina cristagalli* agglutinin (ECA), a feature used to purify the gp40 protein by eluting the gp40 containing O-tGlcNAc from a ECA-agarose column (Heese-Peck and Raihkel 1998).

The immunological identification of OZ43 with the gp40 antibody, the size similarity between these two proteins and the partial sequence identity, makes it likely that these two proteins share similar functions. However, further studies into sugar binding and localisation of OZ43 will be required for a more definitive determination of its cell wall-associated function.

#### 5.1.10 The identification of a putative lipid transfer protein in abscission zone cell walls of *S. nigra*

The partial internal amino acid sequence obtained from the OZ10 protein was found to have the highest identity with many LTPs previously identified in plants (for example Figure 3.13a). LTPs are well characterised, and non-specific LTPs (nsLTPs) have been purified from various sources of plant material including leaves, stems and flowers (see Park *et al* 2000, Kadar 1997). LTP1s (a subclass of nsLTPs) are between 8 and 10 kDa, consistent with the ca. 10 kDa size of the LTP(s) detected with antibodies raised to LTPs from carrot and *Arabidopsis*. The LTP1 protein consists of 91 to 95 amino acids, and so the internal sequence obtained from *S. nigra* of 18 residues accounted for approximately 20 percent of the total protein with a 90 percent identity to a LTP from *Arabidopsis*. All known LTP1s sequenced from plants have eight strictly conserved

amino acid residues forming four disulphide bridges (Kader 1996) and one of the conserved cysteine residues aligns with the sequence obtained from OZ10.

In higher plants, LTPs are encoded by a multigene family. In *A. thaliana*, at least 15 genes have been identified (Arondel 2000), and it is likely that individual LTPs carry out specific functions (Kader 1996). The two antibodies used to detect LTP in the *P. vulgaris* extracts appear to show the proteins accumulate in the same tissue, possibly because these antibodies are detecting the same isoform of LTP. The LTP protein appears the least abundant in the pulvinus before and after ethylene treatment, and is expressed at the same level in the primary zone in both the fresh and ethylene treated tissues. The effect of ethylene treatment (or ageing) of the bean petiole results in an increase in the expression of the LTP protein. This petiole-localised increase may be because the isoform of LTP recognised by the antibodies is stress and/or ethylene induced only in these tissues. In these experiments, the effects of ethylene were not separated from tissue ageing effects using 1-MCP, for example. The recognition pattern of the LTP antibody raised to the recombinant carrot LTP antibody and the purified *Arabidopsis* protein, with respect to location in abscising tissue and stress responses in other tissues, has not been described previously.

Although discovered over 25 years ago, LTPs have yet to be assigned a biological function (Park 2000) although these proteins are relatively abundant. For example, a non specific LTP (WAX9) may constitute 90 percent of all wax associated proteins in broccoli (Pyee *et al* 1994), and it has been calculated using ELISAs and immunoblotting that LTPs make up four percent of soluble proteins extracted from maize seedlings (Douliez *et al* 2001).

A role in plant defence has been proposed for LTPs, which has been supported by recent evidence. Some members of the LTP family have been shown to act as antifungal and antibacterial and antiviral agents *in vitro* (ChangJin *et al* 2002, Regente and Canal 2000, Garcia-Ollmedo *et al* 1995). A review of LTPs by Kader (1996) describes how LTP1s (typically 9 to 10 kDa) are from a multigene family of secreted plant LTPs that are constitutively expressed in specific tissues and/or induced in response to biotic and abiotic stress. LTPs have been shown to interact with receptors on the plasma membrane that have previously been identified as elicitor receptors (Kader 1997).

Elicitin is known as an elicitor of plant defence mechanisms, a protein that loads and unloads lipid molecules, and shares some structural and functional properties with LTPs. It is known that the elicitin-sterol complex is required for recognition by the receptors, but the importance of the LTP-lipid complex formation for elicitin receptor recognition and activation is unknown (Buhot *et al* 2001). It is not yet known whether LTP plays a role in the inhibition of the damage caused by pathogens (Arondael *et al* 2000). The high isoelectric point of these proteins may indicate that they act as membrane permeable agents or their induction may be incidental as cutin biosynthesis is generally stimulated by infection (Kadar 1996).

In terms of biochemical data, the function originally assigned to these proteins in plants was the transfer of lipids between intracellular membranes. However, gene expression data indicates that with gene product accumulation in peripheral layers including the epidermis, LTPs may function more in the secretion of lipids into the cell wall space such as in the shuttling of cutin monomers from their site of synthesis towards the cuticle (Clark and Bohnert 1999, Kader 1996, Hendriks *et al* 1994, Sterk *et al* 1991). The 'cutin theory' is also supported by the observations that LTPs are mainly located in the cell wall and are secreted. As secreted proteins they are present mainly in the surface wax especially in young leaves where cutin deposition is active. Non-specific LTPs have a broad range of substrate specificity and are capable of transferring several classes of phospholipids including phosphatidylcholine, phosphatidylinositol and phosphatidylethanolamine and several galactolipids but not triacylglycerols (Travino and O'Connell 1998, Kader 1997).

#### 5.1.11 Cellulase in the zone cell walls of *S. nigra*

As part of the identification of zone-specific proteins in *S. nigra*, antibodies raised against proteins known to be associated with the abscission process were used.

The antibody raised to the bean abscission cellulase (BAC) detected a protein of ca. 36 kDa in the ethylene treated tissues (MRE and ZONE) of *S. nigra* and, as expected, ca. 51 kDa in the pulvinus and the primary abscission zone of the ethylene treated bean tissues. The deduced molecular weight of the mature cellulase 9.5 protein, from the 1.6 kbp transcript in *P. vulgaris*, is 53 kDa (Tucker *et al* 1988). However, the purification of this isoenzyme using different techniques appears to affect the apparent molecular

size. Koehler and co-workers describe the purification of pI 9.5 from kidney bean (*P. vulgaris*) using affinity chromatography, native and SDS-PAGE (Koehler *et al* 1981). Antibodies raised to this purified isoenzyme were monospecific and identified the cellulase 9.5, in common with this thesis as being 49 kDa.

The ca. 36 kDa protein resolvable with Western analysis using the BAC antibody in the ethylene-treated cells of *S. nigra* is not specifically induced in the zone cells, and is considerably smaller than previously identified cellulase proteins which are between 51 and 68 kDa (Trainotti *et al* 1999). Therefore, it appears that the ca. 36 kDa protein is similar to, but not a cellulase enzyme that is induced by ethylene treatment.

The abscission-associated cellulase identified in *S. nigra* cells (*JET1*) has a deduced molecular weight of 54 kDa (Taylor *et al* 1994). Taylor and co-workers (1994) found an abscission-induced cellulase from *S. nigra* (*JET1*) by screening a cDNA library with pBAC10, produced from mRNA extracted from ethylene-treated leaflet abscission zones. The cellulase encoded by *JET1* has a sequence homology of 67 percent with BAC and 48 percent with avocado Cell1 at the amino acid level.

## 5.2 The *in vitro* approach to study abscission cell differentiation

For the second part of this thesis, the affects of exogenous and endogenous levels of the two plant hormones IAA and ethylene during the formation of secondary abscission zones in bean petiole explants have been examined.

### 5.2.1 The role of auxin in the determination of abscission events

The IAA concentration in the petiole sections during the differentiation of the secondary abscission zones was measured using an antibody immobilised ELISA. When examining the role of auxin (IAA) in the differentiation process, the success rate (65 to 80 percent) of secondary zone cell formation was a factor to be considered. Collecting and sectioning explants that were not going to form zones successfully may affect the interpretation of the IAA concentrations measured in petiole tissues. For IAA measurements at 6, 16 and 26 h, the most turgid and vigorous petioles were collected, as these were most likely to form adventitious abscission zones. By the 26 h sampling point, there was a weakening of the explant at the site the zone was to form. This was apparent before a noticeable difference in the development of colour (green/yellow)

either side of the zone. Thus some attempt was made to measure any changes in the concentration of IAA in petiole tissues destined to form secondary abscission zones.

Prior to the use of the commercially-available monoclonal antibody, an attempt was made to produce polyclonal antibodies (PcAbs) to IAA and so provide a large source for use in the assays. IAA is a small hormone, and therefore a weak immunogen, so to increase its immunogenicity it was conjugated to BSA. Sembdner and collaborators provide an explanation of plant hormone conjugation (Sembdner *et al* 1994). There are two main types of antigens produced for generating antibodies to IAA. The Mannich formaldehyde reaction (Pence and Caruso 1987) couples the ring of the IAA to the carrier protein, thought to occur through the indolic nitrogen. The antibodies raised to this antigen will recognise free IAA with the advantage that the methylation of the carboxyl group (which commonly uses the highly toxic and explosive diazomethane) can be avoided (Caruso *et al* 1993). The disadvantage of this method is the polyclonal antibody titres generated with this antibody have been reported to be lower because of the unstable IAA-N conjugate bond (Pengelly and Meins 1977). The second approach for generating the IAA antigen is to couple the protein through the carboxyl group using either the mixed anhydride or the carbodiimide reaction (Hock 1992). In this study, to maximise the PcAb IAA titres, IAA was conjugated through the carboxyl group to BSA using the carbodiimide method. A less commonly used antigen (IAA-C5-BSA) conjugates the BSA to the benzene moiety. The advantages are the same as for the IAA-N conjugate with a similar result when used in an ELISA (Marcussen *et al* 1989).

In this study, the maximum titre of polyclonal IAA IgG antibodies produced, through the BSA-IAA immunisation procedure, was not sufficient to use in an ELISA to measure the amount of IAA in the bean petiole samples. A large proportion of the antibodies produced to this conjugate recognise parts of BSA alone (a protein with a molecular mass of 68 000), even though each BSA molecule was coated with many IAA molecules. The presence of BSA antibodies did not effect sample ELISA readings for IAA in plant tissues but the observed difference in the titres between the two moieties of the conjugate suggests either the immunogenicity of the conjugate was not sufficient to elicit a high response to IAA or the conjugation reaction itself was not as efficient as in previously studies (Hock *et al* 1992). Hock and collaborators used the method of conjugation and immunisation described in this study, and produced

antibodies of sufficient titre to use in measuring IAA in plant samples with ELISA. The conjugation reaction was repeated using a new preparation of the conjugating reagent EDC, and the effectiveness of conjugation assessed using FPLC (section 2.4.1.1). In comparison with the first conjugation (which is illustrated in section 2.4.1.1), in the second conjugation, the IAA-BSA compound eluted later in the trace (data not shown), suggesting more highly conjugated BSA and a more effective conjugation reaction. It may be that the initial conjugate contained a high proportion of unconjugated or lightly conjugated BSA-IAA molecules and thus resulting in a large proportion of the antibodies produced being against BSA and not IAA. The problem of low titres often seen with IAA PcAb (Artec and Artec 1989) has been overcome with the production of monoclonal antibodies (McAbs). Aside from the advantage of high titres using McAbs, the use of IAA PcAbs with ELISA, even after affinity purification, would have necessitated the purification of the IAA from the tissue extracts because of the likelihood of interfering compounds in the sample. Therefore, instead of immunising the second conjugate to produce a second round of antibodies, the use of monoclonal antibody-based immunoassays were investigated for use in determining the concentration of IAA in plant tissues.

Using the PcAb raised to IAA, the low titres of the IgGs in addition to the similarity of absorbance readings for concentrations of IAA from 0 to 10 pmole/0.1 mL, meant a narrow range of absorbance units was available to calculate the percentage binding of the tracer to the anti-IAA antibody (Figure 4.3b). For calculation of the percentage binding, zero % B (the IAA concentration where there is no change in absorbance with any further increase in IAA), is the value that is determined by the antibody titre as IAA occupies all of the IgG IAA binding sites. At 100% B, the tracer occupies all of the IAA binding sites on the antibody. Although this calculation produces a curve with a steep linear portion, the range of the curve is determined by the titre of the antibody. For the PcAb a range of 10 pmol/0.1 mL was achieved. The difference in the absorbance values measured in the assay, between 0% B and 100% B, is also low, and barely significant when considering the variability between the triplicate readings for each IAA concentration. However, the standard curve generated for the monoclonal antibody had a steep linear portion over an IAA concentration of 0 to 1000 pmol/0.1 mL, covering a one to two absorbance unit change. This range was necessary for the accurate calculation of the percentage binding of the tracer to the antigen binding sites

on the antibody over the IAA sample range measured. It has been reported that sensitivities for enzyme immunoassays have been able to differentiate IAA concentrations as low as 0.2 pmol/0.1 mL using McAbs (Caruso *et al* 1993).

Before using the monoclonal-based immunoassay, it was necessary to screen for compounds in the plant extracts that can interfere with the IAA readings. These can result in either competitive or non-competitive interference in the assay. Competitive inhibition, where the compound competes with the IAA for the binding site on the antibody, gives readings in the assay that are higher than the actual IAA concentration. Non-competitive inhibition occurs when a compound interacts with the IAA and alters it in some way so the IAA is not recognised by the antibody. This can result in lower than actual IAA readings. Combined gas chromatography-mass spectrophotometry (GC-MS) is a physio-chemical method often used in the validation of immunoassay data. Internal radiolabelled standards have also been used (Hoche *et al* 1992). A less costly method, which is commonly reported, and was used in this study, is the construction of dilution curves or cross-reactivity curves from a mixture of a standard hormone concentration and extract.

Cross-reactivity curves, which consist of a standard IAA curve and the same curve with an equal amount of extract added to each standard IAA dilution, indicate if there is interference in the assay. These two curves generated will be parallel to each other if there are no compounds interfering in the assay. However, where curves that are not parallel indicate interference, parallel dilution curves cannot assure the absence of interference. An IAA monoclonal antibody, unlike the polyclonal antibody, is less likely to interact with compounds other than IAA because the nature of the epitope is, in general, more specific to a particular region of the molecule. The parallel dilution curves generated in this study suggest that there were no compounds in the petiole extracts interfering with the ELISA IAA measurements using the monoclonal antibody.

With the monoclonal antibody-based IAA immunoassay tested, IAA concentrations were then measured in a variety of plant tissues that were predicted to have different levels of the hormone. The IAA hormone is produced in the plant locally in young growing regions such as the shoot apex, young leaves and developing seeds (Normanly *et al* 1991). The expanding leaves and roots generally possess the highest concentration

of free IAA (Kowalczyk and Sandberg 2001). Of the 14-day-old bean tissues sampled in this thesis, the free IAA concentration was highest in the shoot (at 750 pmol/g FW) followed by the leaf tissue and then the hypocotyl, petiole and epicotyl.

Various IAA concentrations previously reported in the plant tissues of angiosperms are listed in Table 5.1. The physiological concentration of IAA in carnation stems, mung bean hypocotyls, pea seedlings, vegetative citrus tissues and the monocotyledon maize seedlings ranged from about 30 to 2100 pmol/g FW. The concentration of IAA in the hypocotyl and epicotyl of the bean, although slightly lower, are comparable with the concentration of free IAA in the mung bean hypocotyls. The concentration of IAA in the shoot tip of the bean is significantly higher than that reported in carnation and lower than in the orange shoot tip. As these are all considerably different plants, forming accurate conclusions by direct comparison is not achievable. However, it does show that the overall distribution and range of values of the concentrations of IAA measured in bean in this study appear to be consistent with that previously reported in other plants.

Sample	Tissue level of free IAA (pmol/gram FW)		Method of determination	Reference
Mung bean	Hypocotyl	95	GC-MS	1
Dark grown <i>Zea mays</i> seedlings	Coleoptile			2
	Apex	166-199		
	Base	108-126		
Dark grown <i>Pisum sativum</i> seedlings	Apical	85-90	2	
	Median	53-56		
	Basal	36-39		
Arabidopsis thaliana	Coleoptile tip	615-915	3	
	Seed	223-457		
Chrysanthemum <i>Morifolium</i> (3 fully developed leaves per segment)	Shoot segment		ELISA (Polyclonal)	4
	Shoot tip	170-270		
	Middle	100-210		
	Basal	90-200		
<i>Valencia Orange</i>	Shoot tips	2166	ELISA (monoclonal)	5
	Young leaves	1414		
	Mature leaves	422		

Table 5.1. The reported IAA concentrations within the tissues of various angiosperms. The IAA units vary between studies so have been converted to pmol/g FW so they can be compared to the IAA data collected in this thesis.

#### References

(1) Ben-Efraim *et al*/ 1990, (2) Allen *et al*/ 1982, (3) Ribnickey *et al*/ 1998, (4) Weigel *et al*/ 1984, (5) Sagee *et al*/ 1986.

The assay of different bean tissues had shown that the IAA immunoassay was discerning between tissues with different IAA levels, and that these levels were within the ranges reported for different tissues. So, the next step was to use the immunoassay to measure changes in IAA levels in petiole tissues during the differentiation of a secondary abscission zone. However, the author is aware that the IAA concentrations within the *in vitro* explant system cannot be compared to that of the intact plant for two major reasons. Firstly, it is an explant system (and so is separated from the primary source of endogenous IAA) and secondly, because IAA applied to the explants is at concentrations far exceeding endogenous IAA levels. Thus the use of the term 'low' and 'high' in the following descriptions are comparative terms within the levels noted in the petiole explant tissue.

The amount of IAA in the petiole sections at day 0 (the time of primary abscission, 36 h after exposure to 10 ppm of ethylene) was low in the green and first two yellow sections (the distal 75% of the petiole) and higher in the most proximal yellow section (Y4). The presumed polar movement of the IAA to the proximal section of the explant resulted in the formation of a callus, as IAA promotes the differentiation of cells. This callus was removed before IAA measurement but this pooling of IAA in the proximal explant section may be the cause of the high levels of free IAA observed in the Y4 section. This same pattern of free IAA distribution was followed through (although differing considerably in concentration) to 26 h after the second of the two IAA applications. The differentiation in the petiole into two distinct sections, as observed by green:yellow junction formation, appears at 52 h. A weakening in the petiole at this position, indicating the zone has differentiated and the production of abscission related hydrolytic enzymes is initiated, appears to occur to the majority of the explants at around 26 h after the final IAA application. The signals that trigger the differentiation of the secondary zone will therefore be expected to occur at some point between the final IAA application and the time of evident tissue weakening (between 0 and 26 h).

It is known that the IAA applied to the bean explants disappears over 10 to 12 h (M.T. McManus, *pers comm*) probably through the formation of various conjugates. A major route by which higher plants regulate free IAA levels is through the production of IAA conjugates (Cooke *et al* 2002). At 26 h, the distribution of the free IAA changed dramatically from high concentrations in the proximal portion of the explant to a higher concentration in the green distal portion (although at this time point the entire explant appears green). However, the overall amount of free IAA at 26 h appears very low compared to measurements taken from the other time points. Wiesman and co-workers (1988) found radiolabelled IAA, when introduced to the base of mung bean cuttings to induce adventitious root formation, was metabolised rapidly and after 24 h only a small portion was present as free IAA. In the bean explants, it may be these low free IAA levels at 26 h, combined with the subsequent change in the distribution of IAA along the petiole, triggers the formation of a secondary abscission zone. At 40 h, the free IAA levels remain high in the green tissues when compared with the Y2 and Y3 sections but the amount of free IAA in the Y4 section increases perhaps due to polar transport of liberated free IAA from the IAA conjugates formed earlier. It was observed in a high proportion of the explants, if left to full secondary zone separation, the Y4 section

became greener than the Y2 and Y3 sections and, in a small percentage of the explants, formed another abscission zone at the proximal end of the explant between the Y3 and Y4 segments. At 52 h, the amount of free IAA appears highest in the green section and the Y2 section. This observation may be due to the hydrolysis of IAA from conjugates in the green portion of the explant been transported across the secondary abscission zone in a polar manner to the proximal portion. IAA is associated with young growing tissues and the green portion of the secondary explants is proposed to be the source of the free IAA (McManus *et al* 1998). The IAA concentrations measured in the petiole sections are not consistent with this theory where, in particular at secondary zone separation, the highest concentration of free IAA was measured in the Y4 section, almost three-fold higher than observed in the green section. Warren Wilson and collaborators (1988 a, 1988) found secondary separation layers, which formed in explants of *Impatiens*, were positioned where the auxin concentration decreases in a morphologically upward direction (i.e. against the polar transport flow). They created a mathematical model that will predict the position of a zone forming with a known concentration of IAA applied at the base of the explant (Warren Wilson 1986). The position of secondary zone differentiation in the bean explants, therefore, may also be dependent on the concentration of free IAA that has been observed, in this study, to pool in the morphologically proximal end. It may be the gradient in the morphological upward direction that determines the position at which the zone sites form. The theory, however, does not explain the observation that the distal G1 portion, containing the petiole-pulvinus zone, has a lower concentration of free IAA at separation than the senescing Y4 portion.

What is more certain from these results is that mechanisms whereby free IAA levels are regulated and the influence they have in formation of secondary abscission zones in this explant system is complex. Measuring the free IAA content within a tissue segment, comprising of many different cell types with various compartments, may not give a complete picture of what affect the hormone is having in these tissues. The expression of IAA binding proteins and the proportion of these proteins within each cell that are occupied by auxin are two aspects that will influence the auxin affect. It is becoming clear that subcellular localisations of IAA and the enzymes involved in IAA metabolism and transport are also potential control points (Bartel *et al* 2001).

Application of IAA, as well as inhibiting abscission in primary zones, inhibits BAC accumulation (Taylor *et al* 1994). Radioimmunoassays have shown that the abscission-associated pI 9.5 cellulase accumulates in the primary zones 12 h prior to a decrease the break-strength (Durbin *et al* 1981). The differentiation of these zones is a transdifferentiation event with little to no increase in DNA content but with changes in the nuclear content indicating induced and increased genomic activity (McManus *et al* 1998). The expression of the abscission specific pI 9.5 endo- $\beta$ -1,4-glucanhydrolase has been measured in the secondary zone cells at the time of secondary separation. Thus using the timing of the induction of  $\beta$ -1,4-glucanhydrolase, in combination with microscopic examination, it may be possible to establish the point at which the secondary zone cells differentiate.

To gain a clearer picture on the way the IAA is being utilised in this explant system, an analysis of the IAA-conjugate concentrations at different time points will also be needed. Certain IAA-conjugates have activity in bioassays and tissue culture but the functions of endogenous auxin conjugates remain poorly understood (Ljung *et al* 2002). Hangarter and Good (1981) demonstrated, by observing the enzyme driven hydrolysis of IAA-alanine and IAA-glycine in pea stem segments, that IAA-conjugates can act as slow release sources of IAA. Other roles proposed for IAA-conjugates are to assist in IAA transporting, compartmentalising, as well as in detoxifying excess IAA and protecting the free acid against peroxidative degradation. With the addition of high concentrations of IAA to the bean explant tissue it is assumed most of the IAA will be conjugated. However, some of these forms will be conjugated to act as slow release forms of the hormone, while other conjugates may destine the IAA for turnover. A complete picture of free IAA and IAA conjugate levels is required, therefore, to begin to elucidate the influence of auxin on secondary zone formation

### 5.2.2 The role of ethylene in the differentiation of secondary abscission zones

The earlier work of McManus and colleagues (McManus *et al* 1998) demonstrated that while IAA provided positional information for the differentiation of a secondary zone (i.e. the site of formation was dependent upon the concentration of IAA added), the plant hormone ethylene was also necessary. IAA could be added to explants, but if exogenous ethylene was not applied, then no differentiation occurred. Therefore, as

well as examining changes in IAA concentrations, the evolution of ethylene was examined during secondary zone formation. ACC synthase has been shown to be the enzyme catalysing the rate-limiting step in ethylene biosynthesis. However, closer examination of ACC oxidases both at the gene and protein level suggests that the pathway is also regulated at this catalytic point. Therefore, the initial examination of ethylene biosynthesis during secondary zone formation centred on changes in the accumulation of ACC oxidase protein and ACC oxidase enzyme activity.

The results illustrated that the rates of ethylene evolution differed during secondary zone formation suggesting that there is regulation of the ethylene biosynthetic pathway. The ACC protein expression, as detected using Western analysis, and the ACO enzyme activity appeared to have the same pattern of abundance (to each other) in the fresh petioles and the petiole explants at primary and secondary separation. These results suggest the ACO antibody and the ACO activity assay are detecting and measuring the same isoform of ACO (or different isoforms with the same pattern of expression). However, the ethylene produced from the explant sections, which is highest in the older more senescent tissues, does not appear to be regulated by this isoform, which has relatively low expression and abundance in the highest ethylene producing tissue sections.

In this study, the antibody used to detect ACC oxidase was that raised to the TR-ACO2 protein product expressed in mature green tissues of white clover (Hunter *et al* 1999). Hunter and colleagues found there were three isoforms of ACC oxidase in white clover, designated TR-ACO1, TR-ACO2 and TR-ACO3. Through Northern analysis, *TR-ACO1* appears to be expressed in the apex of the clover stolon, *TR-ACO2* is expressed in the mature green tissues and *TR-ACO3* is present in the senescent tissues. The antibody raised to TR-ACO1 detected a very large (205 kDa) protein following the same expression pattern as the *TR-ACO1* gene. The antibody raised to the *TR-ACO2* gene product recognised the TR-ACO2 protein product (34.5 kDa) expressed in the mature green tissues, with no recognition of protein in the apex of the stolon where TR-ACO1 accumulates. The TR-ACO3 antibody had only weak recognition of a protein of the same size and with the same accumulation pattern as TR-ACO2, and did not detect any protein in the senescent tissues. The detection of the TR-ACO2 protein by the TR-ACO3 antibody is probably due to the high similarity of these two sequences, which, as

shown by phylogenetic analysis, are closer in sequence to each other than all but one ACO previously sequenced (Hunter *et al* 1999). In bean, the antibody recognises a differentially expressed protein of 42 kDa in the non-senescent petiole tissues more strongly than in the senescing tissues. From phylogenetic comparisons of TR-ACO1, 2 and 3 with the amino acid sequences from other ACC oxidases (Hunter *et al* 1999), it was found that TR-ACO2, 3 and an ACO from bean cluster together. This ACO from bean (*PV-ACO1*) was isolated from etiolated seedlings and its expression shown to be regulated by light (Pidgeon *et al* 1997). It was not stated in this paper whether *PV-ACO1* was also expressed in senescent tissue. The protein recognised in bean by the TR-ACO2 antibody in these experiments is possibly *PV-ACO1*, as the amino acid sequences of these two proteins (TR-ACO2 and *PV-ACO1*) are very similar, and the TR-ACO2 antibody, as later shown by Gong and McManus (2000), can recognise a senescent-associated ACC oxidase in stoloniferous white clover, possibly encoded by *TR-ACO3*.

For ACC oxidase activity measurements, the highest activity in the petiole was in the freshly excised tissues, and is considerably lower in the senescent tissues. This is at odds with the ethylene evolution data, which showed that the highest rate of evolution from the senescing tissues (Figure 4.8c). The conditions used for the measurement of ACC oxidase, in particular the pH ranging from 7.0 to 8.1, were designed to favour the activity of the ACC oxidases that have previously been characterised from other species. However, Gong and McManus (2000) found during leaf ontogeny in white clover that the activity of a senescent isoform of ACO becomes apparent if the proteins in the extract are fractionated using hydrophobic interaction chromatography (HIC). The unmasking of ACO activity using HIC suggests there is a proteinaceous inhibitor in the clover extract that is not removed when preparing the extracts for activity measurements by the 30 to 90% ammonium sulfate precipitation or elution from the Sephadex-G25 column. Biochemical characterisation of this senescent-associated enzyme (designated SEII) revealed that it had an optimal pH of 8.5 (compared to 7.5 for the mature green isoform) and different concentrations of cofactors. A similar enzyme to SEII may be present in the senescent bean tissue that catalyses the conversion of ACC to ethylene resulting in the high levels observed in this study. Separation of the proteins in the bean extract using HIC may reveal a senescence-associated ACO in bean that has an associated protein inhibitor.

The TR-ACO2 antibody recognised SEII after HIC (Gong and McManus 2000). However, the TR-ACO2 antibody did not detect any protein in the senescent leaf stages of the stolon in the initial white clover extract (Hunter *et al* 1999). If there is a proteinaceous inhibitor associated with SEII in the extracts (or perhaps more than one) it may also affect the presentation of epitopes that are recognised by the TR-ACO2 antibody.

There has been two published full length ACC oxidase gene sequences from *P. vulgaris* (Pidgeon *et al* 1997), and all of the plant species examined to date contain ACOs are encoded by small multi-gene families (Gong and McManus 2000). The research in this thesis included an investigation of the ACC oxidase genes expressed in the fresh and senescent petiole tissue of bean. Seven clones of ACC oxidase were produced through amplification of cDNA (produced from the extracted total RNA) using primers designed against conserved regions of ACO in white clover. The primers used amplified a ca. 850 bp region from the reading frame of the gene. This section of research appears only in this discussion, and is a supporting point of interest to the ACO protein analysis data. To verify that the *P. vulgaris* clones sequenced represent different genes and to locate possible additional isoforms of the enzyme, there would need to be further cloning and sequencing undertaken. The ACO sequences amplified using RT-PCR provide enough sequence information to differentiate genes (Hunter *et al* 1999). However, amplification of the 3'-UTRs (untranslated regions) using 3'-RACE (Rapid Amplification of cDNA Ends) enables the production of gene-specific probes, as these regions contain significant sequence diversity between ACO genes. Gene-specific probes can then be used in expression studies to determine, using Southern and Northern analysis, the potentially differential expression pattern of different ACO isoforms as illustrated by Hunter *et al* (1999). However, these additional experiments were not undertaken and so just the sequence comparisons can be undertaken.

The ACO sequences obtained by RT-PCR appear to code for two distinct ACO genes. Clones 1 to 6 have between 87 and 95% homology percentage values to each other (Table 5.2). However, Clones 1 to 6, when compared to clone 7 have only 63 to 69% homology to each other (comparing the first 700 bp), indicating that the clone 1-6 sequences and the clone 7 sequence represents two distinct ACO genes

Clone no.	1	2	3	4	5	6	7
1	-	92	93	90	90	88	68
2	92	-	94	89	95	87	65
3	93	94	-	88	90	89	67
4	90	89	88	-	92	88	68
5	90	95	90	92	-	90	69
6	88	87	89	88	90	-	63
7	68	65	67	68	69	63	-

Table 5.2. Nucleotide homology percentage values between the seven putative ACO clones isolated from fresh petiole tissue by RT-PCR.

<i>P. vulgaris</i> Clone number	Gen-bank accession number	Plant species	Score	E value
1 to 6	AF115261 M98357	<i>Trifolium repens</i> (TR-ACO1)	844	0
		<i>Pisum sativum</i> ACC oxidase	230	2e-57
7	VRU06046 AF315316 VRU06047 AF115261 M98357	<i>Vigna radiata</i> (VR1)	720	0
		<i>Vigna radiata</i> ACC oxidase	391	e-105
		<i>Vigna radiata</i> (VR2)	274	2e-70
		<i>Trifolium repens</i> (TR-ACO1)	274	2e-70
		<i>Pisum sativum</i> ACC oxidase	250	3e-63

Table 5.3. ACC oxidase mRNA sequences in the NCBI database from plant with the closest similarities to clones 1 to 6 and clone 7 from *Phaseolus vulgaris* isolated from fresh petiole tissue by RT-PCR.

The sequences from the seven clones were compared to previously identified nucleotide sequences in the NCBI database using a BLAST (nr) search with an expect (E) value at 10 (the default value). The E value is a parameter that describes the number of hits one can "expect" to see just by chance when searching a database of a particular size. It decreases exponentially with the Score (S) that is assigned to a match between two sequences. Essentially, the E value describes the random background noise that exists for matches between sequences. The Expect value is used as a convenient way to create a significance threshold for reporting results. When the Expect value is increased from the default value of 10, a larger list with more low-scoring hits can be reported. The percentage identities in these alignments are not used as a statement of homology in this discussion as it is the length of the sequences compared, directly related to the 'score', which decreases as the sequences become less similar. The E values, therefore are used to rank the sequences in the BLAST search from the most to the least similar to the query sequence.

The six clones (clones 1 to 6) appeared to be the same gene and have the highest homology to *TR-ACO1* from white clover (Table 5.3). The potentially second gene identified here (clone 7) is more similar to a nucleotide sequence from *Vigna radiata*, *VR-ACO1* (Table 5.3), with a score 274 of to *TR-ACO1* (compared to 844 for clone 1 to *TR-ACO1*).

The antibody used to detect the ACO protein, through Western analysis, in this thesis was raised to TR-ACO2. This antiserum does not detect the TR-ACO1 protein (Hunter *et al* 1999), which is more similar in nucleotide sequence to clones 1 to 6 and clone 7 than TR-ACO2 and 3. This suggests the protein that is detected by the TR-ACO2 antibodies in the bean petiole tissues is not translated from either of the sequences from the genes represented by clones 1 to 6 or 7. There is an ACO sequence that has been identified in *P. vulgaris* (PV-ACO1) that clusters (using phylogenetic analysis using the mRNA sequences) with the TR-ACO2 and TR-ACO3 amino acid sequences and may be the gene product the antibody recognises. Another ACO sequence from *P. vulgaris* has been identified since the analysis by Hunter and colleagues (Hunter *et al* 1999) but this too does not appear in the BLAST search when the E value is 10, i.e. this is not the same gene as any of the clones 1 to 7.

Ethylene regulates many aspects of plant growth, development, stress related processes and senescence. Ethylene is normally low in vegetative tissues but can be increased by a variety of stimuli including wounding and IAA and enhances its own production through a positive feed-back loop (Peck and Kende 1995) where both ACO and ACS have been shown to contribute (Kanellis *et al* 1998, Kende and Zeevaart 1997). The ethylene production observed during secondary abscission zone formation in the bean tissues can be formed in response to wounding, application of endogenous IAA and/or as part of the process of senescence.

The mechanisms involved in timing, direction and control of secondary zone differentiation appear, with respect to the ACC oxidase, ethylene and IAA measurements in this chapter, to be regulated in a complex manner. More information into the regulation of each compound within this system will be required to make accurate correlations about these compounds in the formation of secondary abscission zones. However, some correlations do emerge. The ethylene evolved is highest in the tissues where the IAA concentration is highest. If ACO was regulating the production of ethylene then this would be consistent with an IAA-induced ACO. The ACC oxidase activity, when compared with the IAA concentrations, follows a pattern (with the exception of the secondary G1 sample), which is in tissues where the IAA was low there was a high expression and activity of this ACC oxidase enzyme. This would be consistent with the expression of an ACC oxidase, catalysing the conversion of ACC to ethylene, in a process inhibited by IAA. As it is apparent that the ACO measured in the bean tissue was not senescence-associated, another possibility is that it may have been an IAA-induced isoform, perhaps similar to the apex-specific TR-ACO1 of white clover. From the distribution in the tissues it appears most likely the ACO measured in bean is associated with the mature green tissues, its protein expression not unregulated by ethylene. Very recent characterisation of the promoter of *TR-ACO1* has revealed several auxin-response elements suggesting that transcription of the gene is regulated by auxin (B. Chen and McManus *pers comm*).

A recent study (JeongHoe *et al* 2001) measured the affect of applied IAA on ACC oxidase and ACC synthase in mungbean hypocotyls and the subsequent production of ethylene. The major drawback of this study was the limitation of examining only one isoform of ACO and ACS, since both are members of multi-gene families. The

research presented in this paper separates the IAA effects due to applied IAA from those resulting from IAA-induced ethylene. Applied IAA inhibited ethylene action, which resulted in the suppression of *VR-ACO1* and the induction of *VR-ACSI*. The IAA-induced ethylene lead to an accumulation of *VR-ACO1* mRNAs and a reduction of the *VR-ACSI* mRNA. The effect of exogenous ethylene and the ethylene biosynthesis inhibitor aminooxyacetic acid was also examined. Exogenous ethylene increased the transcription level of *VR-ACO1* and reduced that of *VR-ACSI*, but the ethylene inhibitor had the reverse effect. These results imply *VR-ACO1* is under positive feedback control by ethylene and *VR-ACSI* is under negative feedback.

A detailed study of ACC synthase and ACC oxidase gene expression, protein accumulation and the regulation of enzyme activity, is required therefore before the role of ethylene in directing secondary zone formation can be elucidated.

## 5.3 Summary

### 5.3.1 Abscission and abscission cell differentiation:

#### The *in vivo* approach

The major aim of the first part of this thesis was to identify proteins that denote the leaf rachis abscission zone cells of *S. nigra*. Examination of the cell wall protein extracts using SDS-PAGE indicate that there are differences in the repertoire of proteins in the rachis and abscission zone cells before and after ethylene treatment. Moreover, each tissue sampled contains cell wall proteins that are either unique or preferentially expressed and some appear to change in abundance throughout the growing season. In an attempt to characterise some of these proteins that are expressed exclusively in the morphologically distinct abscission zone cells, four peptides were identified through partial internal amino acid sequence obtained from tryptic-digested fragments. Two of these, a superoxide dismutase and ribonuclease were not investigated further as they have previously been identified as pathogen-related proteins, and are likely to be present in the cell walls of both the rachis and the zone cells. Moreover, the sequence fragments obtained for these two proteins comprised 8 and 13 amino acids only, and so it is possible these peptides are from different proteins. The third tryptic fragment identified, through sequence alignment, was a putative lipid transfer protein (LTP). Antibodies were obtained that recognise LTPs from *Arabidopsis* and carrot, and these two antibodies detected a protein of ca.10 kDa in both *S. nigra* and *P. vulgaris*. In the tissues of *S. nigra*, the ca. 10 kDa protein (detected by the LTP antibodies) appeared to be present in a similar abundance in the ethylene-treated (MRE and ZONE) and non-ethylene- treated (MR and OZ) tissues. In the bean petiole tissues, the protein detected by this antibody appeared more abundant in the primary abscission zone and in ethylene-treated petiole tissue. This indicates that the protein is expressed at different levels in specific tissues and, being preferentially expressed in the primary zone, may be associated with a defence response.

The other tryptic fragment from OZ43 possessed high sequence homology to a protein previously partially characterised in the nuclear pore membrane of tobacco suspension cells and designated gp40. A mono-specific antibody was obtained that had been raised to gp40 and was found to recognise a ca. 43kDa protein in the non-ethylene treated

tissues of *S. nigra*. This is referred to as OZ43 although the author concedes that there may be other proteins in the OZ43 protein band identified by SDS-PAGE. This glycoprotein (gp40) possesses high sequence homology to bacterial and mammalian forms of aldose-1-epimerase although, because the protein was modified in the extraction process, activity measurements could not be done. Since the initial identification of gp40, there have been 14 different gp40-like proteins identified in *Arabidopsis*. Although mutarotase activity has been measured in plants previously, there has not been a protein isolated that has been attributed to this observed activity. It appeared probable that this gp40 protein and gp40-like proteins (such as the OZ43 protein) could be actively epimerising aldose sugars in a process closely associated with the cell wall. However, there are no known activities associated with the cell wall that require aldose sugars to be of a certain anomeric configuration. Alternatively, with similarity of the gp40 active site to mammalian sugar binding transporters, the protein may act to transport sugars across the cell wall and membranes and any epimerase activity may be a consequence of transport.

The development of a coupled enzyme assay was undertaken therefore to establish whether the ca. 43kDa protein (OZ43), that was identified with the gp40 antibody, was a mutarotase enzyme. However, the data from these experiments suggested that the mutarotase activity that was detected in the cell wall extracts was not directly associated with this ca. 43kDa protein. Firstly, there was no activity in the specific fraction after Mono-Q ion exchange column chromatography that contained the ca. 43kDa protein recognised by the gp40 antibody. Further, enzyme activity was not found in any of the other fractions suggesting that either the enzyme activity of OZ43 deteriorated during the ion-exchange purification step or that there is a cofactor required for activity that is separated from OZ43 during ion exchange. However, mutarotase is a robust enzyme and there have been not reports of the plant form of this enzyme requiring cofactors. Therefore, these results suggest that the gp40 antibody-recognised OZ43 protein is structurally similar to gp40 (and perhaps shares significant sequence identity) but has no epimerising activity. Although the function of mutarotase in mammals is not known, but different to that characterised in bacteria, these results do not reveal the function of the OZ43 protein in plants but it is quite possibly involved in sugar transport.

In summary, this section of the thesis did identify proteins that were particularly abscission zone cell-specific. The technique of two-dimensional electrophoresis, in common with modern protein identification methods such as MALDI-TOF mass fingerprinting will aid their identification in the cell wall fractions of leaf rachis and abscission zone tissues of *S. nigra*.

### 5.3.2 Abscission and abscission cell differentiation: The *in vitro* approach

The aim of the second part of this thesis was to examine IAA and ethylene during secondary or adventitious abscission zone formation in petiole explants of *P. vulgaris*. Petiole explants from *P. vulgaris* with the distal pulvinus attached were excised at about 14 days after germination. Abscission of the pulvinus occurs after 36 h exposure to ethylene (10 ppm). IAA (1 $\mu$ l of a 1 mM stock) was applied to the pulvinus-petiole abscission zone face at the time of primary abscission (after the removal of the pulvinus) and again eight hours later. The formation of secondary abscission zones occurred at a discrete site along the petiole and removed from the primary zone in 65 to 80 percent of the explants. The reproducible position of the secondary zone differentiation provided a convenient way to section the explants (into four equal sections). The petiole tissue that links the primary zone with the secondary zone (the distal segment) remains green and, in this thesis, is designated as G1. The petiole tissue proximal to the zone senesces and yellows, and was divided into Y2 (immediately proximal to the secondary zone), Y3 (mid way) and Y4 (the most proximal tissue).

During secondary zone formation, the concentration of free IAA in the petiole tissue changed dramatically, with measurements ranging between 6 and 2608 pmol/g, fresh weight (FW) of tissue. The IAA concentration in the petioles at separation at the primary zone before IAA was added was lower in the G1 and Y2 sections (ca. 30 pmol/g FW) when compared with the Y3 and Y4 sections (166 and 271 pmol/g FW respectively). At 6 h after the application of IAA, the concentration of IAA had increased to 146 pmol/g FW in the G1 section, remained the same in the Y2 section and increased to 208 and 423 pmol/g FW in the Y3 and Y4 sections respectively. At 26 h after the application of IAA, and approximately at the time of differentiation of the secondary zone, the IAA concentration was similar to the petioles after 6 h (179 and 21 pmol/g FW for G1 and Y2 respectively) and significantly lower in the Y3 and Y4

sections (35 and 69 pmol/g FW respectively). At 40 h, the concentrations of IAA in both the G1 and Y4 sections are the highest during this time course (2147 and 2608 pmol/g respectively) and comparatively low in the Y2 and Y3 sections (24 and 103 pmol/g respectively). At the first point at which the green:yellow tissue can be ascertained (at 52 h) the IAA concentration was dramatically higher in the G1 and Y2 tissues (1125 and 1090 pmol/g FW respectively) compared to measurements in the Y3 and Y4 sections at 52 h of 17 and 107 pmol/g FW respectively. At separation at the secondary abscission zone, the IAA measurements in the G1, Y2 and Y4 sections were 405, 315 and 1198 pmol/g FW respectively.

The production of ethylene in the petiole sections mirrors the ageing and senescing of the tissues. The fresh tissues produce the lowest amounts of ethylene and the senescent tissues (Y2, Y3, Y4) at secondary separation produce the most ethylene. However, the ACC oxidase (ACO) activity and the protein expression does not follow the same pattern. The freshly excised tissue had the highest ACC oxidase activity (ca. 0.26 nmol/h/mg protein for the entire petiole) when compared with the tissues at separation of the pulvinus at primary abscission (G1, 0.053 nmol/h/mg protein and Y2/Y3/Y4 0.021 nmol/h/mg protein) and at secondary zone formation where G1 increased to 0.097 nmol/h/mg and remained the same in the Y2/Y3/Y4 section. A 42 kDa protein was detected by the ACO antibody that followed the same pattern of expression as the activity assays. It appears the protein that is being detected with the ACC oxidase activity assay and the one detected with the antibody are either the same isoform of ACC oxidase or expressed in the same abundance in the same tissues. Sequencing of seven ACO clones generated from mRNA extracted from fresh petiole tissue suggested there are at least two different ACO isoforms occur in the fresh petiole tissue. Combining this sequence data with the sequences found previously, there appears to be a total of at least four isoenzymes of ACC oxidase in *P. vulgaris*. The differential expression of the bean ACO detected with the TR-ACO2 antibody, shows that, as illustrated in white clover, different isoforms of ACO are differentially regulated in tissues at different developmental stages.

However, together these results show that the mechanisms involved in the timing, direction and control of secondary zone differentiation appear, with respect to ACC oxidase activity, ethylene evolution and changes in IAA concentration to be regulated in

complex manner. More information into the regulation of each compound within this system will be required to make accurate correlations about these compounds and the formation of secondary abscission zones.

## 5.4 Future directions

The information gathered from this *in vitro* study of the of the plant growth regulators, ethylene and auxin, during the differentiation of secondary abscission zones presents many interesting avenues for future research.

The concentration of free IAA along the petiole explants, after IAA is applied to the abscission face, appears to be regulated through conjugation and hydrolysis, of at least some of these conjugates, back to free IAA. Discovery of the specific spatial signals, known to be directed by IAA, that trigger secondary zone differentiation will be assisted with research into how free IAA and IAA conjugates are regulated in this system. One approach to find the time at which this transdifferentiation event occurs may involve the use of protein determinants that are unique to the bean zone cells in the same way as discussed in chapter three.

The detection of an isoform of ACC oxidase that appears to be differentially regulated in the fresh tissues and the primary and secondary zones at separation, that does not have increased expression or activity with increased ethylene production, suggests there are other isoforms of ACC oxidase operating in this system that are associated with senescence. Discovering all of the members of this multigene family and examining their differential expression will aid in our understanding of how this enzyme may assist in the regulation of ethylene production and its inducing factors in this system. Examining ethylene and IAA regulation of ACC oxidase will aid in our understanding of the mechanisms regulated by ethylene that make it an essential molecule for triggering the differentiation of secondary zones.

## Appendix A

Calculation of percentage binding (%B) of the IAA-alkaline phosphatase conjugate (tracer)

Non specific binding (NSB)

= 0% binding of the tracer

= 100  $\mu$ L solution containing IAA (1000 pmol) + 20  $\mu$ L of tracer

(i.e. where IAA is saturating the IgG IAA binding sites)

Zero binding ( $B_0$ )

= 100% binding of the tracer

= 100  $\mu$ L buffer + 20  $\mu$ L tracer

(i.e. where there is no IAA in the reaction)

$$\%B = \frac{(\text{Standard or Sample absorbance} - B_0 \text{ absorbance})}{(B_0 \text{ absorbance} - \text{NSB absorbance})} \times 100$$

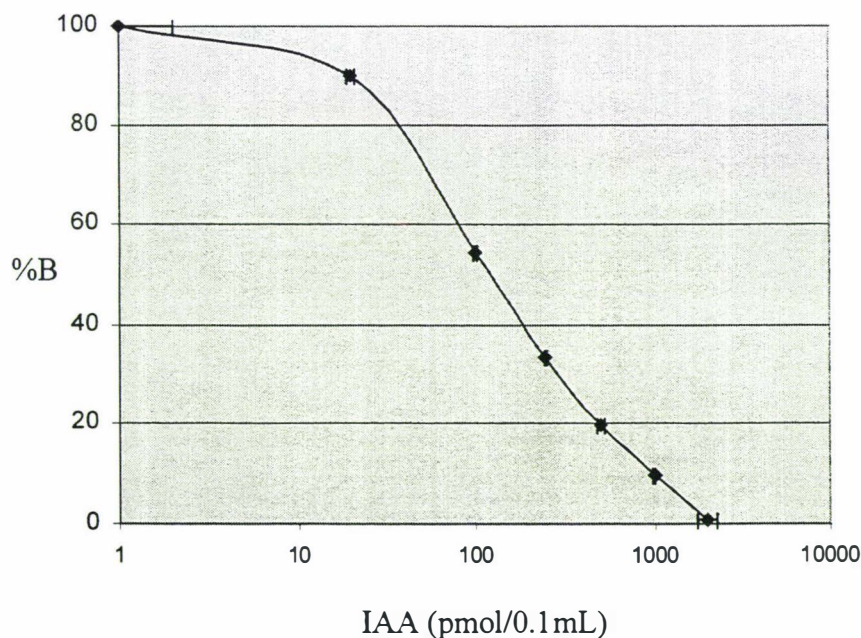


Figure A. Optimised standard curve generated using the monoclonal antibody. \*%B refers to the percentage binding of the alkaline-phosphatase conjugate to the IAA antibody.

## Appendix B

An example calculation for the determination of the polyclonal titres

Calculation of the approximate concentration of polyclonal Immunoglobulin Gs (IgGs), raised to the BSA-IAA conjugate, that recognise BSA, using ELISA.

One  $\mu\text{g}$  of BSA will saturate with a 1/10 dilution of IgG from the DEAE column

One  $\mu\text{g}$  of BSA is  $1.47 \times 10^{-11}$  moles

As there are 2 moles of BSA per 1 mole of IgG,  $7.3 \times 10^{-12}$  moles of IgG react with 1  $\mu\text{g}$  BSA

The reaction volume is 100  $\mu\text{L}$ , converting to mol/L gives  $7.3 \times 10^{-8}$  mol/L

The dilution of the antisera is 1/1000, therefore, the titer of the BSA antibodies in the partially purified IgG preparation from the DEAE column is  **$7.3 \times 10^{-5}$  mol/L**

### **The titer of IAA-CH<sub>3</sub> antibodies in the antisera**

One  $\mu\text{g}$  of IAA is  $5.26 \times 10^{-9}$  moles

As there are 2 moles of IAA-CH<sub>3</sub> per 1 mole of IgG,  $1.05 \times 10^{-8}$  moles of IgG react with 1  $\mu\text{g}$  IAA-CH<sub>3</sub>

The reaction volume is 100  $\mu\text{L}$ , converting to mol/L gives  $1.05 \times 10^{-4}$  mol/L

There is no dilution of the antisera therefore the titer of IAA-CH<sub>3</sub> antibodies is  **$1.05 \times 10^{-4}$  mol/L**

# Bibliography

**Abeles FB and Rubinstein B. (1964)** Regulation of ethylene evolution and leaf abscission by auxin. *Plant Physiol.* 39: 963-969.

**Abeles FB. (1969)** Abscission: The role of cellulase. *Plant Physiol.* 44: 447-452.

**Addicot FT. (1982)** Abscission. University California Press, Berkeley

**Allen JRF, Rivier L and Pilet P-E. (1982)** Quantification of indol-3-yl acetic acid in pea and maize seedlings by gas chromatography-mass spectrophotometry. *Phytochem.* 21: 525-530.

**Ameisen JC. (1996)** The origin of programmed cell death. *Science* 272: 1278-1279.

**Aronel V, Vergnolle C, Cantrel C and Kader J. (2000)** Lipid transfer proteins are encoded by a small multigene family in *Arabidopsis thaliana*. *Plant Sci.* 157: 1-12.

**Artec RN and Artec JM. (1989)** Use of a monoclonal antibody for the determination of free indole-3-acetic acid. *J. Plant . Physiol.* 135: 631-634.

**Bailey JM, Fishman PH and Pentchev PG. (1967)** Studies on mutarotases I. Purification and properties of a mutarotase from higher plants. *J. Biol. Chem.* 242: 4263-4269.

**Bailey JM, Fishman PH and Pentchev PG. (1970)** Studies on mutarotases II. Enzyme levels in a sugar reabsorption in developing rat kidney and intestine. *J. Biol. Chem.* 245: 559-563.

**Bandurski RS and Schulze A. (1977)** Concentration of indole-3-acetic acid and its derivatives in plants. *Plant Physiol.* 60: 211-213.

**Bandurski RS, Cohen JD, Slovin JP and Reinecke DM. (1995)** Auxin biosynthesis and metabolism. In *Plant hormone physiology, biochemistry, molecular biology.* Dordrecht, The Netherlands.pp. 39-65 (Ed. P.J. Davis) Kluwer Academic Publishers

**Barlier I, Kowalazyl M, Marchant A, Ljung K, Bhalerao R, Bennett M, Sandberg G and Bellini C. (2000)** The *sur2* gene of *A. thaliana* encodes the cytochrome P450 CYP8B1, a modulator of auxin homeostasis. *Proc. Natl. Acad. Sci.* 97: 14819-14824.

**Bartel B and Fink. (1995)** ILR1, an amidohydrolase that releases active indole-3-acetic acid from conjugates. *Science* 268: 1745-1748.

**Bartel B, LeClere S, Magidin M and Zolman BK. (2001)** Inputs to the active indole-3-acetic acid pool: de novo synthesis, conjugate hydrolysis, and indole-3-butyric acid  $\beta$ -oxidation. *J. Plant Growth Reg.* 20: 198-216.

**Beal JM and Whiting AG. (1945)** Effect of indoleacetic acid in inhibiting stem abscission in *Mirabilis jalapa*. Bot. Gaz. 106: 420-431.

**Becana M, Paris FJ, Sandalio LM and Rio LAd. (1989)** Isoenzymes of superoxide dismutase in nodules of *Phaseolus vulgaris* L., *Pisum sativum* L., and *Vigna unguiculata* (L.). Plant Physiol. 90: 1286-1292.

**Ben-Efraim I, Gad AE, Cohen P, Reymond P and Pillet P-E. (1990)** The effect of 4-chlororesorcinol on the endogenous levels of IAA, ABA and oxidative enzymes in cuttings. Plant Growth Reg. 9: 97-106

**Beyer EM. (1973)** Abscission: support for a role of ethylene modification of auxin transport. Plant Physiol. 48: 202-218.

**Bialek K and Cohen JD. (1986)** Isolation and partial characterisation of the major amide linked conjugate of indole-3-acetic acid from *Phaseolus vulgaris* L. Plant Physiol. 80: 99-104.

**Bleeker AB and Patterson SE. (1997)** Last exit: Senescence, abscission, and meristem arrest in *Arabidopsis*. Plant Cell 9: 1169-1179.

**Bodson M and Verhoyen MNJ. (2000)** Anatomical study of abscission zone formation and development on wild tomato species, *Lycopersicon pennellii*. Acta Hort. 514: 193-196.

**Boller T, Gehri A, Mauch F and Vogeli U. (1983)** Chitinase in bean leaves: induction by ethylene, purification, properties and possible function. Planta 157: 22-31.

**Bonghi C, Ferrarese L, Ruperti B, Tonutti P and Ramina A. (1998)** Cellulase and polygalacturonase involvement in abscission of leaf and fruit explants in peach. Physiol. Plant. 102: 342-356.

**Bornmann CH, Addicott FT, Lyon JL and Smith DE. (1968)** Anatomy of gibberellin induced stem abscission in cotton. Am. J. Bot 1968: 369-375.

**Bowler C and Chua N. (1994)** Emerging themes in plant signal transduction. The Plant Cell 6: 1529-1541.

**Bowler C, Camp WV, Montagu MV and Inze D. (1994)** Superoxide dismutase in plants. Crit. Rev. Plant Sci. 13: 199-218.

**Bowles DJ. (1990)** Defence-related proteins in higher plants. Annu. Rev. Biochem. 59:873-907.

**Brett CT and Hillman. (eds). (1985)** Biochemistry of plant cell walls. Cambridge; New York: Cambridge University Press.

**Brummell DA, Catala C, Lashbrook CC and Bennett AB. (1997)** A membrane-anchored E-type endo-1, 4-beta- glucanase is localised on the golgi and plasma membranes in higher plants. Pro. Natl. Acad. Sci. USA. 94: 4794-4799.

- Buchanan-Wollaston V. (1997)** The molecular biology of leaf senescence. *J. Exp. Bot.* 307: 181-199.
- Buhot N, Douliez JP, Jacquemard A, Marion D, Tran V, Maume BF, Milat ML, Ponchet M, Mikes V, Kader JC and Blein JP. (2001)** A lipid transfer protein binds to a receptor involved in the control of plant defence responses. *FEBS Letters* 509: 27-30.
- Burg SP and Burg EA. (1966)** The interaction between auxin and ethylene and its role in plant growth. *Proc. Natl. Acad. Sci.* 55: 262-269.
- Burns JK, Nairn CJ and Lewandowski DJ. (1996)** Cell wall hydrolase activity and cellulase gene expression during abscission of Valencia citrus fruit and leaves. *Pro. Florida State Hort. Soc.* 108: 254-258.
- Burns JK and Lewandowski DJ. (2000)** Genetics and expression of pectinmethylesterase, endo- beta-glucanase, and polygalacturonase. *Acta Hort.* 535: 65-80.
- Camp WV, Montagu MV and Inze D. (1994)** Superoxide dismutases: roles in stress tolerance. In *Causes of photooxidative stress and amelioration of defence systems in plants.* (Eds. C.H. Foyer and P.M. Mullineaux) CRC Press.
- Campillo Ed, Reid PD, Sexton R and Lewis LN. (1990)** Occurance and localisation of 9.5 cellulase in abscising and nonabscising tissues. *The Plant Cell* 2: 254-245.
- Campillo ED and Lewis LN. (1992)** Identification and kinetics of accumulation of proteins induced by ethylene in bean abscission zones. *Plant Physiol.* 98: 955-961.
- Campillo ED and Bennett AB. (1996)** Pedicel breakstrength and cellulase gene expression during tomato flower abscission. *Plant Physiol.* 111: 813-820.
- Candenas E. (1989)** Biochemistry of oxygen toxicity. *Ann. Rev. Biochem.* 58: 79-110.
- Carland FM and McHale NA. (1996)** LOP1: a gene involved in auxin transport and vascular patterning in *Arabidopsis*. *Development* 122: 112-115.
- Carpita N, Tierney M and Cambell M. (2001)** Molecular biology of the plant cell wall: searching for the genes that define structure, architecture and dynamics. *Plant Mol. Biol.* 47: 1-5.
- Caruso JL, Pence VC and Leverone LA. (1993)** Immunoassay methods of plant hormone analysis. 433-447.
- Cass LG, Kirven KA and Christoffersen RE. (1990)** Isolation and characterisation of a cellulase gene family member expressed during fruit ripening. *Mol. Gen. Gent.* 223: 76-86.
- Cassab GI. (1998)** Plant cell wall proteins. *Ann. Rev. Plant. Physiol. Plant Mol. Biol.* 49: 281-309.

**Castellano JM, Chamarro J and Vioque B. (1998)** Ethylene biosynthesis in transgenic auxin-overproducing tomato plants. In EU-TMR-Euroconference Symposium, Thira (Santorini) Greece. pp. 397-398. (Eds. A.K. Kanellis, C. Chang, H. Klee, A.B. Bleeker, J.C. Pech and D. Grierson) Kluwer Academic Publishers.

**Chang C, Kwok SF, Bleeker AB and Meyerowitz EM. (1993)** *Arabidopsis* ethylene-response gene ETR1: Similarity of product to two component regulators. *Science* 262: 539-544.

**ChangJin P, Ryoung S, JeongMee P, GilJe L, JinSam Y and KyungHee P. (2002)** Induction of pepper cDNA encoding a lipid transfer protein during the resistance response to tobacco mosaic virus. *Plant Mol. Biol.* 48: 243-254.

**Chauvaux N, Child R, John K, Ulvskov P, Borkhardt P, Prinsen E and Onckelen HAV. (1997)** The role of auxin in cell separation in the dehiscence zone of oil seed rape pods. *J. Exp. Bot.* 48: 1423-1429.

**Chen R, Hilson P, Sedbrook J, Rosen E, Casper T and Masson PH. (1998)** The *Arabidopsis thaliana* AGRVITROPHIC1 gene encodes a component of polar auxin-transport efflux carrier. *Proc. Natl. Acad. Sci. USA* 95: 15112-15117.

**Cho HT and Cosgrove DJ. (2000)** Altered expression of expansin modulates leaf growth and pedicel abscission in *Arabidopsis thaliana*. *Proc. Natl. Acad. Sci. USA* 97: 9783-9788.

**Clark AM and Bohnert HJ. (1999)** Cell-specific expression of genes of the lipid transfer protein family from *Arabidopsis thaliana*. *Plant Cell Physiol.* 40: 69-76.

**Coenen C and Lomax TL. (1997)** Auxin-cytokinin interactions in higher plants: old problem and new tools. *TIPS* 2: 351-355.

**Cohen JD and Bandurski RS. (1978)** The bound auxins: protection of indole-3-acetic acid from peroxidase-catalysed oxidation. *Planta* 139: 203-208.

**Cooke TJ, Poli D, Sztein AE and Cohen JD. (2002)** Evolutionary patterns in auxin action. *Plant Mol. Biol.* 49: 319-338.

**Corke FM and Roberts K. (1997)** Large changes in the population of cell wall proteins accompany the shift to cell elongation. *J. Exp. Bot.* 48: 971-977.

**Cosgrove DJ. (1993)** How do plant cell walls extend? *Plant Physiol.* 102: 1-6.

**Cosgrove DJ. (2000)** Expansive growth of plant cell walls. *Plant Physiol. Biochem.* 38: 109-124.

**Coupe SA, Taylor JE and Roberts JA. (1995)** Characterisation of an mRNA encoding a metallothioneine-like protein that accumulates during ethylene promoted abscission in *Sambucus nigra* L. leaflets. *Planta* 197: 442-447.

**Coupe SA, Taylor JE and Roberts JA. (1997)** Temporal and spatial expression of mRNAs encoding pathogenesis-related proteins during ethylene-promoted abscission in *Sambucus nigra*. *Plant, Cell and Env.* 20: 1517-1524.

**Creelman RA and Mullet JE. (1997)** Oligosaccharides, brassinolides, and jasmonates: Nontraditional regulators of plant growth, development, and gene expression. *The Plant Cell* 9: 1211-1223.

**Crowler JR. (1995)** Basic immunology. ELISA: Theory and Practice. Human Press Inc.: 1-107.

**Dale JE and Milthorpe FL. (1981)** General features of the production and growth of leaves. The growth and functioning of leaves. Cambridge University Press. 151-178.

**Darly CP, Forrester AM and McQueen-Mason SJ. (2001)** The molecular basis of plant cell wall extension. *Plant Mol. Biol.* 47: 179-195.

**Delarue M, Prinsen E, van HO, Caboche M and Bellini C. (1998)** Sur2 mutants of *A. thaliana* define a new locus involved in the control of auxin homeostasis. *Plant J.* 14: 603-611.

**DellaPenna D, Lashbrook CC, Toenjes K, Giovannoni JJ, Fischer RL and Bennett AB. (1990)** Polygalacturonase isoenzymes and pectin depolymerisation in transgenic rin tomato fruit. *Plant Physiol.* 94: 1882-1886.

**Devoto A, Clark AJ, Nuss L, Cervone F and Lorenzo GD. (1997)** Developmental and pathogen-induced accumulation of transcripts of polygalacturonase-inhibiting protein in *Phaseolus vulgaris* L. *Planta* 202: 284-292.

**Doorn WGV and Stead AD. (1997)** Abscission of flowers and floral parts. *J. Exp. Bot.* 48: 821-837.

**Douliez JP, Pata C, Rabsona H, Molle D and Marion D. (2001)** Disulfide bond assignment, lipid transfer activity and secondary structure of a 7-kDa plant lipid transfer protein, LTP2. *Eur. J. Biochem.* 268: 1400-1403.

**Duff SMG, Sarath G and Plaxton WC. (1994)** The role of acid phosphatases in plant phosphorous metabolism. *Physiol. Plant.* 90: 791-800.

**Dunkley HM and Golden KD. (1998)** ACC oxidase from *Carica papaya*: Isolation and characterisation. *Physiol. Plant* 103: 225-232.

**Dupille E and Zacarias L. (1996)** Extraction and biochemical characterisation of wound-induced ACC oxidase from citrus peel. *Plant Sci.* 114: 53-60.

**Durbin ML, Sexton R and Lewis LN. (1981)** The use of immunological methods to study the activity of cellulase enzymes ( $\beta$ -1, 4-glucan 4-glucan hydrolase) in bean leaf abscission. *Plant Cell and Env.* 4: 67-73.

**Duverger E, Pellerin-Mendes C, Mayer R, Roche C-C and Monsigny M. (1995)** Nuclear import of glycoconjugates is distinct from the classical NLS pathway. *J. Cell. Sci.* 108: 1325-1332.

**Ehness R., Ecker M., Godt D. E. and T. R. (1997)** Glucose and stress independently regulate source and sink metabolism and defence mechanisms via signal transduction pathways involving protein phosphorylation. *The Plant Cell* 9: 1825-1841.

**Epstein E and Sagee O. (1992)** Effect of ethylene treatment on transport and metabolism of indole-3-butyric acid in citrus leaf. *Plant Growth Reg.* 11: 357-362.

**Escribano MI, Merodio C and John P. (1996)** Characterisation of 1-aminocyclopropane-1-carboxylate oxidase partially purified from cherimoya fruits. *J. Agric. Food Chem.* 44: 730-735.

**Esquerre-Tugaye M-T, Boudart G and Dumas B. (2000)** Cell wall degrading enzymes, inhibitory proteins, and oligosaccharides participate in the molecular dialogue between plants and pathogens. *Plant Physiol. Biochem.* 38: 157-163.

**Eyal Y, Meller Y, Lev-Yadun S and Fluhr R. (1993)** The basic type PR-1 promoter directs ethylene responsiveness, vascular and abscission zone-specific expression. *Plant J.* 4: 225-234.

**Favaron F, D'Ovidio R, Porceddu E and Alghisi P. (1994)** Purification and molecular characterisation of a soybean polygalacturonase-inhibiting protein. *Planta* 195: 80-87.

**Ferguson IB. (1983)** Calcium stimulation of ethylene production induced by 1-aminocyclopropane-1-carboxylic acid and indole-3-acetic acid. *J. Plant Growth Reg.* 2: 205-214.

**Fernandez-Maculet JC and Yang, SF (1992)** Extraction and partial characterization of the ethylene-forming enzyme from apple fruit. *Plant Physiol* 99: 751-754

**Ferrarese L, Trainotti L, Moretto P, Laureto P, Rascio N and Casadoro G. (1995)** Differential ethylene-inducible expression in cellulase plants. *Plant Mol. Biol.* 29: 735-747.

**Fischer C, Speth V, Fleig-Eberenz S and Neuhaus G. (1997)** Induction of zygotic polyembryos in wheat: influence of auxin polar transport. *The Plant Cell* 9: 1767-1780.

**Fishman PH, Kusiak JW and Bailey JM. (1973)** Studies on mutarotase: Photooxidation reactions and nature of the enzyme catalysis. *Biochem.* 12: 2540-2544.

**Fleur R and Mattoo AK. (1996)** Ethylene: biosynthesis and perception. *Crit. Rev. Plant Sci.* 15: 497-523

**Franco AR, Gee MA and Guilfoyle TJ. (1990)** Induction and superinduction of auxin-responsive mRNAs with auxin and protein synthesis inhibitors. *J. Biol. Chem.* 26: 15845-15849.

- Friml J and Palme K. (2002)** Polar auxin transport - old questions and new concepts? *Plant Mol. Biol.* 49: 273-284.
- Fry SC. (1995)** Polysaccharide-modifying enzymes in the plant cell wall. *Ann. Rev. Plant Physiol. Plant Mol. Biol.* 46: 497-520.
- Fukuda H and Komamine A. (1987)** Lignin synthesis and its related enzymes as markers of tracheary-element differentiation in single cells isolated from the mesophyll of *Zinnia elegans*. *Planta* 155: 423-430.
- Fukuda. (1997)** Tracheary element differentiation. *The Plant Cell* 9: 1147-1156.
- Galston AW and Sawhney RK. (1990)** Polyamines in plant biology. *Plant Physiol.* 94: 406-410.
- Galston AW. (2001)** Plant biology - retrospect and prospect. *Curr. Sci.* 80: 143-152.
- Gatz C and Hillen W. (1986)** *Acinetobacter calcoaceticus* encoded mutarotase: nucleotide sequence analysis of the gene and characterisation of its secretion in *E.coli*. *Nucl. Acids. Res.* 14: 4309-4323.
- Gatz C, Altschmied J and Hillen W. (1986)** Cloning and expresion of the *Acinetobacter calcoaceticus* mutarotase gene in *Escherichia coli*. *J. of Bacteriol.* 168: 31-39.
- Getzoff ED, Cambelli DE, Fisher CL, Parge HE, Viezzoli MS, Banci L and Hallewell RA. (1992)** Faster superoxide dismutase mutants designed by enhancing electrostatic guidance. *Nature* 358. 347-351.
- Gong D and McManus M. (2000)** Purification and characterisation of two ACC oxidase expressed differentially during leaf ontogeny in white clover. *Physiol. Plant.* 110: 13-21.
- Gonzalez-Bosch C, Campillo Ed and Bennett AB. (1997)** Immunodetection and characterisation of tomato endo-beta-1, 4-glucanase Cell protein in flower abscission zones. *Plant Physiol.* 144. 1541-1546.
- Gonzalez-Carranza ZH, Lozoya-Gloria E and Roberts JA. (1998)** Recent developments in abscission: Shedding light on the shedding process. *TIPS.* 3: 8-12.
- Guilfoyle TJ. (1985)** Auxin regulated gene expression in higher plants. *Crit. Rev. Plant Sci.* 4
- Guinn G and Brummett DL. (1988)** Changes in free and conjugated indole-3-acetic acid and abscisic acid in young cotton fruits and their abscission zones in relation to fruit retention during and after moisture stress. *Plant Physiol.* 86: 28-31.
- Hahlbrock K and Scheel D. (1989)** Physiology and molecular biology of phenylpropanoid metabolism. *Ann. Rev. Plant Physiol. Plant Mol. Biol.* 40: 347-369.

**Hall JL and Sexton R. (1974)** Fine structure and cytochemistry of the abscission zone cells of *Phaseolus vulgaris*. II. Localisation of peroxidase and acid phosphatase in the separation zone cells. *Ann. Bot* 157: 855-858.

**Hames BD and Rickwood D (eds.) (1981)** Gel electrophoresis of proteins: A practical approach. IRL Press Ltd. Oxford.

**Hamilton AJ, Lycett WL and Grierson D. (1990)** Antisense gene that inhibits synthesis of the hormone ethylene in transgenic plants. *Nature* 346 (6281): 284-287.

**Hamilton AJ, Bouzawen M and Grierson D. (1991)** Identification of a tomato gene for the ethylene-forming enzyme by expression in yeast. *Proc. Natl. Acad. Sci. USA* 88: 7434-7437.

**Hangarter RP and Good NE. (1981)** Evidence that IAA conjugates are slow-release sources of free IAA in plant tissues. *Plant Physiol.* 68: 1424-1427.

**Harpster MH, Brummell DA and Dunsmuir P. (1998)** Expression analysis of a ripening-specific, auxin-repressed endo-1,4- $\beta$ -glucanase gene in strawberry. *Plant Physiol.* 118: 1307-1316.

**Harris N, Taylor JE and Roberts JA. (1997)** Characterisation and expression of an mRNA encoding a wound-induced (Win) protein from ethylene treated tomato leaf abscission zone tissue. *J. Exp. Bot* 48: 1223-1227.

**Hasenstein KH, Blancaflor EB and Lee JS. (1999)** The Microtubule cytoskeleton does not integrate auxin transport and gravitropism in maize roots. *Physiol.Plant.*105: 729-738.

**Hawes MC and Lin H-J. (1990)** Correlation of pectolytic enzyme activity with the programmed release of cells from root caps of peas (*Pisum sativum*). *Plant Physiol.* 94: 1855-1859.

**Hay A, Watson L, Zhang C and McManus M. (1998)** Identification of cell wall proteins in roots of phosphate-deprived white clover plants. *Plant Physiol. Biochem.* 36: 305-311.

**Hedden P. (1993)** Modern methods for the quantitative analysis of plant hormones. *Ann. Rev. Plant Physiol. Plant Mol. Biol.* 44: 107-129.

**Heese-Peck A and Raikhel NV. (1998)** A glycoprotein modified with terminal N-acetylglucosamine and localised at the nuclear rim shows sequence similarity to aldose-1-epimerase. *The Plant Cell* 10: 599-612.

**Henrissat B, Coutinho PM and Davis GJ. (2001)** A census of carbohydrate-active enzymes in the genome of *Arabidopsis thaliana*. *Plant Mol. Biol.* 47: 55-72.

**Henry EW and Ananich ME. (1986)** Superoxide dismutase activity in ethylene-treated bean abscission zone tissue (24-120hrs). In *Plant Growth Regulator Society of America*, Florida. pp. 115-128.

- Hilt C and Bessis R. (2000)** An *in vitro* model to study abscission in grapevine (*Vitis vinifera* L.). *Vitis* 39: 85-86.
- Hoche V, Scotta B, Maldiney R, Bonnet M and Miginiac E. (1992)** Changes in indole-3-acetic acid levels during tomato seed development. *Plant cell reports*. 11: 253-256.
- Hock B, Liebmann S, Beyrle H and Dressel K. (1992)** Phytohormone analysis by enzyme immunoassay. *Meth in Micro*. 24: 249-270.
- Hoffman NE and Yang SF. (1982)** Enhancement of wound-induced ethylene synthesis by ethylene in preclimateric cantaloupe. *Plant Physiol*. 69(2): 317-322.
- Hoffman NE, Yang SF and McKeon T (1982)** Identification of 1-(malonylamino)cyclopropane-1-carboxylate as a major conjugate of 1-aminocyclopropane-1-carboxylic acid, an ethylene precursor in higher plants. *Biochem. Biophys. Res. Commun*. 104: 765-770.
- Hong SB, Sexton R and Tucker ML. (2000)** Analysis of gene promoters for two tomato polygalacturonases expressed in abscission zones and the stigma. *Plant Physiol*. 123: 869-881.
- Hunter DA, Yoo S-D, Butcher SM and McManus MT. (1999)** Expression of 1-aminocyclopropane-1-carboxylate oxidase during leaf ontogeny in white clover. *Plant Physiol*. 120: 131-141.
- HyungTaeg C and Cosgrove DJ. (2000)** Altered expression of expansin modulates leaf growth and pedicel abscission in *Arabidopsis thaliana*. *Proc. Natl. Acad. Sci. USA* 97: 9783-9788.
- HyunSook C, YongGu C, MiYoung P, MyungChul L, MooYoung E, Kang BG and WooTaek K. (2000)** Hormonal cross-talk between auxin and ethylene differentially regulates the expression of two members of the 1-aminocyclopropane-1-carboxylate oxidase gene family in rice (*Oryza sativa* L.). *Plant and Cell Physiol*. 41: 354-362.
- Iannetta PPM, Wyman M, Neelam A, Jones C, Taylor MA, Davis HV and Sexton R. (2000)** A casual role for ethylene and endo- $\beta$ -1, 4-glucanase in the abscission of red-raspberry (*Rubus idaeus*) drupelets. *Physiol. Plant*. 110: 535-543.
- Jackson MB and Osborne DJ. (1970)** Ethylene, The natural regulator of leaf abscission. *Nature* 225: 1019-1022.
- Jain PC and Singh GB. (1995)** An overview of different types of polarimeters. *Indian sugar* 45: 479-481.
- Jang CS, Chung JE, Cho YG and An G. (1997)** Characterisation of two rice MADS-box genes in control of flowering time. *Mol. Cell* 7: 559-566.
- JeongHoe K, WooTaek K and Kang BG. (2001)** IAA and N<sup>6</sup>-benzyladenine inhibit ethylene-regulated expression of ACC oxidase and ACC synthase genes in mungbean hypocotyls. *Plant and Cell Physiol*. 42: 1056-1061.

**Johnson PR and Ecker JR. (1998)** The ethylene gas signal transduction pathway: a molecular prospective. *Ann. Rev. Gen.* 32: 227-254.

**Jones JF and Kende H. (1979)** Auxin-induced ethylene biosynthesis in subapical stem sections of etiolated seedlings of *Pisum sativum* L. *Planta* 146: 649-656.

**Jones AM. (1990)** Do we have the auxin receptor yet? *Physiol. Plant.* 80: 154-158.

**Jones AM, Im KH, Savka MA, Wu MJ, Derwitt NG, Shillito R and Binns AN. (1998)** Auxin-dependent cell expansion mediated by over expressed auxin binding protein 1. *Science* 282: 1114-1117.

**Jose-Estanyol M and Puigdomenech P. (2000)** Plant cell wall glycoproteins and their genes. *Plant Physiol. Biochem.* 38: 97-108.

**Kacperska A and Kubacka-Zebalska M. (1989)** Formation of stress ethylene depends on both ACC synthesis and on the activity of free radical-generating systems. *Physiol. Plant.* 77: 321-327.

**Kader J. (1996)** Lipid-transfer proteins in plants. *Ann. Rev. Plant. Mol. Biol.* 47: 627-654.

**Kader J. (1997)** Lipid transfer proteins: A puzzling family of proteins. *TIPS* 2: 66-70.

**Kalaitzis P, Koehler SM and Tucker ML. (1995)** Cloning of a tomato polygalacturonase expressed in abscission. *Plant Mol. Biol.* 28: 647-656.

**Kalaitzis P, Solomos T and M.L.Tucker. (1997)** Three different polygalacturonases are expressed in tomato leaf and flower abscission, each with a different temporal expression pattern. *Plant Physiol.* 113: 1303-1308.

**Kaneko TS, Kuwabara C, Tomioka S and Suzuki K. (1998)** A 60 kDa polypeptide of cell wall acid phosphatase from tobacco cells. *Phytochem.* 48: 1125-1130.

**Kawaguchi M and Syono K. (1996)** The excessive production of indole-3-acetic acid and its significance in studies of the biosynthesis of this regulator of plant growth and development. *Plant Cell Physiol.* 37: 1043-1048.

**Kazokas WC and Burns JK. (1998)** Cellulase activity and gene expression in citrus fruit abscission zones during and after ethylene treatment. *J. Amer. Soc. Hort. Sci.* 123: 781-786.

**Kemmerer CL and M.L.Tucker. (1994)** Comparative study of cellulases associated with adventitious root initiation, apical buds, and leaf, flower, and pod abscission zones in soybean. *Plant Physiol.* 104: 557-562.

**Kende H. (1993)** Ethylene Biosynthesis. *Ann. Rev. Plant Mol. Biol.* 44: 283-307.

**Kende H and Zeevaart JAD. (1997)** The five "classical" plant hormones. *The Plant Cell* 9: 1197-1210.

**Kanellis A, Chang C, Kende H and Grierson D. (1997)** Biology and biotechnology of the plant hormone ethylene.

**Kenis JD and Trippi VS. (1982)** Activity of peroxidase and its regulation to aging and abscission in *Phaseolus vulgaris*. *Phyton Argentina* 42: 17-24.

**Keston AS. (1954)** Occurrence of mutarotase in animals: Its proposed relationship to transport and reabsorption of sugar and insulin. *Science* 120: 355-356.

**Koehler DE, Lewis LN, Shannon LM and Durbin ML. (1981)** Purification of a cellulase from kidney bean (seedling) abscission zones. *Phytochem.* 20: 409-412.

**Kosugi Y, Oyomada N, Satoh S, Yoshioka T, Onodera E and Yamada Y. (1997)** Inhibition by 1-aminocyclopropane-1-carboxylate of the activity of 1-aminocyclopropane-1-carboxylate oxidase obtained from senescing petals of carnation flowers. *Plant Cell Physiol.* 38: 312-318.

**Kowalczyk M and Sandberg G. (2001)** Quantitative analysis of indole-3-acetic acid metabolites in *Arabidopsis*. *Plant Physiol.* 127: 1845-1853.

**Kuai J and Dilley DR. (1992)** Extraction, partial purification and characterisation of 1-aminocyclopropane-1-carboxylate oxidase from apple fruit. *Postharv. Biol. Technol.* 1: 203-211.

**Laemmli UK. (1970)** Cleavage of structural proteins during the assembly of the bacteriophage T4. *Nature* 680-685.

**Lakshman P, Ng SK, Loh CS and Goh CJ. (1997)** Auxin, cytokinin and ethylene differentially regulate specific developmental stages associated with shoot bud morphogenesis in leaf tissues of Mangosteen cultured *in vitro*. *Plant Cell Physiol.* 38: 59-64.

**Lamgrimini LM. (1991)** Peroxidase, IAA oxidase and auxin metabolism in transformed tobacco plants. *Plant Physiol.* 96: 77.

**Larson RA. (1988)** The antioxidants of higher plants. *Phytochem.* 27: 969-978.

**LaRue CD. (1936)** Effect of auxin on the abscission of petioles. *Proc. Natl. Acad. Sci. USA* 22: 254-259.

**Lashbrook CC, Gonzalez-Bosch C and Bennet AB. (1994)** Two divergent endo- $\beta$ -1,4-endoglucanase genes exhibit overlapping expression in ripening fruit and abscising flowers. *Plant Cell* 6: 1485-1493.

**Lashbrook CC, Giovannoni JJ, Hall BD, Fischer RL and Bennett AB. (1998)** Transgenic analysis of tomato endo- $\beta$ -1, 4-glucanase gene function. Role of cell in floral abscission. *Plant J.* 13: 303-310.

- Latche KA, Dupille E, Rombaldi C, Cleyet-Marel JC, Lelievre JM and Pech JC. (1992)** Purification, characterisation and subcellular localisation of ACC oxidase from fruits. In Cellular and molecular aspects of the plant hormone ethylene. pp. 39-45 (Eds. J.C. Pech, A. Latche and C. Balague) Kluwer Academic Publishers, Dordrecht, Netherlands.
- Lewis LN and Varner JE. (1970)** Synthesis of cellulase during abscission of *Phaseolus vulgaris* leaf explants. *Plant Physiol.* 46: 194-199.
- Liu W, Sheu H and Zhou Q. (1984)** Peroxidase activity in the pedicel abscission zone of young cotton boll. *Acta. Phytophysiol. Sin.* 10: 169-174.
- Ljung K, Hull AK, Kowalczyk M, Marchant A, Celenza J, Cohen JD and Sandberg G. (2002)** Biosynthesis, conjugation, catabolism and homeostasis of indole-3-acetic acid in *Arabidopsis thaliana*. *Plant Mol. Biol.* 49: 249-272.
- Llop-Tous I, Dominguez-Puigjaner E, Palomer X and Vendrell M. (1999)** Characterisation of two divergent endo- $\beta$ -1,4-glucanase cDNA clones highly expressed in the non-climateric strawberry fruit. *Plant Physiol.* 119: 1415-1421.
- Lomax TL. (1995)** Auxin transport. *Plant Hormones: Physiology, Biochemistry and Molecular Biology.* Davis P.J. ed.: 509-530.
- Loopstra CA, Mouradov A, Vivian-Smith A, Glassick TV, Gale BV, Southerton SG, Marshall H and R.D T. (1998)** Two pine endo- $\beta$ -1,4-glucanases are associated with rapidly growing reproductive structures. *Plant Physiol.* 116(3). 959-967.
- Luschnig C. (1999)** Two pieces of the auxin puzzle. *TIPS* 4: 162-163.
- Magnus V, Nigovic B, Hangarter RP and Good NE. (1992)** N-(indole-3-ylacetyl)amino acids as sources of auxin in plant tissue culture. *Plant Growth Reg.* 11: 19-28.
- Mao Long, Dillara Begum, Chuang HueyWan, Budiman MA, Szymkowlak EJ, Irish EE and Wing RA. (2000)** Jointless is a MADS-box gene controlling tomato flower abscission zone development. *Nature (London).* 406 (6798): 910-913.
- Marcussen J, Ulvskov P, Olsen CE and Rajagopal R. (1989)** Preparation and properties of antibodies against indoleacetic acid (IAA)-C5-BSA, a novel ring-coupled IAA antigen, as compared to two other types of IAA-specific antibodies. *Plant Physiol.* 89: 1071-1078.
- Mauch F, Hadwiger LA and Boller T. (1988)** Antifungal hydrolases in pea tissue. I. Purification and characterisation of two chitinases and two beta-1,3-glucanases differentially regulated during development and in response to fungal infection. *Plant Physiol.* 87: 325-333.
- McGarvey D and Christoffersen RD. (1992)** Characterisation and kinetic parameters of ethylene-forming enzyme from avocado fruit. *J. Biol. Chem.* 267: 5964-5967.

- McManus MT, McKeamting J, Secher DS, Osborne DJ, Ashford D, Dwek RA and Rademacher TW. (1988)** Identification of a monoclonal antibody to abscission tissue that recognises xylose/fucose-containing N-linked oligosaccharides from higher plants. *Planta* 175: 506-512.
- McManus MT and Osborne DJ. (1989)** Identification of leaf abscission zones as a specific class of target cells for ethylene. In: *Cell Separation in Plants, NATO ASF Series, Vol H35, Pp 201-210.* Springer Verlag, Berlin, Heidelberg.
- McManus MT and Osborne DJ. (1990)** Evidence for the preferential expression of particular proteins in leaf abscission zones of the bean *Phaseolus vulgaris*. *J. Plant Physiol.* 136: 391-397
- McManus MT and Osborne DJ. (1990a)** Identification of polypeptides specific to rachis abscission zone cells of *Sambucus nigra*. *Physiol. Plant.* 79: 471-478.
- McManus MT and Osborne DJ. (1991)** Identification and characterisation of an ionically-bound cell wall glycoprotein expressed preferentially in the leaf rachis abscission zone of *Sambucus nigra* L. *J. Plant Physiol.* 137:251-255.
- McManus MT. (1994)** Peroxidases in the separation zone during ethylene-induced bean leaf abscission. *Phytochem.* 35: 567-572.
- McManus MT, Thompson DS, Merriman C, Lyne L and Osborne DJ. (1998)** Transdifferentiation of mature cortical cells to abscission zone cells in *Phaseolus vulgaris* (L.). *Plant Physiol.* 116: 892-897.
- MeiChu C, ShuJen C, LinYun K, YeeYung C and ShangFa Y. (2002)** Subcellular localisation of 1-aminocyclopropane-1-carboxylic acid oxidase in apple fruit. *Plant and Cell Physiol.* 43: 549-554.
- Micheli F. (2001)** Pectin methylesterases: cell wall enzymes with important roles in plant physiology. *TIPS* 6: 414-419.
- Minorsky PV. (2002)** The wall becomes surmountable. *Plant Physiol.* 128: 345-353.
- Moore DJ. (1968)** Cell wall dissolution and enzyme secretion during leaf abscission. *Plant Physiol.* 43: 1545-1549.
- Moya-Leon MA and John P. (1995)** Purification and biochemical characterisation of 1-aminocyclopropane-1-carboxylate oxidase from banana fruit. *Phytochem.* 39: 15-20.
- Mudway GK and Delong A. (2001)** Polar auxin transport: controlling where and how much. *TIPS* 6: 535-542.
- Mulhern SA, Fishman PH, Kusiak JW and Bailey JM. (1973)** Physical characteristics and chemi-osmotic transformations of mutarotase from various species. *J. Biol. Chem.* 248: 4163-4173.
- Nakamura S, Mori H, Sakai F and Hayashi T. (1995)** Cloning and sequencing of cDNA for poplar endo-1, 4-beta-glucanase. *Plant and Cell Physiol.* 36: 1229-1235.

- Napier RM and M.A.Venis. (1995)** Tansley review no. 79: Auxin action and auxin binding proteins. *New Phytol.* 129: 167-201.
- Napier RM. (2001)** Models of auxin binding. *J. Plant Growth Reg.* 20: 244-254.
- Neal MW and Florini JR. (1973)** A rapid method for desalting small volumes of solution. *Analytical Biochem.* 55: 328-330.
- Nelson T and Dengler N. (1997)** Leaf vascular pattern formation. *Plant Cell* 9: 1121-1135.
- Nicol F, His I, Jauneau A, Vernhettes S, Canut H and Hofte H. (1998)** A plasma membrane-bound putative endo-1, 4-beta-D-glucanase is required for normal wall assembly and cell elongation in *Arabidopsis*. *EMBO J.* 17: 5563-5576.
- Normanly J, Slovin JP and Cohen JD. (1995)** Rethinking auxin biosynthesis and metabolism. *Plant Physiol.* 107: 323-329.
- Normanly J. (1997)** Auxin metabolism. *Physiol. Plant* 100: 431-442.
- Normanly J and Bartel B. (1999)** Redundancy as a way of life - IAA metabolism. *Curr. Opin. Plant Biol.* 2: 207-213.
- Oberegger H, Zadra I, Schoeser M, and Haas H. (2000)** Iron starvation leads to increased expression of Cu/Zn-superoxide dismutase in *Aspergillus*. *FEBS Letters.* 485: 113-116.
- Osborne DJ. (1968)** Hormonal mechanisms regulating senescence and abscission. In *Biochemistry and physiology of plant growth substances.* pp. 815-840 (Eds. F. Wightman and G. Setterfield) Runge Press, Ottawa.
- Osborne DJ. (1979)** Auxin and ethylene and the control of cell growth. Identification of three classes of target cells. In *Plant growth regulation.* pp. 161-171 (Ed. P. Pilet) Springer-Verlag, Berlin, Germany.
- Osborne DJ. (1989)** Abscission. *Crit. Rev. Plant Sci.* 8: 103-129.
- Osborne DJ, McManus MT and Webb J. (1985)** Target cells for ethylene action. In *Ethylene and plant development.* (Eds. G. Tucker and J.A. Roberts). Butterworths, London. pp. 197-212
- Osborne DJ and McManus MT. (1986)** Flexibility and Commitment in plant cells during differentiation. *Curr. Top. Dev. Biol.* 20: 383-396.
- Osborne DJ and Sargent JA. (1976)** The positional differentiation of abscission zones during the development of the leaves of *Sambucus nigra* and the response of the cells to auxin and ethylene. *Planta* 132: 197-204.
- Ostergaard L, Petersen M, Mattsson O and Mundy J. (2002)** An *Arabidopsis* callose synthase. *Plant Mol. Biol.* 49: 559-566.

- Ostin A, Kawalczyk M, Bhalerao RP and Sandberg G. (1998)** Metabolism of indole-3-acetic acid *Arabidopsis*. *Plant Physiol.* 118: 285-296.
- Palme K and Galweiler L. (2000)** PIN-pointing the molecular basis of auxin transport. *Curr. Opin. Plant Biol.* 2: 375-381.
- Park S, Jauh G, Mollet J, Eckard KJ, Nothnagel EA, Walling LL and E.M.Lord. (2000)** A lipid transfer-like protein is necessary for lily pollen tube adhesion to an *in vitro* stylar matrix. *The Plant Cell* 12: 151-163.
- Parry G, Marchant A, May S, Swarup R, James N, Graham N, Allen T, Martucci T, Yemm A, Napier R, Manning K, King G and Bennet M. (2001)** Quick on the uptake: characterisation of a family of plant auxin influx carriers. *J. Plant Growth Reg.* 20: 217-225.
- Peck SC and Kende H. (1995)** Sequential induction of ethylene biosynthetic enzymes by indole-3-acetic acid in etiolated peas. *Plant Mol. Biol.* 293-301.
- Pence VC and Caruso JL. (1987)** ELISA determination of IAA using antibodies against ring-linked IAA. *Phytochem.* 26: 1251-1255.
- Peng J, Richards DE, Hartley NM, Murphy GP, Devos KM, Flintham JE, Beales J, Fish LJ, Worland AJ, Peica F, Sudhakar D, Christou P, Snape JW, Gale MD and N.P.Harberd. (1999)** 'Green revolution' genes encode mutant gibberellin response modulators. *Nature* 400: 256-261.
- Pengelly WL and Jr. FM. (1977)** A specific radioimmunoassay for nanogram quantities of auxin, indole-3-acetic acid. *Planta* 136: 173-180.
- Pennell RI and Lamb C. (1997)** Programmed cell death in plants. *The Plant Cell* 9: 1157-1168.
- Peterson M, Sander L, Child R, Onckelen HV, Ulvskov P and Borkhardt B. (1996)** Isolation and characterisation of a pod dehiscence zone -specific polygalacturonase from *Brassica napas*. *Plant Mol. Biol.* 31: 517-527.
- Pidgeon CM, Reid DM and Facchini PJ. (1997)** Light-induced changes in ethylene production in *Phaseolus vulgaris* cv. Taylor. *Plant Physiol.* 114: S-165.
- Pierik RLM. (1973)** Secondary abscission and parthenocarpic fruit growth in apple and pear flowers *in vitro*. *Acta Hort.* 34: 299-309.
- Pierik RML. (1977)** Induction of secondary abscission in apple pedicels *in vitro*. *Physiol. Plant.* 39: 271-274.
- Pierik RML. (1980)** Hormonal regulation of secondary abscission in pear pedicels. *Physiol. Plant* 48: 5-8.

- Plummer JA, Vine JH and Mullins MG. (1991)** Regulation of stem abscission and callus growth in shoot explants of sweet orange [*Citrus sinensis* (L.) Osbeck]. *Ann. Bot.* 67: 17-22.
- Poolman B, Royer TJ, Mainzer SE and Schmidt BF. (1990)** Carbohydrate utilisation in *Streptococcus thermophilus*: Characterisation of the genes for aldose-1-epimerase (mutarotase) and UDPglucose 4-epimerase. *J. Bacteriol.* 172: 4037-4047.
- Poovaiah BW and Rasmussen HP. (1973)** Peroxidase activity in the abscission zone of bean leaves during abscission. *Plant Physiol.* 52: 263-267.
- Price NC and Stevens L. (1989)** The purification of enzymes. In: *Fundamentals of enzymology*. Oxford, New York pp. 17-50. Oxford University Press.
- Pyee J, Hongshi Y and Kolattukudy PE. (1994)** Identification of a lipid transfer protein as the major protein in the surface wax of broccoli (*Brassica oleracea*) leaves. *Arch. Biochem. Biophys.* 311: 460-468.
- Quarrie SA, Whitford PN, Appleford NEJ, Wang TL, Cook SK, Henson IE and Loveys BR. (1988)** A monoclonal antibody to (S)-abscisic acid: Its characterisation and use in radioimmunoassay for measuring abscisic acid in crude extract of cereal and lupin leaves. *Planta* 173: 130-139.
- Quirino BF, Noh Y, Himelblau E and Amasino RM. (2000)** Molecular aspects of leaf senescence. *TIPS* 5: 278-282.
- Regente MC and Canal Ldl. (2000)** Purification, characterisation and antifungal properties of a lipid transfer protein from sunflower (*Helianthus annuus*) seeds. *Physiol. Plant.* 110: 158-163.
- Reid PD, Strong HG, Lew F and Lewis LN. (1974)** Cellulase and abscission in the red kidney bean (*Phaseolus vulgaris*). *Plant Physiol.* 53: 732-737.
- Reid MS. (1985)** Ethylene and abscission. *Hort. Sci.* 20 (1): 45-50.
- Reinhardt D, Kende H and Boller T. (1994)** Subcellular localisation of ACC oxidase in tomato cells. *Planta* 195: 142-146.
- Reiter W. (1998)** The molecular analysis of cell wall components. *TIPS* 3: 27-31.
- Reiter W-D and Vanzin GF. (2001)** Molecular genetics of nucleotide sugar interconversion pathways in plants. *Plant Mol. Biol.* 47: 95-113.
- Ribnicky DM, Cooke TJ and Cohen JD. (1998)** A micotechnique for the analysis of free and conjugated indole-3-acetic acid in milligram amounts of plant tissue using a benchtop gas chromatograph-mass spectrophotometer. *Planta* 204: 1-7.
- Riov J and Bangerth F. (1992)** Metabolism of auxin in tomato fruit. *Plant Physiol.* 300: 1396-1402.

- Roberts IN, Lloyd CW and Roberts K. (1985)** Ethylene-induced microtubule reorientations: mediation by helical rays. *Planta* 164: 439-447.
- Roberts JA, Taylor JE, Coupe SA, Harris N and Webb STJ. (1992)** Changes in gene expression during leaf abscission. In *Cellular and molecular aspects of the plant hormone ethylene*, France. pp. 272-277. Kluwer Academic Publishers.
- Roberts JA, Whitelaw CA, Gonzalez-Carranza ZH and McManus MT. (2000)** Cell separation processes in plants - models, mechanisms and manipulation. *Ann. Bot.* 86: 223-235.
- Robertson D, Davies DR and Gerrish C. (1995)** Rapid changes in oxidative metabolism as a consequence of elicitor treatments of suspension cultured cells of French bean (*Phaseolus vulgaris* L.). *Plant Mol. Biol.* 27 (1): 59-67
- Robertson D, Mitchell GP, Gilroy JS, Gerrish C, Bolwell GP and Slabas AR. (1997)** Differential extraction and protein sequencing reveals major differences in patterns of primary cell wall proteins from plants. *J. Biol. Chem* 272: 15841-15848.
- Rubery PH and Sheldrake AR. (1974)** Carrier-mediated auxin transport. *Planta* 118: 101-121.
- Rubinstein B and Leopald AC. (1963)** Analysis of the auxin control of bean leaf abscission. *Plant Physiol.* 38: 262-267.
- Ruperti B, Whitelaw CA and Roberts JA. (1999)** Isolation and expression of an allergen-like mRNA from ethylene treated *Sambucus nigra* leaflet abscission zones. *J. Exp. Bot.* 50: 733-734.
- Sack FD. (1987)** The development and structure of stomata. *Stomatal function* Stanford University Press: 59-89.
- Sagee O, Maoz A, Mertens R, Goren R and Riov J. (1986)** Comparisons of different enzyme immunoassays for measuring indole-3-acetic acid in vegetative citrus tissues. *Physiol. Plant.* 68: 265-270.
- Salvi G, Giarizzo F, DeLorenzo G and Cervone F. (1990)** A polygalacturonase-inhibiting protein in the flowers of *Phaseolus vulgaris* L. *J. Plant Physiol.* 136: 513-518.
- Sargent JA, Osborne DJ and Dunford SM. (1984)** Cell separation and its hormonal control in *Gramineae*. *J. Exp. Bot.* 35: 1663-1667.
- Satina S, Blake AF and Avery AG. (1940)** Demonstration of the three germ layers in the shoot apex of *Datura* by means of induced polyploidy in periclinal chimeras. *Am. J. Bot.* 27: 895-905.
- Schumacher K, Schmitt T, Rossberg M, Schmitz G and Theres K. (1999)** The lateral suppressor (Ls) gene of tomato encodes a new member of the VHIID protein family. *Proc. Natl. Acad. Sci. USA* 96: 290-295.

- Sembdner G, Atzorn R and Schneider G. (1994)** Plant hormone conjugation. *Plant Mol. Biol.* 26: 1459-1481.
- Sexton R, Durbin ML, Lewis LN and Thompson WW. (1980)** Use of cellulase antibodies to study leaf abscission. *Nature* 283: 873-875.
- Sexton R, Durbin ML, Lewis LN and Thompson WW. (1981)** The immunochemical localisation of 9.5 cellulase in abscission zones of bean (*Phaseolus vulgaris* cv. Red kidney). *Protoplasm* 109: 335-347.
- Sexton R. and Roberts JA (1982)** Cell biology of abscission. *Ann. Rev. Plant Physiol.* 33: 133-162.
- Sexton R, Campillo Ed, Duncan D and Lewis LN. (1990)** The purification of an anther cellulase (beta (1:4) 4-glucanhydrolase) from *Lathyrus odoratus* L. and its relationship to the similar enzyme found in abscission zones. *Plant Science* 67: 169-176.
- Sexton R, Laird G, Dorn W and van WG. (2000)** Lack of ethylene involvement in tulip abscission. *Physiol. Plant.* 108: 321-329.
- Shani Z, Dekel M, Tsabary G and Shoseyov O. (1997)** Cloning and characterisation of elongation specific endo-1, 4-beta-glucanase (cell) from *Arabidopsis*. *Plant Mol. Biol.* 34: 837-842.
- Shastri NV, Dias S and Aishwarya D. (2002)** Polygalacturonase inhibiting proteins (PGIPs) of plants. *J. Plant Biochem. Biotech.* 11: 11-20.
- ShengCheng W, Blumer JM, Darvill AG and Albersheim P. (1996)** Characterisation of an endo-beta-1, 4-glucanase gene induced by auxin in elongating pea epicotyls. *Plant Physiol.* 110: 163-170.
- Showalter AM. (1993)** Structure and function of plant cell wall proteins. *Plant Cell.* 1: 9-23.
- Sisler EC, Serek M, Dupille E and Goren R. (1999)** Inhibition of ethylene responses by 1-methylcyclopropene and 3-methylcyclopropene. *Plant Growth Reg.* 27: 105-111.
- Sitbon F, Ostin A, Sundberg B, Olsson O and Sandberg G. (1993)** Conjugation of IAA in wild-type and IAA-overproducing transgenic tobacco plants, and identification of the main conjugates by frit-fast atom bombardment liquid chromatography-mass spectrophotometry. *Plant Physiol.* 101: 313-320.
- Slater A, Maunders MJ, Edwards K, Schuch W and Grierson D. (1985)** Isolation and characterisation of cDNA clones for tomato polygalacturonase and other ripening-related proteins. *Plant Mol. Biol.* 5: 137-147.
- Slovin JP and Cohen JD. (1993)** Auxin metabolism in relation to fruit ripening. *Acta Hort.* 329: 84-89.
- Smallwood M, Knox JP and Bowles DJ. (1996)** Membranes: Specialized functions in plants. Oxford. Pp 61-79. BIOS Scientific Publishers.

- Smith JJ, Ververidis P and John P. (1992)** Characterisation of the ethylene-forming enzyme partially purified from melon. *Phytochem.* 31: 1485-1494.
- Smolen G and Bender J. (2002)** *Arabidopsis* cytochrome P450 cyp83B1 mutations activate the tryptophan biosynthetic pathway. *Genetics* 160: 323-332.
- Steffens GJ, Michelson AM, Otting F, Puget K, Strassburger W and Flohe L. (1986)** Primary structure of Cu-Zn superoxidase dismutase of *Brassica oleracea* proves homology with corresponding enzymes of animals, fungi and prokaryotes. *Biol. Chem. Hoppe-Seyler* 367: 1007-1016.
- Sterk P, Booij H, Schellekens GA and Kammen AV. (1991)** Cell-Specific expression of the carrot EP2 lipid transfer protein gene. *The Plant Cell* 3: 907-921.
- Stuttle GW and Gage J. (1990)** Gibberellin inhibits fruit abscission following seed abortion in peach. *J. Amer. Soc. Hort. Sci.* 115: 107-110.
- Stzein AE, Cohen JD, Fuente IG and Cooke TJ. (1999)** Auxin metabolism in mosses and liverworts. *Amer. J. Bot.* 86: 1544-1555.
- Suzuki T. (1991)** Shoot-tip abscission and adventitious abscission of internodes in mulberry (*Morus alba*). *Physiol. Plant.* 82: 483-489.
- Szymkowiak EJ and Irish EE. (1999)** Interactions between jointless and wild-type tomato tissues during development of the pedicel abscission zone and the inflorescence meristem. *The Plant Cell* 11: 159-175.
- Tabuchi T, Daimon T, Ito S, Nishiyama M, Arai N and Tanaka H. (2000)** Anatomical study of abscission zone formation and development on wild tomato species, *Lycopersicon pennellii*. *Acta Hort.* 514: 193-196.
- Taylor JE, Tucker GA, Lasslett Y, Smith CJS, Arnold CM, Watson CF, Schuch W, Grierson D and Roberts JA. (1990)** Polygalacturonase expression during leaf abscission of normal and transgenic tomato plants. *Planta* 183: 133-138.
- Taylor JE, Webb STJ, Coupe SA, Tucker GA and J.A.Roberts. (1993)** Changes in polygalacturonase activity and solubility of polyuronides during ethylene-stimulated leaf abscission in *Sambucus nigra*. *J. Exp. Bot.* 258: 93-98.
- Taylor JE, Coupe SA, Picton SJ and Roberts JA. (1994)** Isolation and expression of a mRNA encoding an abscission-related B-1,4-glucanase from *Sambucus nigra*. *Plant Mol. Biol.* 24: 961-964.
- Taylor JE and Whitelaw CA. (2001)** Signals in abscission. *New Phytol.* 151:323-339
- Thimann KV. (1988)** A history of the knowledge of auxin. *Plant Physiology and Biochemistry of Auxins in Plants* Kutacke, M. *et al*, eds. SPB Academic Publishing, Prague, Czechoslovakia: 3-11.

- Thoma S, Kaneko Y and Somerville C. (1993)** A non-specific lipid transfer protein from *Arabidopsis* is a cell wall protein. *Plant J.* 3: 427-436.
- Thomas RG. (1988)** *Biology of Plants. Manual. Botany and Zoology*, Massey University, Palmerston North.
- Thompson DS and Osborne DJ. (1994)** A role for the stele in intertissue signalling in the initiation of abscission in bean leaves. *Plant Physiol.* 105: 341-347.
- Tonutti P, Cass LG and Christoffersen RE. (1995)** The expression of cellulase gene family members during induced avocado fruit abscission and ripening. *Plant. Cell and Env.* 18: 709-713.
- Trainotti L, Farrarese L and Casadoro G. (1998)** Characterisation of cCel3, a member of the pepper endo-beta-1, 4-glucanase multigene family. *Hereditas (Landskrona).* 128: 121-126.
- Trainotti I, Farrarese L, Poznanski E and Vecchia FD. (1998)** Endo-beta-1, 4-glucanase activity is involved in the abscission of pepper flowers. *J. Plant Physiol.* 152: 70-77.
- Trainotti L, Spolaore S, Pavanello A, Baldan B and Casadoro G. (1999)** A novel E-type endo- beta- 1, 4-glucanase with a putative cellulose-binding domain is highly expressed in ripening strawberry fruits. *Plant Mol. Biol.* 40: 323-332.
- Trevino MB and O'Connell MA. (1998)** Three drought responsive members of the nonspecific lipid-transfer protein gene family in *Lycopersicon pennellii* show different developmental patterns of expression. *Plant Physiol.* 116: 1461-1468.
- Trewavas AJ and Malho R. (1997)** Signal perception and transduction: The origin of the phenotype. *Plant Cell* 9: 1181-1195.
- Tucker ML, Sexton R, Campillo Ed and Lewis LN. (1988)** Bean abscission cellulase. Characterisation of cDNA and regulation of gene expression by ethylene and auxin. *Plant Physiol.* 88: 1257-1262.
- Tucker ML and Milligan SB. (1991)** Sequence analysis and comparison of avocado fruit and bean abscission cellulase. *Plant Physiol.* 95: 928-933.
- Tucker ML, Baird SL and Sexton R. (1991)** Bean leaf abscission: tissue specific accumulation of cellulase mRNA. *Planta* 186: 52-57.
- Tuominen H, Ostin A, Sandberg G and Sundberg B. (1994)** A novel metabolic pathway for indole-3-acetic acid in apical shoots of *Populus tremula* (L.) x *Populus tremuloides* (Michx.). *Plant Physiol.* 106: 1511-1520.
- Ueda J, Miyamoto K and Hashimoto M. (1996)** Jasmonates promote abscission in bean petiole explants: its relationship to the metabolism of cell wall polysaccharides and cellulase activity. *J. Plant Growth Reg.* 15: 189-195.
- Varner JE and Lin L. (1989)** Plant cell wall architecture. *Cell* 56: 231-239.

- Vered R and Fluhr R. (1993)** Ethylene signal is transduced via protein phosphorylation events in plants. *The Plant Cell* 5: 523-530.
- Ververidis P and John P. (1991)** Complete recovery *in vitro* of ethylene forming enzyme activity. *Phytochem.* 30: 725-727.
- Vioque B and Castellano JM. (1994)** Extraction and biochemical characterisation of 1-aminocyclopropane-1-carboxylate oxidase from pear. *Physiol. Plant* 90: 334-338.
- Vizzotto G, Ramina A and Masia A. (1986)** Peroxidase and IAA-oxidase activity in peach fruit and leaf abscission. *Acta Horticulturae.* 179: 693-696.
- Vogelsang R and Barz W. (1993)** Purification, characterisation and differential hormone regulation of a B-1,3-glucanase and two chitinases from chickpea (*Cicer arietinum* L.). *Planta* 60-69.
- Wang KLC, Li H and Ecker JR. (2002)** Ethylene biosynthesis and signalling networks. *Plant Cell* 14: Suppl: s131-s151.
- Warren Wilson J, Warren-Wilson PM and Walker ES. (1987)** Abscission sites in nodal explants of *Impatiens sultani*. *Ann. Bot.* 60: 511-530.
- Warren Wilson J, Walker ES and Wilson PMW. (1988)** The role of basipetal auxin transport in the positional control of abscission sites induced in *Impatiens sultani* stem explants. *J. Bot.* 62: 487-495.
- Warren Wilson J, Warren Wilson PM and Walker ES. (1988a)** Effects of applied IAA on the position of abscission sites induced in wounded explants from *Impatiens sultani* internodes. *Ann. Bot.* 62: 233-243.
- Warren Wilson J, Palni LMS and Wilson PMW. (1999)** Auxin concentrations in nodes and internodes of *Impatiens sultani*. *Ann. Bot.* 83: 285-292.
- Webster BD and Leopold C. (1972)** Stem abscission in *Phaseolus vulgaris* explants. *Bot Gaz.* 133: 292-298.
- Weigel U, Horn W and Hock B. (1984)** Endogenous auxin levels in terminal stem cuttings of *Chrysanthemum morifolium* during adventitious rooting. *Physiol. Plant.* 61: 422-428.
- Weir DM. (ed.) (1978)** Application of immunological methods. Blackwell Scientific Publications. Oxford.
- Wiesman Z, Riov J and Epstein E. (1988)** Comparison of movement and metabolism of indole-3-acetic acid and indole-3-butyric acid in mung bean cuttings. *Physiol. Plant.* 3: 556-560.
- Willats WGT, Steele-King CG, McCartney L, Orfila C, Marcus SE and Knox JP. (2000)** Making and using antibody probes to study plant cell walls. *Plant Physiol. Biochem.* 38: 27-36.

**Wing RA, Zhang H-B and Tanksley SD. (1994)** Map-based cloning in crop plants. Tomato as a model system: I. Genetic and physical mapping of jointless. *Mol. Gen. Genetics* 242: 681-688.

**Wojtaszek P and Bolwell GP. (1995)** Secondary cell-wall-specific glycoprotein(s) from french bean hypocotyls. *Plant Physiol.* 108: 1001-1012.

**Worley CK, Zenser N, Ramos J, Rouse D, Leyser O, Theologis A and Callis J. (2000)** Degradation of Aux/IAA proteins is essential for normal auxin signalling. *Plant J.* 21: 553-562.

**Wright M and Osborne DJ. (1974)** Abscission in *Phaseolus vulgaris*. The positional differentiation and ethylene-induced expansion growth of specialised cells. *Planta* 120: 163-170.

**Yang SF and Hoffman NE. (1984)** Ethylene biosynthesis and its regulation in higher plants. *Ann. Rev. Plant Physiol.* 35: 155-189.

**Yang SF and Dong JG. (1993)** Recent progress in research of ethylene biosynthesis. *Bot. Bull. Acad. Sin.* 34: 89-101.

**Yao C, Conway WS and Sams CE. (1995)** Purification and characterisation of a polygalacturonase-inhibiting protein from apple fruit. *Phytopath.* 85: 1373-1377.

**Yen S, Chung M, Chen P and Yen H. (2001)** Environmental and developmental regulation of the wound-induced cell wall protein WI12 in the Halophyte ice plant. *Plant Physiol.* 127: 517-528.

**Yoon I. S., Mori H, Kim JH, Kang BG and Imaseki H. (1997)** VR-ACS6 is an auxin inducible 1-aminocyclopropane-1-carboxylate synthase gene in mungbean (*Vigna radiata*). *Plant Cell Physiol.* 38: 217-224.

**Yoshii H and Imaseki H. (1982)** Regulation of auxin-induced ethylene biosynthesis. Repression of inductive formation of 1-aminocyclopropane-1-carboxylate synthase by ethylene. *Plant and Cell Physiol.* 23: 639-649.

**Zhang Z, Schofield CJ, Baldwin JE, Thomas P and John P. (1995)** Expression, purification and characterisation of ACC oxidase from tomato in *E. coli*. *Biochem. J.* 307: 77-85.